Bruker Corporation

Almanac 2010

- 50 Years of Innovation

think forward

www.bruker.com

Bruker – the performance leader in life science and analytical systems.

Right from the beginning, which is now fifty years ago, Bruker has been driven by a single idea: to provide the best technological solution for each analytical task.

Today, worldwide more than 4,000 employees are working on this permanent challenge at over 70 locations on all continents. Bruker systems cover a broad spectrum of applications in all fields of research and development and are used in all industrial production processes for the purpose of ensuring quality and process reliability.

Bruker continues to build upon its extensive range of products and solutions, its broad base of installed systems and a strong reputation amongst its customers. Indeed, as our customers would expect, Bruker as one of the world's leading analytical instrumentation companies, continues to develop state-of-the-art technologies and innovative solutions for today's analytical questions.

Bruker. Think forward!

ISBN 978-3-929431-24-7

Bruker is the performance leader in the following technology platforms and product lines:

Magnetic Resonance
- Nuclear Magnetic Resonance (NMR)
- Electron Paramagnetic Resonance (EPR)
- Magnetic Resonance Imaging (MRI)
- Bench-top TD-NMR Process and GA Systems
- Superconducting Magnets

X-Ray and Elemental Analysis
- X-RayDiffraction (XRD)
- X-Ray Spectrometry (XRF)
- X-Ray Crystallography (SCD)
- EDS and X-Ray Microanalysis
- Optical Emission Spectroscopy (OES)
- Combustion Analysis for Metals

Life Sciences Mass Spectrometry
- MALDI TOF/TOF Mass Spectrometry
- Ion Trap Mass Spectrometry
- ESI-(Q)-TOF Mass Spectrometry
- ESI/MALDI-FTMS
- UHR-TOF MS

Molecular Spectroscopy
- FT-Infrared Spectroscopy (FT-IR)
- Near Infrared Spectroscopy (NIR)
- Raman Spectroscopy

Chemical, Biological, Radiological, Nuclear and Explosives (CBRNE) Detection
- GC-Mass Spectrometry
- Ion Mobility Spectrometry (IMS)
- FT IR Stand-off Detection
- Biological Classification and Identification Systems
- Explosives Detection Systems

Superconductor Wire Products and Devices
- Low temperature superconductors (LTS)
- High-temperature superconductors (HTS)
- Hydrostatic Extrusions
- Magnets
- Synchrotron instrumentation

Life Science

Quality & Process Control

Materials Research

Food & Environment

Pharma & Biotech

Clinical Research

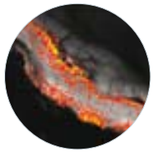

Bruker AXS

Bruker AXS GmbH
Oestliche Rheinbrückenstr. 49
76187 Karlsruhe
Germany
Tel: +49 (7 21) 5 95-28 88
Fax: +49 (7 21) 5 95-45 87
info@bruker-axs.de
www.bruker-axs.com

Bruker AXS Inc.
5465 East Cheryl Parkway
Madison, WI 53711
USA
Tel: +1 (8 00) 2 34-XRAY
Tel: +1 (6 08) 2 76-30 00
Fax: +1 (6 08) 2 76- 30 06
info@bruker-axs.com
www.bruker-axs.com

Bruker AXS K.K.
3-9-A, Moriya-cho,
Kanagawa-ku,
Yokohama-shi
Kanagawa 221-0022
Japan
Tel: +81 (45) 4 53-19 60
Fax: +81 (45) 4 40-07 57
info@bruker-axs.jp
www.bruker-axs.com

Bruker BioSpin

Bruker BioSpin GmbH
Silberstreifen 4
76287 Rheinstetten
Germany
Tel: +49 (7 21) 51 61-0
Fax: +49 (7 21) 51 71 01
nmr@bruker-biospin.de
epr@bruker-biospin.de
mri@bruker-biospin.de
www.bruker-biospin.com

Bruker BioSpin Corp.
15 Fortune Drive
Billerica, MA 01821-3991
USA
Tel: +1 (9 78) 6 67-95 80
Fax: +1 (9 78) 6 67-09 85
sales@bruker-biospin.com
www.bruker-biospin.com

Bruker EST

Bruker EAS GmbH
Ehrichstr. 10
63450 Hanau
Germany
Tel: +49 (6181) 4384-4100
Fax: +49 (6181) 4384-4400
info@advancedsupercon.com
www.advancedsupercon.com

Bruker Daltonics

Bruker Daltonik GmbH
Fahrenheitstr. 4
28359 Bremen
Germany
Tel: +49 (4 21) 22 05-0
Fax: +49 (4 21) 22 05-103
CBRN Detection
Tel: +49 (3 41) 24 31-30
sales@bdal.de
www.bdal.de

Bruker Daltonics Inc.
40 Manning Road
Manning Park
Billerica, MA 01821
USA
Tel: +1 (9 78) 6 63-36 60
Fax: +1 (9 78) 6 67-59 93
ms-sales@bdal.com
www.bdal.com

Bruker BioSciences Pty. Ltd.
Unit 1/28A, Albert St.
Preston, VIC. 3072
Australia
Tel: 1300 BRUKER
Tel: +61 (3) 94 74 70 00
Fax: +61 (3) 94 74 70 70
sales@bruker-daltonics.com.au
www.bdal.com

Bruker Optics

Bruker Optik GmbH
Rudolf-Plank-Str. 27
76275 Ettlingen
Germany
Tel: +49 (72 43) 5 04-20 00
Fax: +49 (72 43) 5 04-20 50
info@brukeroptics.de
www.brukeroptics.de

Bruker Optics Inc.
19 Fortune Drive,
Manning Park
Billerica, MA 01821-3991
USA
Tel: +1 (9 78) 4 39-98 99
Fax: +1 (9 78) 6 63-91 77
info@brukeroptics.com
www.brukeroptics.com

Bruker Optik Asia Pacific Ltd.
Unit 509, 5/F, Tower II,
Enterprise Square No. 9,
Sheung Yuet Road
Hong Kong
Tel: +8 52-27 96-61 00
Fax: +8 52-27 96-61 09
asiapacific@brukeroptics.com.hk
www.brukeroptics.com

Australia
Bruker BioSpin Pty. Ltd.
Tel: +61 (2) 95 50-64-22
sales@bruker.com.au

Bruker BioSciences Pty. Ltd.
Tel: 1300 BRUKER
+61 (0)3 9474 7000
sales@bruker-daltonics.com.au
baxs@bruker-axs.com.au

Austria
Bruker Austria GmbH
Tel: +43 (1) 8 04-78 81-0
sales@bruker.com.at
office@bruker.at

Belgium
Bruker Belgium SA/NV
Bruker Daltonics SPRL/BVBA
Tel: +32 (2) 7 26-76 26
daltonics@bruker.be
bruker@bruker.be

Brazil
Bruker do Brasil, Ltda.
Tel: +55 (11) 55 94-50 30
Tel: +55 (11) 50 52-55 37
info@bruker.com.br

Bruker AXS do Brasil
Tel: +55 (11) 55 94-50 30

Canada
Bruker BioSpin Ltd.
Bruker Daltonics Ltd.
Bruker Optics Ltd.
Tel: +1 (905) 8 76-46 40
Tel: +1 (604) 5 91-72 99
info@bruker.ca
info@brukeroptics.com

Bruker AXS
Tel: +1 (608) 2 76-30 00
Tel: +1 (800) 2 34-XRAY
info@bruker-axs.com

France
Bruker BioSpin S.A.
Tel: +33 (3) 88 73 68 00
bruker@bruker.fr

Bruker AXS S.A.S.
Tel: +33 (1) 60 95 90 00
secret@bruker-axs.fr

Bruker Daltonique S.A.
Tel : +33 (3) 88 06 60 40
infomasse@bruker.fr

Bruker Optics S.a.r.l.
Tel: +33 (1) 64 61 81 10
bruker@bruker.fr

Germany
Bruker BioSpin GmbH
Tel: +49 (7 21) 51 61-0
nmr@bruker-biospin.de
epr@bruker-biospin.de

Bruker BioSpin MRI GmbH
Tel: +49 (7 21) 51 61-6500
mri@bruker-biospin.de

Bruker AXS GmbH
Tel: +49 (7 21) 5 95-28 88
info@bruker-axs.de

Bruker Daltonik GmbH, Bremen
Tel: +49 (4 21) 22 05-0
sales@bdal.de

Bruker Daltonik GmbH, Leipzig
Tel: +49 (3 41) 24 31-30
sales@bdal.de

Bruker Optik GmbH
Tel: +49 (72 43) 5 04-2000
info@brukeroptics.de

Bruker AXS Microanalysis GmbH
Tel: +49 (30) 67 09 90-0
info-ma@bruker-axs.de

Bruker Nano Division of Bruker AXS Microanalysis GmbH
Tel: +49 (24 07) 56 42-0
info@bruker-nano.de

Bruker-Elemental GmbH
Tel: +49 (28 24) 97 65 00
info@bruker-elemental.de

Bruker Optik GmbH, Leipzig
Tel: +49 (3 41) 2 41 09-10
info@brukeroptics.de

Bruker Optik GmbH, Bremen
Tel: +49 (4 21) 2 23 19-10
info@brukeroptics.de

India
Bruker India Scientific Pvt. Ltd.
Tel: +91 (80) 23 61 25 20
cv.manjunath@bruker-biospin.in

Bruker AXS Analytical Instruments Pvt. Ltd. (New Delhi)
Tel: +91 (11) 24 61 01 23

Bruker Optik GmbH (Mumbai)
Tel: +91 (22) 67 42 40 23
branchoffice.india@brukeroptics.de

Israel
Bruker Scientific Israel Ltd.
Tel: +9 72 (8) 9 47-77 05
bsis@bruker.co.il

Italy
Bruker BioSpin S.r.l.
Tel: +39 (02) 70 63 63 70
bruker@bruker.it

Bruker AXS S.r.l.
Tel: +39 (02) 70 63-63 70
axs@bruker.it

Bruker Daltonics S.r.l.
Tel: +39 (0733) 28 31 41
bruker@bdal.it

Bruker Optics Srl
Tel: +39 (02) 70 63 63 70
optics@bruker.it

Japan
Bruker BioSpin K.K.
Tel: +81 (2 98) 52-12 34
info@bruker-biospin.jp

Bruker AXS K.K.
Tel: +81 (45) 4 53-19 60
service@bruker-axs.jp

Bruker Daltonics K.K.
Tel: +81 (45) 4 40-04 71
info@bruker.co.jp

Bruker Optics K.K.
Tel: +81 (3) 58 16-21 25
Tel: +81 (6) 63 94-89 89
info@bruker-optics.jp

Latvia
Bruker Baltic Ltd.
Tel: +371 67 38 39 47
office@bruker-baltic.lv

Maghreb
Bruker AXS S.A.S.
Tel: +33 (1) 60 95-90 00

Malaysia
Bruker Malaysia SDN Bhd
Bruker Optics Malaysia
Tel: +60 (3) 56 21 83 03
tak@bruker.com
malay@brukeroptics.com.hk

Mexico
Bruker Mexicana, SA de CV
Tel: +52 (55) 56 30 57 47
mexico-sales@bruker.com
ventasmexico@bdal.com
info-axs@bruker.com.mx
mexico@brukeroptics.com

The Netherlands
Bruker BioSpin B.V.
Tel: +31 (75) 6 28-52 51
biospin@bruker.nl

Bruker AXS B.V.
Tel: +31 (15) 2 15-24 00
info@bruker-axs.nl

Bruker Daltonics B.V.
Tel: +31 (75) 6 28-52 51
daltonics@bruker.nl

Bruker Optics B.V.
Tel: +31 (15) 2 15 24 30
optics@brukeroptics.nl

New Zealand
Asia-Pacific Area Headquarters
Tel: +64 (21) 64 08 01
chs@dbal.com
bruker.asiapacific@bdal.com

The Nordic Countries
Bruker BioSpin Scandinavia AB
Tel: +46 (8) 6 55 25 10
nmr-support@bruker.se

Bruker AXS Nordic GmbH
Tel: +46 (8) 6 55 25 60
info@bruker-axs.se

Bruker Daltonics Scandinavia AB
Tel: +46 (8) 6 55 25 40
ms-sales@bruker.se

Bruker Optics Scandinavia AB
Tel: +46 (8) 6 55 25 30
optics@bruker.se

People's Republic of China
Bruker BioSpin AG Ltd.
Tel: +86 (10) 68 47-2015
jia.wei@bruker-biospin.cn

Bruker AXS Beijing Office
Tel: +86 (10) 68 48-69 46
service@bruker-axs.com.cn

Bruker Daltonics Inc. Beijing Representative Office
Tel: +86 (10) 68 47 40 93-5
hank.wang@bruker.com.cn

Bruker Optics
Hong Kong
Tel: +852 27 96 61 00
Shanghai
Tel: +86 (21) 62 49-90 60
Beijing
Tel: +86 (10) 68 47-20 60
asiapacific@brukeroptics.com.hk
optics@bruker.com.cn

Poland
Bruker Polska Sp.z.o.o.
Tel: +48 (61) 8 68-90 08
secretariat@bruker.poznan.pl

Russia and the CIS
Bruker Russia Ltd.
Tel: +7 (4 95) 5 02-90 06
info@bruker.ru

Singapore
Bruker Singapore Office
Tel: +65 65 00 72 88
sales@bruker.com.sg

South Africa
Bruker South Africa (Pty) Ltd.
Bruker Daltonics SA (Pty) Ltd.
Tel: +27 (11) 4 63-60 40
info@bruker.co.za

South Korea
Bruker BioSpin Korea Co. Ltd.
Tel: +82 (2) 5 93-54 54
nmrsales@bruker.co.kr

Bruker BioSciences Korea Co. Ltd.
Tel: +82 (2) 596 32 32
info@bdal.co.kr

Bruker Optics Korea Ltd.
Tel: +82 (2) 5 93-61 66
brukeroptics@brukeroptics.co.kr

Spain
Bruker Española S.A.
Bruker BioSciences Española SA
Tel : +34 (91) 4 99 40 80
Tel : +34 (91) 6 55 90 13
Tel : +34 (91) 4 49 38 12
bruker@bruker.es

Switzerland
Bruker BioSpin AG
Tel : +41 (44) 8 25-91 11
sales@bruker-biospin.ch

Bruker AXS GmbH
Tel: +49 (721) 5 95-28 88
info@bruker-axs.de

Bruker Daltonics GmbH
Bruker Optics GmbH
Tel: +41 (44) 8 25-91 11
daltonics@bruker.ch
optics@bruker.ch

Taiwan
Bruker Daltonics Inc.
Tel: +886 (2) 89 82 37 10
taiwan_service@bruker.com.tw

Bruker Optics Taiwan Ltd.
Tel: +886 (2) 22 76 73 58
taiwan@brukeroptics.idv.tw

Thailand
Bruker BioSpin AG
Bruker Southeast Asia
Tel: +66 (2) 6 42-69 00
kkbsea@bruker.co.th
kdcbsea@bruker.co.th
neukbsea@bruker.co.th

Bruker Optik Thailand
Tel: +66 (2) 6 32-28 82-5
thai@brukeroptics.com.hk

United Kingdom
Bruker BioSpin Ltd.
Bruker BioSpin MRI Ltd.
Bruker AXS Ltd.
Bruker Daltonics Ltd.
Bruker Optics Ltd.
Tel: +44 (24) 76 85 52 00
sales@bruker.co.uk
sales@biospin-mri.bruker.co.uk
info@bruker-axs.co.uk
sales@daltonics.bruker.co.uk
sales@optics.bruker.co.uk

United States
Bruker BioSpin Corporation
(Northeast/U.S. Headquarters)
Tel: +1 (9 78) 6 67-95 80
sales@nmr.bruker-biospin.com
epr@bruker.com
mri@bruker-biospin.com

(West Coast)
Tel: +1 (5 10) 6 83-43 00
wcoast@bruker-biospin.com

(Mid-Atlantic)
Tel: +1 (3 02) 8 36-90 66
ma@bruker-biospin.com

(Southeast)
Tel: +1 (3 02) 8 36-90 66
soeast@bruker-biospin.com

(South)
Tel: +1 (2 81) 2 92-24 47
so@bruker-biospin.com

Bruker AXS Inc.
Madison, WI
Tel: +1 (6 08) 2 76-30 00
Tel: +1 (8 00) 2 34-XRAY
info@bruker-axs.com

Bruker Daltonics Inc.
Billerica, MA
Tel: +1 (9 78) 6 63-36 60
ms-sales@bdal.com

Bruker Daltonics Inc.
Fremont, CA
Tel: +1 (5 10) 6 83-43 00
ms-sales@bdal.com

Bruker Optics Inc.
Tel: +1 (9 78) 4 39-98 99
info@brukeroptics.com

Additional information
www.bruker.com/offices

Bruker Corporation

The Bruker Group is a leading provider of high-performance scientific instruments and solutions for molecular and materials research, as well as for industrial and applied analysis. Bruker Corporation (Nasdaq: BRKR), headquartered in Billerica, Massachusetts, is the publicly traded parent company of Bruker Scientific Instruments Division (Bruker AXS, Bruker BioSpin, Bruker Daltonics, Bruker Optics) and Bruker Energy & Supercon Technologies (BEST) Division.

Bruker AXS

Bruker AXS is a leading global developer and manufacturer of analytical X-ray systems, optical emission spectrometers and combustion analyzers for elemental analysis, materials research and crystallographic investigations. Bruker AXS' innovative solutions enable a wide range of customers in research and industry – including chemistry, petrochemistry, pharmacy, metals and steel, semiconductor, cement, minerals and mining, automotive, forensics, environmental, art and conservation, nanotechnology and life sciences – to make technological advancements and to accelerate their progress.

Bruker BioSpin

Bruker BioSpin is the global market and technology leader in analytical magnetic resonance instruments including NMR, preclinical MRI and EPR. The company delivers the world's most comprehensive range of magnetic resonance research tools enabling life science, materials science, analytical chemistry, process control and clinical research. Bruker BioSpin is also the leading manufacturer of superconducting high and ultra high field magnets for NMR and MRI.

Bruker Daltonics

Bruker Daltonics is a leading manufacturer of mass spectrometry (MS) instruments and accessories for life science, pharmaceutical, biochemical and chemical research as well as for more routine analytical tasks in forensics and food safety. Technical solutions are based on a comprehensive range of MALDI-TOF/TOF, ESI-(Q)-TOF, UHR-TOF, ESI-ITMS, ESI/MALDI-FTMS mass spectrometry systems, as well as automated sample handling systems and productivity enhancing software designed to answer our customers' needs. Bruker Daltonics is also a global leader in nuclear, biological and chemical detection, with a CBRNE product line based on a broad array of technologies, including mass spectrometry and ion mobility spectrometry.

Bruker Optics

Bruker Optics offers the industry's most comprehensive range of product offerings and solutions based on vibrational spectroscopy. Products include FT-IR spectrometers; from the world's smallest in size to the highest in resolution, Near Infrared and Raman spectrometers. Whether it's a high-end research system, a life sciences instrument, a routine quality control tool or a process analyzer, Bruker Optics offers a wide variety of innovative analytical solutions.

Bruker EST

Bruker Energy & Supercon Technologies Division is a leading manufacturer and developer of a broad range of high-performance superconductor wire products and devices.

Bruker – the group with analytical excellence, long time experience and global presence.

Bruker AXS facilities

Bruker BioSpin facilities

Bruker Daltonics facilities

Bruker Optics facilities

Bruker Australia

Bruker Japan

Bruker Germany

Bruker France

Bruker 1960-2010

- 50 Years of Innovation

The Beginnings

Prof. Günther Laukien

The Bruker group of companies owes its existence to Dr. Günther Laukien, who moved to the Institute for Experimental Physics in Stuttgart shortly after finishing his studies in Physics in Tubingen in 1952. From 1952 to 1957, he pursed post-doctoral research in NMR Spectroscopy, and in 1958 published a pioneering paper on high-frequency nuclear magnetic resonance. This paper described the theoretical aspects that were known at the time, while also covering the practical aspects of constructing experimental systems. In 1960, he was appointed as a Professor for Experimental Physics in Karlsruhe.

At that time, laboratories in the US were already building the first high-resolution systems for use in analytical chemistry. Dr. Laukien recognized the power in this technique and the need for a system not yet produced commercially. He set out to fill this need by establishing his own company.

Bruker Physik-AG was officially incorporated on September 7, 1960, originally located in the backyard of a Karlsruhe residence. The development of NMR spectrometers began with the production of laboratory magnets and power supplies.

Bruker Physik AG's first operational facility in Hardtstraße, Karlsruhe, Germany.

By 1963, the rapidly-growing Bruker Physik employed a staff of 30 developing both high-resolution NMR and EPR. With a rapidly expanding market, Bruker quickly outgrew its space and moved to an undeveloped parcel in Forchheim, where it was able to build a facility to better meet it's expanding needs.

Why the Name Bruker?

In 1960, university professors were not allowed to commit to commercial work whilst in a position of research and teaching.

This meant that Professor Laukien could not be named as a founding member; thus co-founder Dr. Emil Bruker gave the company its name.

1963: Bruker NMR pulse spectrometer.

High-Resolution NMR at Trüb Täuber; The Onset of Bruker in Switzerland

In Zurich in 1960, Trüb Täuber & Company, a manufacturer of complex measuring instruments for the power station industry, had a small research department that focused on NMR spectrometers and electron microscopes.

Their NMR research had benefited directly from close cooperation with the ETH Swiss Federal Institute of Technology in Zurich, namely Professors Günthard, Primas and subsequent Nobel Prize Laureate, Richard Ernst.

Operating at 25 MHz, and equipped with a permanent magnet, their first KIS spectrometers were 2 meters tall.

Early NMR Spectrometer

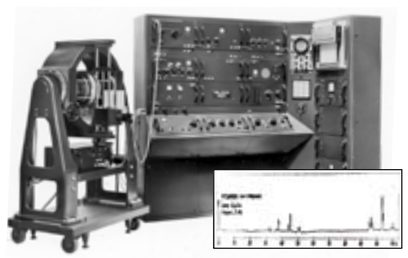

1960: 25 MHz permanent magnet KIS1 NMR system. Spectra required in 12 hours of acquisition time. Spectra courtesy: Prof. R. Ernst

In 1962, with competitor systems featuring significantly higher field strengths, a new spectrometer, the KIS 2, was developed based on a five-ton magnet that enabled high-resolution spectroscopy at field strengths up to 90 MHz. Around twenty KIS 25 MHz and KIS 2 instruments were installed in Switzerland, France, Belgium and Germany.

When Trüb Täuber fell into financial difficulty midway through the 1960s, Günther Laukien founded Spectrospin AG specifically to preserve its former NMR department.

Bruker-Spectrospin Cooperation

The establishment of Spectrospin AG set the scene for close cooperation and a strong synergistic relationship with Bruker. The introduction of manufacturing agreements saw Bruker specialize in magnets and power supplies while simultaneously closing down its development of high-resolution instruments, leaving Spectrospin AG to focus on the high-resolution instruments and equally close down its development of EPR.

An ambitious development project was then launched to exploit valve-free, solid-state technology. By 1967 successful system demonstrations of the first fully transistorized instrument immediately led to the delivery of the first HFX 90 to the Technical University Berlin.

The HFX 90 was the first production spectrometer in the world to offer three independent channels for locking, recording and decoupling, working exclusively with frequency sweep.

Multinuclear NMR

1967: HFX 90, the first fully transistorized NMR system, equipped with three independent channels.

New experiments became possible, while previously impossible or extremely difficult experiments became routine. Pioneering innovations included spin spectroscopy (homo and hetero), decoupling, accumulation and completely reproducible scales. To display all the new details made possible by the system, a new recorder with 60 cm paper width had to be developed.

Other developments were also rapidly progressing at Bruker, including EPR spectrometers, pulse spectrometers and magnets applied in physics.

The first demonstrations for American customers took place in 1967. Yale University purchased two systems, with the first spectrometer being delivered in 1968 by air cargo.

1968: First HFX 90 for the United States (Yale Univ.) being loaded onto a Boeing 707.

Shortly after this installation, Bruker opened its first US office in Elmsford, New York, and proceeded to quickly secure a considerable customer base.

At the end of 1970, Spectrospin AG moved to new, modern premises in Fällanden, near Zurich, that provided more space and dedicated production facilities. Expansion also saw Bruker extend its facilities in Forchheim. Consequently, both companies were well equipped to meet the challenges of the next decade.

Fourier Transform (FT)

In 1964, Richard Ernst was the first to develop a functioning FT process that delivered a significant increase in sensitivity. However, skepticism regarding experiment length and long ^{13}C relaxation times meant the system was never commercialized.

1971: WH 90, the first FT-only NMR Spectrometer.

Another problem with ^{13}C was the lack of decoupling to achieve pure shift spectra with improved signal-to-noise ratio. Richard Ernst was again the pioneering figure, being the first to describe noise decoupling, which solved the problem.

Bruker's continuing development of pulse spectrometry saw the first high-power radio frequency amplifier that could transmit a pulse as well as decouple. This was followed by a new form of

Birth of ^{13}C FT NMR

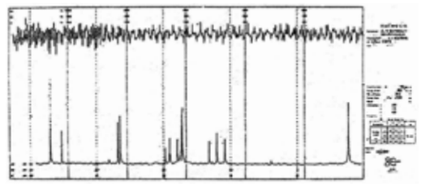

1969 : One of the first ^{13}C FT Spectra. Measuring time now reduced to 200 seconds.

broadband decoupling, which was significantly more effective than Ernst's method, and simpler to implement. The new technology delivered unique experimental opportunities that remained unmatched by Bruker's competitors right through to the 1980s.

1973: NMR spectrometer based on superconducting magnet technology.

In 1969, Bruker unveiled the world's first FT-NMR spectrometer that enabled broadband proton decoupling. Developed in Elmsford, the new spectrometer delivered sensational results. The new, superior and revolutionary ^{13}C spectra made a significant impact when presented at the ^{13}C conference in Anaheim, California.

Driven by its unmatched FT-NMR technology, Bruker's share of the market expanded considerably. In addition, the development of pulse spectrometry resulted in the construction of the minispec, a spectrometer dedicated to industrial applications.

First Industrial NMR Applications

1975: minispec p20 NMR spectrometer.

The Bruker Group

During the 1960s, it had become evident that to be a key player in the analytical instrument market, a worldwide presence was required with contacts for customers and researchers at a local level.

The first step had been toward America, a growing hub of NMR research at the time. Despite local market dominance by US companies, success was rapid, driven by Bruker's unequalled technologies and the widespread approval of the NMR community.

This was followed in 1971 with the establishment of Bruker SA in France. Bruker moved into new production facilities in Wissembourg and quickly started producing sub-units.

Throughout the early 1970s sales offices appeared all over Europe, including the UK and Italy.

In 1969, during the 25th anniversary of the discovery of EPR in Kazan, Bruker undertook its first activities in, what was then, the USSR.

A new office was also established in Israel, strengthening relations with the country and with the Weizman Institute in particular.

In 1972, expansion reached Australia, where collaboration with local company Selby signified Bruker's arrival.

1975: Mr. Fanf Yi, PRC Vice President and President of the Chinese Academy visits the Bruker stand at a trade show in Beijing.

In 1975, Bruker arrived in China. A very successful appearance at the Swiss Industrial Exhibition in Beijing led to the immediate sale of two WH 90 NMR spectrometers.

1975: Ceremony for breaking ground in Tsukuba, Japan.

Japan, South Korea and Taiwan sales offices soon followed, and in 1976 Bruker opened its first facility in Japan.

Bruker was also successful in South America, with the first instrument installations taking place in Venezuela.

FT-IR

Bruker began the development of new infrared spectrometers in the 1970s. Launched in 1974, the IFS 110 was the beginning of a very successful product line that ultimately led to the foundation of the Bruker Optics division.

1974: IFS 110, Bruker's first FT-IR spectrometer.

Today, Bruker Optics offers a comprehensive vibrational spectroscopy product-line that includes both the world's smallest benchtop FT-IR spectrometer for routine use, and the world's highest resolution FT-IR for advanced research applications.

Magnetic Resonance Imaging

Bruker Medizintechnik GmbH was founded in 1975, offering a product range of mobile defibrillators. By the late 1970s, Bruker was producing NMR tomographs for clinical and pre-clinical environments, leading to whole body clinical scanner instrumentation.

The Onset of Magnetic Resonance Imaging

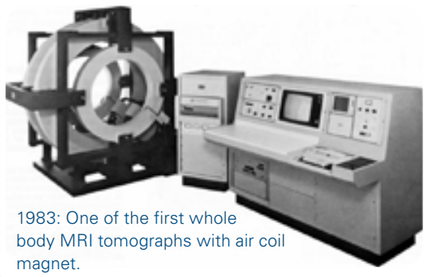

1983: One of the first whole body MRI tomographs with air coil magnet.

Over time Bruker shifted its focus towards pre-clinical instrumentation, a move which saw the company develop as market leader in the field, a position maintained by Bruker BioSpin MRI today.

Marine Research

Bruker Meerestechnik GmbH was founded in 1977, producing small submersibles for the shelf research and oil exploration sectors, and for tourism (including the largest tourist submarine in the world to date). Bruker's increasing on analytical instrumentation led to the later sale of this division.

1978: Bruker submersible 'Meermaid' in action.

Partnership with IBM

The late 1970s was a time of global diversification, and IBM's subsidiary, IBM Instruments, sought an interest in Bruker's wide-ranging product range. IBM invested in Bruker in 1978, and the partnership witnessed the development of a large range of instruments for gas chromatography, liquid chromatography and polar graphs, and optimized IR, NMR and TD-NMR instruments for routine applications and specific sales initiatives in the American markets.

The relationship lasted for 10 years, until Bruker repurchased the IBM holding and integrated a portion of the developed systems into its own product range.

Expansion at Karlsruhe

Unable to expand significantly in Forchheim, Karlsruhe became the focus for new production facilities.

In 1982 the company purchased a large factory complex in Karlsruhe-Rheinhafen that was perfectly suited to the production of magnets for particle physics research. The site remains the ideal location for magnet production.

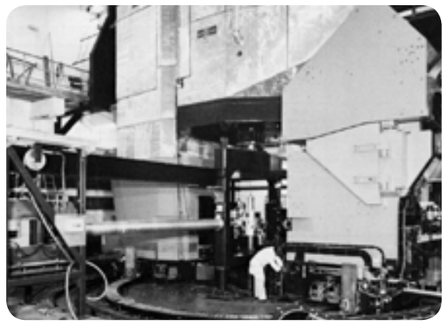

1984: Final assembly of the particle spectroscopy magnet in the Rheinhafen plant.

In 1991 the Ettlingen site witnessed the opening of its first building – the Bruker NMR Imaging Development and Application Center – an NMR tomography development, production and demonstration center.

To guarantee the provision of high-quality electronic components for numerous Bruker divisions, Bruker Elektronik GmbH was established in 1985, equipped with state-of-the-art production and testing equipment.

With an ever-increasing number of biological applications using magnetic resonance spectroscopy, the company formed the Bruker BioSpin Group in 2001, bringing together all BioSpin companies specializing in magnetic resonance, to ensure market-leading focus and commitment.

Mass Spectrometry

Industrial production of the first mass spectrometers began in the 1940s. In Germany, an early mass spectrometer was developed in 1948 by Dr. L. Jenckel, head of Atlas MAT (Mess- und Analysentechnik) in Bremen.

In 1977 "Dr. Franzen Analysentechnik" was founded in Bremen as a spin-off company from Atlas MAT. Dr. Franzen developed the first table-top mass spectrometer, based on a quadrupole mass filter and coupled to a GC.

A few years later, in 1980, Bruker acquired this company and renamed it "Bruker-Franzen Analytik", adding robust quadrupole mass spectrometers to the Bruker portfolio. That same year the first mobile detection system, the MM1, proved successful in both the civilian and military markets.

Mass Spectrometer

1980: MM1 the first mobile detection system.

Thanks to Bruker's existing expertise in NMR and superconducting magnet technology, Bruker Spectrospin in Switzerland successfully developed a new type of mass spectrometer, with the first installations of FT-ICR mass spectrometry systems taking place in 1982.

An innovative collaboration with the Technical University of Munich in 1983 resulted in a project to investigate resonant laser mass spectrometry. The project's success ultimately led to Bruker's introduction of time-of-flight mass spectrometers, an intrinsic part of the product range to this day.

50 Years of Innovation

Mass Spectrometry

1980s: Early FT ICR mass spectrometer.

In 1990, together with scientists from the former Academy of Science, Bruker founded Bruker Saxonia in Leipzig. As a subsidiary company of Bruker-Franzen Analytik, Bruker Saxonia was dedicated to ion mobility spectrometry.

In 1997 Bruker-Franzen Analytik GmbH was renamed Bruker Daltonik GmbH. The name was chosen to honor John Dalton for his work in formulating the theory of the atomic structure of matter.

The development of two new ionization procedures in the late 1980s, electrospray and MALDI, enabled the ionization and analysis of biomolecules. This paved the way for the application of mass spectrometry in molecular biology and molecular medicine. The development of these ionization procedures was honored with a Nobel Prize in 2002.

In 1997 the company witnessed a change in leadership, brought about by the death of its founder, Günther Laukien. His death was a great loss to the company and the scientific community at large because his ideas, his motivation, and his competence as both scientist and entrepreneur were major driving forces behind the company's success.

His wife and four sons have continued to lead the company in accordance with his vision and beliefs, and the same forward-thinking spirit that drives progress to this day.

With the spectrometers being continuously enhanced, Bruker mass spectrometry experienced unexpected growth. Mass spectrometry became a solid base for ground-breaking research in a broad range of sciences, comprising pharmaceutical, life sciences and clinical research.

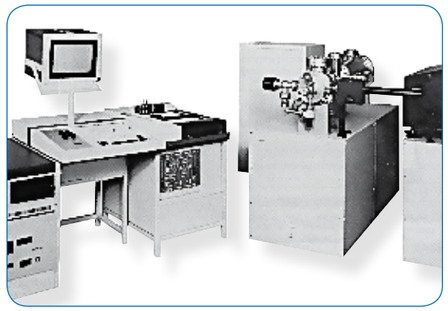

1987: Early MS TOF spectrometer.

Moreover, Bruker has recently obtained the first IVD-CE mark for the MALDI-TOF-based microbial identification workflow solution, the MALDI Biotyper. This system is pioneering the advancement of mass spectrometry in clinical diagnostics. Global mass spectrometry operations later fell under the umbrella of the Bruker Daltonics Group.

X-ray Technologies

In 1997 Bruker acquired the X-ray spectroscopy division of Siemens AG, which included prime manufacturing facilities in Karlsruhe and Madison, Wisconsin. Commercial growth, combined with additional company acquisitions, quickly launched Bruker AXS as a leading provider of X-ray analytical instrumentation, significantly extending Bruker's technology portfolio.

D8 ADVANCE, new generation of X-ray powder diffraction instrument launched in 1997.

Superconducting Wire Technologies

Superconducting magnets, an essential component in several Bruker product lines, require special qualities of wire critical for high-end performance. In order to secure a guaranteed quality of supply, Bruker acquired the wire manufacturer Vacuumschmelze, in Hanau in 2003.

Magnets and power supplies for physics research have been a key constituent for Bruker since its beginnings in 1960. In 2009, the acquisition of ACCEL significantly strengthened Bruker's position as a leading developer in the sector. The expanding product range, has resulted in a new division, Bruker Energy and Supercon Technologies.

1975: Power supplies for nuclear physics research.

Bruker Corporation

The organizational restructuring of Bruker began in 2000, as the company adapted to meet the needs of today's markets and environments. The Bruker Daltonics group became the first Bruker company to be listed on the NASDAQ stock exchange market, followed by the Bruker AXS group in 2001.

The synergies generated from the improved integration across development, production and sales were quickly recognized, leading to the development of combined systems that would deliver significant customer benefits. Consequently, in 2003, the Daltonics and AXS groups were soon merged into a single listed company.

In 2006, the Bruker Optics group followed suit, and finally the magnetic resonance business, the Bruker BioSpin Group, in 2008.

This unification under one new parent company, the Bruker Corporation, has created one of the strongest brands in analytical instrumentation.

Bruker Corporation headquarters in Billerica, Massachusetts, USA.

Bruker Today

In 2008 Bruker Corporation revenues exceeded the US$ 1 billion mark for the first time, directly attributable to the company's exceptional customer service, innovation, continuity, and product quality.

The unique scope of the Bruker product range remains ground-breaking and influential, evidenced by the many product lines that lead their respective markets.

Bruker's growth in size has further fueled its highly dynamic nature, driving the introduction of many key innovations throughout 2009.

Positive and committed progress is assured through reliance on more than 4000 highly motivated employees, and through continuing excellent customer relations.

Bruker is convinced that these are the ideal conditions for developing innovative solutions for tomorrow's analytical questions, thereby securing an ever-successful future.

Content

BRUKER

Bruker BioSpin

Nuclear Magnetic Resonance

Solutions for Life Sciences
and Analytical Research

think forward

AVANCE III

The AVANCE™ III is the ultimate NMR platform for life-sciences and materials research. Robust, automated and easy-to-use it is the ideal NMR analysis system for the pharmaceutical, biotech, and chemical industries, for metabonomics, materials science, molecular diagnostics, and much more. With the enhanced architecture of the AVANCE III, we introduce the fastest and most flexible, high-performance NMR spectrometer on the market.

The AVANCE III is the newest generation in the very successful AVANCE series, which has established Bruker BioSpin as the clear technological and market leader in NMR and pre-clinical MRI worldwide. The AVANCE III spectrometer architecture is designed around an advanced digital concept which provides an optimized pathway for high-speed RF generation and data acquisition with highly modular and scalable transmitters and multiple receiver channels.

The AVANCE III platform provides 25 ns event timing (12.5 ns clock), and simultaneous phase, frequency and amplitude switching with capabilities that exceed the requirements of even the most demanding solid-state NMR experiments. The second-generation digital receiver technology delivers high dynamic range, high digital resolution and large-bandwidth digital filtering. The unique digital lock system provides the utmost in field/frequency stability.

AVANCE III 1000 MHz Console

AVANCE III Features

- Patented Direct Digital Synthesis
- One-chip RF generation
- Timing Resolution: 12.5 ns
- Minimum event time: 25 ns
- Phase resolution: 0.0055°
- Frequency resolution: 0.005 Hz
- Advanced ADC with an effective resolution of up to 22 bits

NMR Magnets

Bruker BioSpin has specialized in the design and production of magnets and cryogenic systems for a wide range of applications, becoming the world's largest manufacturer of superconducting magnets for NMR. Bruker BioSpin is engaged in every aspect of the magnet business including research and development, production and testing, individual site planning, as well as service and support.

UltraStabilized

UltraStabilized™ is our innovative magnet technology for Ultra-High Field NMR at 750 MHz to 1000 MHz. This proprietary technology provides reliable, stable operation at reduced helium bath temperature and ambient pressure.

UltraShield UltraStabilized

The US² represents the efficient combination of Bruker BioSpin's renowned magnet technologies (UltraStabilized™ and UltraShield™) for enhanced system performance and siting flexibility at Ultra-High Field strength.

UltraShield Plus

The UltraShield™ Plus magnets represent the latest and most advanced technology ever developed. These actively shielded magnets provide the smallest stray field and the greatest immunity to external field transients, in combination with the highest performance.

Electromagnetic Disturbance Suppression (EDS)

Our EDS technology achieves the highest level of shielded performance by simultaneously reducing both the stray field and the influence upon magnet stability of external electromagnetic field disturbances.

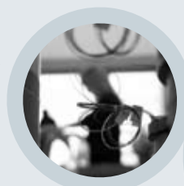

NMR Probes

Solids Probes

Our comprehensive range of the most advanced solids probes are ideal for inorganic and biological samples using experiments such as CP, d.CP, MQMAS, or REDOR.

Maximal spinning rates are 70 kHz for the ultra-high speed 1.3-mm MAS probe for materials science, 30 kHz for the 3.2-mm triple-resonance E^{free} MAS probe for protein research, and 15 kHz for the 4-mm HR-MAS probe with Z gradient for metabolomics studies.

X Observe Probes

These probes are optimized for observation of X-nuclei. They are available in selective or broadbanded versions for double, triple and quadruple resonance experiments, including automated tuning and matching.

^{1}H Inverse Probes

The inner coil of these versatile probes, in multinuclear or selective configuration, is fully optimized for ^{1}H observation at highest sensitivity with optimal lineshape. The available configurations and choices of X-nuclei are identical to those for X Observe Probes.

BBFOplus SmartProbe

Inverse MicroProbes

For highest ^{1}H sensitivity per mole of substance, e.g. in natural products applications, Bruker BioSpin offers 1- and 1.7-mm ^{1}H/^{13}C/^{15}N fixed-frequency probes.

BBFO^{plus} SmartProbe™

Bruker BioSpin's new BBFO^{plus} SmartProbe™ delivers highest sensitivity on both the multinuclear and proton channel. The SmartProbe design exclusively features a broadband frequency channel enabling fully automated applications on protons and the widest range of X-nuclei. This unique probe technology enables fluorine applications including ^{19}F observe with ^{1}H decoupling and vice versa.

BBFO^{plus} SmartProbe Applications with X-nuclei

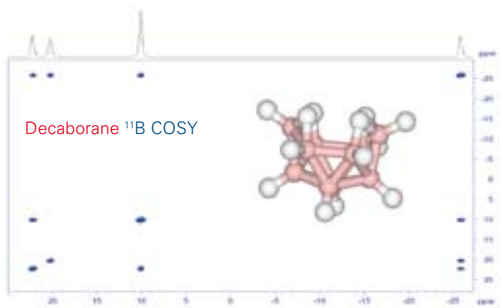

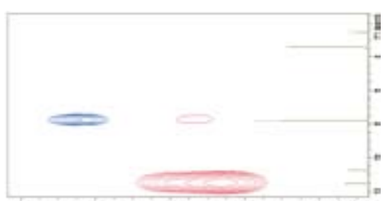

Comparison of the 19F, 1H HOESY and HMBC experiment. While the HOESY spectrum has a correlation to the proton of the heterocycle, the HMBC shows a correlation to the NH protons.

CryoProbes

CryoProbe™ technology has delivered the single largest increase in detection sensitivity ever achieved in the evolution of NMR equipment. The factor 3-4 jump in sensitivity allows the use of correspondingly smaller sample quantities that are impractical with conventional probes, or enables the user to increase sample throughput up to 16-fold.

Product Lines

Bruker BioSpin offers the largest range of CryoProbe configurations from 400 MHz to 1000 MHz, including proton optimized probes such as our 1.7- and 5-mm inverse triple-resonance probes, as well as 10-mm dual ^{13}C observe probes.

The 1.7-mm Micro-CryoProbe offers an increase in sensitivity per mole of more than an order of magnitude compared to a conventional 5-mm probe. For optimal X-nucleus detection we offer the 5-mm Quad CryoProbe in ^{13}C/^{31}P/^{19}F/^{1}H and ^{15}N/^{13}C/^{31}P/^{1}H versions. All high-resolution CryoProbes are equipped with a ^{2}H lock and a Z-gradient. A ^{1}H micro-imaging CryoProbe is also offered to enhance the study of sample structure and properties in the micrometer range.

QCI CryoProbe

CryoPlatform

Every CryoProbe is interfaced with a fully automated universal CryoPlatform™, which controls the closed-cycled cooling system and guarantees excellent stability during experiments of any length. Once a CryoProbe is in the cold state it is just as easy to use as a conventional probe. The temperature of the sample, while just millimeters away from the cold RF coils, is stabilized at a user-defined value within the usual accessible range.

Nitrogen Liquifier

The Bruker Smart Nitrogen Liquifier (BSNL) is an accessory that uses the extra cooling capacity of the latest generation CryoPlaform™ to re-condense the evaporating nitrogen gas from the magnet dewar. While standard magnets have a nitrogen refill interval of 2–3 weeks, the new BSNL greatly extends this time or even makes refilling unnecessary.

QCI CryoProbe: Protein Research

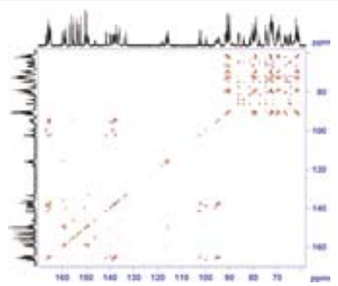

2D ^{13}C observe TOCSY with ^{31}P & ^{15}N & ^{1}H decoupling, 4 mg ^{15}N/^{13}C labeled RNA 14-mer, experiment time 40 min.

QCI CryoProbe: Small Molecule Applications

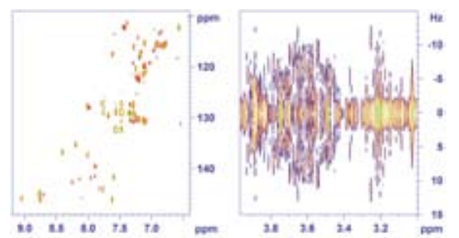

2D J-RES aliphatic region. Sample: 350 ml unbuffered male urine in shaped sample tube.

TopSpin

TopSpin™ is our market leading software package for acquiring, processing and analyzing NMR data. TopSpin was designed as a highly intuitive interface for Windows® and Linux® users, utilizing the widespread standards from word processing, graphics, or presentation programs and providing the same convenient look-and-feel for your NMR applications.

Features

- Available for Windows® or Linux® PC
- New Flow User Interface consistent with latest PC standards, the perfect solution for both beginner and expert
- Individual user customization (fonts, colors, menus, toolbars, commands)
- Comprehensive on-line-documentation for both the software and its applications
- Support tools for regulatory compliance (audit trailing, electronic signature)
- Flexible licensing for various usage, including student license

Data Evaluation

TopSpin provides a wealth of data processing visualization and administration features, including:

- Comprehensive set of functionalities for dealing with 1D to 5D data including automatic forward/backward or delayed linear prediction
- Inverse Fourier transform processing of rows, columns, planes and subcubes of nD datasets
- Interactive and automatic multi-dimensional peak picking and integration.

One can automatically process series of data sets, import a variety of NMR data formats, and administer groups of data sets to manage projects. The experienced user can write TopSpin extensions in C or Python, including graphic displays. TopSpin includes, as an option, a small molecular structure elucidation suite with automatic spectra analysis, isomer generation and shift prediction-based structure rating.

TopSpin User Interface

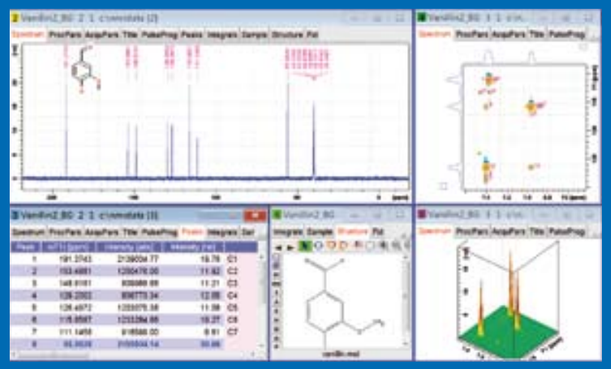

Automation

AVANCE™ NMR systems meet the most demanding of automation needs by streamlining every aspect of NMR analysis, including sample submission, sample preparation, automatic probe tuning, data acquisition, processing, data distribution and archiving. Depending upon the laboratory's needs or goals, automation may involve high-throughput screening, overnight automation or multi-user open access.

ICON-NMR

This productivity tool excels whenever large numbers of samples are submitted for standardized experiments, or when many users access the spectrometer. ICON-NMR™ supports sample changers and sample preparation robots. The user can set up or supervise measurements remotely via a Web browser from a desktop or pocket PC.

SampleJet

The SampleJet™ changer for 300-700 MHz NMR systems offers both high-throughput as well as individual sample capabilities in a single NMR sample changer. Its versatile design can accept samples from five 96-position racks, allowing batch analysis of up to 480 tubes. In addition, the SampleJet easily accepts single tube samples via a separate carousel that can hold up to forty-seven 1-, 1.7-, 3- and 5-mm tubes.

B-ACS 60/120

The Bruker Automatic Sample Changer (B-ACS) provides dialog-guided steps which allow the user to easily and effectively perform automatic (continuous) experiments on most 300-950 MHz systems. Bruker offers the B-ACS™ in 60- or 120-sample versions for 1–10-mm sample tubes with random sample shuffling, optional bar code reader for sample identification, and individual sample temperature control with an optional sample heater.

ICON-NMR

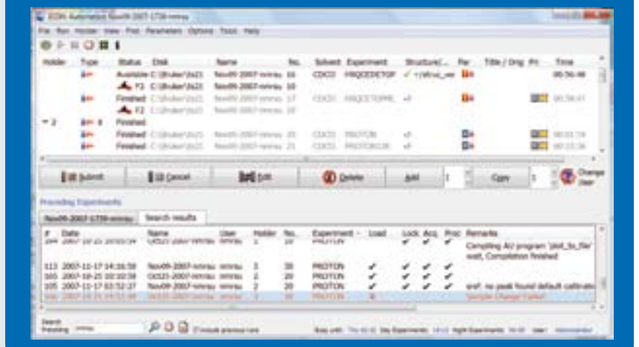

Metabolic Profiler

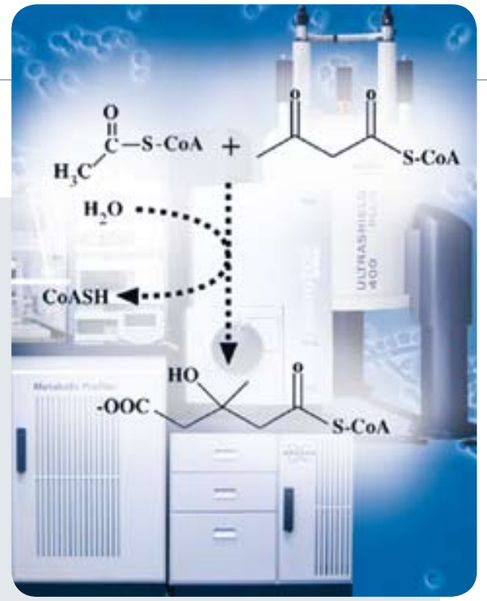

Metabolic profiling and finger printing is a key process in the pharmaceutical industry for studying drug efficacy or toxicology. In clinical research, metabolic profiling helps to identify biomarker compounds for early disease detection and monitoring, and enables researchers to study the effects of drugs in biological systems in a rapid and robust method.

Integrated Analysis

The Metabolic Profiler™ is a dedicated, integrated LC-NMR/MS solution for metabolic analysis featuring an AVANCE NMR spectrometer and a micrOTOF-Q II™ from Bruker Daltonics. This system provides a simple, easy to use and inexpensive base to acquire the spectroscopic data needed for basic metabolic profiling. The system delivers the integration of automated sample handling, acquisition, collection and archiving of your data, and enables the comparative and statistical analysis needed for your research.

Data Management

SampleTrack™ is an Oracle® based information system, which utilizes SQL tools for organizing, searching and archiving sample information, which can simplify experimental control of large sample sets.

Analysis with AMIX

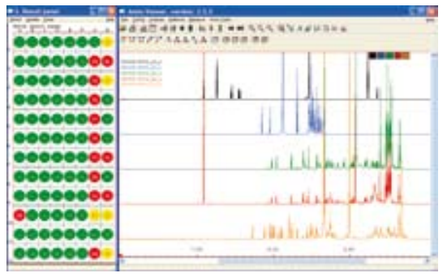

AMIX™ analyzes data and is linked to the Spectral Database for further comparative analysis.

Statistical Analysis

The AMIX program provides a comprehensive range of powerful tools that enable statistical and spectroscopic analyses of both your NMR and MS data. AMIX features Pattern Match - which can define spectral patterns in multiple ways and project these to spectra. In addition, the Multi-Integration features can be used to identify and quantify metabolites in complex mixtures.

Reference Compound Spectral Database

The most complete metabolite NMR spectral database available which contains over 12,500 spectra of the most common endogenous metabolites. By taking into account the effects of pH, field strength and by using one as well as two dimensional NMR data, the database enables the assignment of metabolites in biofluids, cell extracts and tissues in a unique and unambiguous way. With the database linked to AMIX this allows for automatic investigations, such as matching to mixture spectra. Direct integration into statistical data evaluation is also possible.

Hyphenation

Major tools for small molecule research and mixture analysis include HPLC, SPE, NMR and MS. Bruker offers hyphenated systems to meet various research needs. While NMR can be used to investigate the complete mixture, LC-NMR can analyse the individual compounds separated by the chromatography. Such an LC-NMR interface could easily be added to the Metabolic Profiler thereby also enabling hyphenated LC-(SPE)-NMR(/MS) applications. By combining the structural resolving power of NMR for the separated compounds with the mass accuracy of the micrOTOF, we can offer the most complete system for structural analysis available today.

LC-(SPE)-NMR

Two different methods for coupling are possible: Either by coupling the chromatography system directly to the NMR spectrometer, or by the intermediate collection of the samples. Direct coupling can be performed as stopflow or on-flow analysis. For intermediate collection loop-storage or collection on solid phase extraction(SPE)-cartridges is possible. The use of SPE provides an efficient interface between chromatography and NMR even enabling the analysis of low level metabolites.

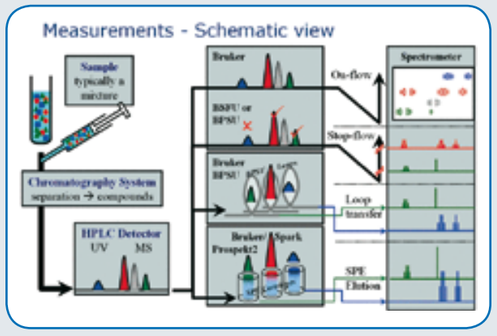

Hyphenated system including sample preparation, NMR, LC and MS

LC-SPE-NMR-MS Results

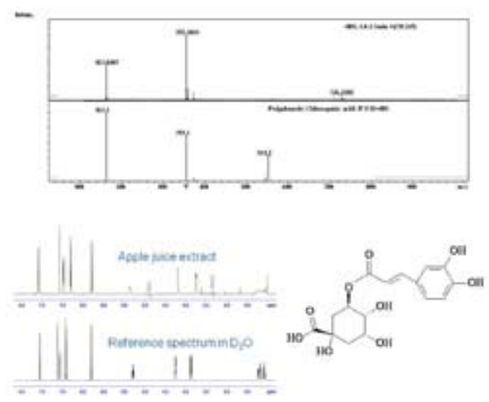

LC-(SPE)-NMR-MS of Apple Juice high resolution mass spectra from m/z 355.1034 (upper part) of chlorogenic acid and the comparison with ion trap library (lower part)
^{1}H NMR spectrum of chlorogenic acid and the comparison with reference compound commercially available.

Sensitivity Boost for Biomolecular NMR

263 GHz AVANCE™ III Solid-State DNP-NMR Spectrometer

Bruker BioSpin's 263 GHz AVANCE DNP-NMR Spectrometer is the world's first commercially available solid-state DNP-NMR system. The 263 GHz spectrometer enables extended DNP solid-state NMR experiments, delivering unsurpassed sensitivity for exciting new applications. Signal enhancements from a factor of 20 to 80 are possible on a wide range of samples, with ongoing system optimization delivering even higher DNP efficiency. The new high-power gyrotron system, powering microwaves at 263 GHz, is robust, safe and easy-to-use, enabling long term DNP experiments without time limits. Experiments are performed at a low temperature of ~100 K using Bruker's innovative low-temperature MAS probe for sample polarization in-situ, directly at the NMR field.

DNP-Enhanced CPMAS of ^{13}C-Proline

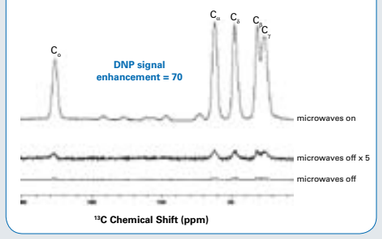

Features

- Turn-key solution for DNP-enhanced solids NMR experiments at high-field
- Polarization enhancement yields up to a factor of 80 gain in sensitivity for solid-state NMR
- Unique high-power (25 W) 263 GHz microwave source
- Easy-to-use software-controlled high-power gyrotron (9.7 T)
- Optimum beam propagation to the sample ensured by microwave transmission lines
- New low-temperature MAS probe technology with built-in waveguide and cold spinning gas supply
- AVANCE III 400 wide-bore NMR system

DNP-Enhanced Experiments

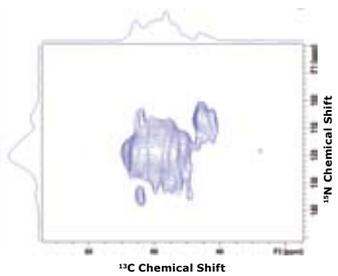

DNP-enhanced NMR experiments on ^{15}N Proteorhodopsin (WHYIF-reversely labeled) with 10 mM TOTAPOL. 6 mg of sample in 3.2 mm rotor. 8 kHz MAS at 105 K. ^{15}N-^{13}C NCA correlation experiment to natural abundance ^{13}C. ^{15}N Proteorhodopsin (WHYIF-reversed labeled), 6 mg, 10 mM TOTAPOL. 40 hour experiment time.

Microwaves on continuously. Sample courtesy of L. Shi, E. Lake, L. Brown, V. Ladizhansky, University of Guelph

Complete Molecular Confidence

Complete Molecular Confidence™ (CMC) is a unique, fully integrated NMR-LC/MS-X-ray based solution delivering on-the-fly molecular formulae determination and automated structure verification for small molecules and natural products. This novel solution can deliver publication quality results and high-confidence, analytical support for chemical synthesis, reference library screening, and verification.

Complementary Modalities

CMC incorporates Bruker's complementary analytical techniques; NMR and X-ray for structure verification, MS for molecular formula determination. Analysis is based on data combined from all techniques which results in higher reliability and robustness in high-throughput library screening of small molecules.

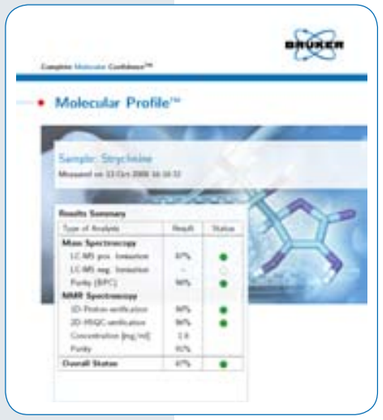

Molecular Profile

CMC yields the Molecular Profile in the form of a compact report, detailing metrics for the quality of the fit of the molecular formula, as well as any other sum formula candidates. It delivers a probability for the verification of the proposed molecular structure, purity information and approximate quantity of the sample.

Features

- Automated molecular formula determination and structure proposals by electrospray mass spectrometry using SmartFormula3D
- Fast and automated structure verification by Nuclear Magnetic Resonance
- Optimum confidence for small molecule characterization
- Unique tool for compound library screening
- Identification of impurities
- Enhanced productivity for synthetic chemists
- Quantitation of compounds
- Combines Bruker's AVANCE™ III NMR and micrOTOF-Q™ II MS cutting edge technologies
- Automated structure determination using novel X2S Crystal-to-Structure X-ray system (optional)

JuiceScreener

The JuiceScreener™, combined with its SGF Profiling™ technique, can deliver huge amounts of information derived from one single experiment, instead of multiple individual analysis steps. This provides higher throughput and reliability than conventional techniques, leading to a significant reduction of cost per sample. This enables up to 5 times more sample investigations with no change in budget, resulting in an improved and more comprehensive quality control screening.

Push-Button Routine

SGF Profiling is a fully automated push-button routine that needs no interaction from the operator. From sample bar code registration, preparation and handling, to data acquisition and statistical evaluation, all steps are under the control of SampleTrack™, Bruker's laboratory information system.

Spectroscopic Database

The screening is based on an extensive spectroscopic database that includes thousands of NMR spectra from mainly authentic juices. Currently the data base includes about 40 different fruit types from more than 50 production sites worldwide. In addition, the database also provides access to hundreds of small molecule compounds for further analysis of unknown ingredients.

Features

- Fully automated push-button NMR solution including evaluation and reporting
- Simultaneous absolute quantification of all relevant organic ingredients for juice assessment
- High-throughput with minimal sample preparation
- Reduced cost per sample
- Reliable screening method providing targeted and non-targeted multi-marker analyses
- Enables the detection of unexpected fraud
- Screening is based on an extensive NMR spectroscopic database of more than 3000 reference juices, obtained from production sites all over the world
- Complex statistical models enable the analysis of: origin authenticity, species purity, fruit content, false labeling, production process control and sample similarity

Origin Authentification of Orange Juice

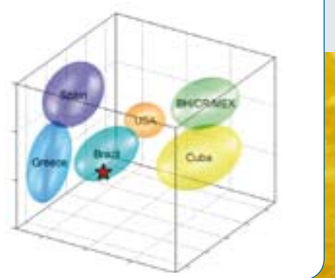

Immediate Access to Latest Technologies

Contract Bruker Analytical Services

Everyone can now benefit from Bruker's latest technologies and instrumentation, and unmatched experience in analytical applications. We offer supporting services that include advanced high-resolution NMR and mass spectrometry applications. Our customers can benefit from access to the latest developments in the field through Bruker's cooperations with academic and industrial research labs. Our experts can also assist you with special customized projects.

Benefits

- Short and long term support increases project handling capacity
- Latest, most advanced Bruker technologies
- Unique analytical expertise and knowledge
- Method development and feasibility studies

Advanced NMR Services

- Structure verification and elucidation
- Reaction and purity control
- Quantitative analysis
- Variable temperature experiments
- Screening methods for pharmaceutical and clinical research
- Food quality control
- Metabonomics studies
- Natural product analysis

Additional Analytical Services

- Mass Spectrometry & Imaging
- EPR (ESR) Spectroscopy
- TD (Time Domain) NMR Spectroscopy
- X-ray Diffraction, Crystallography & Fluorescence
- FT-IR Spectroscopy & Microscopy
- Raman Spectroscopy & Microscopy
- HPLC

Customized Projects

When additional measures are needed, our technical experts will discuss the range of special capabilities available to you. Whether it is a short term project where specialized equipment is a necessity, method development is required or feasibility studies are needed, we can help you with our extensive resources.

Ultra-High Field NMR

AVANCE™ 1000 System with CryoProbe™

Bruker BioSpin launches a breakthrough one Gigahertz Ultra-High Field AVANCE 1000 MHz NMR spectrometer. It incorporates the world's first 23.5 Tesla standard-bore (54 mm) superconducting NMR magnet. The high-field strength and high-field stability, in combination with the first 5-mm triple-resonance CryoProbe, enables unique 1 GHz NMR applications.

Bruker is proud to be able to deliver such an outstanding instrument to NMR researchers who wish to push the frontiers in biochemistry, structural biology and molecular research areas. The first Avance 1000 system was installed to the new 'Centre de RMN à Très Hauts Champs' in Lyon, France in July 2009.

- World's first standard-bore, high-homogeneity 1 GHz NMR magnet
- Persistent superconducting magnet
- UltraStabilized™ sub-cooling technology
- Magnetic field strength of 23.5 Tesla
- Proton NMR frequency of 1000 MHz
- Standard bore size of 54 mm

Combination of 1 GHz and CryoProbe

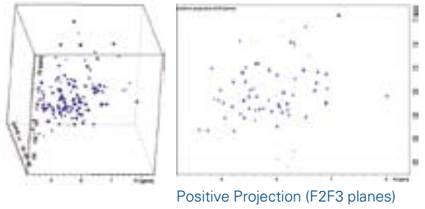

Positive Projection (F2F3 planes)

3D TROSY-HNCA - Fast Acquisition: non-uniform sampling mode, 10% sparse matrix (10% of regular sampled data points actually recorded), MDD Processing (Orekhov et al.), experimental time: 80 min.

Solid-State NMR at 23.5 T: ^{11}B MAS

Sodium-Borosilicate Glass (8 mol% Na_2O / 31 mol% B_2O_3 / 61 mol% SiO_2)

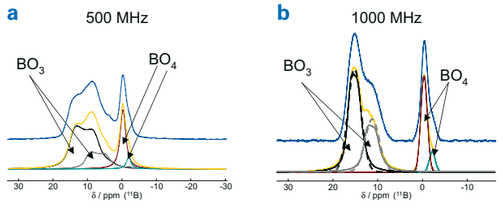

Spectra of a sodium borosilicate glass at 11.7 T (500 MHz, **a**) and at 23.5 T (1000 MHz, **b**) and their spectral deconvolution. The 23.5 T spectrum clearly shows markedly enhanced resolution. Gaussian line shapes suffice to compose the spectrum, indicating that in contrast to the 11.7 T spectrum almost no residual second order broadening is visible.

Biological Solid State NMR

TL_2 and E^{free} and 1.3mm MAS product lines

The so-called BioSolids probe product line is based on one of two technologies, TL_2 or E^{free}. For optimum performance these probes are configured as fixed frequency triple resonance probes, most often requested for proton, carbon and nitrogen. TL_2 probes yield the best overall sensitivity with high ^{1}H sensitivity for inverse detection experiments.

700 MHz CPMAS Applications

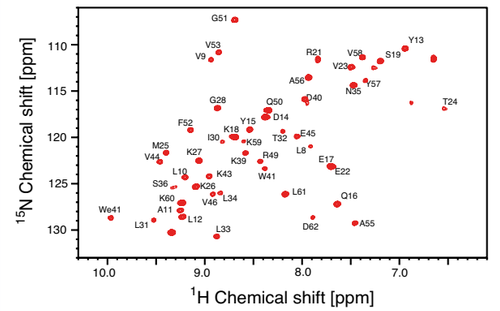

^{15}N -^{1}H inverse detected solid state NMR experiment on SH3. Data kindly provided by Bernd Reif (V. Chevelkov, K. Rehbein, A. Diehl and B. Reif, Angew. Chem. Int. Ed. 45: 3878-3881 (2006)

E^{free}

E^{free} probes are specifically designed to minimize RF heating. The two coil configuration provides enhanced sensitivity for ^{13}C and ^{15}N and the highest tuning and matching stability for safe, long term experiments. Minimized RF heating ensures the integrity of your protein, even while operating at room temperature.

TL_2

TL_2 technology is the choice when high-decoupling fields are needed for optimum decoupling in J-coupling based experiments and when sample heating is not an issue. TL_2 probes are best used for dry and non-salty samples, or samples that are kept in a frozen state.

1.3-mm MAS

The 1.3-mm probe product line provides the highest spinning speeds coupled with high-sensitivity and RF fields. Where sample heating might become an issue, convenient low power decoupling can be employed.

500 MHz CPMAS Applications

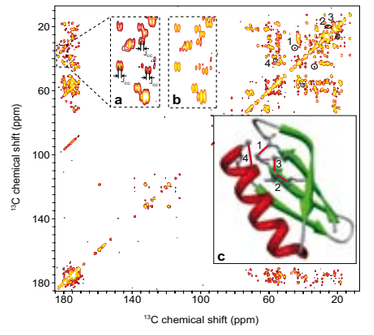

2D ^{13}C-^{13}C PAR correlation spectra of [U-^{13}C, ^{15}N]-GB1 obtained at nr= 65 kHz and no (^{1}H) = 500 MHz with 10 ms PAR mixing. Panel (c) illustrates some of the representative long distance contacts that are observed in an experiment with 10 ms PAR mixing. The crosspeaks corresponding to the contacts in panel (c) are circled and marked with numbers in the spectrum.
(Lewandowski et al, J. Phys. Chem. B, 2009, 113 (27), pp 9062-9069)

Small Molecule Analysis

TopSpin™ Structure Verification

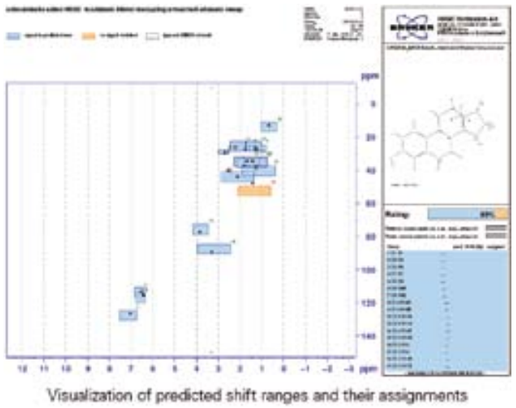

Visualization of predicted shift ranges and their assignments

The automatically generated plots provide a quick overview on the consistency of structure and spectrum leaving the specialist free to focus on evaluation.

Bruker's HSQC structure verification aid is based on a 1D proton and carbon prediction. The prediction generates an error bar for each calculated chemical shift, whose size depends on the accuracy with which the shift can be predicted. In an HSQC, when the structure used for the prediction fits the spectrum, this will result in areas that contain the cross signals of the acquired spectrum.

A plot that shows spectrum, structure and predictions is automatically generated. With this readily accessible information, the spectroscopist can decide whether or not the structure fits the spectrum.

Quantitative NMR - CMCQ

In drug discovery, the majority of expensive, false positive screening results originate from erroneous assumptions regarding the concentrations of screening compounds. NMR has been proven superior to other typical methods used for concentration determination.

Bruker provides a complete, highly automated workflow for determining NMR-based high-quality concentrations. Analysis proposals are presented in an intuitive GUI that automatically generates concentration reports for entire well-plates.

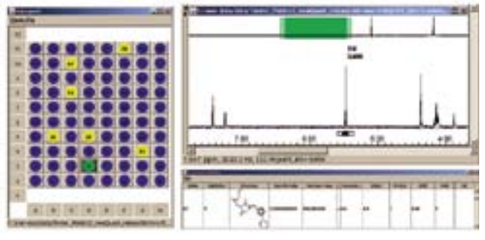

Intuitive GUI for manual control of automatically generated CMCQ results

Structure Elucidation

TopSpin™ Structure Elucidation

The elucidation of molecular structures from NMR data is a common and often tedious task. Bruker BioSpin is implementing a set of tools in TopSpin to facilitate this task. Starting from a chemical formula and common NMR experiments, peaks are automatically selected and entered into a correlation table. This information is then interpreted by a structure-determination algorithm and structures consistent with the data are generated. These structures can then be ranked in accordance to comparison with chemical shift predictions, thus narrowing down the possibilities, assisting the researcher in determining their structure.

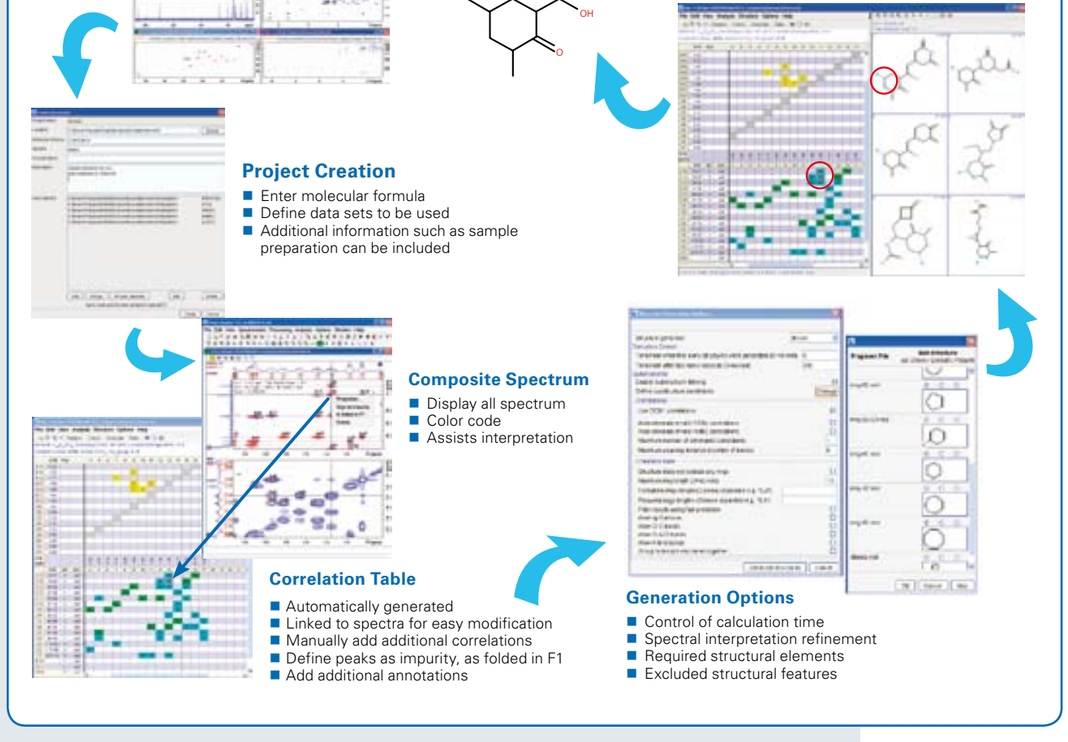

Analysis of Natural Products

High-Performance NMR Solutions

Recent advances in Bruker's NMR technology now deliver the high-performance solutions necessary to address the complex structural questions confronting natural products researchers. Improvements in probe design and receivers provide the highest NMR sensitivity available on the market. These hardware developments, in combination with our new software packages, provide the perfect complement of tools for optimizing your productivity and making new discoveries.

Screening

Bruker software and hardware assists in both of these processes by providing the automation, the instrument stability and the analysis capabilities needed to complete these tasks on both pure materials and complex mixtures. Any spectrum may be added to spectral data bases for rapid comparisons with new samples to determine sample similarities and differences. Analysis capabilities enable the user to find known compounds or fragments, categorize spectra, and find unique NMR spectra.

Screening

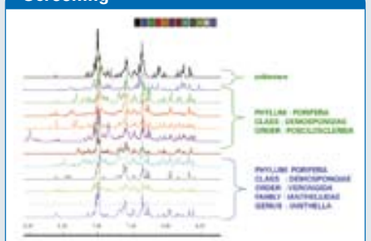

AMIX MATCH successfully classified the unknown natural product extract sample to the proper taxonomy using a user generated spectral base linked with known taxonomy data. Spectra and taxonomy data kindly supplied by Cherie Motti, AIMS, Australia.

Sensitivity

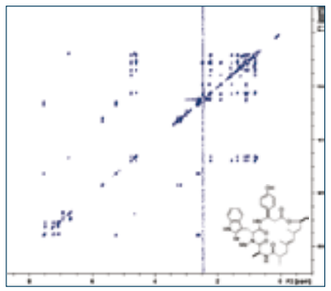

25 µg of Jaspamide isolated from sponge acquired in $CDCl_3$ on a 1-mm MicroProbe at 700 MHz. ^1H TOCSY spectrum acquired using 32 scans. Total acquisition time 2 hours 15 min. Sample was kindly provided by Tadeusz Molinski, UCSD.

Mixture Analysis

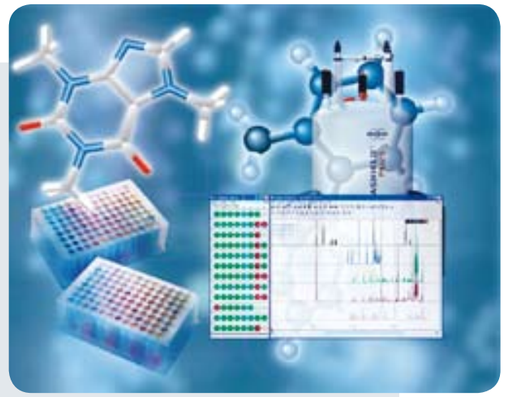

AMIX™ is a unique and powerful software tool which facilitates and automates the comparative analysis of large sets of spectra for a variety of chemical, biological and medical applications; e.g. the analysis of complex mixtures, detection and quantification of metabolites in body fluids, structure verification in combinatorial chemistry (AutoDROP™) and parallel synthesis, and assessment of protein-ligand binding assays.

Study of Protein-Ligand Interaction

Peak tracing in set of HSQC spectra enables the study of protein-ligand interaction.

Statistics

The available statistical methods include PCA and co-variance analysis to study hidden phenomena in ensembles of spectra, model building and classification to test if new spectra fits a given set of spectra, and PLS to correlate ensembles with external information. Multiple window techniques allow various AMIX tools to be linked and provide unsurpassed interaction between statistics and spectroscopy.

Spectra Bases

AMIX can be used to manage and manipulate so-called user-expandable spectra bases, containing 1D and 2D spectra in an optimally compressed format which retains the full information content of the original data.

Sophisticated routines are included for searching the spectra bases, for displaying results, and for preparing the data for statistical or correlation analysis.

Data Visualization

A powerful front end to AMIX is the AMIX-Viewer, a multiple-object viewer which offers unequaled display and analysis capabilities with direct access to data from flow-injection NMR and hyphenated techniques. Thus, 1D, 2D, and 3D NMR data sets, molecular structures, MS and MS^n data, UV absorption and chromatogram data can be readily visualized and correlated in an efficient manner.

AMIX software package

High-Performance Power Supplies

High-Voltage Power Supplies

Bruker high-voltage power supplies find their main applications in IOT- and Klystron based RF transmitters in Particle Physics. Our power supplies provide high-voltages of up to 50 kV at broad range, from 1 kW up to several Megawatts. The compact solid-state design is based either on the latest switch mode technique or, in the case of highest power applications, based on SCR (Thyristor) control.

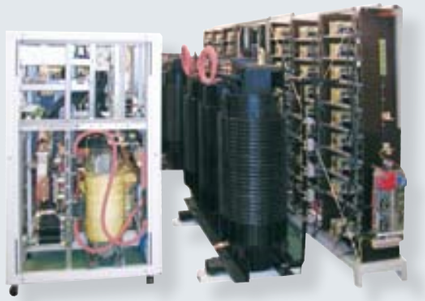

Klystron power supply for the MAMI C race track microtron, Mainz University, Germany.

High-Current Power Supplies

Bruker high-current power supplies are employed in industry and particle physics research worldwide. Our high-current power supplies, available for pulsed or DC, monopolar, bipolar or four-quadrant operation, deliver high-currents of up to 30.000 A. Based on the latest switch mode technology they ensure optimum efficiency and enable stand-alone, fail-safe operation. The option of linear mode regulation provides maximum stability and minimum noise and fluctuations from 1% to better than 1 ppm (part per million).

For high power applications, our high-current power supplies benefit from SCR (Thyristor) control. We offer single- and multi-channel supplies starting in the 100 Watt range going up to several Megawatts.

RF Transmitters

Bruker Radio Frequency Transmitters are established in nuclear physics applications all over the world. Our high-voltage power supplies, capable of emitting power from 100 Watt up to 300 kW and more, benefit from modern switch mode design for optimum efficiency and feature SCR (Thyristor) control to handle the highest power applications.

Choose from single or stacked solid-state amplifiers, whilst IOT amplifiers deliver optimum peak power conversion efficiency.

For arc protection our emitter tubes operate with defined stored energy, with optional solid-state crowbar circuits to protect the sensitive elements.

Start-up and operating procedures are handled automatically ensuring stand-alone, fail-safe operation, while a solid-state safety system ensures maximum protection for the transmitter elements and the user applications.

RF IOT high-power transmitter at ELBE FZD Rossendorf, Dresden, Germany.

Content:

MRI Products

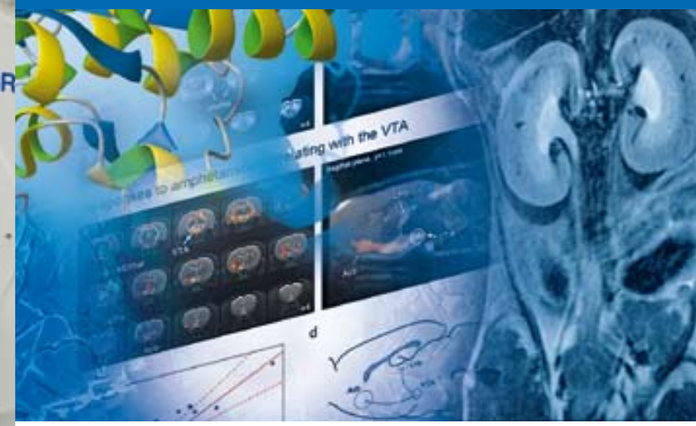

Magnetic Resonance Imaging

Solutions for Molecular Imaging and Preclinical Research

think forward

BioSpec

The BioSpec® series is designed for the emerging market of preclinical and molecular MRI. State-of-the-art MRI CryoProbe™ technology together with ultra-high field USR magnets deliver high-spatial resolution *in vivo* enabling customers to come closer to the molecular and cellular level. Thanks to its innovative modular concept, virtually any small animal MR imaging application in life science, biomedical and preclinical research can be conducted. Whatever your application is, the BioSpec series will deliver the optimum solution, will perfectly equip you for the most demanding tasks and challenges.

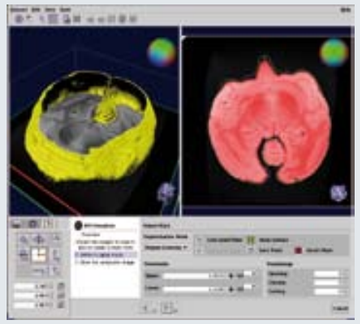

Standard and optional Product Features

- High-end UltraShield™ Refrigerated (USR) magnets from 4.7 up to 11.7 Tesla
- A wide range of bore sizes (16 to 40 cm) for investigations on any kind of animals
- Helium zero-boil-off and nitrogen free magnets for reduced service costs
- Scalable AVANCE III architecture with up to 16 receiver and 6 transmitter channels
- Parallel imaging (GRAPPA) for almost all applications including EPI
- Multiple transmit imaging applications
- BGA-S gradients with highest amplitudes, slew rates, shim strengths, and duty cycles
- Motorized animal positioning for increased throughput
- IntraGate™ - Self gated steady-state cardiac imaging (no external triggering devices)
- Phased-array RF coil technology for maximum sensitivity and minimum scan times
- MRI CryoProbe™ delivers an exceptional increase in sensitivity to 250 %
- ParaVision® - Intuitive software package, for multi-dimensional MRI/MRS data acquisition,reconstruction, analysis and visualization

Innovative Animal MRI Solutions for Molecular and Preclinical Imaging

BioSpec benefits from the excellence of Bruker BioSpin, the global market and technology leader in analytical magnetic resonance instruments including NMR, preclinical MRI and EPR. With an install base of over 500 MRI systems worldwide and more than 40 local Bruker offices on all continents, you can rely on our long term expertise and dedicated after sales support.

DTI of the Song Control System (SCS) of Starlings

DTI is used to quantify seasonal changes in the SCS. The density of axonal connections changes under hormonal influences.

Courtesy: De Groof, A. Van der Linden, RUCA, Antwerp, Belgium.

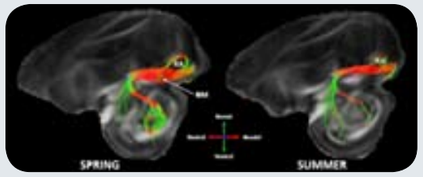

Cardiac Angiography

Visualization of coronary arteries in vivo (mice) using IntraGate.

Mouse Abdomen

T2 RARE abdominal mouse imaging with excellent contrast.

Courtesy: D. Elverfeldt, B. Kreher, J. Hennig et al., University Hospital Freiburg, Germany.

ClinScan

With the ClinScan® you enter the field of translational research and molecular imaging. The ClinScan, a 7 T animal MRI and MRS scanner is designed to further facilitate translational research from 'mice to men' in the field of pre-clinical and molecular imaging.

ClinScan is Bruker BioSpin's solution for an emerging market of research MRI systems that allows a direct and fast transfer of preclinical studies on animal models to clinical studies on humans.

By virtue of the strategic alliance with Siemens Medical Solutions on human high-field MR systems, ClinScan uses the clinical user interface *syngo*® MR. Its operation is identical to that of Siemens MAGNETOM TIM systems.

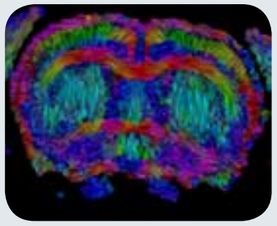

DTI tractography of rat brain

Product Description

- 7 T Bruker USR magnet (Ultra Shielded Refrigerated, bore size 20 cm or 30 cm)
- Bruker gradient and shim coil (gradient strength of 290 mT/m or 630 mT/m, slew rate of 1160 T/m/s or 6300 T/m/s)
- Bruker RF array coil technology in combination with numerous animal handling accessories
- Siemens MAGNETOM Avanto technology with up to 32 receive channels
- Clinical routine user interface *syngo* MR to enable efficient workflow and highly automated state-of-the-art MRI and MRS applications on small animals

Multi Modality Imaging - MRI/PET

Simultaneous in-vivo imaging of a F-18-FDG labeled mouse heart at 7 T. PET and MRI acquisition was done in parallel without interference between the two modalities.

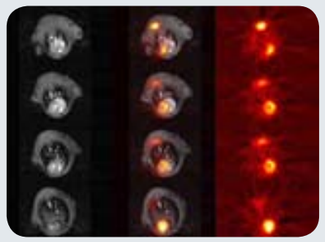

Courtesy: B. Pichler, H. Wehrl, M. Judenhofer et al., Laboratory for Preclinical Imaging University Tübingen, Germany

ClinScan systems are designed for translational molecular MRI and provide the clinical routine user interface *syngo* MR that facilitates straightforward transfer of protocols from benchtop to bedside and vice-versa

Small Animal MRI Solution for Molecular Imaging and Translational Research

Clinical User Interface syngo® MR

- Parallel working and one-click exams are supported efficiently.
- Parallel scanning and reconstruction are standard. Images can be loaded and used for graphical slice planning during reconstruction.
- iPAT (integrated Parallel Acquisition Techniques) further increase the acquisition speed. iPAT is fully compatible with the optional phased array coils.
- Dynamic Analysis evaluation and Mean Curve software allow the calculation of functions and dynamic examinations.
- IDEA sequence development environment with research agreement.

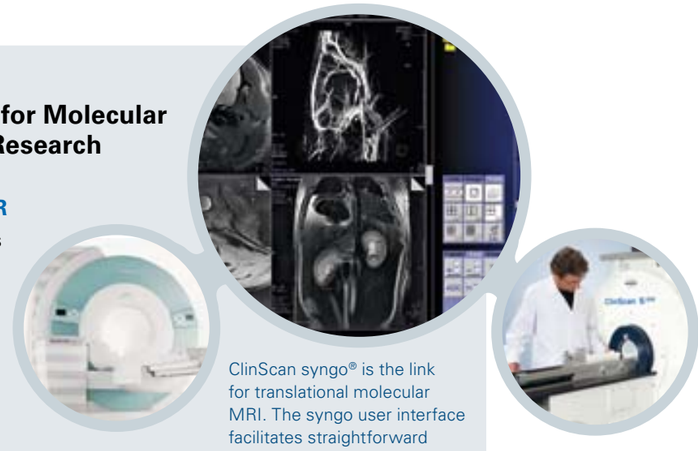

ClinScan syngo® is the link for translational molecular MRI. The syngo user interface facilitates straightforward transfer of protocols from bench top to bedside and vice-versa.

Cardiac Imaging

- True FISP & 2D/3D FLASH segmented
- Magnetization prepared TrueFISP
- Prospective triggering & retrospective gating
- Retrospectively gated cine imaging
- Phase sensitive IR

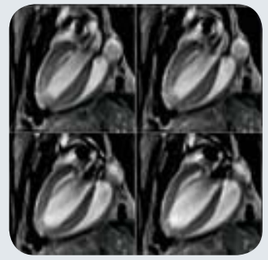

Cine cardiac imaging

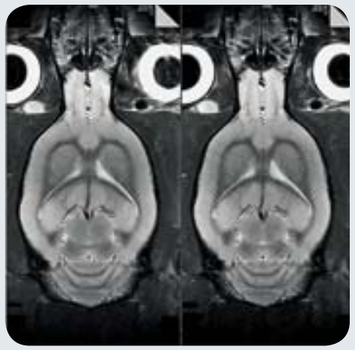

Rat brain, TSE, GRAPPA iPAT, TR: 2 s, TEeff: 45 ms, Resolution: 78 x 78 µm², iPAT factor 1 (left), iPAT factor 2 (right)

PharmaScan

Dedicated MR Scanner for Pharmaceutical, Biomedical and Molecular Imaging Research

The PharmaScan® is a high-field, easy-to-use and at the same time easy-to-install and very cost-effective MR-system. It is designed for MRI applications on small animals such as mice and rats in the field of routine pharmaceutical, biomedical and molecular imaging research. With the integrated automatic image acquisition and analysis, fast and reliable results can be obtained by simple operation of the system by non-academic personnel, without compromising full flexibility for the MR expert.

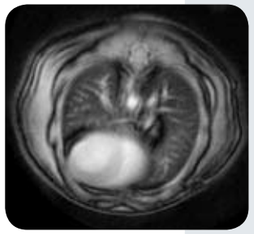

Mouse Lung Imaging using Ultra Short TE (UTE) Imaging

Radial scan with ultra short TE enables the visualization of detailed lung structures without using expensive hyperpolarized helium techniques.

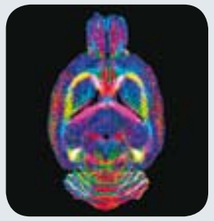

High-Resolution DTI

Coronal map of the major principle diffusion direction of a rat brain. The diffusion tensor imaging, with 30 diffusion directions, is acquired by the segmented echo planar imaging technique.

Standard and optional Product Features

- ^{1}H MRI and MRS routine system, optimized for small rodents (such as rats, mice, gerbils)
- Actively shielded magnets at 4.7 T and 7 T allows easy and cost-efficient siting
- 16 cm clear bore size with 72 mm free access for the animal
- Parallel imaging (GRAPPA)
- High-performance BGA-9 or BGA-9S (as an option) gradients with highest amplitude, slew rates, shim strengths, and duty cycles optimized for small animal imaging
- No Faraday cage required
- 25 m^2 floor space required
- Scalable AVANCE III architecture incorporates up to 4 receivers
- AutoPac™ - Motorized, positioning system for routine animal handling and increased animal throughput
- IntraGate™ - Self gated steady-state cardiac imaging requiring no external trigger devices
- Phased-array RF coil technology for increased sensitivity and reduced scan times
- MRI CryoProbe™ - Sensitivity increase up to a factor of 2.5
- ParaVision® - Fully intuitive software package for multi-dimensional MRI/MRS data acquisition, reconstruction, analysis and visualization

USR™ Magnets

Combining High-Field Magnet Performance with Easy Handling and Siting

The UltraShielded Refrigerated (USR) horizontal bore magnet product line features ultra-high magnetic fields and variable bore sizes in combination with easy handling and siting. Field strengths offered from 4.7 up to 11.7 T deliver optimum sensitivity for high-resolution MRI and MRS. The various bore diameters from 16 to 40 cm ensure optimal experimental performance on a wide range of animal MRI applications. Active shielding based on our well-proven UltraShield™ technology provides minimum stray fields. For ease of operation all USR magnets are nitrogen-free and include helium refrigeration for zero boil-off and minimum service intervals.

Features

- Ultra-high magnetic fields
- Variable bore sizes
- Highest field homogeneity
- Compact magnet design
- Excellent field stability
- Optimum external disturbance suppression
- Minimum stray fields
- Easy and cost efficient siting
- Nitrogen free
- Helium refrigeration (zero boil-off[1])
- Longer service intervals (two years)
- Cold delivery and fast installation
- Over 100 USR installations worldwide

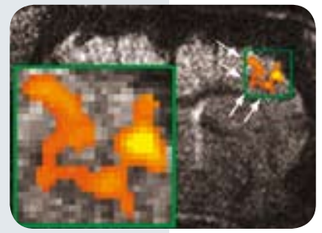

High resolution BOLD activation measured at 11.7 T USR magnet.

Courtesy: J.Seehafer, M.Hoehn, MPI for Neurological Research, Cologne, Germany

USR Magnet Product Line for a wide range of applications

	47/40 USR	70/20 USR	70/30 USR	94/20 USR	94/30 USR	117/16 USR
^{1}H Frequency (MHz)	200	300	300	400	400	500
Field Strength (T)	4.7	7.0	7.0	9.4	9.4	11.7
Bore Diameter (cm)	40	20	31	21	31	16
Length (m)	1.49	1.31	1.49	1.49	2.01	1.46
Width (m)	1.65	1.12	1.65	1.65	1.71	1.65
Height (m)	2.37	2.14	2.37	2.37	2.40	2.37
Field Drift (ppm/h)	<0.05	<0.05	<0.05	<0.05	<0.05	<0.05
Weight (kg)	4.700	2.500	5.200	5.500	11.500	7.000
Stray Field (radial x axial) (m x m)	2 x 3	1.5 x 1.5	2 x 3	2.0 x 3.0	2.3 x 3.3	1.7 x 2.8
Service Interval (year)	2	2	2	2	2	2
Zero Boil-off	Yes[1]	Yes[1]	Yes[1]	Yes[1]	Yes[1]	Yes[1]

USR systems are available with field strengths ranging from 4.7 to 9.4 T and bore sizes of 16, 20, 30 or 40 cm as shown in the table.

[1]With a valid service contract

BGA-S Gradient Series

Maximum Gradient and Shim Performance in Animal MRI

The Bruker gradient series BGA-S™ delivers unsurpassed performance for the whole range of animal MRI applications. The unique design provides highest gradient strengths and slew rates required for high field animal imaging. The high cooling efficency results in unmatched duty cycles and as a consequence of it, modern imaging sequences with minimum field of view and a high number of slices for long experiment times can easily be performed. The integrated shim coils add up to ultra-strong shim capabilities. The BGA-S gradients can be operated as inserts and are easily exchangeable for maximum flexibility.

Specifications

	BGA-6S	BGA-9S	BGA-12S	BGA-20S
Outer diameter [mm]	113	150	198	303
Inner diameter [mm]	60	90	114	200
Strength* [mT/m] at I_{max}	1000	740	660	300
Slew rate* [T/m/s] at U_{max}	11250	6600	4570	1100
Gradient linearity/DSV [% / mm]	± 5 / 35	± 5 / 60	± 4 / 80	± 3 / 130
Number of RT Shims	9	9	9	9
Max. cont. gradient all axis [mT/m each axis]	500	190	210	87
Max. continous gradient one axis [mT/m]	350	130	167	60
U_{max} [V]/I_{max} [A]	300/100	300/200	500/300	500/300

* Output values have been measured on MRI system

Product Description

- Highest gradient strengths up to 1000 mT/m
- Highest slew rates
- Excellent duty cycle specifications
- Very high gradient linearity
- Optimal gradient shielding
- Maximum shim performance

MRI CryoProbe

New Signal-to-Noise Horizons in Small Animal MRI

Bruker now offers a new series of MRI CryoProbes for MRI systems. They feature very low temperature, closed cycle cooled RF-coils and preamplifiers offering an increase in signal-to-noise ratio (SNR) to a factor of 2.5 over standard room temperature RF-coils in routine MRI applications. The use of the MRI CryoProbe in routine imaging of the mouse brain *in vivo* at 9.4 T delivers outstanding image quality. The increased signal-to-noise ratio enables one to acquire high-resolution images of the microscopic structures in the mouse brain down to the cellular level.

Product Description

- Increase in sensitivity to more than 250 %
- Flexible design for easy siting
- Standardized interface allowing different MRI CryoProbes to be used with one cooling system
- Efficient design allows minimal distances between RF-coil and object
- Carefully controlled thermal environment with no cold surfaces in contact with animal
- Cooling down outside the magnet possible

CryoProbe Spine Imaging

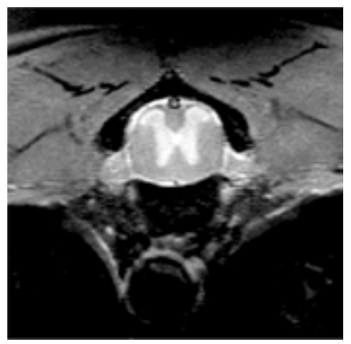

T_2 spine imaging of mouse at 46 µm in-plane resolution, total scan time < 7 min.

Comparison with Nissle staining

Comparison of micro-structures in the mouse cerebellum with histological Nissle staining (left). Identification of anatomical structures like white matter, granular layers, molecular layers and Purkinje cell layers are possible.
Courtesy: Baltes C. et al., ETH Zurich, Switzerland

ParaVision® 5.0

Ultimate MR-Acquisition and Processing in Preclinical Research and Life Science

ParaVision is Bruker's software package for multi-dimensional MRI/MRS data acquisition, reconstruction, analysis and visualization for its BioSpec, PharmaScan and MicroImaging product lines. It offers an intuitive routine user interface and cutting-edge techniques for animal MR imaging and spectroscopy - including a rich palette of powerful image evaluation and visualization tools.

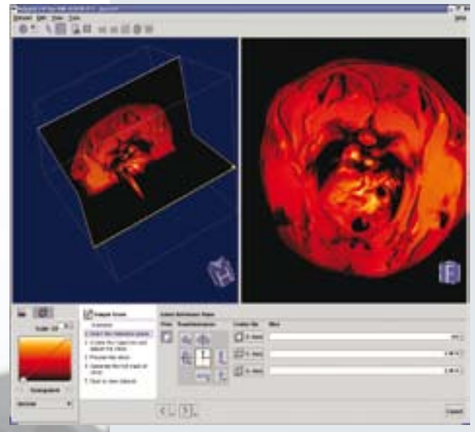

Product Description

- Intuitive routine workflow
- Application-oriented, ready-to-use protocols
- Self-acting, method-specific scanner adjustments
- Automatic instrumentation recognition
- Parallel imaging option for all suitable acquisition techniques with automatic generation of composed images/ spectra
- Half-Fourier (Partial-Fourier) encoding
- Real-time display of acquired and reconstructed data
- Data archiving including DICOM export
- Development environment with powerful tools for rapid prototyping of user-defined experiments and professional method implementation

New Reconstruction and Processing Features

- Push-button GRAPPA reconstruction
- Sum of squares and phase-sensitive phased-array reconstruction
- Phased-array spectroscopy reconstruction
- Partial Fourier reconstruction
- EPI reconstruction with efficient ghost suppression
- Navigator techniques to reduce motion artifacts in EPI and SPIRAL
- 2D and 3D region growing
- Display and analysis of time-course data with the fitting tool "ISA"
- Frame-selective loading of image sequences for display, e.g. either timecourse frames or slices for a multi-slice movie dataset
- 3D visualization with surface rendering
- Image mask inversion

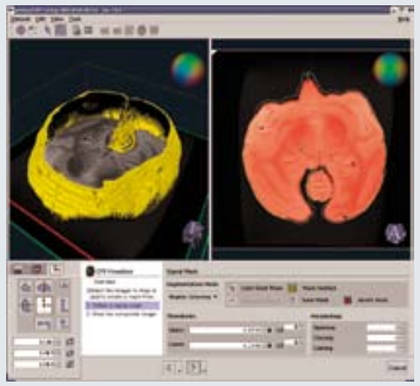

Beyond Standard BioSpecs

Vertical BioSpec

The vertical BioSpec® has been engineered for MR research investigations of non-human primates. It enables specifically fMRI studies on monkeys as they are particularly receptive to behavioral conditioning while sitting in upright position. The vertical BioSpec are offered with two different magnet types operating at 4.7 T and 7 T which both have a high-magnetic field stability and excellent homogeneity. The actively shielded gradient coil with integrated shims is especially designed for a vertically oriented magnet.

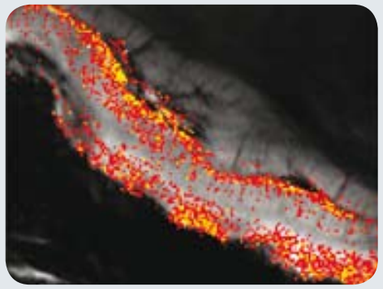

Anatomical and Functional Resolution

fMRI-EPI-image with a resolution of (125 x 125 x 660) μm^3 in the monkey visual cortex. Fine details of the visual cortex (Gen=Gennari Line) including small cortical vessels are visualized. Each BOLD-pixel represents as few as approx. 600 neurons.

Courtesy: N. Logothetis, MPI for Biological Cybernetics, Tübingen, Germany

Ultra-High Field MRI

Bruker BioSpin is offering up to 17 T horizontal MRI BioSpec, enabling high-resolution in vivo preclinical MRI on small animals at a microscopic scale. The magnet with a bore size of 25 cm is based on Bruker's UltraStabilized™ subcooling technology offering excellent field homogeneity and stability.

A new BGA-S™ gradient coil with unsurpassed specifications regarding gradient field strength, gradient slew rate, and gradient duty cycle provides best MRI performance.

These innovations will push the current limits of animal MR imaging towards higher spatial and spectral resolution, enabling new applications in the field of molecular imaging and preclinical research.

Micro-Imaging

CryoProbe for Micro-Imaging

The extension of Bruker BioSpin's cryogenic NMR probe expertise into the field of MRI microscopy leads to new and exciting opportunities. Micro-imaging techniques for small samples with diameters up to 5 mm benefit from CryoProbe technology and a factor 4 improvement in sensitivity. The result is improved image quality, increased spatial resolution and/or reduced scan times. The MIC CryoProbes for ^{1}H at 400-600 MHz offer variable temperature operation over the range from 0 to 80 °C and are used with a Bruker BioSpin Micro2.5 gradient system in vertical wide-bore magnets with bore sizes of 89 mm or larger. The newly developed dual $^{1}H/^{13}C$ micro-imaging CryoProbe is also available.

Research Possibilities

- Investigations on plants, insects and other small animals, embryos, or histological tissue samples.
- Studies of porous and inhomogeneous objects at intermediate field strengths with minimum susceptibility distortions and highest sensitivity.
- Studies of fast dynamic processes.
- Microliter spectroscopy.

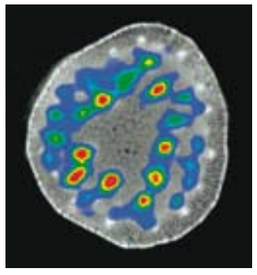

Detection of sugar transport. An Angiocanthos plant was fed with ^{13}C labelled glucose. The C1-^{13}C bound protons (coloured) overlayed to a proton image of the system cross-section C1 α-Glucose (93 ppm (^{13}C), 5.42 ppm (^{1}H)), system field strength 9.4 T, cyclic J cross polarization method in-plane resolution of ^{13}C image: 156 x 156 µm², slice thickness: 5 mm total scan time 4:00 h.

Courtesy of
M. Wenzler, Max Planck Institut
für chemische Ökologie, Jena, Germany

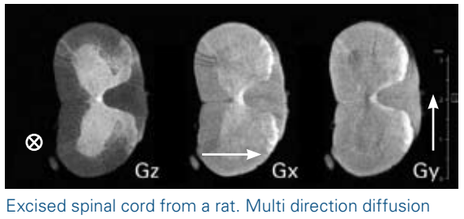

Excised spinal cord from a rat. Multi direction diffusion anisotropy experiment along three main axes (b=1088 s/mm²) at a spatial resolution of 23 x 23 mm², slice thickness 250 µm, total scan time 22 min.

Sample provided by
C. Faber, T. Weber, Univ. of Würzburg, Germany

IntraGate

IntraGate™ is Bruker's unique self-gated cardiac MRI technique, delivering unsurpassed high-quality CINE cardiac imaging without any external triggering hardware. With IntraGate, the cardiac and respiratory cycles are derived from navigator signals that enable the acquisition and retrospective reconstruction of cardiac and respiration movies with full coverage of the R-R interval. In addition, self-gating with IntraGate guarantees a steady state condition during acquisition, thus avoiding the flashing effects common to conventional ECG triggering and respiratory gating. IntraGate is available for *BioSpec®*, *PharmaScan®* and Mirco-Imaging systems.

Features:

- Cardiac and respiratory movies with full coverage of the R-R interval, or respiratory cycle, respectively
- Combined cardiac and respiration movies
- Different reconstruction possibilities of a single data set
- Multi-slice data sets can be acquired in less than 5 minutes
- Time course function enables observation of non-cyclic motion like peristalsis or uptake of contrast agents
- Synchronous multi-slice CINE frames
- No triggering devices necessary
- Steady-state acquisition
- High-temporal and spatial resolution
- Predictable scan times in comparison to conventional triggering
- Image quality independent from cardiac rate

Navigator Signal Processing

The IntraGate navigator signal records physiological motion. Cardiac and respiratory traces can be separated from the navigator signal individually. Using this information, acquired data are rearranged according to their corresponding cardiac and/or respiratory phases. Cardiac motion, respiratory motion and combined cardiac and respiratory motion can be visualized from just one single data set. Temporal resolution of the CINE movies can be changed without reacquiring the data.

Navigator Signal Time Course

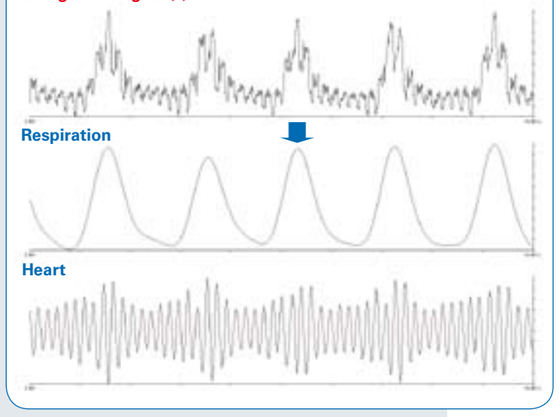

High-Resolution Cardiac MRI

IntraGate CINE of a mouse heart at the ultra-high-field of 11.7 T with (110 x 110) µm² in plane resolution

Content

EPR Products

Electron Paramagnetic Resonance

Solutions for Life Science and Analytical Research

ELEXSYS-II E780

The World's First Commercial mm-wave 263 GHz EPR Spectrometer

Bruker BioSpin has pioneered the world's first commercial mm-wave 263 GHz EPR spectrometer, ELEXSYS-II E780, representing a first step for Bruker's EPR division into quasi-optical microwave technology. It incorporates a unique superconducting magnet that can be ramped up to 12 T and is combined with new probe technology for optimum sensitivity, even on large samples up to 5 mm. Based on the well-proven Bruker ELEXSYS concept it provides multiple turn-key operation modes including, CW-, Pulse-EPR, ENDOR and ELDOR, thus enabling research groups for the first time, to routinely use very high frequency EPR technology.

Features

- Enables mm-wave very-high field EPR at 263 GHz
- Quasi optical front-end featuring reflection and induction detection
- Superconducting EPR magnet incorporating 12 T main coil and 0.2 T sweep coil
- Multiple turn-key operation modes including CW-, Pulse-EPR, ENDOR and ELDOR
- High-sensitivity single mode resonator
- Non-resonant probe for samples up to 5 mm
- Variable sample temperature from 4 to 300 K
- Safe and robust operation
- Runs routine software package Xepr

263 GHz Examples

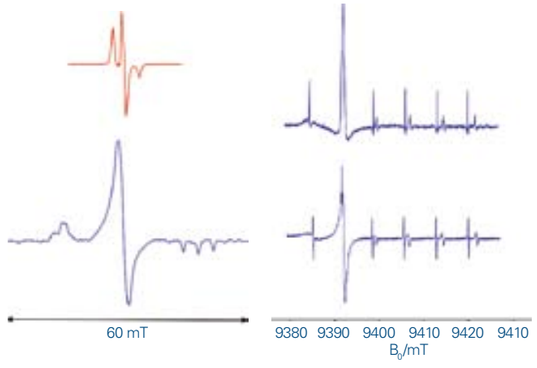

Tempol in polystyrene, 2 mW microwave power, modulation 10 G / 100 kHz, $5x10^{15}$ spins

Mn^{2+} in CaO, dispersion (top) and absorption (bottom) signal, sample volume 80 µl, microwave power 0.2 mW, modulation 1 G / 100 kHz

A Complete System

The ELEXSYS-II E780 is equipped with a quasi-optical front-end, featuring reflection and induction detection with safe and robust operation. The front-end is interfaced with a single mode resonator for highest sensitivity, and with a non-resonant probe featuring a larger diameter for samples up to 5 mm, both of which allow low temperature measurements down to 4 Kelvin. As with all other ELEXSYS systems, the E780 is driven by the proprietary Intermediate Frequency (IF) concept for optimum phase stability and pulse precision, and runs the Bruker software package Xepr, for routine and assisted expert workflows.

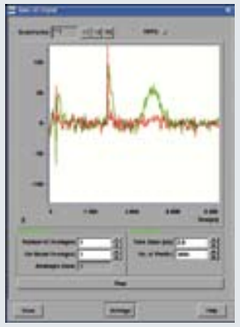

Spin echo of the E'center in quartz:
- Single shot
- Non-resonant probe
- Pulse sequence: 0.7-2-0.7 us

Very High-Field EPR Magnets

The ELEXSYS-II E780 is based on a unique superconducting magnet with specifications that match the the needs of very-high field EPR applications.

- Vertical field
- 89-mm bore
- Main field 0–12 T in < 100 min (21 bit)
- Homogeneity 10 ppm in 10 mm dsv
- High-resolution sweep coil (19 bit)
- High-resolution range 0.2 T

Quasi optical front-end of ELEXSYS-II E780

ELEXSYS-II Series

Redefining research level EPR

Introduced in 1997 the ELEXSYS has become the renowned research platform for modern EPR. Over the years a constant technical evolution has assured to keep track with new emerging demands of the EPR society. The second generation of the pulse devices SpecJet-II and PatternJet-II have been launched in 2006 and just recently DICE-II has become available.

Yet another major development step has now created ELEXSYS-II. The OS9 acquisition server has been replaced and the SuperX microwave bridge has been redesigned with improved specifications. The new multi-purpose signal processing unit (SPU) plays a central role in the expanded capabilities of the ELEXSYS-II, replacing the signal channel, fast digitizer, and rapid scan with a single integrated unit offering unprecedented performance and specifications.

ELEXSYS-II: The only commercial spectrometer series which covers all EPR techniques

	L-Band	S-Band	X-Band	K-Band	Q-Band	W-Band	mm-wave
CW-EPR	•	•	•	•	•	•	•
FT-EPR	•	•	•		•	•	•
CW-ENDOR			•		•		
Pulse-ENDOR			•		•	•	•
Pulse-ELDOR	•	•	•		•	•	•
Imaging	•	•	•				
Saturation recovery	•	•	•		•		
Rapid scan	•	•	•	•	•		
Transient EPR			•		•	•	
ODMR			•		•		

ELEXSYS-II E500 CW-EPR

SuperX: an ELEXSYS feature for the ultimate sensitivity in CW-EPR

The X-Band ELEXSYS instruments are equipped with the SuperX feature. SuperX comprises a selected high-power, ultra-low-noise Dual-Gunn source, and the super-high-Q cavity. The combination of these devices has resulted in an order of magnitude increase in sensitivity for CW-EPR in X-band. As one measure for sensitivity we specify a weak-pitch signal-to-noise of 3000:1 for the E 500 CW-EPR spectrometer.

Cu^{2+} histidine at 20 K and 20 dB power

Xepr for experiment design and data handling

Unprecedented flexibility and ease of use are the attributes of the Xepr software. Whether you are dealing with a simple CW experiment or a complicated multiple-resonance 2D experiment, the graphical user interface of Xepr ensures easy instrument control, experiment definition and execution. .

E 500 Accessories

- Teslameter
- Field-Frequency lock
- N_2 and Helium VT systems
- automated goniometer
- DICE-II ENDOR system
- microwave frequencies from L- to W-Band
- numerous dedicated probeheads
- large selection of magnet systems

E500 Highlights

- SuperX microwave units of world record sensitivity
- rapid scan module
- stationary and time resolved experiments
- multi purpose signal processing unit
- reference free spin counting

Standard super-high-Q cavity for ELEXSYS Systems

ELEXSYS-II E580 FT/CW

Pulsed EPR was initially the pride of selected laboratories until a real breakthrough was made by Bruker with the introduction of the ESP380 spectrometer in 1987. This event marked the beginning of a new era and set the standard for all future technical developments in EPR. The new generation of ELEXSYS-II FT/CW spectrometers has now been extended in frequency range ut to 263 GHz. With the recent introduction of the second generation pulse programmer and transient recorder, PatternJet-II and SpecJet-II, improvements in digital resolution and averaging capabilities have again pushed up the performance level of the E580.

PatternJet-II

Virtually no experimental limits are imposed by the PatternJet Series of pulse programmers. Designed for the needs of EPR this pulse programmer features a dynamic range of 10^9 , i.e. ns resolution over a time scale of up to one second. The well established concept of our first generation PatternJet has been technically enhanced and carried on to the second generation PatternJet-II. A 1 GHz clock, ultra low jitter and increased memory size are the cornerstones for a further increase in experimental flexibility and precision in data acquisition.

SpecJet II

With the first generation of SpecJet a dramatic improvement in pulse-EPR sensitivity could be achieved by high-speed signal averaging. The SpecJet-II now further enhances the abilities to capture fast and short lived transient signals. The real time display of the averaged echo/FID can now be toggled between time and FT mode and greatly facilitate spectrometer handling and signal optimization. With a sampling rate of up to 1 GHz and a pulse programmer with 1 GHz clock, the SpecJet-II is the perfect partner for meeting the evolving needs of pulsed EPR.

ESEEM Application

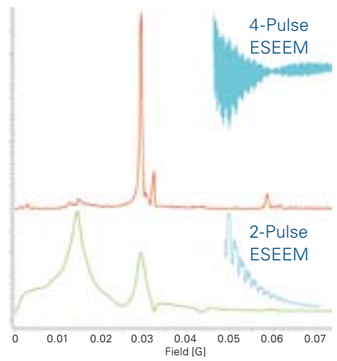

Numerous ESEEM sequences are available for increased sensitivity and resolution: 4-pulse (top) vs. the 2-pulse (bottom) ESEEM spectrum of powder spin label.

ELEXSYS-II E540 System

Biomedical research by EPR imaging is a rapidly growing field. Bruker's response to this development is the E540. Based on the proven ELEXSYS architecture, this instrument operates at 1 GHz and provides the seamless integration of imaging techniques into EPR spectroscopy. The imaging accessory can also be adapted to an X-band spectrometer for material science applications.

Gradient and Magnet System

EPR imaging uses continuous microwave irradiation and stepped field gradients in 3 dimensions. The 3D gradient coils provide up to 40 G/cm and are mounted on the pole faces of a dedicated L-band magnet or an X-band magnet.

To assure optimum performance, we have developed a variety of probes dedicated to specific applications.

E540R23

This probe has an access diameter of 23 mm, assuring a high-filling factor (sensitivity) for "small" animals.

E540R23

E540R36

This probe has an access diameter of 36 mm and is well suited for whole body mice and rat brain applications. An electronic matching control compensates effects from animal motion.

E540SC

The surface coil is designed for localized spectroscopy with or without magnetic field gradients. An electronic auto-matching and auto-tuning circuit assures ease of handling and compensates the undesired effects of animal movement during data acquisition.

Imaging Software

The graphical user interface provides a comprehensive, easy-to-use software package for all aspects of EPR imaging in 3 dimensions as well as spectral-spatial imaging in 4 dimensions. The ImageViewer supports further analysis and visualization of the images, and the oximetry software package allows precise determination of tissue oxygen levels.

E540SC

E540R36

ELEXSYS-II Multi-Frequency

Multi-frequency EPR is commonly understood in terms of its relation to CW-EPR spectroscopy. Bruker's commercial Multi-frequency/Multi-resonance EPR covers both, CW-EPR and FT-EPR as well as Pulse-ENDOR and Pulse-ELDOR at a multitude of microwave frequencies. Thanks to the ELEXSYS platform design and the advantageous intermediate frequency (IF) concept, every ELEXSYS spectrometer can be expanded for state-of-the-art multi-frequency experiments; now and in the future. All features of the X-Band CW/FT microwave bridge are transferred to the new operating frequency. For each frequency band a dedicated probe provides a maximum of sensitivity and ease of use.

High-Frequency/High-Field EPR and ENDOR at 94 GHz

The ELEXSYS family of EPR spectrometers includes two W-band systems, the E600 and E680. The former is optimized for CW-EPR experiments at 94 GHz, while the E680 operates in both CW and FT-mode.

The variable-temperature W-band TeraFlex probehead operates from 4 K to 300 K. This resonator is available as an EPR and EPR/ENDOR version. Samples can be exchanged at any temperature.

6 T EPR SC

The second generation of W-band super conducting magnet features a horizontal field, a main coil with 6 T sweep range, permanent leads and a 2000 G high-resolution sweep coil. Easy and safe operation is accomplished conveniently by software only, which allows switching between the two operation modes just by a mouse click.

SuperQ-FT

One building block, introduced in 2002, is called SuperQ-FT, a Pulsed EPR microwave bridge operating at Q-band (4 GHz). The SuperQ-FT can be configured as a stand-alone unit or as an upgrade for an X-band E580. The ER5107D2 resonator is available as an EPR and EPR/ENDOR version.

W-band magnet

SuperL-FT

The Bruker IF Concept not only allows to up covert to higher frequency but also to down convert to a lower operating frequency. This is realized for the first time with the CW/FT microwave bridge SuperL-FT. Combined with a local oscillator at 8.5 GHz, all features of the X-Band CW/FT microwave bridge are transferred to a frequency range of 0.8 – 1.4 GHz.

SuperS-FT

The latest addition to our IF multi-frequency pulse-EPR suite operates in S-band (3.4 – 3.8 GHz) in CW and pulse mode. The SuperS-FT is available as an add-on to an X-band E580 spectrometer for X/S dual band operation.

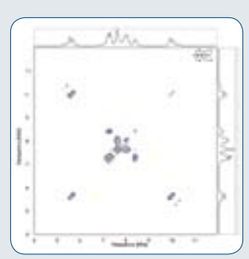

^{2}H Q-Band single crystal HYSCORE

ESEEM Application

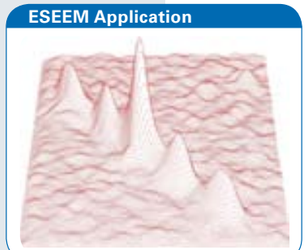

S-Band HYSCORE of BDPA

Multi-Resonance Accessories

Flexline
Pulse-ENDOR
Resonator
EN4118X-MD4

E560D-P DICE-II Pulse-ENDOR System

The DICE unit has been the cornerstone of pulse-ENDOR applications over many years. Now the second generation, DICE-II, has been developed with numerous enhanced specifications. To mention just one, the frequency range is 1 - 650 MHz covered by two bands.

DICE-II supports all known pulse-ENDOR and related techniques and in addition opens the way to new applications and pulse sequences. Multi-frequency pulse-ENDOR is supported by probeheads in X-, Q-, W- and mm-wave-band .

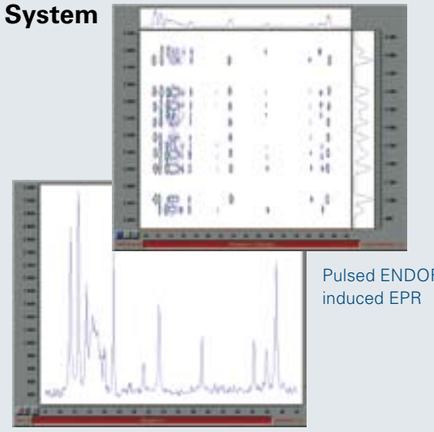

Pulsed ENDOR-induced EPR

Davies ENDOR spectrum

E580-400 Pulse-ELDOR unit

Electron-Electron Double Resonance (ELDOR) has become a major tool in EPR applications over the last few years. The E580-400 ELDOR unit is available as an accessory to the E580 FT/CW-EPR system and transfers to all other bands generated by the IF concept.

Typical experiments that can be performed with the ELDOR unit:

- Saturation Recovery ELDOR to measure molecular dynamics
- ELDOR-detected NMR to measure the ENDOR-equivalent nuclear-spin spectrum
- DEER to measure electron-electron spin distances
- Hyperfine Selective ENDOR to correlate the ENDOR and hyperfine spectrum

Specifications

- Digitally controlled solid-state microwave oscillator
- Frequency range of 800 MHz
- Pulse switching unit with 80 dB isolation
- Amplitude control with 30 dB dynamic range
- Fully software controlled

In order to make full use of the 800 MHz frequency range the ELDOR unit is complemented by the ultra broad band Flexline resonator series.

EMX*plus*

The foundation of EPR

The EMXplus is the next generation of Bruker's successful EMX spectrometer line, well-known for its premium performance in CW-EPR research. The design of the EMXplus reflects its dedication to the heart of the matter: rapid and high-quality data.

Simply power-on the EMXplus and start your EPR journey. Following self-validation procedures, the EMXplus is ready to use via Bruker's WIN-ACQ software.

The Perfect Duo I

The Signal Channel and Field Controller work together seamlessly to provide practically unlimited resolution on both axes: field and signal intensity.

The Perfect Duo II

The EMXplus Signal Channel now offers two detection channels in one. Simultaneous quadrature and 1st & 2nd harmonic detection schemes are just a mouse click away.

Accessories & Options

- The PremiumX microwave package for enhanced sensitivity
- The Variable Temperature Controller can be incorporated into the EMXplus console
- The ER036TM Teslameter ensures precise g-factor determination in combination with the integrated microwave counter
- The EMX-ENDOR package allows CW-ENDOR experiments to be performed on EMXplus Systems
- The full range of microwave frequencies from L- to Q-Band

Ultra-high-resolution over large sweep

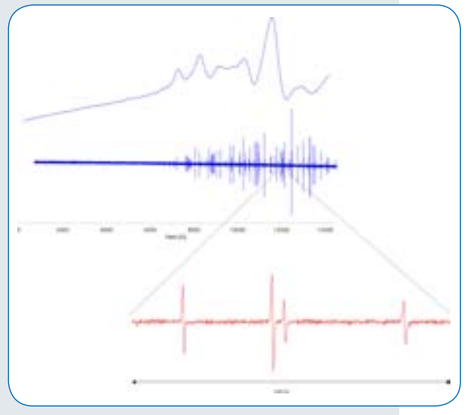

The spectra show oxygen in air at ambient pressure (top) and reduced pressure (middle) measured at Q-Band. A sweep range of 14 kG was recorded with 180000 points, resulting in a resolution of 80 mG, sufficient for the line width of 300 mG at reduced pressure.

EMX*micro*

The EMXmicro completes the EMX family and features an electronics cabinet with the footprint of a PC tower. The instruments micro cabinet can be combined with all electromagnets and microwave bridges from L- to Q-Band.

The standard software of the EMX series for data acquisition and processing is provided by WinACQ and WinEPR

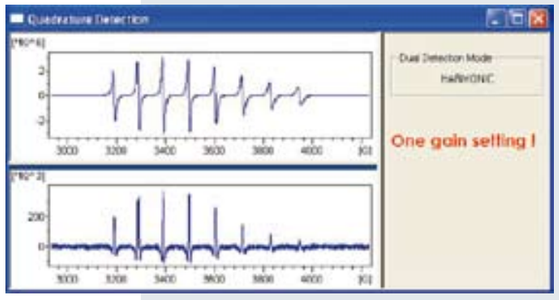

Dual-mode simultaneous detection of 1st and 2nd harmonic EPR spectrum of a vanadyl sample

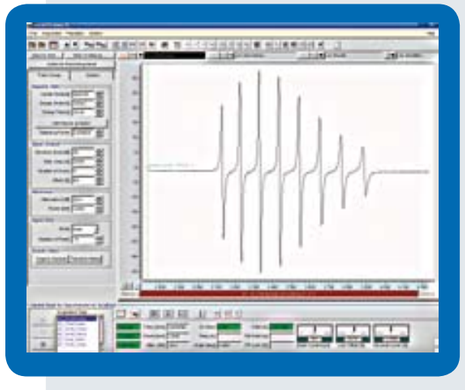

Xenon user interface

Xenon

This new software package is an option for the EMXmicro/plus series. It features a Linux® front end PC with a new graphical user interface integrating acquisition and processing in a user friendly environment. Xenon features numerous novel tools for data acquisition and processing, e.g. the direct spin counting method without reference sample.

e-scan

Bruker BioSpin's e-scan product line of table-top EPR (ESR) readers offer dedicated and tailored turn-key systems for specific Quality Control applications as well as systems for medical and pharmaceutical R&D applications of Reactive Oxygen Species (ROS) and Reactive Nitrogen Species (RNS). All e-scan systems have been designed for and have proven rock-solid in 24/7 operation with the best possible price-performance ratio available today.

A few example applications fields for e-scan:

- Irradiation Dosimetry with Alanine Dosimeters (ISO/ASTM method)
- Food Irradiation Control (EU standard methods)
- Beer Shelf Life: flavour stability and antioxidant stability (patented application)
- Biomedical EPR research: ROS and RNS detection and quantification

e-scan food control inserts (left) and the cavity template. (right).

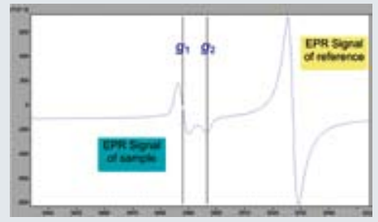

EPR spectrum of an irradiated chicken bone recorded with the e-scan Food Analyzer.

Content:

For research use only.
Not for use in diagnostic procedures.

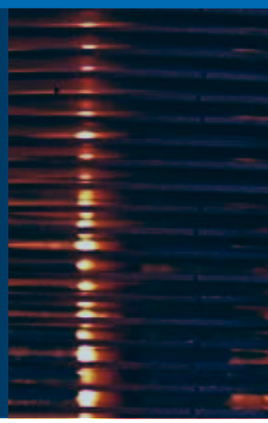

Mass Spectrometry

- Solutions for Life Science Research

think forward

MALDI-TOF and TOF/TOF

The well-known Bruker Daltonics FLEX MALDI-TOF-series stands for maximum performance and reliability. Applications-specific solution packages, like MALDI Molecular Imager or MALDI Biotyper, provide maximum flexibility and scalability of the system to answer challenging questions in expression proteomics, clinical proteomics and functional genomics.

autoflex III smartbeam

microflex

autoflex III smartbeam

Innovative MALDI-TOF and TOF/TOF MS technology for reliable and detailed protein characterization, high-resolution MALDI imaging and validated biomarker discovery. The innovative smartbeam-II™ laser technology in combination with dedicated high-speed bioinformatics enables LC MALDI and MALDI imaging applications with unrivalled speed, improved sensitivity and excellent resolution. smartbeam-II outclasses YAG-only laser technology and provides top-performance with any chosen matrix – with an adjustable laser repetition rate from 1 – 200Hz and computer-controlled, adjustable laser focus size from 10 – 100 µm for highest spatial resolution.

microflex LT/microflex

The microflex instruments are affordable, easy-to-use and compact benchtop MALDI-TOF systems with superior performance. The modular design supports different and growing user requirements. Unbeaten 15k resolution and microScout MALDI targets in 1/4 MTP format distinguish the microflex from other benchtop MALDI-TOF systems.

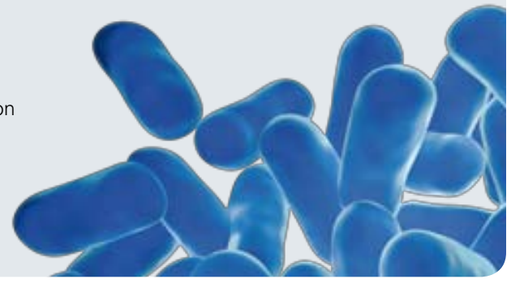

Ultra-high Productivity and Superb Performance

Sample preparation

Data acquisition

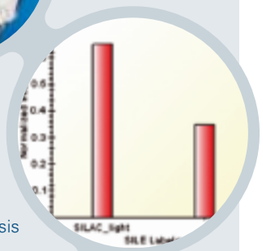

Data analysis

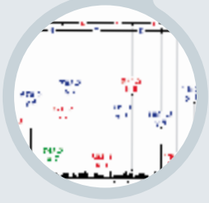

Peptide ID (see Application Note MT-86)

ultrafleXtreme

ultrafleXtreme

Attain a spectacular level of mass spectrometry performance: Incredible sensitivity, resolution and mass accuracy for high-success expression proteomics, quantitation and advanced biomarker discovery studies. First commercially available 1 kHz smartbeam-II™ laser technology gives access to superior performance in any proteomics project.

Our TOF/TOF technology provides enhanced ion optics for cutting-edge MS/MS experiments and second generation PAN™ “panoramic” resolution allows impressive simultaneous mass resolution across a wide mass range leading to reliable top-down sequencing capabilities.

The latest innovation in MALDI mass spectrometry is the TOF/TOF technology for ultimate performance in both 2D gel-based and LC-based proteome analysis. Our patented LIFT™ technology with up to 1 kHz data acquisition rate and a highly automated workflow provide high-quality MALDI-TOF and TOF/TOF information from minute sample amounts in just seconds.

ION Trap

Bruker's novel amaZon ion trap series opens up new performance levels for any kind of analytical requirements.

Equipped with dual ion funnel transfer for 10x improved sensitivity, novel technology for highly accelerated data acquisition as well as a mass resolving power up to 20,000, this ion trap reaches unrivalled data quality and extreme flexibility for a broad variety of complementary applications like proteomics, metabolomics, compound screening and identification as well as chemical analysis.

The amaZon series is available in two versions: amaZon ETD for proteomics, and amaZon X for small molecule analysis and applied markets.

The amaZon series of ion traps equipped with the renowned spherical high-capacity trap, combined with an ingenious detector design, offers high performance and superior data quality for a large range of applications – tailored for highest productivity. Transforming speed to information, the amaZon series perfectly answers today's challenges in molecular characterization.

amaZon ETD

Spherical ion traps are ideal tools for ETD & PTR:

1. Simultaneous storage of + and – ions with direct ETD reaction as soon as anions enter the trap
2. Cations and anions are pushed towards the center of the trap: Excellent cross section for ionion-reactions
3. Perfect combination of resolution for up to 6+ charge states at high-scan speed of 4,600 u/sec
4. High m/z range of 3,000 u
5. Easy and fast switching between ETD and PTR simply by changing electrical potentials
6. High-mass accuracy (< 0.15 Da) for fast protein database searches and successful de novo sequencing. Features that translate directly to highly efficient ETD reaction and superior data acquisition.

Exceed the Limits of all Previous Ion Trap Technologies

amaZon X / amaZon ETD

The new amaZon series incorporates key inventions for unprecedented capabilities:

- First ion trap system with dual ion funnel transfer for 10x improved sensitivity over current platforms
- Unrivalled scan speed of 52,000 u/sec at better than unit resolution for fastest UPLC applications and a maximum duty cycle in data-dependant MS/MS and MS^n
- Ultimate ion trap mass resolving power up to 20,000 in full scans across the 50-3,000 m/z range at HPLC speed.
- Latest ETD/PTR technology for most efficient, extremely robust and sensitive peptide and protein fragmentation. The combination of bottom-up CID or ETD and top-down ETD/PTR provides new ways for detailed protein characterization in, e.g. the unambiguous elucidation of post-translational modifications and the full coverage of the amino acid sequence including N- and C-termini.

ETD was first commercially available on Bruker ion traps and is incorporated in all amaZon ETD systems or available as a field upgrade for all amaZon X systems.

- "Zero Delay Alternating" for high-speed ion polarity switching without any sensitivity and time compromise. Up to 20 Hz MS data acquisition in both polarities provides for an ideal combination with fast UPLC separation. Supported by spectral MS^n libraries, the amaZon is the ultimate mass spectrometer for MS/MS based multi-compound screening.

ESI-TOF

High-mass accuracy with high-dynamic range

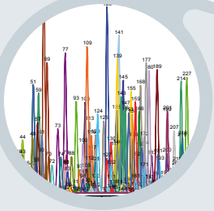

Automated detection of multiple compounds and ID of unknowns (see Technical Note ET-12)

High-resolution Extracted Ion Chromatogram (hrEIC)

Detect multiple targets within one LC-run

Get ultimate confidence in your results. Bruker Daltonics' micrOTOF II™ and micrOTOF-Q II™ mass spectrometers feature the very lastest technology developments to provide maximum certainty in your research in Small Molecule Identification, Metabolomics or Proteomics.

Precious sub-ppm confidence is available for formula determination in pharmaceutical impurity analysis, metabolite identification, pesticide screening and toxicology & doping analysis.

Simultaneously, three dimensions of information promote your analytical tasks to unrivaled heights of confidence:

1. Measure with unequalled accurate mass.
2. Validate with sub-ppm confidence using unequaled True Isotopic Pattern (TIP) analysis.
3. Benefit from accurate mass and TIP also in fragments analysis in MS/MS mode with the micrOTOF-Q II.

Highest confidence in analytical and scientific tasks is achieved by the concurrent availability of market-leading sensitivity, wide dynamic range mass accuracy and superb focus resolution power.

micrOTOF II focus

Featuring a mass resolution exceeding 16,500 FWHM and mass accuracy of better than 2 ppm in combination with true isotopic pattern analysis, micrOTOF II is the perfect choice for straightforward formula determination of small molecules, quality control of intact proteins, and metabolic studies.

micrOTOF II

Easy Formula Determination

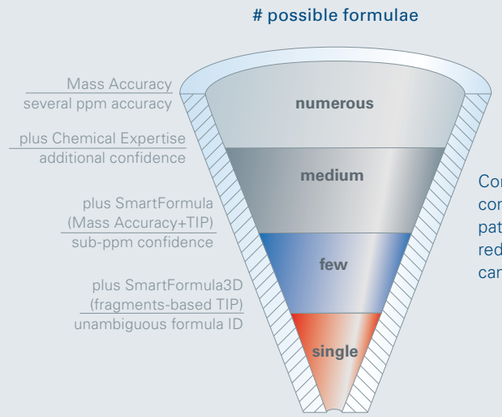

Confident determination of the elemental composition of a LC-MS peak. Isotopic pattern information – SmartFormula 3D – reduces the number of molecular formula candidates dramatically.

micrOTOF-Q II

micrOTOF-Q II

Precise mass, SmartFormula 3D™, MS/MS: Bruker Daltonics' new micrOTOF-Q II™ ESI-Qq-TOF mass spectrometer features the very latest technology developments to provide maximum certainty in research in Small Molecule Identification, Metabolomics or Proteomics. Easy formula determination of small molecules, metabolic studies, analysis of complex mixtures, digests and in-depth evaluation of intact proteins are key applications. With a superb quadrupole mass filter and a quadrupole collision cell, the entire mass range of fragment ions is available at increased sensitivity for time-of-flight mass analysis.

UHR-TOF

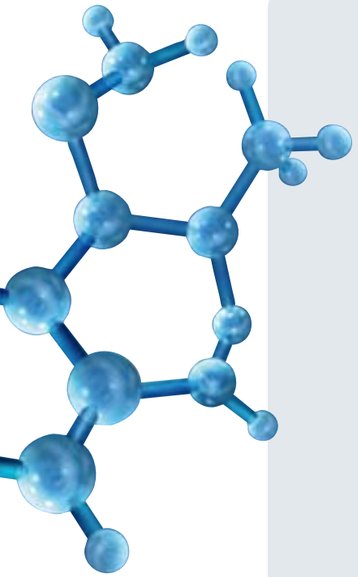

Both, mass accuracy and resolution are maintained, even at an acquisition rate of 10 spectra/s.

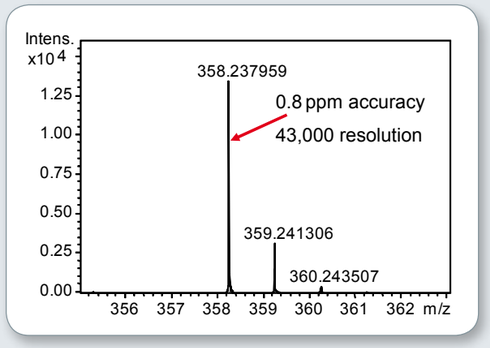

maXis

The latest development from Bruker, the novel UHR-TOF ultra-high resolution technology, again proves Bruker Daltonics leadership in the design of cutting-edge mass spectrometry.

Maximum information @ maximum speed

maXis™ is a high-resolution tandem mass spectrometer offering a no-compromise solution for exceptional accurate mass, high-resolution and high-sensitivity analysis at a speed able to take full advantage of ultra-high performance chromatography.

With resolution in excess of 40,000 FWHM and MS and MS/MS mass accuracy typically between 600 – 800 ppb at speeds of up to 20 full spectra per second simultaneously, no other mass spectrometer is better equipped to deliver definitive data on complex samples in proteomics, metabolomics and small molecule identification challenges.

FTMS

solariX ®

solariX, the next-generation hybrid Qq-FTMS, is an easy to use, high-performing system that is equipped to address the most challenging proteomics and complex mixture applications.

The broad-band, ultra-high resolving power (> 1,000,000 @ m/z 400, 7 T) is essential for tackling complex mixtures, especially those that are not amenable to on-line separation techniques such as; hydrocarbon related analysis ("petroleomics"), environmental analysis, and metabolomics.

For applications that require high-performance LC-MS or LC-MS/MS, the solariX is ideally suited. New functionality provides more resolution when it is needed most and with optional, faster acquisitions for MS/MS data.

Added top-down versatility is provided with fully enabled Electron Transfer Dissociation (ETD). This exciting new technique, combined with FTMS performance, is superb for the comprehensive analysis of proteins and peptides and their subtle, posttranslational modifications.

The solariX can be configured with Dual ESI/MALDI (based on advanced ion funnel technology) and a range of API source options (APCI, GC-APCI, APPI). Low maintenance, refrigerated magnets are standard with solariX and can be configured with one of several magnetic field options (7T, 9.4T, 12T and 15T).

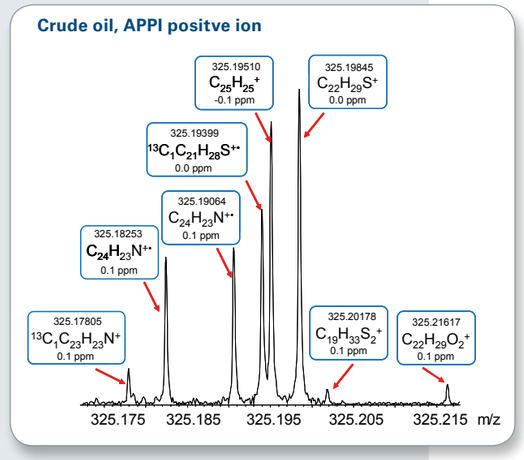

solariX

Ion Sources

The key to performance and flexibility

In Mass spectrometry, the performance of the MS system in terms of mass resolution, mass accuracy and mainly sensitivity, depends strongly on the method of ion generation. There is no single ion source for any application; polar and non-polar, big and small molecules require different ionization techniques. Especially for LC/MS systems there are numerous ion sources available to meet any possible application. Bruker Daltonics offers the biggest variety of ion sources, all of them with special features and some of them really unique.

API sources

In general atmospheric pressure ionization (API) is more gentle than vacuum ionisation techniques like electron impact (EI). Therefore API is used for larger molecules like peptides which would undergo uncontrollable fragmentation at vacuum ionisation.

GC/APCI

The GC/APCI source allows the coupling of a GC on a Bruker LC-MS (TOF-MS, UHR-TOF, FTMS). If just a few samples need to be analysed by a high-resolution MS there is no need anymore for an expensive, dedicated GC. Switchhing from LC to GC and vice versa can be done within minutes without breaking the vacuum. This option allows for the first time the coupling of a GC with a real high-performance mass spectrometer for unambigous formula determination or high-resolution extracted ion chromatograms.

micrOTOF II with GC/APCI source and heated transfer line.

Types of ion sources and their fields of application taking the molecular weight and the polarity of the analyte into account.

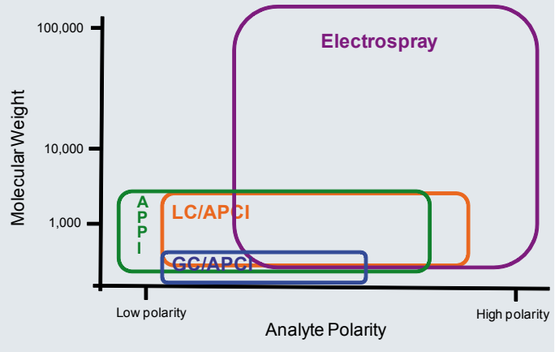

HPLC for nano-LC-MS/MS Proteomics

EASY-nLC: "One Click" separation

It is easy to handle, steady and reliable. It is a 1D-nanoflow HPLC system tailored to the requirements of today's proteomics applications. It is the straightforward gateway to proteomics discovery and provides the researcher with:

- Simplicity: Easy installation & operation
- Reliability: Robust & steady
- Low-Maintenance: Split-free gradient mixing
- A 2D LC-kit is available as an option
- Efficiency: minimum peak widths < 5 sec.
- Compact design with small footprint

EASY-nLC

Ease of use and split-free flows

The EASY-nLC is a compact, innovative and affordable nano-HPLC system for state-of-the-art proteomics laboratories. Split-free binary gradient mixing down to the low nanolitre/min range are made possible by precise direct drive pumps. Bruker Daltonics' Compass™ software environment fully integrates the EASY-nLC with Bruker Daltonics mass spectrometry systems.

Maximize productivity

Easy-nLC operation is optimized for Bruker Daltonics mass spectrometry instrumentation, whether it is connected online to amaZon X or amaZon ETD ion traps, micrOTOF ESI-TOF systems, FTMS sytems or the PROTEINEER fc II MALDI sample collector for offline measurements with FLEX series MALDI-TOF/TOF instruments. Intuitive and simple software allows the integrated control of the whole experiment.

Compass - the common user interface

Bruker Daltonics' unified software environment for all life science instruments integrates our successful modules for instrument control, data acquisition, processing and interpretation with a new, global method management. The optional Compass Security Pack provides all necessary functions to support work in compliance with FDA and EU regulations (21CFR part 11/Annex 11).

The database system for proteomics project management

ProteinScape is Bruker Daltonics' central bioinformatics platform for storage and processing of MS data. The embedded processing pipeline maximizes the outcome and reliability of your protein identification. ProteinScape is the bioinformatics backbone of the HUPO Brain Proteomics Project.

Proteomics Solutions

Protein characterization

The Proteomics solution is a comprehensive, integrated platform supporting all major LC and gel-based strategies that allow to identify and quantify proteins at proteomic scale. The ProteinScape™ software is the bioinformatics heart, providing a single software platform for identification and quantification by gel-based analysis, label-free and labeling technologies such as SILAC, ICPL or iTRAQ™, using any of Bruker Daltonics mass spectrometer platforms. Reporting tools following the HUPO-PSI guidelines accelerate the publication process of proteomics studies dramatically, using ProteinScape. Both, top-down and bottom-up strategies are supported comprising detailed protein characterization tools unique in the market: PTM discovery with ETD II on amaZon enables powerful phosphorylation, glycosylation and epigenomic work; top-down protein sequencing provided by the MALDI-TDS on the ultrafleXtreme with ISD and T^3-Sequencing is replacing Edman-sequencing in the near future for N- plus C-terminal sequencing of intact proteins even in case of N-terminal protein modification.

Easy and intuitive data evaluation and comprehensive data reporting with ProteinScape 2.

MALDI imaging

The MALDI Molecular Imager™ is based on solariX and FLEX-series MALDI-TOF MS with smartbeam-II™ laser technology to combine MALDI-TOF MS technology with histological tissue imaging. The system enables high-sensitivity imaging of protein biomarker candidates in biological and clinical research based on their spatial distribution in tissue sections. The complete imaging solution provides all tools necessary for successfull MALDI imaging: the fully-automated ImagePrep™ station, mass spectrometry, as well as data analysis and statistical evaluation software.

MALDI imaging of rat brain. See Application Note MT-91 for details.

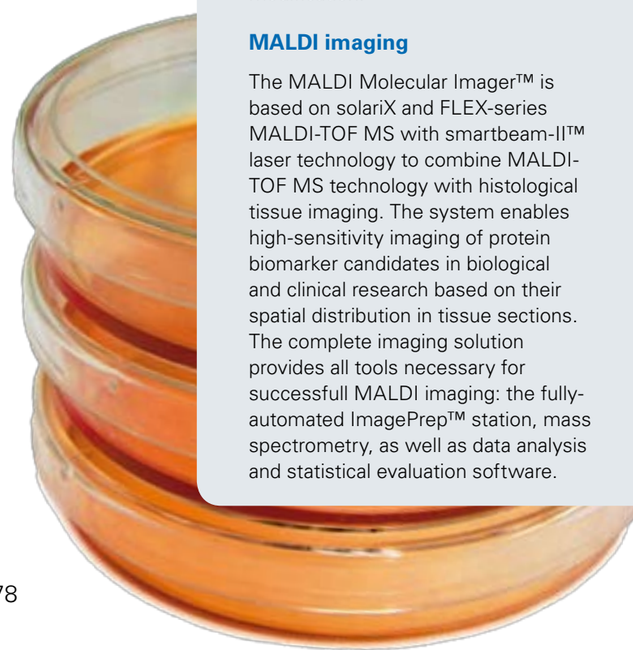

ID of microorganisms

The MALDI Biotyper allows fast and reliable identification and classification of microorganisms, such as bacteria, archaea, yeasts or fungi. Single bacterial colonies can be directly taken from the agar plate and transferred onto a MALDI sample target. There is neither a need for any prior PCR amplification, nor for the usage of selective growth media nor for any other preassumptions, which may influence the outcome of the analysis. The MALDI Biotyper software identifies microorganisms by the species-specific signal patterns contained in their respective molecular profiles.

Lipidomics

The direct coupling of thin layer chromatography with MALDI is enabled by a new adapter target for Merck´s 5*7.5 cm aluminum backed HPTLC plates and a dedicated software that controls the acquisition of MALDI-TLC mass chromatograms and their analysis. MALDI-TLC provides direct access to molecular information for various applications: from quick tests in the organic synthesis lab to identify side products to lipidomics and lipid profiling and all analysis of groups of organic molecules for which no stale HPLC procedure is available.

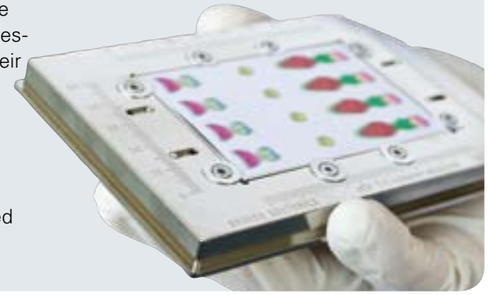

Chemistry

Polymer analysis

MALDI-TOF mass spectrometry and PolyTools™ software enable for the rapid determination of monomer units and end groups of oligomeric resolved polymer mass spectra. Characteristic values of the polymer, like weight average molecular weight (MW), number average molecular weight (MN), polydispersity and degree of polymerization are automatically calculated from the mass spectra.

Petroleomics

Crude oil is a very complex mixture. The analysis of the elemental composition of single compounds of crude oil is achieved using ultra-high resolution Fourier Transform Mass Spectrometry (FTMS). Quantitative information of compound classes in crude oil is indispensable in many industries. Applying different ionization techniques such as ESI, APCI and APPI in negative and positive mode enables the comprehensive classification of crude oil.

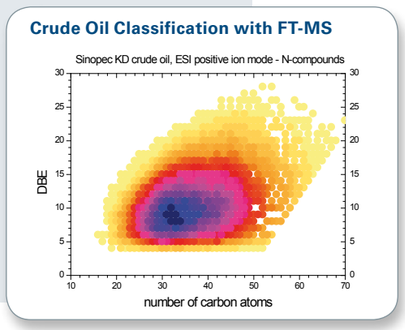

DBE Plot vs. carbon atoms of compound class N in positive ion mode of crude oil 3/1.

Small Molecules Applications

Identification of unknowns

The precise mass TOF-MS systems by Bruker are ideally suited for the identification of unknown substances in an LC run. The combination of accurate mass information and True Isotopic Pattern allows an unrivalled confidence in the outcome and a dramatic reduction in the remaining number of possible formulae. Common structure elucidation algorithms are just using the exact mass and isotopic pattern of the precursor ion and the exact mass of the fragment ions. By SmartFormula 3D the isotopic pattern of the fragment ions is used additionally. By this possibility the number of possible hits is in most cases reduced to 1. The sophisticated algorithm combines the information of precise mass with multistep fragmentation, thus dramatically reducing the number of possible formulae.

Analysis of fragments ions reduces possible formulae to just one candidate

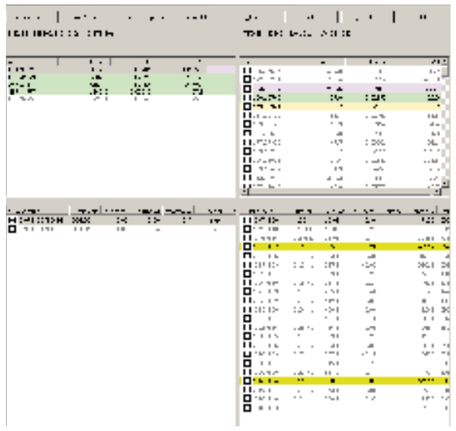

List of sum formulae after reduction by accurate mass and True Isotopic Pattern.

Screening of multiple pesticides in a single run

The usefulness of LC/MS/MS for the unambiguous identification and quantification of pesticides in complex matrixes are well known as the ESI-TOF system can generate high-specificity without limiting the number of simultaneously observed target compounds. Further benefits are:

1. Due to mass accuracy apparently independent of peak intensity, it is possible to generate extracted ion traces with a window down to a few mDa, allowing for extreme selectivity and simple and fast identification.
2. Due to the conserved correct isotopic pattern, it is possible to reduce the number of possible hits within a given mass interval by at least an order of magnitude. The derived SmartFormula strongly helps to find the correct elemental composition.

List of compounds detected

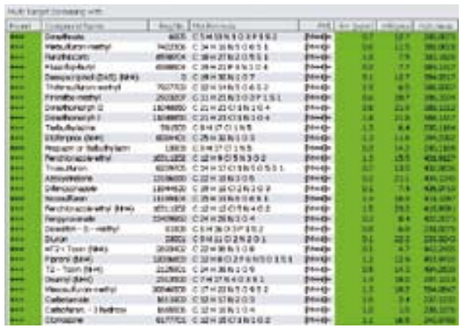

Analysis of a complex pesticide mixture detected with one single run. Resulting search in TargetAnalysis database based on accurate mass, isotope pattern and retention time identified more than 250 compounds in a mass range from m/z 100 to m/z 1000.

Metabolite detection

The major task of metabolite identification is rapid and reliable elucidation of structural changes. This fact applies to metabolism of both xenobiotics and endogenous compounds. Liquid chromatography hyphenated to atmospheric pressure ionization mass spectrometers (LCMS) has become an integral part of metabolite identification, and especially ion trap mass spectrometers with their multiple MS capability have proven excellent tools for this purpose. Since data acquisition is performed nowadays in an automated fashion, data interpretation has emerged as new bottleneck in the identification process. The integrated solution provided by Bruker Daltonik, consisting of a state-of-the-art MS (either ion trap, TOF or FTMS) and a sophisticated software combination of DataAnalysis. and MetaboliteTools provides novel tools for both metabolite prediction as well as sophisticated detection and thus significantly speeds up data interpretation in this specific application.

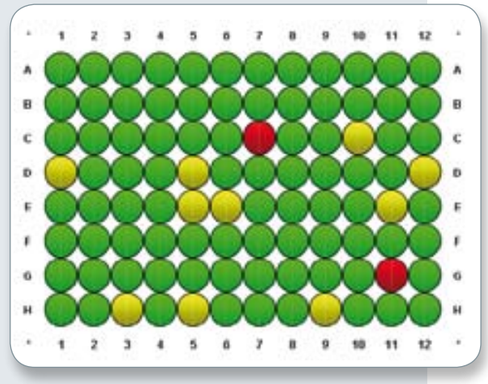

OA/QC

Deliver an expert analytical result first time to every walkup lab user, whatever their knowledge or experience. Compass OpenAccess™ is the ideal client/server software system to combine with the unique chemical formula generation capabilities of the Bruker Daltonics micrOTOF II™, defining a new level of certainty in chemical information from open-use LC/MS.

Compass OpenAccess allows the guided use of LC/MS systems, all under a simple user interface to select appropriate analytical tasks with prepared SOPs. It automatically handles even more advanced analytical tasks on behalf of the user, such as automated analysis of isotopic patterns and evaluation of chemical species using SmartFormula™.

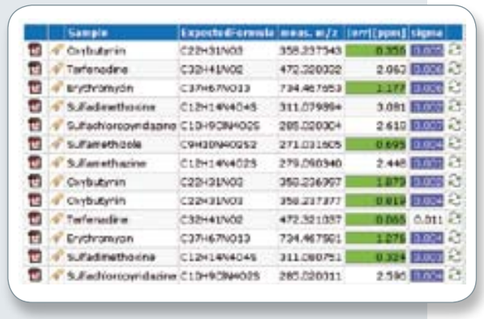

Confirmation of formulae at a glance: Color-based confirmation is visualized in a well-plate representation. More details are obtained from a result table of compounds using Compass OpenAcess QC.

Content:

CBRN Products

CBRN

Chemical, Biological, Radiological and Nuclear Detection

Prepared for a World of Changing Threats

The complete product line for CBRN detection

CBRN detection technology has always been the core competence of Bruker Daltonics. As the first supplier on the market, we cover the complete range of chemical, biological and nuclear detection. Bruker is specialized in development, engineering and manufacturing of military hardened and easy-to-use analytical systems and is ISO9001 certified.

The product line supports all possible use cases for the detection of various threats, and includes handheld point detectors as well as detection systems for reconnaissance vehicles, shipboard or stationary use. Bruker provides sophisticated CBRN evaluation and monitoring software.

Safety and Security

Major events such as summits, concerts, parades or sporting events are part of critical infrastructure and may be targets of terrorist attacks with CWA and TIC. Harbor and airport areas as well as any public buildings are also most sensitive in terms of any release of hazardous agents. Stationary and mobile Bruker detection equipment can be integrated into monitoring systems for critical infrastructure.

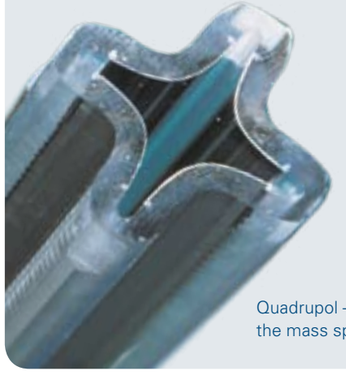

Quadrupol – heart of the mass spectrometer

Bruker offers a wide product range including

- Mobile Mass Spectrometers
- Ion Mobility Spectrometers for real time detection of CWA and TIC
- Stand-off detectors based on passive FTIR
- Radiation Meters
- Non invasive identification of CWA in ammunition

System Integration

Our CBRN detectors can be easily integrated into any kind of CBRN detection system. The systems are deployed under various environmental conditions. Ruggedised design and sophisticated accessories allow flexible and extensive applications for the detection of hazardous compounds by mounting the systems on vehicles, ships, helicopters, shelters or by hand-held use under field conditions. Sophisticated software supports the integration of our CBRN detectors. Bruker has over twenty years of experience in systems integration.

Bruker Detection confronts the needs of airport-, emergency responder-, event- and border-security personnel not only with military equipment. Special designed products face these challenges.

RAID-AFM

The innovative RAID-AFM is the only available stationary IMS without a radioactive source. It can be deployed for chemical and radiological detection in vulnerable areas such as airports, sea ports, sports arenas and other public facilities.

RAID-AFM (NC-Version)

Mobile-IR

Mobile-IR

Most chemical substances have their own infrared signature; just like a fingerprint. With the new portable FT-IR spectrometer Mobile-IR, it is easy to identify unknown chemicals in just a few seconds, by comparing the fingerprint of the substance with included data bases. Unlike other portable instruments, the Bruker Mobile-IR is designed to be used under adverse conditions. It is waterproof to IP67 standards, and offers a high degree of shock protection.

E²M

The enhanced environmental mass spectrometer E²M is a mobile, compact and lightweight GC/MS system for fast, reliable onsite identification of organic chemicals from any medium (soil, water, air). Typical fields of application are environmental protection, mobile on-site analysis and event monitoring. The E²M fully supports first responders and homeland security detection and identification activities.

E²M

Stay Prepared – Prepared for the Worst

The challenge of asymmetric threats in various environments requires highly flexible equipment. Bruker Detection provides a assuring track record of such equipment, used all over the world. As technology market leader for more than 25 years we are ready to “Stay prepared – prepared for the worst”.

Stand-off detector for atmospheric pollutants

A compact, mobile infrared detector for real-time remote sensing of chemical agent clouds. All known CWA and important Toxic Industrial Chemicals (TICs) can be automatically identified and monitored over a distance of several kilometres – either stationary or on the move. Latest developments have resulted in linking two ore more RAPID’s to setup a triangulation system and allowing tomographic reconstruction of CWA clouds.

RAPID – easily deployable chemical stand-off capabilty on various platforms.

RAPID

MM series

The new MM2 sets a milestone in GC/MS technology with a volume of 43 litres and a weight of 35 kg. Equipped with improved Gas Chromatography/ Mass Spectrometry technique it represents the new generation of quadrupole mass spectrometers. The MM2 is optimized for long-term chemical reconnaissance in various armoured vehicles, as well as for mobile chemical agent inspection and detection missions.

MM2

RAID series

A series of chemical monitors, covering multiple tasks including monitoring of collective protection facilities and CBRN filter stations, as well as handheld point detection for personnel protection purposes. Based on the well-established Ion Mobility Spectrometry, all important CWA and Toxic Industrial Chemicals (TIC) can be monitored.

The innovative RAID-XP combines chemical and radiological detection into one system.

The RAID-M 100 is distinguished by its flexible and easy use for portable and hand-held deployment. It is designed for fast and sensitiv detection and identification of CWA and TICs.

The RAID-S2 is specially designed for long term operations. The instrument can either be operated separately, or several instruments can be connected in networks.

The µRAID is a compact, easy-to-use IMS based chemical agent detector for personal use.

Integrated RAID-S2 sensors

RAID-XP

µRAID

RAID-M 100

Content:

Vibrational Spectroscopy

Advanced Research and QA/QC Solutions
Based on Infrared and Raman Spectroscopy

FT-IR

Bruker Optics has the industry's most comprehensive FT-IR product-line; from the world's smallest FT-IR spectrometer to the world's highest resolution.

ALPHA

About the size of a lab book, the world's smallest FT-IR spectrometer ALPHA will play a big part in your daily routine. Plug & play set-up, easy-to-use software, combined with QuickSnap™ sampling modules assure powerful and reliable FT-IR analysis you expect from Bruker. ALPHA is ideal for academic teaching and routine industrial applications.

ALPHA with ATR Sampling Module

Mobile-IR Portable FT-IR

Material Identification Anywhere! Bruker's Mobile-IR is a self-contained, rugged portable FT-IR spectrometer that provides benchtop performance, wider spectral coverage and higher spectral resolution. It's ideal for crime scene investigation, environmental monitoring and hazardous material identification applications.

Mobile-IR

EM27 Open Path FT-IR

Providing laboratory grade performance, the EM27 open-path FT-IR can easily be deployed in the field for various environmental air monitoring applications. Emissions from smoke stacks and waste disposals, hazardous emissions from chemical accidents can be observed with an operating range of up to several kilometers.

EM27 Open Path FT-IR

Most Comprehensive FT-IR Product Line; from the Smallest in Size to the Highest in Resolution

TENSOR 27 FT-IR Spectrometer

TENSOR Series

If you need a FT-IR spectrometer that can rapidly identify, quantify and verify your routine samples, TENSOR is the right tool for your laboratory. It combines the highest performance and outstanding flexibility with ease of use. A full line of sample compartment and external FT-IR accessories enable it to be used for various challenging applications.

VERTEX 70 FT-IR Spectrometer

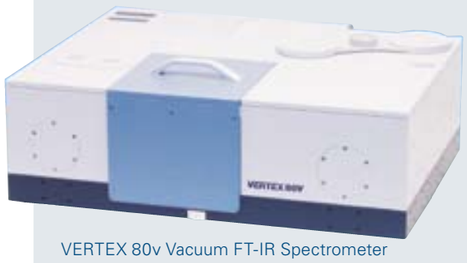

VERTEX 80v Vacuum FT-IR Spectrometer

VERTEX Series

The VERTEX Series is built on a fully upgradeable optics platform that is designed with the utmost flexibility in mind. Multiple input and exit ports allows users to connect various external and internal accessories and components to customize the instrument based on applications. VERTEX spectrometers share a wide range of features and utilize patented RockSolid™ and UltraScan™ interferometer designs. With the vacuum models, peak sensitivity in the mid-, near- and far IR regions is obtained without the fear of masking very weak spectral features by air water vapor absorptions.

IFS 125HR

IFS 125 Series

The IFS 125 is built for performance with each instrument component optimized to approach the theoretical limit of sensitivity. It offers the highest spectral resolution available down to 0,001 cm^{-1}, a resolving power of up to 10^6 and the wide wavelength range from 5 cm^{-1} in the far-IR/THz to 50,000 cm^{-1} in the UV. The mobile IFS 125/M is dedicated to gas phase absorption studies, frequently applicable to atmospheric research.

Raman

The Raman effect is based on the inelastic scattering of monochromatic light with matter. As the complementary vibrational technique of IR spectroscopy Raman provides detailed molecular structure information. Due to its nondestructive characteristic, Raman spectroscopy is ideally suited for in-situ analysis of macro and micro samples ranging from materials research to quality control. The Raman spectrum reveals valuable information about crystallinity, polymorphism and phase transitions. Raman spectroscopy combines high-information content, no sample preparation and the use of fiber optic probes for remote sampling.

Bruker Optics added FT-Raman capabilities to its product line shortly after the technique was first reported in late 1980s. Since then, continual hardware and software improvements, as well as the development of various sampling accessories, helped Bruker maintain the tradition of innovation and excellence in this scientific instrumentation technique. Today, Bruker offers a variety of Raman (both dispersive and Fourier transform) instruments for laboratory and process applications.

MultiRam

The MultiRAM is a stand-alone high-performance Fourier transform Raman spectrometer. It has a large sample compartment to utilize an extensive range of pre-aligned sampling accessories that are designed to accommodate all types of sample formats; from powders to liquids in vials.

MultiRam Stand-Alone FT-Raman

RAMII FT-Raman Module

Designed as an add-on module, Bruker's RAM II is a dual-channel FT-Raman spectrometer that can be coupled to VERTEX series multi range FT-IR spectrometers. It combines fast and easy sample handling and maximum suppression of disturbing fluorescence, expected from FT-Raman.

RAMII coupled to VERTEX 70 FT-IR

FT-IR & Raman Microscopy

Sample visualization is the important first step in the analysis of almost any sample. Infrared and Raman spectroscopy are versatile and powerful analytical techniques that can be applied to micro-analysis. Bruker's FT-IR and Raman microscopes are built on state-of-the-art optical microscopy platforms that provide optimal sample visualization and also feature chemical imaging and mapping. Areas of applications include material science, forensics, mineralogy, failure analysis, content uniformity, sample homogeneity and quality control.

HYPERION 2000
coupled to TENSOR 27

HYPERION™ Series

Featuring full automation, infrared chemical imaging, crystal-clear sample viewing and a wide variety of IR and visible objectives, the HYPERION™ series provide everything needed to conduct the most demanding micro-analysis easily and efficiently. It can be coupled to TENSOR and VERTEX Series FT-IR Spectrometers.

The HYPERION™ 3000 represents the pinnacle of infrared microspectroscopy, incorporating state-of-the-art Focal Plane Array detectors for the most demanding infrared imaging applications. High-resolution chemical images can be collected in a matter of seconds.

SENTERRA Raman Microscope

SENTERRA™

Bruker's SENTERRA™ is an easy to use Raman microscope that combines many novel features such as the patented SureCal permanent calibration, fluorescence rejection and on-demand confocal depth profiling. With a wide variety of excitation lasers providing high-spectral resolution, it is ready to challenge any microanalysis research applications.

RamanScopeIII

When sample fluorescence is a problem, FT-Raman microscopy with near infrared 1064 nm excitation is frequently the only solution. RamanScopeIII can be coupled to Bruker's FT-Raman spectrometers, and be combined with the SENTERRA™ dispersive Raman microscope as a hybrid solution.

FT-NIR

Discover the flexibility of Near Infrared Spectroscopy

Choosing the best possible sampling method is crucial when solving a specific analysis task. Near-Infrared Spectroscopy (NIR) is an ideal technique for both on-line as well as in the laboratory. It offers several advantages over traditional methods, including the ability to make measurements remotely over fiber optics, rapid results, and multiplexing capability.

NIR spectroscopy has largely replaced a number of wet chemical analysis methods. With the fiber optics and the integrating sphere sampling techniques, NIR spectroscopy does not require any sampling preparation. It is a fast and precise tool for the nondestructive analysis of liquids, solids and paste-like materials, saving costs by reducing time and reagent use.

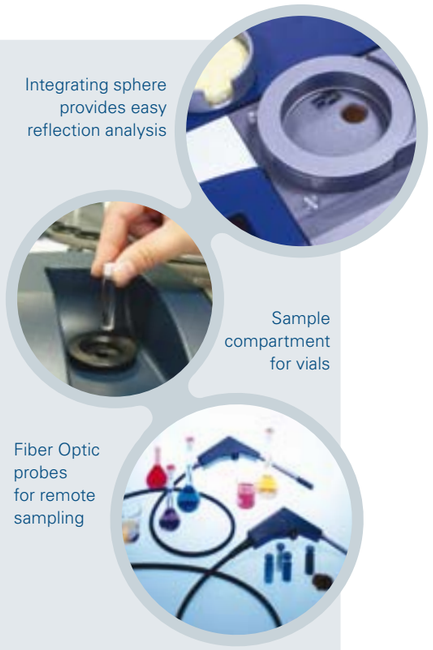

MPA Multi Purpose Analyzer

Bruker's dedicated FT-NIR spectrometer MPA offers everything you need for the analysis of liquids, solids, powders and tablets. Selection of the different measurement accessories is completely software controlled and validated, without the need for any manual exchange.

MPA

MATRIX™ Series

The award winning MATRIX™ series process-ready FT-NIR Spectrometers incorporate state-of-the-art optics for outstanding sensitivity and stability. Available configurations include fiber optic coupling up-to 6 probes and integrating sphere.

MATRIX-I

Process Analytical Technologies

Today, many companies are not only striving to manufacture high-quality products, but also increase production efficiency by installing the analytical systems directly into their production plants. This improves process verifiability and gives the company the opportunity to optimize material use.

Bruker's technology base includes FT-IR, FT-NIR, Dispersive NIR and Raman Spectroscopy. This allows us to offer a choice of analytical solutions based on applications or sampling points. The robust design of our spectrometers enable use in tough conditions in the production plant.

MATRIX-F duplex FT-NIR Spectrometer

MATRIX-F FT-NIR Spectrometers

The award winning MATRIX-F FT-NIR spectrometers allow the direct measurement in process reactors and pipelines, leading to a better understanding and control of the process. Its innovative design provides consistent high-quality results, less downtime and direct method transfer.

MATRIX-MF FT-IR Reaction Monitoring

MATRIX-MF FT-IR Spectrometers

Utilizing the information rich mid-IR region for use in both laboratory and process environments, the MATRIX-MF is a process ready spectrometer that is ideal for real-time monitoring and analysis of chemical and biological reactions.

SENTINEL Dispersive Process Raman

SENTINEL Raman Spectrometer

With patented automatic calibration, curve slit correction for aberration free imaging and the low noise CCD, Bruker's SENTINEL Raman spectrometer brings innovative insight to process monitoring and control applications.

Content:

Time Domain NMR

Time Domain Benchtop NMR Analyzers

the minispec TD-NMR Analyzers

The minispec benchtop product lines utilize Time-Domain (TD-)NMR spectroscopy, a method similar to High-Resolution NMR and Magnetic Resonance Imaging, MRI. Unique permanent magnet and radio frequency (RF) technologies are applied to investigate the sample as a whole, non-destructively and non-invasive.

Turn-key solutions for Quality Control (QC) are offered with straight-forward calibrations comprising well-known international recognized standard methods according to ISO, ASTM and AOCS. the minispec series provide also a sound basis for R&D applications like MRI contrast agent research, droplet size determination of emulations and obesity research

the minispec mq Series

the minispec mq Series

The award winning mq series covers a wide range of applications and offer expansion capabilities for both routine quality control and R&D.

With the addition of innovative accessories and readily exchangeable probe assemblies, the mq series is suited to a full range of time domain NMR measurements. Typical applications include pharmaceutical contactless check weighing, contrast agent analysis, droplet size determination in emulsions, and others.

the minispec LF Series

Bruker's minispec LF Series Whole Body Composition Analyzers provide a precise method for measurement of Lean Tissue, Fat, and Fluid in live mice and rats. The longitudinal studies are possible as the animal is carefully handled without the need for anesthesia. Measurements with the LF Series are done in minutes without the need for any sample preparation.

the minispec LF90

Dedicated Solutions for Industrial Quality Control

the minispec Plus software displays results in seconds

the minispec turn-key analysis workflow

Readily available calibration standards, such as for the spin finish analysis

No sample preparation, just insert sample into the minispec mq_{one}

the minispec mq_{one}

The mq_{one} takes the minispec mq series product line further into the realm of routine industrial applications. The minispec mq_{one} analyzer is not just a benchtop system; it is a dedicated analyzer providing a complete solution off the shelf. With easy installation, comprehensive calibration and calibration transfer standards, the mq_{one} is ready to use in minutes.

the minispec mq_{one} Analyzers

- mq_{one} SFC Analyzer
  Solid-Fat Content (ISO, AOCS)
- mq_{one} Seed Analyzer
  Oil and Moisture (ISO, IUPAC, AOCS)
- mq_{one} Hydrogen Analyzer
  Hydrogen in Fuels (ASTM)
- mq_{one} Spin Finish Analyzer
  Finish on Fibre, Oil-Pick-Up (OPU)
- mq_{one} Polymer Analyzer
  Xylene-soluble in PP
- mq_{one} Total Fat Analyzer
  Precise Fat Quantitation

the minispec mq_{one}

HyperQuant

HyperQuant™ is a benchtop time-domain NMR reader that precisely and quantitatively delivers both the magnetic hyperpolarization and thermal polarization status of a sample. This proprietary solution applies a unique permanent 0.94 Tesla magnet system combined with an innovative MR probe design and novel NMR pulse sequence capabilities. This unique combination enables quantification of the thermal polarization level of ^{13}C-labeled samples using volumes as low as 1 ml. The hyperpolarization enhancement factors can be obtained directly on the sample of interest, without the need for a separate calibration reference.

Features

- Direct quantification of magnetic hyperpolarization and thermal polarization levels
- Calibration-free technology based on direct comparison of hyperpolarized and thermally polarized state
- Turn-key ^{13}C application
- Proven bench-top TD-NMR design
- Unique 0.94 T permanent magnet system
- Only 1 ml of sample volume required
- Tracing of the ^{13}C hyperpolarization decay
- Thermal signal determination with 99% accuracy
- Quantifying concentrations of fully labeled ^{13}C samples
- External trigger interface to HyperSense®
- Applicable to all hyperpolarization methods including DNP and Para-Hydrogen

^{13}C measurement

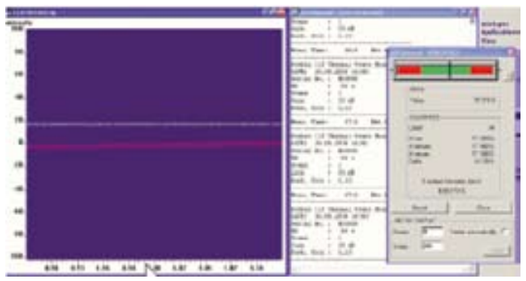

^{13}C TD-NMR signal of the thermally polarized (right) with statistics on the superior restability (left)

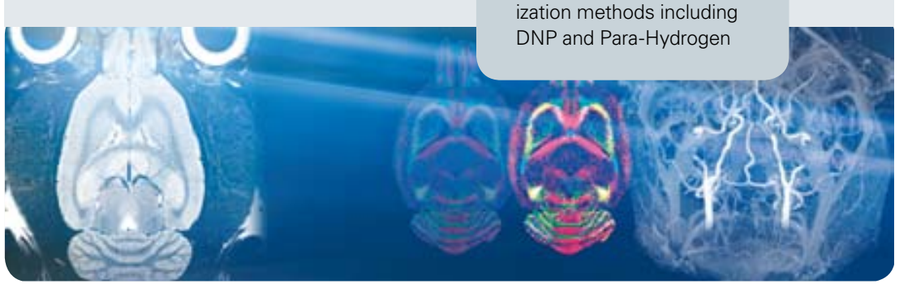

Effect of Hyperpolarization

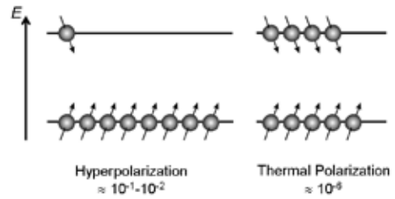

Hyperpolarization

Hyperpolarization promises to be a useful technique with its potential to boost contrast in MRI and sensitivity in solid-state NMR. Hyperpolarization provides a means to increase the nuclear magnetic polarization by orders of magnitude (enhancement factors of 100,000) from the otherwise physical limit of the thermal Boltzmann polarization. Hyperpolarization can be obtained by various mechanisms, both physical and chemical in nature, such as DNP (dynamic nuclear polarization) and parahydrogen induced polarization (PHIP). Typically labeled ^{13}C samples are utilized because of the preferential MR properties of the ^{13}C nucleus.

Direct Quantification

HyperQuant delivers a unique direct quantification of the enhancement factor, by being able to measure both the hyperpolarized and the thermally polarized state of the ^{13}C sample. Thus, it does not require a separate calibration reference.

Applications

For academic researchers and manufacturers of hyperpolarization systems, HyperQuant delivers quantitative measurements for research studies and product validation. In the research field of hyperpolarized agents in MRI or NMR, HyperQuant provides a precise measure of the enhancement factor.

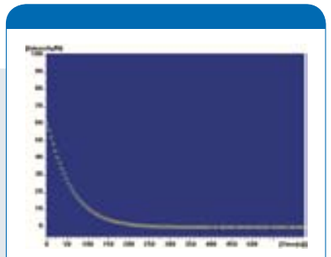

Decay of the Hyperpolarized ^{13}C signal

Quantifying Hyperpolarization

The hyperpolarization is quantified by using a carefully calibrated small flip angle excitation pulse. The measurement hardly affects the polarization state of the sample. Alternatively, HyperQuant can also closely trace the decay rate of the hyperpolarization.

Thermal Polarization

The thermal polarization of ^{13}C labeled samples is enabled by a unique combination of a 0.94 T magnet, a high Q ^{13}C probe (10 MHz) and a multipulse NMR sequence. The plug-and-play concept of the probes allows for easy exchange and handling. In addition, 40 MHz ^{1}H probes are also available.

Pulse Flip Angle Calibration

Key to the precise determination of the enhancement factor is the automatic flip angle calibration to determine and validate both the 90° and 180° pulse length.

Content:

Advanced Analytical Solutions

- XRD, XRF, SC-XRD, AFM, MA, OES, CA

think forward

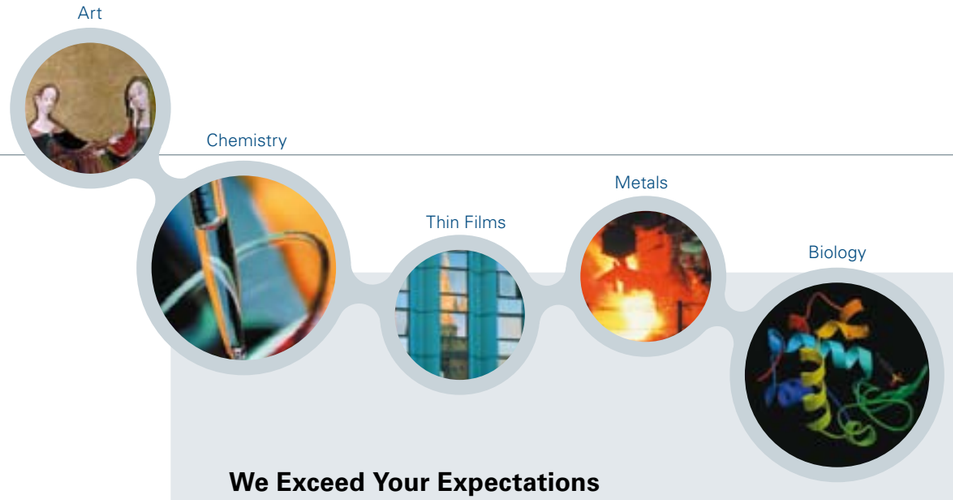

We Exceed Your Expectations

Professional Competence

Bruker AXS is a worldwide market leader in providing advanced X-ray and optical emission systems and complete solutions for structure and elemental analysis using X-ray diffraction (XRD), X-ray fluorescence (XRF/OES) and crystallographic diffraction techniques. Our products fit the analytical requirements of customers in materials research, life science, quality control, and process analysis. They provide essential information about the molecular structure, material and structural parameters of thin film and bulk material as well as elemental composition of solids and liquids.

High-Performance

Bruker AXS X-ray systems emphasize modularity and flexibility, enabling an entry-level system to be reconfigured or upgraded to meet changing requirements. We offer the widest available variety of X-ray sources, optics, sample environments and detectors, along with expert advice on configuring the optimal system. All of our systems and solutions are easy to operate, robust and compact, with degrees of automation ranging from none to one-button operation. Professional training and worldwide service is in place to support the customer.

SUPER SPEED SOLUTIONS

Bruker AXS breaks all records. The SUPER SPEED components ensure breathtaking speed at high-sensitivity resolution – without sacrificing reliability and flexibility. The X-ray diffraction SUPER SPEED SOLUTIONS enable an unprecedented throughput in research and development.

- TURBO X-RAY SOURCE
- VÅNTEC-1 detector – instant diffraction snapshots
- LYNXEYE™ – rapid powder diffraction
- HI-STAR detector – super sensitive XRD²
- VÅNTEC-2000 detector – ultra size XRD²

A History of Innovation Leadership

Bruker AXS is constantly redefining the performance and quality standards in X-ray analysis. Breakthrough innovations and continual improvements upon established techniques provide our customers with analytical possibilities that were considered beyond reach only a short while ago. Examples include our revolutionary detection technologies, multilayer X-ray optics, and ability to perform XRF analysis of light or trace elements.

X-ray Powder Diffraction

Table-top, automated, or scientific workshorse instrumentation

X-ray diffraction expands analytical capabilities down to the nanometer range. Our highly accurate, reliable and fast diffraction solutions are accompanied by an intuitive and clearly laid-out user interface, easy handling, and individual data presentation, as well as perfect integration and communication capabilities.

D8 ADVANCE

D4 ENDEAVOR

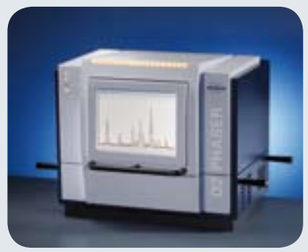

D2 PHASER

Applications

- Crystalline phase identification
- Crystalline phase quantification
- % crystallinity
- Crystallite size determination
- Crystal structure analysis
- Texture and preferred orientation
- Microstrain
- Residual stress
- Depth profiling
- Polymorph screening
- High temperature
- Low temperature
- Humidity
- Phase transition
- Nanoparticles

Powder diffraction at it's best

DAVINCI.DESIGN

The D8 ADVANCE with DAVINCI.DESIGN facilitates a pioneering diffractometer concept, which eliminates the problems of awkward configuration and adjustments once and for all. It is extremely easy to exchange all components and geometries, thanks to the multi-level design:

- DAVINCI.SNAPLOCK: alignment- and tool-free optics change
- DAVINCI.MODE: real-time component recognition, configuration and conflict detection
- DIFFRAC.DAVINCI: graphical representation of the actual goniometer showing all beam path components including their status, enabling immediate measurements as well as the creation of measurement methods.

Total Flexibility with DIFFRAC.Suite

DIFFRAC.Suite is the benchmark program suite for all routine and research applications in powder diffractometry, generally ackowledged in literature as the most innovative, powerful and intuitive software package. DIFFRAC.Suite has a remarkable tradition in introducing most significant scientific innovations into the powder diffraction community, and consequently performed best repeatedly in international round robins for phase identification and ab-initio structure determination.

X-ray Diffraction

Quick-Change Artists without Limits

The capabilities provided by the D8 DISCOVER, laboratory X-ray diffraction enters new frontiers in the nano-world and materials research so that synchrotron measurement campaigns become obsolete in many cases.

D8 DISCOVER

Applications

- Crystalline phase identification
- Crystalline phase quantification
- % crystallinity
- Crystallite size determination
- Crystal structure analysis
- Texture and preferred orientation
- Microstrain and relaxation
- Residual stress
- Layer thickness
- Layer roughness
- Lattice parameter
- Chemical composition
- Lateral structures
- Defects
- Depth profiling
- Real space mapping
- Microdiffraction
- Polymorph screening
- High-temperature
- Low temperature
- Humidity
- Phase transition
- Nanoparticles

High-Throughput Applications

Screening a large number of samples quickly and completely requires dedicated instrumentation and extensive knowledge of the analytical process. Extremely large amounts of data need to be handled, especially in catalyst development and pharmaceutical research. Unique applications from Bruker AXS extract authoritative results from the most varied of sample characteristics, parameters and correlations, e.g.:

- Laser/Video system for precisely focused, automated alignment
- Eulerian cradles 2D Detectors, robotic wafer handling
- Powerful X-ray sources, innovative detectors
- Integrated Analytical Intelligence with POLYSNAP software

Enter the Universe of Nanostructure Analysis

SAXS²

The innovative Small Angle X-ray Scattering System NANOSTAR is the ideal tool for investigating precipitants in bulk materials and macromolecules like protein solutions with a size on the order of 10 to 1000 Ångstrom.

NANOSTAR-U

Applications

- Small Angle X-ray Scattering (SAXS)
- Grazing-incidence SAXS (GI-SAXS)
- Wide Angle X-ray Scattering (WAXS)
- Nanography
- Particle size
- Particle size distribution
- Particle shape
- Orientation distribution
- Particle distances
- Low temperature
- High-temperature
- Glazing Incidence Small Angle X-ray Scattering (GISAXS)

D8 FABLINE

The D8 FABLINE is the only X-ray metrology instrument with four combined applications:

- High-Resolution X-Ray Diffraction (HRXRD)
- X-ray Reflectivity (XRR)
- Micro X-ray Fluorescence (µXRF)
- Grazing incidence Diffraction (GID)

Göbel and Montel Mirror

The highest performance can only be achieved with the most modern instruments. With the invention of the Göbel Mirror, Bruker AXS raised the standards for diffraction and SAXS. Göbel Mirrors are X-ray optics with incomparable precision: The mirrors have length and width in the centimeter range, the contour accuracy is in the micrometer range and the roughness is in the nanometer range.

- Maximum flux
- Perfect beam homogeneity
- Highest spectral purity
- Bragg-Brentano, parallel beam, or focusing geometries

X-ray Fluorescence Analysis

Defining the World of Elements in Seconds

X-ray fluorescence spectrometry is the most effective way to perform multi-elemental analysis determining concentrations in all forms of samples: solids, powders and liquids. Based on the renowned XFlash® silicon drift detector technology Bruker AXS energy dispersive X-ray fluorescence (EDXRF) systems offer highest analytical precision and stability. The S2 PICOFOX allows the analysis of thin films as well as the analysis of traces down to 0.1 ppb using total reflection X-ray fluorescence (TXRF). The S2 RANGER with TouchControl™ provides you with instant answers for element concentrations from Na to U in unknown samples.

S2 PICOFOX: True Trace Element Analysis by TXRF

Applications

- Fresh water, sea water
- Sewage, sludge
- Pharmaceuticals
- Blood, urine
- Proteins, macromolecules
- Food, dietary supplements
- Wine, beverages
- Nanoparticles
- Washcoats
- Contaminations
- Aerosols
- Thin films

S2 RANGER: EDXRF with TouchControl™

Applications

- Petrochemicals
- Minerals and mining
- Slags
- Cement
- Geology
- Pharmaceuticals
- Metals and alloys
- Soil, sediments and waste

TouchControl™

Reliable results and error-free instrument operation is the key to success. This is why Bruker AXS developed the intuitive instrument operation with touch screen. With minimum training, even inexperienced operators can obtain optimum results. And your analytical data are safe due to the unique TouchControl™ concept.

- Easy-to-use – intuitive operation
- No mouse or keyboard needed
- Minimal training required
- Immediate results on the touch screen
- Compact all-in-one design

Unrivalled

Analytical Performance

Our wavelength dispersive X-ray fluorescence (WDXRF) systems provide you with excellent analytical results for elements from Be to U in your samples. They feature high accuracy and the best achievable precision for effective process and quality control. They are reliable and robust for all industrial applications, yet flexible and powerful for all non-routine applications in research and development.

S8 TIGER - S8 LION: Excellence in WDXRF

S8 LION

Applications

- Cement
- Industrial Minerals
- Mining

S8 TIGER: TouchControl™ and SampleCare™

Applications

- Petrochemicals
- Plastics and polymers
- Cement
- Geology
- Metals and alloys
- Precious metals
- Minerals and mining
- Glass and ceramics
- Chemicals and catalysts
- Pharmaceuticals
- Soil, sediments and waste
- Foods

Intuitive easy operation TouchControl™

Easiest operation due to intuitive touchscreen interface tailored for industrial environments

- No operator training required
- Standalone operation in tough environments (no PC, mouse or keyboard)
- Unmatched data integrity
- Online language switch with free selection: English, German, French, Chinese, Russian, Spanish, Korean

Micro-X-ray Fluorescence Analysis

M1 and M4 Tabletop Micro-XRF Spectrometer Series

M4 TORNADO

µ-XRF is the method of choice for the elemental analysis of inhomogeneous or irregularly shaped samples as well as small samples or even inclusions. Bruker's M1 and M4 tabletop spectrometers offer maximum versatility for all applications, whether for routine analysis in quality control or for individual setups analyzing special samples.

Applications

- Minerals
- Metals and alloys
- Electronic components (RoHS)
- Particles
- Forensics
- Layers
- Art conservation, archeology

M1 MISTRAL and M1 ORA

Applications

- Jewelry
- Metals and alloys
- Layers (M1 MISTRAL)

Highlights of Innovation Leadership

Using policapillary optics Bruker's micro-XRF spectrometers can illuminate areas down to 30 µm in diameter with maximum X-ray intensity. The integrated Peltier-cooled XFlash® Silicon Drift Detectors process highest count rates at optimal energy resolution. Short measurement times and fast sample stages lead to extremely quick results regarding the elemental composition of a sample.

- Spatially resolved analysis of arbitrarily shaped samples, including fine structures
- No cooling media or consumables required
- Non-destructive measurement without sample preparation
- Outstanding analytical flexibility

ARTAX - High Spatial Resolution, Portable, Non-destructive

The ARTAX is a unique, portable micro-XRF spectrometer designed to meet the requirements for a spectroscopic analysis of immobile and valuable objects on site, i.e. in archeometry and restoration. It can be used for both spot measurements and high-resolution 1D and 2D mapping.

Applications

- Non-destructive element analysis in
- Art conservation, archeology and archeometry
- Metals, alloys, sheet metal
- Thin layers

ARTAX

Handheld XRF Spectrometry

XRF Elemental Analyzer

The Bruker handheld XRF analyzers provide quick and easy non-destructive analysis. The S1 TURBO^{SD} and S1 SORTER enable fast analysis and ID of most alloys. The TRACER III-V and III-SD tube based systems include the Bruker /NASA joint patented vacuum system and high-resolution detector allows for laboratory grade results of elements from Mg to U.

Applications

- Analysis of metal alloys for Positive Material Identification (PMI)
- Non-destructive testing with grade ID and chemistry
- Light element capability: Mg, Al, Si, P
- Scrap metal recycling
- QA/QC in the manufacturing environment

S1 TURBO^{SD}

TRACER III-V

Applications

- Art conservation, archaeology and archeometry
- Research and teaching tool for universities
- Research and development
- Selected by leading museums like the Getty and MOMA

Highlights of Innovation Leadership

- Light element analysis – Mg, Al, Si, P, S and Cl without vacuum or He
- SDD provides rapid analysis and ID for alloys
- TÜV SÜD certification – trusted the world over!
- Joint Bruker/NASA patent, earned NASA's Space Seal for vacuum technology
- Tube-based XRF for handheld elemental analysis – no radioactive materials
- PDA based analyzer

Optical Emission Spectrometry

High-End Elemental Analysis of Metals

Spark optical emission spectrometers (S-OES) are the ideal instruments for all types of metals. From pure metal trace analysis to high alloyed grades, spark OES covers the complete range from sub-ppm to percentage levels. All relevant elements can directly be analyzed simultaneously.

Spark spectrometer instruments cover all types of metal applications. Our range of high-end instruments allows our customers to elevate their business into new levels of quality and process control.

Q4 TASMAN/Q6 COLUMBUS – Benchtop metals analyzer

Highlights of Innovation Leadership

Pioneering Channeltron technology

Q8 MAGELLAN and Q6 COLUMBUS feature the latest technology in photomultiplier detectors:
- Lowest dark current
- Large dynamic range
- Highest sensitivity
- Improved limits of detection
- Impressive stability and repeatability

Spark stand with co-axial argon flow

The innovative co-axial argon flow represents the culmination of our efforts to further improve performance:
- Extended cleaning intervals
- Low argon consumption
- Better analytical quality
- Reduced operation costs

Q4 TASMAN (CCD)

Q6 COLUMBUS (CPM)

Channel photomultiplier (CPM)

Pneumatic sample clamp

Metal samples

Photomultiplier optic

Measuring results

Applications

Iron and steel and its alloys
- Aluminium and its alloys
- Copper and its alloys
- Nickel and its alloys
- Cobalt and its alloys
- Magnesium and its alloys
- Lead and its alloys
- Tin and its alloys
- Titanium and its alloys
- Zinc and its alloys

Q8 CORONADO – Analysis automation

Applications

- Process analysis of steels
- Process analysis of cast iron
- Process analysis of aluminum
- Process analysis of copper

Q8 MAGELLAN – Stationary vacuum spectrometer

Applications

Elemental analysis of:
- Iron and steel alloys and its traces
- Nitrogen in steel
- Aluminium alloys and its traces
- Copper alloys and its traces
- Oxygen in copper
- Nickel alloys and its traces
- Cobalt alloys and its traces
- Magnesium alloys and its traces
- Tin alloys and its traces
- Lead alloys and its traces
- Titanium alloys and its traces

Highlights of Innovation Leadership

Complete software package

Spectrometer software QMATRIX is an easy to use front-end interface:
- QMATRIX for the routine analysis
- Regression software for calibration
- SQL for data treatment

Automation control software QMATION

The Q8 CORONADO is controlled by the powerful QMATION software:
- Net framework technology
- Graphical user interface for providing system status

Gas Analyzers - C, S, O, N, H in Solids

Our innovative analysis instruments allow automatic and fast determination of Carbon, Sulfur, Oxygen, Nitrogen and Hydrogen in solids. Our instruments provide highly accurate measurement within a short analysis time and are highly reliable and userfriendly.

The state-of-the-art technology allows not only the use for quality control but also in the various fields of material development. The “One-4-All” analysis software is clear and simply structured and universal for all instruments.

G4 ICARUS HF

CS analyzer with high-frequency furnace

G4 ICARUS TF

CS analyzer with high-temperature tube furnace

Highlights of Innovation Leadership

CS-Analysis

G4 ICARUS analyzers are designed for simultaneous or individual, fast and accurate determination of carbon and sulfur in various metallic and non-metallic materials.

G4 ICARUS features:

- Continuously adjustable HF furnace power for optimum sample combustion
- Alternative version with external high-temperature tube furnace up to 1550° C
- Short analysis time, nearly maintenance-free operation
- Long term stable, selective solid-state NDIR detectors
- Automatic base line compensation/zero adjustment and Automatic Level Control

Applications

- Iron, steel and alloys
- Aluminum and alloys
- Titanium and alloys
- Zirconium and alloys
- Ores, minerals
- Coal, coke and ash
- Catalysts

G4 ICARUS HF ceramic crucible

G4 PHOENIX DH tube Ø 30 mm

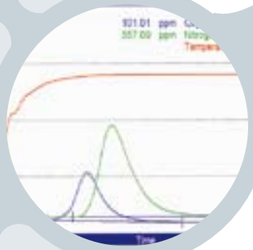

G4 ICARUS TF ceramic boat

One-4-All software

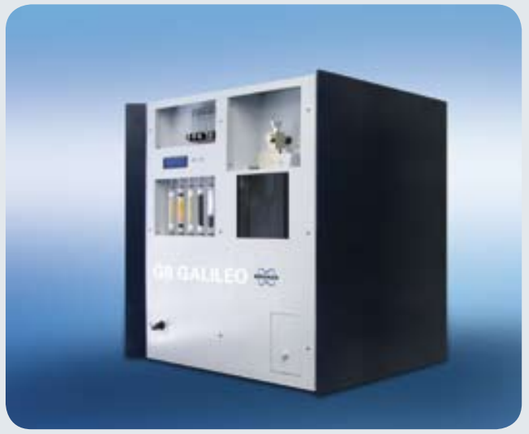

G8 GALILEO

O, N, H analyzer

Applications

- Iron, steel and alloys
- Aluminum and alloys
- Copper and alloys
- Titanium and alloys
- Zirconium and alloys
- Ores
- Ceramics
- Minerals

Highlights of Innovation Leadership

ON/H-Analysis

G8 GALILEO delivers fast and automatic determination of oxygen, nitrogen and hydrogen in solids by carrier gas method, melt and hot extraction. Different configurations for simultaneous or single element determination are available.

G8 GALILEO features:

- Electrode furnace with programmable temperature up to 2500°C, contact-free optical sensor for temperature measurement
- Selective solid-state NDIR-detector for CO, long term stable thermal conductivity cell for N_2/H_2
- Optional automatic furnace cleaning system with dust removal and optional automatic crucible changer
- External furnace for diffusible Hydrogen with ramping functions optional

G4 PHOENIX

Determination of diffusible hydrogen

Applications

- Steel
- Aluminum
- Weld material
- Weld seams

Microanalysis (EDS) and Electron Backscatter Diffraction (EBSD)

Accurate, Fast and Easy to Use

Rough surfaces, particles, thin layers, bulk samples … The QUANTAX family of EDS instruments tackles even your toughest challenges with unprecedented speed, accuracy and ease-of-use. The unique LN_2-free XFlash® Silicon Drift Detectors (SDD), together with our state-of-the-art Hybrid Pulse Processor technology, deliver both the highest available energy resolution and over ten times the speed of conventional Si(Li)-based systems.

The QUANTAX EDS microanalysis system works in conjunction with Scanning Electron Microscopes, as well as Transmission Electron Microscopes (TEM) with the worldwide first SDD designed for TEM - the XFlash® 5030 T. In addition QUANTAX also provides the option of EBSD analysis with the fully integrated QUANTAX CrystAlign.

QUANTAX 800

Applications

- Metals and alloys
- Semiconductors
- Layers and coatings
- Minerals
- Glasses
- Nano-materials
- Plastics and organic solids
- Biological samples
- Forensics

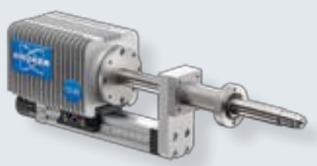

XFlash® 5000 series for SEM

e-Flash for EBSD

XFlash® 5030 T for TEM

Highlights of Innovation Leadership

QUANTAX EDS for Nanoanalysis

- With XFlash® world wide leading SDD technology
- For SEM and TEM
- High collecting efficiency
- Unmatched energy resolution
- Superb light element performance

QUANTAX CrystAlign - Discover Fast and Easy to Use EBSD

- Revolutionary in-situ tiltable e⁻Flash detector
- Simultaneous EBSD and EDS analysis
- Live data processing during acquisition
- Fast analysis and minimum drift

Chemical Crystallography

Absolute Clarity for your Results

Single Crystal X-ray diffraction is the method of choice for determining the 3-dimensional structure of any kind of chemical compound. The method provides accurate and precise measurements of molecular dimensions in a way that no other investigative technique can begin to approach. The APEX II line of Chemical Crystallography Solutions features easy to use, state-of-the-art software, the fastest, most sensitive low noise APEX II CCD detector, integrated with the most flexible and precise sample motion available. A broad selection of dedicated X-ray sources including sealed tube microfocus tube, rotating anodes and dual wavelength options completes the system to give you the best data possible. The newly released APEX DUO provides two X-ray sources and enables the scientist to select Mo- or Cu-radiation for absolute structure determination just with a mouse click.

Applications

- Structural determination of new molecules and minerals
- Comprehensive treatment of absorption effects by intuitive correction methods
- Absolute structure determination on molybdenum and copper radiation
- Integrated treatment of twinned samples
- Electron charge density studies by high-angle diffraction
- Structural investigation of high-pressure phases
- Modulated structures
- Diffuse scattering

Highlights of Innovation Leadership

APEX II Detector

The APEX II CCD detector provides ultimate sensitivity for data collection on small or weakly diffracting crystals.

- 4 K CCD Chip (16 megapixel)
- 1:1imaging, no reduction taper
- Highest signal to noise
- Superior dynamic range
- Anti blooming mode
- Optimized for Cu- and Mo-radiation

Automated Crystal-Structure Analysis

Walk-up X-ray Structure Determination for Chemists

Bruker AXS' SMART X2S is the first benchtop X-ray crystallography system for fully automated 3D chemical structure determination. It is designed for use by chemists who have no special training in crystallography.

The SMART X2S takes small molecule structure determination to the next level of convenience by automating the previously difficult aspects of X-ray structure determination, from sample loading through data collection all the way to report generation and data archiving. Its compact design, low maintenance, low cost of ownership and easy and intuitive operation through a touch screen graphical interface are truly groundbreaking

Highlights of Innovation Leadership

AUTOSTRUCTURE™

The ground-breaking program suite for fully automatic determination of 3D crystal structures of organic and inorganic molecules from X-ray data. It allows solving and refining structural parameters routinely, providing the crucial tool to make accurate chemical X-ray structure determination quick and easy.

- Fast, reliable, intuitive-to-use, fully-automated
- Results verified using IUCr standard structure checkers
- Cascades through Patterson, direct- and dual-space methods to increase structure solution success

SMART X2S

Applications

- Structural information for routine samples when you need it – quickly, reliably and cost effectively
- X-ray structure determination with no or little background in crystallography
- Unambiguous synthesis control for working chemists

Biological Crystallography

High-Class Performance of True Brilliance

No other field in crystallography has developed as rapidly as biological crystallography. This is because single crystal diffraction is the ideal tool for obtaining accurate structural models of the molecules of life: such as nucleic acids, proteins, and viruses. The sheer volume and complexity of structural biology projects has steadily increased in recent years. In order to meet the demands of structural biologists Bruker AXS has further improved the performance and ease-of-use of its solutions. Today we offer systems with highest intensity, sensitivity, and reliability. Consequently, the investigation of weakly diffracting samples and small crystals for a complete in-house data collection or prior to a synchrotron trip has become a routine.

X8 PROSPECTOR

Features

- Designed for fast protein screening
- Intuitive software
- Minimal down-time
- Lowest cost of ownership
- Small footprint
- IμS microfocus source with three years of warranty on the tube
- Most sensitive 16 Mega pixel CCD detector

Highlights of Innovation Leadership

The IμS microfocus source is an outstanding X-ray source for point-focus applications combining the advantage of a traditional sealed tube and a rotating anode generator. Running at only 30W, the tube has a long lifetime and water cooling is not required. Despite this low power consumption, the beam produced has a high brilliance and unprecedented high flux, outperforming a traditional 300 micron rotating anode generator.

Scanning Probe Microscopy

Analyze Nanometer Size Surface Structures within Minutes

The N8 range of instruments provides a complete set of solutions for atomic force and scanning probe microscopy (SPM). All systems are based on the unique NANOS SPM head. These instruments can accurately analyze a wide variety of different sample characteristics associated with SPM. It is only a matter of selecting the appropriate measurement mode and probe. Supported are contact mode, non-contact mode, intermittent contact mode, scanning tunneling microscopy, magnetic and electrostatic force microscopy, and many more.

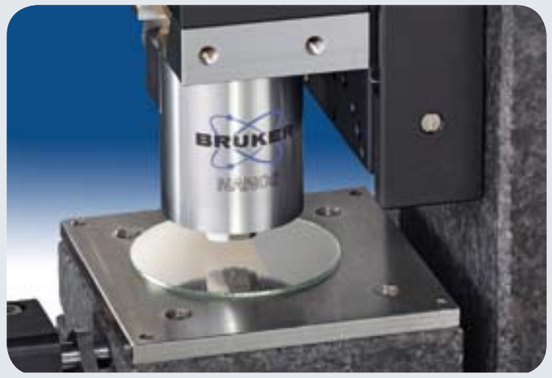

Highlights of Innovation Leadership

NANOS

The NANOS is the only SPM head that approximates the size and shape of a standard microscope objective. It therefore fits any commercially available microscope and can be used to unite optical and SPM analysis in a single instrument.

- Changing between optical microscopy and SPM by a simple turn of the microscope turret
- Unique feedback cycle for compact SPM head design, yet providing fast and accurate results
- Contact and oscillation modes (non-contact, intermittent contact)
- Easy to replace measuring probe, no adjustment required
- Wide variety of measuring modes supported
- Can be used to upgrade existing research grade microscopes

N8 NEOS

The N8 NEOS combines optical microscopy and scanning probe microscopy in a single, optimized set-up that reduces vibration and thermal drift. The combination of the NANOS measuring head and a powerful optical microscope allows unequalled productivity in performing high-resolution surface inspection.

High-Class Performance of True Brilliance

N8 RADOS

The N8 RADOS combines a high quality research microscope, a scriber and the NANOS AFM measuring head on a single automated platform. After locating a region of interest with the microscope the AFM scan is started at the press of a button. After completion the press of another button can be used to scribe the location on the sample.

N8 TITANOS

The N8 TITANOS provides sub-nanometer resolution on a fully-automated, in-line capable and rigid single-plane setup for the analysis of samples with a size of up to 300 mm². The open architecture accommodates the NANOS AFM measuring head, while allowing various other optical measuring devices or microscopes to be added to the system.

Applications

- Semiconductors
- Hard Disk/CD/DVD inspection
- Material science
- Nano-particles and structures
- Metrology
- Polymers
- Catalysts
- Life Science

Highlights of Innovation Leadership

Alignment-free cantilver & automated routines guarantee fastest time to results

- No moving part for beam alignment, tip saving auto-retract features
- Tip deflection & amplitude automatically calibrated in nm not V
- Compatible with bright field, dark field, DIC, fluorescence microscopy and even Raman
- Unobstructed sample view, the sample image is observed, not the back of the cantilever.

Content:

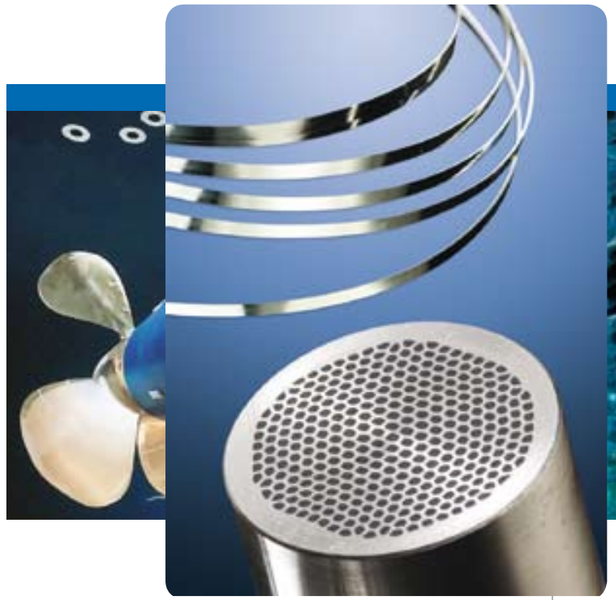

Advanced Superconductors

Authority in Superconductivity

Manufacturing Site

Bruker EAS - low temperature superconductors

Bruker EAS, based in Hanau, Germany, has been a world leading manufacturer of low temperature superconductor (LTS) wire for over 40 years, an experience unparalleled in the industry. Its LTS wire is used for clinical MRI, scientific instruments including NMR, EPR, and FTMS, as well as for large-scale research applications in high-energy physics and fusion projects. We continue to be a partner in major superconductivity projects worldwide, with a track record of excellence.

Bruker HTS - high-temperature superconductors

Bruker HTS has now become Europe's leading company in the area of high-temperature superconductivity, a key technology of the 21st Century. Our research and development teams of over 30 people develop Bismuth (Bi) and Yttrium (Y)-based high-temperature superconducting technologies. Bruker HTS provides industrial superconductors and application solutions to a wide range of customers.

Hydrostatic Extrusions Limited - hydrostatic extrusion

Developed by Asea, the hydrostatic extrusion process uses a fluid compression medium under very high-pressure to force material through a precision made die.

Applications

Rotating Machines

High-temperature superconductors (HTS) now overcome the limitations of these machines, replacing copper wire with new, virtually resistance-free superconductors. HTS technology permits new machine designs, combining substantial weight and size reduction together with operational benefits.

Cables

Providing dependable electricity in today's megacities, across networks, and over vast distances has become a critical challenge in our increasingly energy demanding world. HTS play a vital role in building the power cable of the future. Their unique ability to carry currents at over ten times the amount of conventional wires, provide substantially lower losses, and allow more compact designs makes them ideally suited to meet the requirements of densely populated urban environments and critical high-power links.

Magnets

Superconducting magnets represent by far the largest market for superconducting technologies today. Low temperature and high-temperature superconductors provide vast benefits to increase performance and efficiency

Fault Current Limiters

Electric power disruptions cause hundreds of millions of dollars worth of economic loss every year to the world's leading economies. Worldwide energy demand is increasing rapidly, requiring new solutions to dramatically improve the reliability of our energy supply. Fault Current Limiters are new devices, using the unique electrical properties of HTS to almost instantaneously protect power grids against short circuits and thereby prevent costly outages.

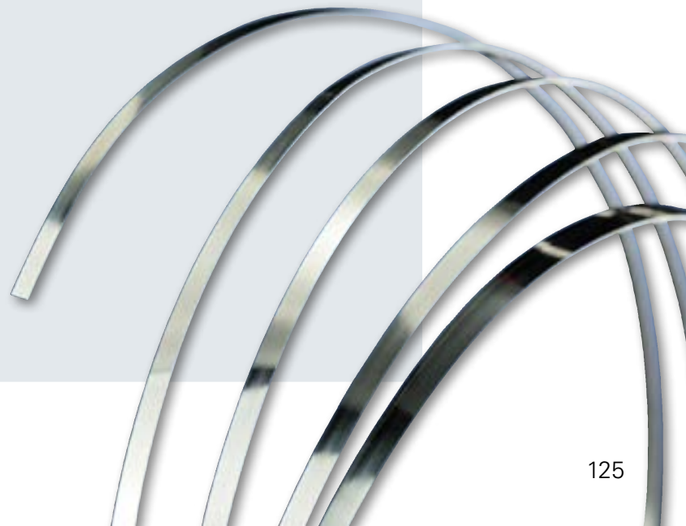

Low Temperature Superconductors (LTS)

Our LTS products are used in a wide range of applications, including clinical MRI and ultra-high-field NMR as well as energy storage, high-energy physics and fusion research, addressing the world's energy needs.

NbTi Superconductors

NbTi superconductors are high-performance superconductors and the workhorse of the world's superconductor industry. Their major market is in clinical MRI, with well over 1,000,000 kilometers of NbTi wire produced to date. Other large markets include Nuclear Magnetic Resonance (NMR) Spectroscopy, particle accelerators for high-energy

Customized Superconductors

Our customized products include superconductors with highly specialized performance characteristics. We have delivered specially alloyed or reinforced conductors and conductors with ultra thin filaments to some of the most demanding customers world wide. Between 2000 and 2005 we had delivered over 40,000 km of thin filament NbTi conductors to the LHC particle accelerator project at CERN. By 2007 we delivered over 60 km of aluminum clad NbTi cables with a total of 15,000 kilometers of NbTi wire to the Euratom "Wendelstein" fusion project.

Nb3Sn Superconductors

Nb3Sn superconductors are high-performance superconductors and the gold standard of the world's superconductor industry. Their distinguishing characteristic among LTS conductors is the extraordinary performance under ultra-high magnetic fields. They are indispensable for the high-field magnets in Nuclear Magnetic Resonance (NMR) and Mass Spectroscopy (FTMS), which today routinely exceed 20 Tesla. Large fusion projects also rely on Nb3Sn for magnets exceeding field strengths of 14 Tesla, paving the way to a future with clean and abundant energy.

The portfolio encompasses innovative "Powder-In-Tube" Nb3Sn conductors, which combine extremely high-currents with unmatched workability and high-field performance.

High-Temperature Superconductors (HTS)

Bruker HTS is a leading manufacturer of HTS materials and devices, based on its broad conductor technology platform. Bruker HTS products and services enhance the reliability and efficiency of electrical power grids and large energy demanding applications. Conductors and components made by Bruker HTS are used to build a new generation of compact high-power devices such as motors, generators, cables and transformers as well as high-field magnets for medical and research applications.

HTS Tapes

Bruker HTS tape products are able to carry more than ten times the electricity of a comparable copper wire. They are designed with electric power and magnet applications in mind. Bruker HTS commercially produces HTS tapes of the highest quality, using state-of-the-art production technology. Our products can be optimized to meet a large range of demanding applications. All Bruker HTS tapes are available with reliable electrical insulation.

Current Leads

Today's superconducting applications operate at temperatures as low as -270° Celsius. Current leads transfer electric current from room temperature to these extremely low temperature operating conditions. Our robust HTS technology reduces heat leakage to the cryogenic envelope by an order of magnitude and is used in a wide range of applications, from MRI to large scale and cryogen free magnets.

Coils

HTS coils are used for a wide range of applications in magnet and electric power technology. In all of these applications, the end-user benefits from reduced operating cost, a more compact design, and high reliability of operation.

Roebel Conductors

Roebel conductors are designed for high total currents. The transposition adds the advantage of equivalence of elementary tapes. This is of benefit for magnets as well as for AC applications (low loss). The Roebel conductors may be made by an odd number of transposed tapes, bare or insulated; the actual transposition scheme is usually designed to fit the requirements of the application. This cable has the advantage of high-mechanical flexibility and high-current at the same time.

Metal Matrix Extrusions

Our hydrostatically extruded metal product line includes Cuponal™ copper clad aluminum wire and sections for the aircraft industry and electric power equipment. We also offer extrusion services for aluminum, superconductors and other alloys.

Cuponal

Cuponal is a bi-metal conductor developed to provide an economic alternative to solid copper. CUPONAL is produced by the hydrostatic extrusion process, and consists of a solid core of electrical grade aluminum with a pressure bonded outer layer of high-conductivity copper.

CUPONAL therefore offers economic and weight saving advantages over solid copper, while retaining the surface properties of a copper busbar. It is often possible to substitute a copper bar with a Cuponal bar of equal dimensions. This yields the maximum cost saving.

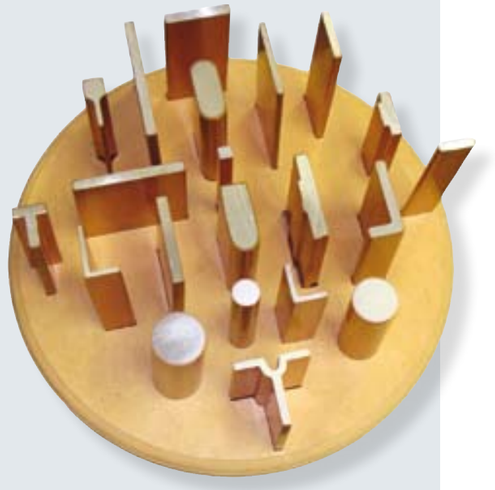

Tolling Service

Materials extruded by the hydrostatic process exhibit very important characteristics of uniform fine grain structure, high-dimensional accuracy and has cross-sectional relationships identical to the input material. This delivers a high-quality feedstock material for onward processing with less waste.

Hydrostatically extruded aluminum, in particular, requires little or no further preparation for operations such as impact extrusion or forging.

Composite materials, e.g. superconductors, where there is a requirement for exact replication of cross-sectional parameters, can only be extruded by the hydrostatic process.

Tables and Others Useful Information

NMR Tables

Isotopes sorted according to spin and nucleon numbers

		Isotope	Spin
1	H	Hydrogen	1/2
3	H	Tritium *	1/2
3	He	Helium	1/2
13	C	Carbon	1/2
15	N	Nitrogen	1/2
19	F	Fluorine	1/2
29	Si	Silicon	1/2
31	P	Phosphorus	1/2
57	Fe	Iron	1/2
77	Se	Selenium	1/2
89	Y	Yttrium	1/2
103	Rh	Rhodium	1/2
107	Ag	Silver	1/2
109	Ag	Silver	1/2
111	Cd	Cadmium	1/2
113	Cd	Cadmium	1/2
115	Sn	Tin	1/2
117	Sn	Tin	1/2
119	Sn	Tin	1/2
123	Te	Tellurium	1/2
125	Te	Tellurium	1/2
129	Xe	Xenon	1/2
169	Tm	Thulium	1/2
171	Yb	Ytterbium	1/2
183	W	Tungsten	1/2
187	Os	Osmium	1/2
195	Pt	Platinum	1/2
199	Hg	Mercury	1/2
203	Tl	Thallium	1/2
205	Tl	Thallium	1/2
207	Pb	Lead	1/2
209	Po	Polonium *	1/2
211	Rn	Radon *	1/2
225	Ra	Radium *	1/2
239	Pu	Plutonium *	1/2
251	Cf	Californium *	1/2
2	H	Deuterium	1
6	Li	Lithium	1
14	N	Nitrogen	1
7	Li	Lithium	3/2
9	Be	Beryllium	3/2
11	B	Boron	3/2
21	Ne	Neon	3/2
23	Na	Sodium	3/2
33	S	Sulfur	3/2
35	Cl	Chlorine	3/2
37	Cl	Chlorine	3/2
39	K	Potassium	3/2
41	K	Potassium	3/2
53	Cr	Chromium	3/2
61	Ni	Nickel	3/2
63	Cu	Copper	3/2
65	Cu	Copper	3/2
69	Ga	Gallium	3/2
71	Ga	Gallium	3/2
75	As	Arsenic	3/2
79	Br	Bromine	3/2
81	Br	Bromine	3/2
87	Rb	Rubidium	3/2
131	Xe	Xenon	3/2
135	Ba	Barium	3/2
137	Ba	Barium	3/2
139	Ce	Cerium *	3/2
155	Gd	Gadolinium	3/2
157	Gd	Gadolinium	3/2
159	Tb	Terbium	3/2
189	Os	Osmium	3/2
191	Ir	Iridium	3/2
193	Ir	Iridium	3/2
197	Au	Gold	3/2
201	Hg	Mercury	3/2
227	Ac	Actinium *	3/2
231	Pa	Protactinium *	3/2
17	O	Oxygen	5/2
25	Mg	Magnesium	5/2
27	Al	Alumin(i)um	5/2
47	Ti	Titanium	5/2
55	Mn	Manganese	5/2
67	Zn	Zinc	5/2
85	Rb	Rubidium	5/2
91	Zr	Zirconium	5/2
95	Mo	Molybdenum	5/2
97	Mo	Molybdenum	5/2
99	Ru	Ruthenium	5/2
101	Ru	Ruthenium	5/2
105	Pd	Palladium	5/2
121	Sb	Antimony	5/2
127	I	Iodine	5/2
141	Pr	Praeseodymium	5/2
145	Pm	Promethium *	5/2
151	Eu	Europium	5/2
153	Eu	Europium	5/2
161	Dy	Dysprosium	5/2
163	Dy	Dysprosium	5/2
173	Yb	Ytterbium	5/2
185	Re	Rhenium	5/2
187	Re	Rhenium	5/2
229	Th	Thorium *	5/2
237	Np	Neptunium *	5/2
241	Am	Americium *	5/2
243	Am	Americium *	5/2
10	B	Boron	3
39	Ar	Argon *	7/2
43	Ca	Calcium	7/2
45	Sc	Scandium	7/2
49	Ti	Titanium	7/2
51	V	Vanadium	7/2
59	Co	Cobalt	7/2
123	Sb	Antimony	7/2
133	Cs	C(a)esium	7/2
139	La	Lanthanum	7/2
143	Nd	Neodymium	7/2
145	Nd	Neodymium	7/2
147	Sm	Samarium	7/2
149	Sm	Samarium	7/2
165	Ho	Holmium	7/2
167	Er	Erbium	7/2
175	Lu	Lutetium	7/2
177	Hf	Hafnium	7/2
181	Ta	Tantalum	7/2
235	U	Uranium *	7/2
245	Cm	Curium *	7/2
249	Bk	Berkelium *	7/2
253	Es	Einsteinium *	7/2
73	Ge	Germanium	9/2
83	Kr	Krypton	9/2
87	Sr	Strontium	9/2
93	Nb	Niobium	9/2
99	Tc	Technetium *	9/2
113	In	Indium	9/2
115	In	Indium	9/2
179	Hf	Hafnium	9/2
209	Bi	Bismuth	9/2
138	La	Lanthanum	5
212	Fr	Francium *	5
50	V	Vanadium	6
176	Lu	Lutetium	7

* Unstable isotope with lifetime suitable for NMR.

NMR Frequency Tables

NMR Frequencies vs. Bruker Field Strengths – sorted by increasing atomic number

Isotope		Spin	Nat. Abund. (%)	Receptivity		Larmor Frequencies (MHz) vs. Bruker Field Strengths (Tesla)											
				Natural rel. ^{13}C	Molar rel. ^{1}H	Freq. to 3 decimals are experimental for IUPAC Standards; freq. to 2 dec. are calculated from magn. moments											
						7.04925	9.39798	11.7467	14.0954	16.4442	17.6185	18.7929	19.9673	21.1416	22.3160	23.4904
1	H	1/2	99.9885	5.87E+03	**1.00E+00**	**300.130**	**400.130**	**500.130**	**600.130**	**700.130**	**750.130**	**800.130**	**850.130**	**900.130**	**950.130**	**1000.130**
2	H	1	0.0115	6.52E−03	9.65E−03	46.072	61.422	76.773	92.124	107.474	115.150	122.825	130.500	138.175	145.851	153.526
3	H	1/2		-	1.21E+00	320.131	426.795	533.459	640.123	746.786	800.118	853.450	906.782	960.114	1013.446	1066.778
3	He	1/2	1.34E-04	3.48E−03	4.42E−01	228.636	304.815	380.994	457.173	533.352	571.441	609.531	647.620	685.710	723.799	761.889
6	Li	1	7.59	3.79E+00	8.50E−03	44.167	58.883	73.600	88.316	103.032	110.390	117.748	125.106	132.464	139.822	147.180
7	Li	3/2	92.41	1.59E+03	2.94E−01	116.642	155.506	194.370	233.233	272.097	291.529	310.961	330.393	349.825	369.257	388.688
9	Be	3/2	100.0	8.15E+01	1.39E−02	42.174	56.226	70.277	84.329	98.381	105.407	112.433	119.459	126.485	133.510	140.536
10	B	3	19.9	2.32E+01	1.99E−02	32.245	42.989	53.732	64.476	75.220	80.591	85.963	91.335	96.707	102.079	107.451
11	B	3/2	80.1	7.77E+02	1.65E−01	96.294	128.378	160.462	192.546	224.630	240.672	256.714	272.755	288.797	304.839	320.881
13	C	1/2	1.07	**1.00E+00**	1.59E−02	75.468	100.613	125.758	150.903	176.048	188.620	201.193	213.765	226.338	238.910	251.483
14	N	1	99.636	5.90E+00	1.01E−03	21.688	28.915	36.141	43.367	50.594	54.207	57.820	61.433	65.046	68.659	72.273
15	N	1/2	0.364	2.23E−02	1.04E−03	30.423	40.560	50.697	60.834	70.971	76.039	81.107	86.176	91.244	96.312	101.381
17	O	5/2	0.038	6.50E−02	2.91E−02	40.687	54.243	67.800	81.356	94.913	101.691	108.469	115.248	122.026	128.804	135.582
19	F	1/2	100.0	4.89E+03	8.32E−01	282.404	376.498	470.592	564.686	658.780	705.827	752.874	799.921	846.968	894.015	941.062
21	Ne	3/2	0.27	3.91E−02	2.46E−03	23.693	31.587	39.482	47.376	55.270	59.217	63.165	67.112	71.059	75.006	78.953
23	Na	3/2	100.0	5.45E+02	9.27E−02	79.390	105.842	132.294	158.746	185.198	198.424	211.650	224.876	238.101	251.327	264.553
25	Mg	5/2	10.00	1.58E+00	2.68E−03	18.373	24.494	30.616	36.738	42.859	45.920	48.981	52.042	55.103	58.163	61.224
27	Al	5/2	100.0	1.22E+03	2.07E−01	78.204	104.261	130.318	156.375	182.432	195.460	208.489	221.517	234.546	247.574	260.602
29	Si	1/2	4.685	2.16E+00	7.86E−03	59.627	79.495	99.362	119.229	139.096	149.030	158.963	168.897	178.831	188.764	198.698
31	P	1/2	100.0	3.91E+02	6.65E−02	121.495	161.976	202.457	242.938	283.419	303.659	323.900	344.140	364.380	384.621	404.861
33	S	3/2	0.75	1.00E−01	2.27E−03	23.038	30.714	38.390	46.066	53.742	57.580	61.418	65.256	69.094	72.932	76.770
35	Cl	3/2	75.76	2.10E+01	4.72E−03	29.406	39.204	49.002	58.800	68.598	73.497	78.396	83.295	88.194	93.093	97.992
37	Cl	3/2	24.24	3.88E+00	2.72E−03	24.478	32.634	40.789	48.945	57.101	61.179	65.256	69.334	73.412	77.490	81.568
39	K	3/2	93.258	2.79E+00	5.10E−04	14.005	18.672	23.338	28.004	32.671	35.004	37.337	39.670	42.003	44.337	46.670
41	K	3/2	6.730	3.34E−02	8.44E−05	7.687	10.249	12.810	15.371	17.932	19.213	20.494	21.774	23.055	24.336	25.616
43	Ca	7/2	0.135	5.10E−02	6.43E−03	20.199	26.929	33.659	40.389	47.119	50.484	53.849	57.214	60.579	63.944	67.309
45	Sc	7/2	100.0	1.78E+03	3.02E−01	72.907	97.199	121.490	145.782	170.074	182.220	194.366	206.511	218.657	230.803	242.949
47	Ti	5/2	7.44	9.18E−01	2.10E−03	16.920	22.557	28.195	33.833	39.470	42.289	45.108	47.926	50.745	53.564	56.383
49	Ti	7/2	5.41	1.20E+00	3.78E−03	16.924	22.563	28.203	33.842	39.481	42.300	45.120	47.939	50.759	53.578	56.398
50	V	6	0.250	8.18E−01	5.57E−02	29.924	39.894	49.865	59.835	69.805	74.790	79.775	84.761	89.746	94.731	99.716
51	V	7/2	99.750	2.25E+03	3.84E−01	78.943	105.246	131.549	157.852	184.155	197.306	210.458	223.609	236.761	249.912	263.064
53	Cr	3/2	9.501	5.07E−01	9.08E−04	16.965	22.617	28.270	33.922	39.575	42.401	45.227	48.054	50.880	53.706	56.532
55	Mn	5/2	100.0	1.05E+03	1.79E−01	74.400	99.189	123.978	148.768	173.557	185.951	198.346	210.741	223.135	235.530	247.924
57	Fe	1/2	2.119	4.25E−03	3.42E−05	9.718	12.955	16.193	19.431	22.669	24.288	25.906	27.525	29.144	30.763	32.382
59	Co	7/2	100.0	1.64E+03	2.78E−01	71.212	94.939	118.666	142.393	166.120	177.984	189.847	201.711	213.575	225.438	237.302
61	Ni	3/2	1.1399	2.40E−01	3.59E−03	26.820	35.756	44.692	53.628	62.564	67.032	71.500	75.968	80.436	84.904	89.372
63	Cu	3/2	69.15	3.82E+02	9.39E−02	79.581	106.096	132.612	159.127	185.643	198.901	212.158	225.416	238.674	251.931	265.189
65	Cu	3/2	30.85	2.08E+02	1.15E−01	85.248	113.652	142.055	170.459	198.863	213.065	227.266	241.468	255.670	269.872	284.074
67	Zn	5/2	4.102	6.92E−01	2.87E−03	18.779	25.035	31.292	37.549	43.806	46.934	50.063	53.191	56.319	59.448	62.576
69	Ga	3/2	60.108	2.46E+02	6.97E−02	72.035	96.037	120.038	144.039	168.041	180.041	192.042	204.043	216.043	228.044	240.045
71	Ga	3/2	39.892	3.35E+02	1.43E−01	91.530	122.026	152.523	183.020	213.517	228.765	244.013	259.262	274.510	289.758	305.007

Isotope		Spin	Nat. Abund. (%)	Receptivity		Larmor Frequencies (MHz) vs. Bruker Field Strengths (Tesla) Freq. to 3 decimals are experimental for IUPAC Standards; freq. to 2 dec. are calculated from magn. moments										
				Natural rel. ^{13}C	Molar rel. ^{1}H	7.04925	9.39798	11.7467	14.0954	16.4442	17.6185	18.7929	19.9673	21.1416	22.3160	23.4904
73	Ge	9/2	7.76	6.44E−01	1.41E−03	10.469	13.958	17.446	20.934	24.423	26.167	27.911	29.655	31.399	33.144	34.888
75	As	3/2	100.0	1.49E+02	2.54E−02	51.390	68.513	85.635	102.758	119.881	128.442	137.003	145.564	154.126	162.687	171.248
77	Se	1/2	7.63	3.15E+00	7.03E−03	57.239	76.311	95.382	114.454	133.525	143.061	152.597	162.133	171.668	181.204	190.740
79	Br	3/2	50.69	2.37E+02	7.94E−02	75.195	100.248	125.302	150.356	175.410	187.937	200.464	212.991	225.518	238.045	250.572
81	Br	3/2	49.31	2.88E+02	9.95E−02	81.055	108.061	135.068	162.074	189.081	202.584	216.087	229.591	243.094	256.597	270.100
83	Kr	9/2	11.500	1.28E+00	1.90E−03	11.548	15.395	19.243	23.091	26.938	28.862	30.786	32.710	34.633	36.557	38.481
85	Rb	5/2	72.17	4.50E+01	1.06E−02	28.977	38.632	48.287	57.942	67.597	72.425	77.252	82.080	86.907	91.735	96.562
87	Rb	3/2	27.83	2.90E+02	1.77E−01	98.204	130.924	163.645	196.365	229.086	245.446	261.806	278.166	294.527	310.887	327.247
87	Sr	9/2	7.00	1.12E+00	2.72E−03	13.007	17.341	21.675	26.009	30.342	32.509	34.676	36.843	39.010	41.177	43.344
89	Y	1/2	100.0	7.00E−01	1.19E−04	14.707	19.607	24.507	29.408	34.308	36.758	39.208	41.658	44.108	46.558	49.008
91	Zr	5/2	11.22	6.26E+00	9.49E−03	27.901	37.197	46.494	55.790	65.086	69.734	74.382	79.031	83.679	88.327	92.975
93	Nb	9/2	100.0	2.87E+03	4.88E−01	73.460	97.936	122.413	146.889	171.365	183.603	195.841	208.079	220.317	232.555	244.794
95	Mo	5/2	15.90	3.06E+00	3.27E−03	19.559	26.076	32.593	39.110	45.627	48.885	52.144	55.402	58.661	61.919	65.178
97	Mo	5/2	9.56	1.96E+00	3.49E−03	19.970	26.623	33.277	39.931	46.585	49.911	53.238	56.565	59.892	63.219	66.546
99	Tc	9/2		-	3.82E−01	67.554	90.063	112.571	135.079	157.588	168.842	180.096	191.350	202.604	213.858	225.113
99	Ru	5/2	12.76	8.46E−01	1.13E−03	13.821	18.427	23.032	27.637	32.242	34.545	36.847	39.150	41.452	43.755	46.057
101	Ru	5/2	17.06	1.58E+00	1.57E−03	15.491	20.652	25.814	30.975	36.136	38.717	41.298	43.878	46.459	49.040	51.620
103	Rh	1/2	100.0	1.86E−01	3.17E−05	9.563	12.750	15.936	19.123	22.309	23.902	25.496	27.089	28.682	30.275	31.869
105	Pd	5/2	22.33	1.49E+00	1.13E−03	13.734	18.310	22.886	27.463	32.039	34.327	36.615	38.903	41.191	43.479	45.767
107	Ag	1/2	51.839	2.05E−01	6.74E−05	12.149	16.197	20.244	24.292	28.340	30.364	32.388	34.412	36.436	38.460	40.483
109	Ag	1/2	48.161	2.90E−01	1.02E−04	13.967	18.620	23.274	27.927	32.581	34.908	37.234	39.561	41.888	44.215	46.541
111	Cd	1/2	12.80	7.27E+00	9.66E−03	63.674	84.890	106.105	127.320	148.536	159.144	169.751	180.359	190.967	201.575	212.182
113	Cd	1/2	12.22	7.94E+00	1.11E−02	66.608	88.802	110.995	133.188	155.381	166.478	177.574	188.671	199.767	210.864	221.961
113	In	9/2	4.29	8.85E+01	3.51E−01	65.626	87.491	109.357	131.223	153.089	164.022	174.954	185.887	196.820	207.753	218.686
115	In	9/2	95.71	1.99E+03	3.53E−01	65.766	87.679	109.592	131.504	153.417	164.373	175.330	186.286	197.242	208.198	219.155
115	Sn	1/2	0.34	7.11E−01	3.56E−02	98.199	130.918	163.636	196.355	229.074	245.433	261.793	278.152	294.511	310.871	327.230
117	Sn	1/2	7.68	2.08E+01	4.60E−02	106.943	142.575	178.208	213.840	249.472	267.288	285.104	302.921	320.737	338.553	356.369
119	Sn	1/2	8.59	2.66E+01	5.27E−02	111.920	149.211	186.502	223.792	261.083	279.728	298.374	317.019	335.664	354.309	372.955
121	Sb	5/2	57.21	5.48E+02	1.63E−01	71.823	95.753	119.684	143.615	167.545	179.510	191.476	203.441	215.406	227.372	239.337
123	Sb	7/2	42.79	1.17E+02	4.66E−02	38.894	51.854	64.813	77.772	90.731	97.211	103.691	110.170	116.650	123.129	129.609
123	Te	1/2	0.89	9.61E−01	1.84E−02	78.543	104.713	130.883	157.052	183.222	196.307	209.392	222.477	235.562	248.647	261.731
125	Te	1/2	7.07	1.34E+01	3.22E−02	94.690	126.240	157.790	189.340	220.889	236.664	252.439	268.214	283.989	299.764	315.539
127	I	5/2	100.0	5.60E+02	9.54E−02	60.048	80.056	100.063	120.071	140.078	150.082	160.086	170.090	180.093	190.097	200.101
129	Xe	1/2	26.4006	3.35E+01	2.16E−02	83.467	111.277	139.087	166.897	194.707	208.613	222.518	236.423	250.328	264.233	278.138
131	Xe	3/2	21.2324	3.51E+00	2.82E−03	24.742	32.986	41.230	49.474	57.718	61.840	65.962	70.084	74.206	78.328	82.450
133	Cs	7/2	100.0	2.84E+02	4.84E−02	39.365	52.482	65.598	78.714	91.830	98.388	104.946	111.504	118.062	124.620	131.178
135	Ba	3/2	6.592	1.94E+00	5.01E−03	29.816	39.751	49.685	59.620	69.554	74.521	79.489	84.456	89.423	94.390	99.357
137	Ba	3/2	11.232	4.62E+00	7.00E−03	33.353	44.466	55.579	66.692	77.805	83.361	88.918	94.474	100.031	105.587	111.144
138	La	5	0.090	4.97E−01	9.40E−02	39.600	52.794	65.989	79.183	92.377	98.974	105.572	112.169	118.766	125.363	131.960
139	La	7/2	99.910	3.56E+02	6.06E−02	42.395	56.521	70.647	84.772	98.898	105.961	113.023	120.086	127.149	134.212	141.275
141	Pr	5/2	100.0	1.97E+03	3.35E−01	91.89	122.51	153.12	183.74	214.36	229.67	244.97	260.28	275.59	290.90	306.21

Isotope		Spin	Nat. Abund. (%)	Receptivity		Larmor Frequencies (MHz) vs. Bruker Field Strengths (Tesla) Freq. to 3 decimals are experimental for IUPAC Standards; freq. to 2 dec. are calculated from magn. moments										
				Natural rel. ^{13}C	Molar rel. ^{1}H	7.04925	9.39798	11.7467	14.0954	16.4442	17.6185	18.7929	19.9673	21.1416	22.3160	23.4904
143	Nd	7/2	12.2	2.43E+00	3.39E−03	16.35	21.80	27.25	32.69	38.14	40.86	43.59	46.31	49.04	51.76	54.48
145	Nd	7/2	8.3	3.87E−01	7.93E−04	10.07	13.43	16.78	20.14	23.49	25.17	26.85	28.53	30.20	31.88	33.56
147	Sm	7/2	14.99	1.34E+00	1.52E−03	12.51	16.68	20.84	25.01	29.18	31.26	33.35	35.43	37.52	39.60	41.68
149	Sm	7/2	13.82	6.92E−01	8.52E−04	10.31	13.75	17.18	20.62	24.06	25.77	27.49	29.21	30.93	32.64	34.36
151	Eu	5/2	47.81	5.04E+02	1.79E−01	74.62	99.48	124.34	149.20	174.06	186.49	198.92	211.35	223.78	236.22	248.65
153	Eu	5/2	52.19	4.73E+01	1.54E−02	32.94	43.91	54.88	65.86	76.83	82.32	87.80	93.29	98.78	104.26	109.75
155	Gd	3/2	14.80	1.26E−01	1.45E−04	9.21	12.28	15.35	18.42	21.49	23.03	24.56	26.10	27.63	29.17	30.70
157	Gd	3/2	15.65	3.00E−01	3.26E−04	12.08	16.11	20.13	24.16	28.19	30.20	32.21	34.22	36.24	38.25	40.26
159	Tb	3/2	100.0	4.08E+02	6.94E−02	72.14	96.18	120.22	144.26	168.29	180.31	192.33	204.35	216.37	228.39	240.41
161	Dy	5/2	18.889	5.26E−01	4.74E−04	10.32	13.75	17.19	20.63	24.07	25.78	27.50	29.22	30.94	32.66	34.38
163	Dy	5/2	24.896	1.91E+00	1.31E−03	14.46	19.28	24.10	28.92	33.74	36.15	38.56	40.97	43.38	45.79	48.20
165	Ho	7/2	100.0	1.16E+03	1.98E−01	63.43	84.57	105.71	126.84	147.98	158.54	169.11	179.68	190.25	200.82	211.38
167	Er	7/2	22.869	6.77E−01	5.04E−04	8.66	11.54	14.42	17.31	20.19	21.63	23.08	24.52	25.96	27.40	28.85
169	Tm	1/2	100.0	3.32E+00	5.66E−04	24.82	33.10	41.37	49.64	57.91	62.04	66.18	70.32	74.45	78.59	82.72
171	Yb	1/2	14.28	4.63E+00	5.52E−03	52.521	70.020	87.519	105.019	122.518	131.268	140.017	148.767	157.517	166.266	175.016
173	Yb	5/2	16.13	1.28E+00	1.35E−03	14.61	19.48	24.35	29.22	34.09	36.52	38.96	41.39	43.83	46.26	48.69
175	Lu	7/2	97.41	1.79E+02	3.13E−02	34.27	45.69	57.11	68.53	79.94	85.65	91.36	97.07	102.78	108.49	114.20
176	Lu	7	2.59	6.05E+00	3.98E−02	24.33	32.43	40.53	48.64	56.74	60.80	64.85	68.90	72.95	77.01	81.06
177	Hf	7/2	18.60	1.53E+00	1.40E−03	12.18	16.24	20.30	24.36	28.42	30.45	32.48	34.51	36.53	38.56	40.59
179	Hf	9/2	13.62	4.38E−01	5.47E−04	7.65	10.20	12.75	15.30	17.85	19.13	20.40	21.68	22.95	24.23	25.50
181	Ta	7/2	99.988	2.20E+02	3.74E−02	35.984	47.974	59.964	71.953	83.943	89.938	95.932	101.927	107.922	113.917	119.912
183	W	1/2	14.31	6.31E−02	7.50E−05	12.505	16.671	20.837	25.004	29.170	31.253	33.337	35.420	37.503	39.586	41.669
185	Re	5/2	37.40	3.05E+02	1.39E−01	67.603	90.128	112.652	135.177	157.701	168.964	180.226	191.488	202.751	214.013	225.275
187	Re	5/2	62.60	5.26E+02	1.43E−01	68.284	91.036	113.788	136.539	159.291	170.667	182.042	193.418	204.794	216.170	227.546
187	Os	1/2	1.96	1.43E−03	1.24E−05	6.850	9.132	11.415	13.697	15.979	17.120	18.262	19.403	20.544	21.685	22.826
189	Os	3/2	16.15	2.32E+00	2.44E−03	23.306	31.072	38.837	46.602	54.368	58.251	62.133	66.016	69.899	73.781	77.664
191	Ir	3/2	37.3	6.38E−02	2.91E−05	5.40	7.20	9.00	10.79	12.59	13.49	14.39	15.29	16.19	17.09	17.99
193	Ir	3/2	62.7	1.37E−01	3.73E−05	5.86	7.82	9.77	11.73	13.68	14.66	15.63	16.61	17.59	18.56	19.54
195	Pt	1/2	33.832	2.07E+01	1.04E−02	64.518	86.015	107.512	129.009	150.505	161.254	172.002	182.751	193.499	204.247	214.996
197	Au	3/2	100.0	1.62E−01	2.76E−05	5.31	7.08	8.84	10.61	12.38	13.26	14.15	15.03	15.92	16.80	17.69
199	Hg	1/2	16.87	5.89E+00	5.94E−03	53.756	71.667	89.577	107.488	125.399	134.354	143.310	152.265	161.221	170.176	179.132
201	Hg	3/2	13.18	1.16E+00	1.49E−03	19.843	26.455	33.067	39.678	46.290	49.595	52.901	56.207	59.513	62.819	66.124
203	Tl	1/2	29.52	3.40E+02	1.96E−01	171.444	228.567	285.690	342.813	399.937	428.498	457.060	485.621	514.183	542.745	571.306
205	Tl	1/2	70.48	8.36E+02	2.02E−01	173.127	230.810	288.494	346.178	403.862	432.704	461.546	490.388	519.230	548.071	576.913
207	Pb	1/2	22.1	1.18E+01	9.06E−03	62.789	83.710	104.630	125.551	146.471	156.932	167.392	177.852	188.313	198.773	209.233
209	Bi	9/2	100.0	8.48E+02	1.44E−01	48.229	64.298	80.367	96.437	112.506	120.541	128.575	136.610	144.644	152.679	160.714
209	Po	1/2		-	1.44E−02	73.08	97.42	121.77	146.12	170.47	182.64	194.81	206.99	219.16	231.34	243.51
231	Pa	3/2	100.0	4.06E+02	6.90E−02	72.00	95.99	119.98	143.97	167.96	179.96	191.95	203.94	215.94	227.93	239.93
235	U	7/2	0.7204	6.53E−03	1.54E−04	5.527	7.368	9.209	11.051	12.892	13.813	14.734	15.654	16.575	17.496	18.416

Isotope		Spin	Nat. Abund. (%)	Receptivity		Larmor Frequencies (MHz) vs. Bruker Field Strengths (Tesla) Freq. to 3 decimals are experimental for IUPAC Standards; freq. to 2 dec. are calculated from magn. moments									
				Natural rel. ^{13}C	Molar rel. ^{1}H	7.04925	9.39798	11.7467	14.0954	16.4442	17.6185	18.7929	19.9673	21.1416	22.3160	23.4904
3	H	1/2		–	1.21E+00	320.131	426.795	533.459	640.123	746.786	800.118	853.450	906.782	960.114	1013.446	1066.778
1	H	1/2	99.9885	5.87E+03	**1.00E+00**	**300.130**	**400.130**	**500.130**	**600.130**	**700.130**	**750.130**	**800.130**	**850.130**	**900.130**	**950.130**	**1000.130**
19	F	1/2	100.0	4.89E+03	8.32E–01	282.404	376.498	470.592	564.686	658.780	705.827	752.874	799.921	846.968	894.015	941.062
3	He	1/2	1.34E–04	3.48E–03	4.42E–01	228.636	304.815	380.994	457.173	533.352	571.441	609.531	647.620	685.710	723.799	761.889
205	Tl	1/2	70.48	8.36E+02	2.02E–01	173.127	230.810	288.494	346.178	403.862	432.704	461.546	490.388	519.230	548.071	576.913
203	Tl	1/2	29.52	3.40E+02	1.96E–01	171.444	228.567	285.690	342.813	399.937	428.498	457.060	485.621	514.183	542.745	571.306
31	P	1/2	100.0	3.91E+02	6.65E–02	121.495	161.976	202.457	242.938	283.419	303.659	323.900	344.140	364.380	384.621	404.861
7	Li	3/2	92.41	1.59E+03	2.94E–01	116.642	155.506	194.370	233.233	272.097	291.529	310.961	330.393	349.825	369.257	388.688
119	Sn	1/2	8.59	2.66E+01	5.27E–02	111.920	149.211	186.502	223.792	261.083	279.728	298.374	317.019	335.664	354.309	372.955
117	Sn	1/2	7.68	2.08E+01	4.60E–02	106.943	142.575	178.208	213.840	249.472	267.288	285.104	302.921	320.737	338.553	356.369
87	Rb	3/2	27.83	2.90E+02	1.77E–01	98.204	130.924	163.645	196.365	229.086	245.446	261.806	278.166	294.527	310.887	327.247
115	Sn	1/2	0.34	7.11E–01	3.56E–02	98.199	130.918	163.636	196.355	229.074	245.433	261.793	278.152	294.511	310.871	327.230
11	B	3/2	80.1	7.77E+02	1.65E–01	96.294	128.378	160.462	192.546	224.630	240.672	256.714	272.755	288.797	304.839	320.881
125	Te	1/2	7.07	1.34E+01	3.22E–02	94.690	126.240	157.790	189.340	220.889	236.664	252.439	268.214	283.989	299.764	315.539
141	Pr	5/2	100.0	1.97E+03	3.35E–01	91.89	122.51	153.12	183.74	214.36	229.67	244.97	260.28	275.59	290.90	306.21
71	Ga	3/2	39.892	3.35E+02	1.43E–01	91.530	122.026	152.523	183.020	213.517	228.765	244.013	259.262	274.510	289.758	305.007
65	Cu	3/2	30.85	2.08E+02	1.15E–01	85.248	113.652	142.055	170.459	198.863	213.065	227.266	241.468	255.670	269.872	284.074
129	Xe	1/2	26.4006	3.35E+01	2.16E–02	83.467	111.277	139.087	166.897	194.707	208.613	222.518	236.423	250.328	264.233	278.138
81	Br	3/2	49.31	2.88E+02	9.95E–02	81.055	108.061	135.068	162.074	189.081	202.584	216.087	229.591	243.094	256.597	270.100
63	Cu	3/2	69.15	3.82E+02	9.39E–02	79.581	106.096	132.612	159.127	185.643	198.901	212.158	225.416	238.674	251.931	265.189
23	Na	3/2	100.0	5.45E+02	9.27E–02	79.390	105.842	132.294	158.746	185.198	198.424	211.650	224.876	238.101	251.327	264.553
51	V	7/2	99.750	2.25E+03	3.84E–01	78.943	105.246	131.549	157.852	184.155	197.306	210.458	223.609	236.761	249.912	263.064
123	Te	1/2	0.89	9.61E–01	1.84E–02	78.543	104.713	130.883	157.052	183.222	196.307	209.392	222.477	235.562	248.647	261.731
27	Al	5/2	100.0	1.22E+03	2.07E–01	78.204	104.261	130.318	156.375	182.432	195.460	208.489	221.517	234.546	247.574	260.602
13	C	1/2	1.07	**1.00E+00**	1.59E–02	75.468	100.613	125.758	150.903	176.048	188.620	201.193	213.765	226.338	238.910	251.483
79	Br	3/2	50.69	2.37E+02	7.94E–02	75.195	100.248	125.302	150.356	175.410	187.937	200.464	212.991	225.518	238.045	250.572
151	Eu	5/2	47.81	5.04E+02	1.79E–01	74.62	99.48	124.34	149.20	174.06	186.49	198.92	211.35	223.78	236.22	248.65
55	Mn	5/2	100.0	1.05E+03	1.79E–01	74.400	99.189	123.978	148.768	173.557	185.951	198.346	210.741	223.135	235.530	247.924
93	Nb	9/2	100.0	2.87E+03	4.88E–01	73.460	97.936	122.413	146.889	171.365	183.603	195.841	208.079	220.317	232.555	244.794
209	Po	1/2		–	1.44E–02	73.08	97.42	121.77	146.12	170.47	182.64	194.81	206.99	219.16	231.34	243.51
45	Sc	7/2	100.0	1.78E+03	3.02E–01	72.907	97.199	121.490	145.782	170.074	182.220	194.366	206.511	218.657	230.803	242.949
159	Tb	3/2	100.0	4.08E+02	6.94E–02	72.14	96.18	120.22	144.26	168.29	180.31	192.33	204.35	216.37	228.39	240.41
69	Ga	3/2	60.108	2.46E+02	6.97E–02	72.035	96.037	120.038	144.039	168.041	180.041	192.042	204.043	216.043	228.044	240.045
231	Pa	3/2	100.0	4.06E+02	6.90E–02	72.00	95.99	119.98	143.97	167.96	179.96	191.95	203.94	215.94	227.93	239.93
121	Sb	5/2	57.21	5.48E+02	1.63E–01	71.823	95.753	119.684	143.615	167.545	179.510	191.476	203.441	215.406	227.372	239.337
59	Co	7/2	100.0	1.64E+03	2.78E–01	71.212	94.939	118.666	142.393	166.120	177.984	189.847	201.711	213.575	225.438	237.302
187	Re	5/2	62.60	5.26E+02	1.43E–01	68.284	91.036	113.788	136.539	159.291	170.667	182.042	193.418	204.794	216.170	227.546
185	Re	5/2	37.40	3.05E+02	1.39E–01	67.603	90.128	112.652	135.177	157.701	168.964	180.226	191.488	202.751	214.013	225.275
99	Tc	9/2		–	3.82E–01	67.554	90.063	112.571	135.079	157.588	168.842	180.096	191.350	202.604	213.858	225.113
113	Cd	1/2	12.22	7.94E+00	1.11E–02	66.608	88.802	110.995	133.188	155.381	166.478	177.574	188.671	199.767	210.864	221.961
115	In	9/2	95.71	1.99E+03	3.53E–01	65.766	87.679	109.592	131.504	153.417	164.373	175.330	186.286	197.242	208.198	219.155

NMR Frequency Tables

NMR Frequencies vs. Bruker Field Strengths – sorted with decreasing Larmor frequency

Isotope		Spin	Nat. Abund. (%)	Receptivity		Larmor Frequencies (MHz) vs. Bruker Field Strengths (Tesla) Freq. to 3 decimals are experimental for IUPAC Standards; freq. to 2 dec. are calculated from magn. moments									
				Natural rel. ^{13}C	Molar rel. ^{1}H	7.04925	9.39798	11.7467	14.0954	16.4442	17.6185	18.7929	19.9673	21.1416	22.3160	23.4904
113	In	9/2	4.29	8.85E+01	3.51E–01	65.626	87.491	109.357	131.223	153.089	164.022	174.954	185.887	196.820	207.753	218.686
195	Pt	1/2	33.832	2.07E+01	1.04E–02	64.518	86.015	107.512	129.009	150.505	161.254	172.002	182.751	193.499	204.247	214.996
111	Cd	1/2	12.80	7.27E+00	9.66E–03	63.674	84.890	106.105	127.320	148.536	159.144	169.751	180.359	190.967	201.575	212.182
165	Ho	7/2	100.0	1.16E+03	1.98E–01	63.43	84.57	105.71	126.84	147.98	158.54	169.11	179.68	190.25	200.82	211.38
207	Pb	1/2	22.1	1.18E+01	9.06E–03	62.789	83.710	104.630	125.551	146.471	156.932	167.392	177.852	188.313	198.773	209.233
127	I	5/2	100.0	5.60E+02	9.54E–02	60.048	80.056	100.063	120.071	140.078	150.082	160.086	170.090	180.093	190.097	200.101
29	Si	1/2	4.685	2.16E+00	7.86E–03	59.627	79.495	99.362	119.229	139.096	149.030	158.963	168.897	178.831	188.764	198.698
77	Se	1/2	7.63	3.15E+00	7.03E–03	57.239	76.311	95.382	114.454	133.525	143.061	152.597	162.133	171.668	181.204	190.740
199	Hg	1/2	16.87	5.89E+00	5.94E–03	53.756	71.667	89.577	107.488	125.399	134.354	143.310	152.265	161.221	170.176	179.132
171	Yb	1/2	14.28	4.63E+00	5.52E–03	52.521	70.020	87.519	105.019	122.518	131.268	140.017	148.767	157.517	166.266	175.016
75	As	3/2	100.0	1.49E+02	2.54E–02	51.390	68.513	85.635	102.758	119.881	128.442	137.003	145.564	154.126	162.687	171.248
209	Bi	9/2	100.0	8.48E+02	1.44E–01	48.229	64.298	80.367	96.437	112.506	120.541	128.575	136.610	144.644	152.679	160.714
2	H	1	0.0115	6.52E–03	9.65E–03	46.072	61.422	76.773	92.124	107.474	115.150	122.825	130.500	138.175	145.851	153.526
6	Li	1	7.59	3.79E+00	8.50E–03	44.167	58.883	73.600	88.316	103.032	110.390	117.748	125.106	132.464	139.822	147.180
139	La	7/2	99.910	3.56E+02	6.06E–02	42.395	56.521	70.647	84.772	98.898	105.961	113.023	120.086	127.149	134.212	141.275
9	Be	3/2	100.0	8.15E+01	1.39E–02	42.174	56.226	70.277	84.329	98.381	105.407	112.433	119.459	126.485	133.510	140.536
17	O	5/2	0.038	6.50E–02	2.91E–02	40.687	54.243	67.800	81.356	94.913	101.691	108.469	115.248	122.026	128.804	135.582
138	La	5	0.090	4.97E–01	9.40E–02	39.600	52.794	65.989	79.183	92.377	98.974	105.572	112.169	118.766	125.363	131.960
133	Cs	7/2	100.0	2.84E+02	4.84E–02	39.365	52.482	65.598	78.714	91.830	98.388	104.946	111.504	118.062	124.620	131.178
123	Sb	7/2	42.79	1.17E+02	4.66E–02	38.894	51.854	64.813	77.772	90.731	97.211	103.691	110.170	116.650	123.129	129.609
181	Ta	7/2	99.988	2.20E+02	3.74E–02	35.984	47.974	59.964	71.953	83.943	89.938	95.932	101.927	107.922	113.917	119.912
175	Lu	7/2	97.41	1.79E+02	3.13E–02	34.27	45.69	57.11	68.53	79.94	85.65	91.36	97.07	102.78	108.49	114.20
137	Ba	3/2	11.232	4.62E+00	7.00E–03	33.353	44.466	55.579	66.692	77.805	83.361	88.918	94.474	100.031	105.587	111.144
153	Eu	5/2	52.19	4.73E+01	1.54E–02	32.94	43.91	54.88	65.86	76.83	82.32	87.80	93.29	98.78	104.26	109.75
10	B	3	19.9	2.32E+01	1.99E–02	32.245	42.989	53.732	64.476	75.220	80.591	85.963	91.335	96.707	102.079	107.451
15	N	1/2	0.364	2.23E–02	1.04E–03	30.423	40.560	50.697	60.834	70.971	76.039	81.107	86.176	91.244	96.312	101.381
50	V	6	0.250	8.18E–01	5.57E–02	29.924	39.894	49.865	59.835	69.805	74.790	79.775	84.761	89.746	94.731	99.716
135	Ba	3/2	6.592	1.94E+00	5.01E–03	29.816	39.751	49.685	59.620	69.554	74.521	79.489	84.456	89.423	94.390	99.357
35	Cl	3/2	75.76	2.10E+01	4.72E–03	29.406	39.204	49.002	58.800	68.598	73.497	78.396	83.295	88.194	93.093	97.992
85	Rb	5/2	72.17	4.50E+01	1.06E–02	28.977	38.632	48.287	57.942	67.597	72.425	77.252	82.080	86.907	91.735	96.562
91	Zr	5/2	11.22	6.26E+00	9.49E–03	27.901	37.197	46.494	55.790	65.086	69.734	74.382	79.031	83.679	88.327	92.975
61	Ni	3/2	1.1399	2.40E–01	3.59E–03	26.820	35.756	44.692	53.628	62.564	67.032	71.500	75.968	80.436	84.904	89.372
169	Tm	1/2	100.0	3.32E+00	5.66E–04	24.82	33.10	41.37	49.64	57.91	62.04	66.18	70.32	74.45	78.59	82.72
131	Xe	3/2	21.2324	3.51E+00	2.82E–03	24.742	32.986	41.230	49.474	57.718	61.840	65.962	70.084	74.206	78.328	82.450
37	Cl	3/2	24.24	3.88E+00	2.72E–03	24.478	32.634	40.789	48.945	57.101	61.179	65.256	69.334	73.412	77.490	81.568
176	Lu	7	2.59	6.05E+00	3.98E–02	24.33	32.43	40.53	48.64	56.74	60.80	64.85	68.90	72.95	77.01	81.06
21	Ne	3/2	0.27	3.91E–02	2.46E–03	23.693	31.587	39.482	47.376	55.270	59.217	63.165	67.112	71.059	75.006	78.953
189	Os	3/2	16.15	2.32E+00	2.44E–03	23.306	31.072	38.837	46.602	54.368	58.251	62.133	66.016	69.899	73.781	77.664
33	S	3/2	0.75	1.00E–01	2.27E–03	23.038	30.714	38.390	46.066	53.742	57.580	61.418	65.256	69.094	72.932	76.770
14	N	1	99.636	5.90E+00	1.01E–03	21.688	28.915	36.141	43.367	50.594	54.207	57.820	61.433	65.046	68.659	72.273
43	Ca	7/2	0.135	5.10E–02	6.43E–03	20.199	26.929	33.659	40.389	47.119	50.484	53.849	57.214	60.579	63.944	67.309

NMR Frequency Tables

NMR Frequencies vs. Bruker Field Strengths – sorted with decreasing Larmor frequency

Isotope		Spin	Nat. Abund. (%)	Receptivity		Larmor Frequencies (MHz) vs. Bruker Field Strengths (Tesla) Freq. to 3 decimals are experimental for IUPAC Standards; freq. to 2 dec. are calculated from magn. moments												
				Natural rel. ^{13}C	Molar rel. ^{1}H	7.04925	9.39798	11.7467	14.0954	16.4442	17.6185	18.7929	19.9673	21.1416	22.3160	23.4904
97	Mo	5/2	9.56	1.96E+00	3.49E-03	19.970	26.623	33.277	39.931	46.585	49.911	53.238	56.565	59.892	63.219	66.546
201	Hg	3/2	13.18	1.16E+00	1.49E-03	19.843	26.455	33.067	39.678	46.290	49.595	52.901	56.207	59.513	62.819	66.124
95	Mo	5/2	15.90	3.06E+00	3.27E-03	19.559	26.076	32.593	39.110	45.627	48.885	52.144	55.402	58.661	61.919	65.178
67	Zn	5/2	4.102	6.92E-01	2.87E-03	18.779	25.035	31.292	37.549	43.806	46.934	50.063	53.191	56.319	59.448	62.576
25	Mg	5/2	10.00	1.58E+00	2.68E-03	18.373	24.494	30.616	36.738	42.859	45.920	48.981	52.042	55.103	58.163	61.224
53	Cr	3/2	9.501	5.07E-01	9.08E-04	16.965	22.617	28.270	33.922	39.575	42.401	45.227	48.054	50.880	53.706	56.532
49	Ti	7/2	5.41	1.20E+00	3.78E-03	16.924	22.563	28.203	33.842	39.481	42.300	45.120	47.939	50.759	53.578	56.398
47	Ti	5/2	7.44	9.18E-01	2.10E-03	16.920	22.557	28.195	33.833	39.470	42.289	45.108	47.926	50.745	53.564	56.383
143	Nd	7/2	12.2	2.43E+00	3.39E-03	16.35	21.80	27.25	32.69	38.14	40.86	43.59	46.31	49.04	51.76	54.48
101	Ru	5/2	17.06	1.58E+00	1.57E-03	15.491	20.652	25.814	30.975	36.136	38.717	41.298	43.878	46.459	49.040	51.620
89	Y	1/2	100.0	7.00E-01	1.19E-04	14.707	19.607	24.507	29.408	34.308	36.758	39.208	41.658	44.108	46.558	49.008
173	Yb	5/2	16.13	1.28E+00	1.35E-03	14.61	19.48	24.35	29.22	34.09	36.52	38.96	41.39	43.83	46.26	48.69
163	Dy	5/2	24.896	1.91E+00	1.31E-03	14.46	19.28	24.10	28.92	33.74	36.15	38.56	40.97	43.38	45.79	48.20
39	K	3/2	93.258	2.79E+00	5.10E-04	14.005	18.672	23.338	28.004	32.671	35.004	37.337	39.670	42.003	44.337	46.670
109	Ag	1/2	48.161	2.90E-01	1.02E-04	13.967	18.620	23.274	27.927	32.581	34.908	37.234	39.561	41.888	44.215	46.541
99	Ru	5/2	12.76	8.46E-01	1.13E-03	13.821	18.427	23.032	27.637	32.242	34.545	36.847	39.150	41.452	43.755	46.057
105	Pd	5/2	22.33	1.49E+00	1.13E-03	13.734	18.310	22.886	27.463	32.039	34.327	36.615	38.903	41.191	43.479	45.767
87	Sr	9/2	7.00	1.12E+00	2.72E-03	13.007	17.341	21.675	26.009	30.342	32.509	34.676	36.843	39.010	41.177	43.344
147	Sm	7/2	14.99	1.34E+00	1.52E-03	12.51	16.68	20.84	25.01	29.18	31.26	33.35	35.43	37.52	39.60	41.68
183	W	1/2	14.31	6.31E-02	7.50E-05	12.505	16.671	20.837	25.004	29.170	31.253	33.337	35.420	37.503	39.586	41.669
177	Hf	7/2	18.60	1.53E+00	1.40E-03	12.18	16.24	20.30	24.36	28.42	30.45	32.48	34.51	36.53	38.56	40.59
107	Ag	1/2	51.839	2.05E-01	6.74E-05	12.149	16.197	20.244	24.292	28.340	30.364	32.388	34.412	36.436	38.460	40.483
157	Gd	3/2	15.65	3.00E-01	3.26E-04	12.08	16.11	20.13	24.16	28.19	30.20	32.21	34.22	36.24	38.25	40.26
83	Kr	9/2	11.500	1.28E+00	1.90E-03	11.548	15.395	19.243	23.091	26.938	28.862	30.786	32.710	34.633	36.557	38.481
73	Ge	9/2	7.76	6.44E-01	1.41E-03	10.469	13.958	17.446	20.934	24.423	26.167	27.911	29.655	31.399	33.144	34.888
161	Dy	5/2	18.889	5.26E-01	4.74E-04	10.32	13.75	17.19	20.63	24.07	25.78	27.50	29.22	30.94	32.66	34.38
149	Sm	7/2	13.82	6.92E-01	8.52E-04	10.31	13.75	17.18	20.62	24.06	25.77	27.49	29.21	30.93	32.64	34.36
145	Nd	7/2	8.3	3.87E-01	7.93E-04	10.07	13.43	16.78	20.14	23.49	25.17	26.85	28.53	30.20	31.88	33.56
57	Fe	1/2	2.119	4.25E-03	3.42E-05	9.718	12.955	16.193	19.431	22.669	24.288	25.906	27.525	29.144	30.763	32.382
103	Rh	1/2	100.0	1.86E-01	3.17E-05	9.563	12.750	15.936	19.123	22.309	23.902	25.496	27.089	28.682	30.275	31.869
155	Gd	3/2	14.80	1.26E-01	1.45E-04	9.21	12.28	15.35	18.42	21.49	23.03	24.56	26.10	27.63	29.17	30.70
167	Er	7/2	22.869	6.77E-01	5.04E-04	8.66	11.54	14.42	17.31	20.19	21.63	23.08	24.52	25.96	27.40	28.85
41	K	3/2	6.730	3.34E-02	8.44E-05	7.687	10.249	12.810	15.371	17.932	19.213	20.494	21.774	23.055	24.336	25.616
179	Hf	9/2	13.62	4.38E-01	5.47E-04	7.65	10.20	12.75	15.30	17.85	19.13	20.40	21.68	22.95	24.23	25.50
187	Os	1/2	1.96	1.43E-03	1.24E-05	6.850	9.132	11.415	13.697	15.979	17.120	18.262	19.403	20.544	21.685	22.826
193	Ir	3/2	62.7	1.37E-01	3.73E-05	5.86	7.82	9.77	11.73	13.68	14.66	15.63	16.61	17.59	18.56	19.54
235	U	7/2	0.7204	6.53E-03	1.54E-04	5.527	7.368	9.209	11.051	12.892	13.813	14.734	15.654	16.575	17.496	18.416
191	Ir	3/2	37.3	6.38E-02	2.91E-05	5.40	7.20	9.00	10.79	12.59	13.49	14.39	15.29	16.19	17.09	17.99
197	Au	3/2	100.0	1.62E-01	2.76E-05	5.31	7.08	8.84	10.61	12.38	13.26	14.15	15.03	15.92	16.80	17.69

NMR Properties of Selected Isotopes

Z = proton number, **A** = mass number, **Half-Life** where appropriate in years (y), days (d), hours (h), minutes (m); ***I*** = spin quantum number; **NA** = natural abundance (IUPAC 2003); μ_z = z-component of nuclear magnetic moment in units of the nuclear magneton (μ_N); ***Q*** = electric quadrupole moment in units of $fm^2 = 10^{-30} m^2$ ($1\ fm^2 = 0.01$ barns); calc. magnetogyric ratio $\gamma = \mu_z/\hbar\ I$. Note: for μ_z and ***Q*** the experimental uncertainty begins with the last significant digit.

			Isotope (half-life)	Spin	Nat. Abund. 2003 (TICE 2001)	Rel. Nucl. Magn. Mom. (measured)	Quadrupole Moment	Magnetogyric Ratio (calc., free atom)
Z	A	Sym	Name	*I*	NA (%)	μ_z / μ_N	*Q* [fm^2]	γ [10^7 rad s^{-1} T^{-1}]
0	1	n	Neutron	1/2		-1.9130427		-18.3247183
1	1	H	Hydrogen	1/2	99.9885	2.79284734		26.7522208
	2	H (D)	Deuterium	1	0.0115	0.857438228	0.286	4.10662919
	3	H (T)	Tritium (12.32 y)	1/2		2.97896244		28.5349865
2	3	He	Helium	1/2	0.000134	-2.12749772		-20.3789473
3	6	Li	Lithium	1	7.59	0.8220473	-0.0808	3.937127
	7	Li	Lithium	3/2	92.41	3.2564625	-4.01	10.397704
4	9	Be	Beryllium	3/2	100	-1.17749	5.288	-3.75966
5	10	B	Boron	3	19.9	1.80064478	8.459	2.87467955
	11	B	Boron	3/2	80.1	2.688649	4.059	8.584707
6	13	C	Carbon	1/2	1.07	0.702412		6.728286
7	14	N	Nitrogen	1	99.636	0.40376100	2.044	1.9337798
	15	N	Nitrogen	1/2	0.364	-0.28318884		-2.7126189
8	17	O	Oxygen	5/2	0.038	-1.89379	-2.558	-3.62806
9	19	F	Fluorine	1/2	100	2.626868		25.16233
10	21	Ne	Neon	3/2	0.27	-0.661797	10.155	-2.113081
11	23	Na	Sodium (Natrium)	3/2	100	2.2176556	10.4	7.0808516
12	25	Mg	Magnesium	5/2	10.00	-0.85545	19.94	-1.63884
13	26	Al	Alumin(i)um (7.17E5 y)	5		2.804	27	2.686
13	27	Al	Alumin(i)um	5/2	100	3.6415069	14.66	6.9762780
14	29	Si	Silicon	1/2	4.685	-0.55529		-5.31903
15	31	P	Phosphorus	1/2	100	1.13160		10.8394
16	33	S	Sulfur	3/2	0.75	0.643821	-6.78	2.055685
17	35	Cl	Chlorine	3/2	75.76	0.8218743	-8.165	2.6241991
	37	Cl	Chlorine	3/2	24.24	0.6841236	-6.435	2.1843688
18	39	Ar	Argon (269 y)	7/2		-1.59		-2.17
19	39	K	Potassium (Kalium)	3/2	93.258	0.3915073	5.85	1.2500612
	40	K	Potassium (1.248E9 y)	4	0.0117	-1.298100	-7.3	-1.554286
	41	K	Potassium	3/2	6.730	0.21489274	7.11	0.68614062
20	41	Ca	Calcium (1.02E5 y)	7/2		-1.594781	-6.7	-2.182306
	43	Ca	Calcium	7/2	0.135	-1.317643	-4.08	-1.803069
21	45	Sc	Scandium	7/2	100	4.756487	-22.0	6.508800
22	47	Ti	Titanium	5/2	7.44	-0.78848	30.2	-1.51054
	49	Ti	Titanium	7/2	5.41	-1.10417	24.7	-1.51095
23	50	V	Vanadium (1.4E17 y)	6	0.250	3.345689	21	2.670650
	51	V	Vanadium	7/2	99.750	5.1487057	-5.2	7.0455139
24	53	Cr	Chromium	3/2	9.501	-0.47454	-15	-1.51518
25	53	Mn	Manganese (3.74E6 y)	7/2		*5.024*		6.875
	55	Mn	Manganese	5/2	100	3.46871790	33	6.64525453
26	57	Fe	Iron, Ferrum	1/2	2.119	0.09062300		0.8680627
	59	Fe	Iron (44.507 d)	3/2		-0.3358		-1.0722
27	59	Co	Cobalt	7/2	100	4.627	42 s	6.332
	60	Co	Cobalt (1925.2 d)	5		3.799	44	3.639
28	61	Ni	Nickel	3/2	1.1399	-0.75002	16.2	-2.39477
29	63	Cu	Copper, Cuprum	3/2	69.15	2.227346	-22.0	7.111791
	65	Cu	Copper, Cuprum	3/2	30.85	2.3816	-20.4	7.6043
30	67	Zn	Zinc	5/2	4.102	0.8752049	15.0	1.6766885
31	69	Ga	Gallium	3/2	60.108	2.01659	17.1	6.43886
	71	Ga	Gallium	3/2	39.892	2.56227	10.7	8.18117
32	73	Ge	Germanium	9/2	7.76	-0.8794677	-19.6	-0.9360306
33	75	As	Arsenic	3/2	100	1.43947	31.4	4.59615
34	77	Se	Selenium	1/2	7.63	0.5350743		5.125388

NMR Properties of Selected Isotopes

Theor. NMR freq. ν_o calc. from γ and scaled to ^{1}H = 100.0 MHz; Molar Receptivity **R_M(H)** relative to equal number of protons is proportional to $\gamma^3 I (I+1)$; Receptivity at nat. abundance **R_{NA}(C)** relative to ^{13}C; recommended Reference sample (IUPAC 2001); *experimental* reson. freq. of ref. sample on the unified Ξ scale (at B_0 where TMS (^{1}H) = 100.0 MHz).
Numbers containing E are in exponential format.

		Theoretical NMR Freq. (free atom)	**Molar Receptivity** (rel. ^{1}H)	**Receptivity at Nat. Abund.** (rel. ^{13}C)	**Reference Sample**	**Measured. NMR Freq.** (rel. ^{1}H ref.)
A	**Sym**	ν_o [MHz]	**R_M(H)**	**R_{NA}(C)**	**Reference**	Ξ [MHz]
1	n	68.4979	3.21E–01			
1	H	100.0000	**1.00E+00**	5.87E+03	1% Me_4Si in $CDCl_3$	100.000000
2	D	15.3506	9.65E–03	6.52E–03	$(CD_3)_4Si$ neat	15.350609
3	T	106.6640	1.21E+00		TMS-T_1	106.663974
3	He	76.1767	4.42E–01	3.48E–03	He gas	76.178976
6	Li	14.7170	8.50E–03	3.79E+00	9.7 m LiCl in D_2O	14.716086
7	Li	38.8667	2.94E–01	1.59E+03	9.7 m LiCl in D_2O	38.863797
9	Be	14.0536	1.39E–02	8.15E+01	0.43 m $BeSO_4$ in D_2O	14.051813
10	B	10.7456	1.99E–02	2.32E+01	15% $BF_3.Et_2O$ in $CDCl_3$	10.743658
11	B	32.0897	1.65E–01	7.77E+02	15% $BF_3.Et_2O$ in $CDCl_3$	32.083974
13	C	25.1504	1.59E–02	**1.00E+00**	1% Me_4Si in $CDCl_3$ DSS in D_2O	25.145020 25.144953
14	N	7.2285	1.01E–03	5.90E+00	$MeNO_2$ + 10% $CDCl_3$	7.226317
15	N	10.1398	1.04E–03	2.23E–02	$MeNO_2$ + 10% $CDCl_3$ liquid NH_3	10.136767 10.132767
17	O	13.5617	2.91E–02	6.50E–02	D_2O	13.556457
19	F	94.0570	8.32E–01	4.89E+03	CCl_3F	94.094011
21	Ne	7.8987	2.46E–03	3.91E–02	Neon gas, 1.1 MPa	7.894296
23	Na	26.4683	9.27E–02	5.45E+02	0.1 M NaCl in D_2O	26.451900
25	Mg	6.1260	2.68E–03	1.58E+00	11 M $MgCl_2$ in D_2O	6.121635
26	Al	10.0399	4.05E–02			
27	Al	26.0774	2.07E–01	1.22E+03	1.1 m $Al(NO_3)_3$ in D_2O	26.056859
29	Si	19.8826	7.86E–03	2.16E+00	1% Me_4Si in $CDCl_3$	19.867187
31	P	40.5178	6.65E–02	3.91E+02	H_3PO_4 external $(MeO)_3PO$ internal	40.480742 40.480864
33	S	7.6842	2.27E–03	1.00E–01	$(NH_4)_2SO_4$ in D_2O (sat.)	7.676000
35	Cl	9.8093	4.72E–03	2.10E+01	0.1 M NaCl in D_2O	9.797909
37	Cl	8.1652	2.72E–03	3.88E+00	0.1 M NaCl in D_2O	8.155725
39	Ar	8.1228	1.13E–02			
39	K	4.6727	5.10E–04	2.79E+00	0.1 M KCl in D_2O	4.666373
40	K	5.8099	5.23E–03	3.59E–03	0.1 M KCl in D_2O	5.802018
41	K	2.5648	8.44E–05	3.34E–02	0.1 M KCl in D_2O	2.561305
41	Ca	8.1575	1.14E–02			
43	Ca	6.7399	6.43E–03	5.10E–02	0.1 M $CaCl_2$ in D_2O	6.730029
45	Sc	24.3299	3.02E–01	1.78E+03	0.06 M $Sc(NO_3)_3$ in D_2O	24.291747
47	Ti	5.6464	2.10E–03	9.18E–01	$TiCl_4$ neat + 10% C_6D_{12}	5.637534
49	Ti	5.6479	3.78E–03	1.20E+00	$TiCl_4$ neat + 10% C_6D_{12}	5.639037
50	V	9.9829	5.57E–02	8.18E–01	$VOCl_3$ + 5% C_6D_6	9.970309
51	V	26.3362	3.84E–01	2.25E+03	$VOCl_3$ + 5% C_6D_6	26.302948
53	Cr	5.6638	9.08E–04	5.07E–01	K_2CrO_4 in D_2O (sat.)	5.652496
53	Mn	25.6983	3.56E–01			
55	Mn	24.8400	1.79E–01	1.05E+03	0.82 m $KMnO_4$ in D_2O	24.789218
57	Fe	3.2448	3.42E–05	4.25E–03	$Fe(CO)_5$ + 20% C_6D_6	3.237778
59	Fe	4.0079	3.22E–04			
59	Co	23.6676	2.78E–01	1.64E+03	0.56 m $K_3[Co(CN)_6]$ in D_2O	23.727074
60	Co	13.6026	1.01E–01			
61	Ni	8.9517	3.59E–03	2.40E–01	$Ni(CO)_4$ + 5% C_6D_6	8.936051
63	Cu	26.5839	9.39E–02	3.82E+02	$[Cu(CH_3CN)_4][ClO_4]$ in CH_3CN (sat.) + 5% C_6D_6	26.515473
65	Cu	28.4250	1.15E–01	2.08E+02	$[Cu(CH_3CN)_4][ClO_4]$ in CH_3CN (sat.) + 5% C_6D_6	28.403693
67	Zn	6.2675	2.87E–03	6.92E–01	$Zn(NO_3)_3$ in D_2O (sat.)	6.256803
69	Ga	24.0685	6.97E–02	2.46E+02	1.1 m $Ga(NO_3)_3$ in D_2O	24.001354
71	Ga	30.5813	1.43E–01	3.35E+02	1.1 m $Ga(NO_3)_3$ in D_2O	30.496704
73	Ge	3.4989	1.41E–03	6.44E–01	Me_4Ge + 5% C_6D_6	3.488315
75	As	17.1804	2.54E–02	1.49E+02	0.5 M $NaAsF_6$ in CD_3CN	17.122614
77	Se	19.1587	7.03E–03	3.15E+00	Me_2Se + 5% C_6D_6	19.071513

NMR Properties of Selected Isotopes

Z	**A**	**Sym**	**Name**	***I***	**NA** (%)	μ_z / μ_N	***Q*** [fm^2]	γ [10^7 rad s^{-1} T^{-1}]
	79	Se	Selenium (2.95E5 y)	7/2		-1.018	80	-1.393
35	79	Br	Bromine	3/2	50.69	2.106400	30.5	6.725619
	81	Br	Bromine	3/2	49.31	2.270562	25.4	7.249779
36	83	Kr	Krypton	9/2	11.500	-0.970669	25.9	-1.033097
37	85	Rb	Rubidium	5/2	72.17	1.3533515	27.6	2.5927059
	87	Rb	Rubidium (4.81E10 y)	3/2	27.83	2.751818	13.35	8.786403
38	87	Sr	Strontium	9/2	7.00	-1.093603	33.5	-1.163938
39	89	Y	Yttrium	1/2	100	-0.1374154		-1.316279
40	91	Zr	Zirconium	5/2	11.22	-1.30362	-17.6	-2.49743
41	93	Nb	Niobium	9/2	100	6.1705	-32	6.5674
42	95	Mo	Molybdenum	5/2	15.9	-0.9142	-2.2	-1.7514
	97	Mo	Molybdenum	5/2	9.56	-0.9335	25.5	-1.7884
	99	Mo	Molybdenum (65.924 h)	1/2		*0.375*		3.59
43	99	Tc	Technetium (2.1E5 y)	9/2		5.6847	-12.9	6.0503
44	99	Ru	Ruthenium	5/2	12.76	-0.641	7.9	-1.228
	101	Ru	Ruthenium	5/2	17.06	-0.716	45.7	-1.372
45	103	Rh	Rhodium	1/2	100	-0.08840		-0.84677
46	105	Pd	Palladium	5/2	22.33	-0.642	66	-1.230
47	107	Ag	Silver, Argentum	1/2	51.839	-0.1136797		-1.088918
	109	Ag	Silver	1/2	48.161	-0.13069		-1.2519
48	111	Cd	Cadmium	1/2	12.80	-0.5948861		-5.698315
	113	Cd	Cadmium (7.7E15 y)	1/2	12.22	-0.6223009		-5.960917
49	113	In	Indium	9/2	4.29	5.5289	79.9	5.8845
	115	In	Indium (4.41E14 y)	9/2	95.71	5.5408	81	5.8972
50	115	Sn	Tin	1/2	0.34	-0.91883		-8.8013
	117	Sn	Tin	1/2	7.68	-1.00104		-9.58880
	119	Sn	Tin (Stannum)	1/2	8.59	-1.04728		-10.0317
51	121	Sb	Antimony (Stibium)	5/2	57.21	3.3634	-36	6.4435
	123	Sb	Antimony	7/2	42.79	2.5498	-49	3.4892
	125	Sb	Antimony (2.7586 y)	7/2		*2.63*		3.60
52	123	Te	Tellurium (9.2E16 y)	1/2	0.89	-0.7369478		-7.059101
	125	Te	Tellurium	1/2	7.07	-0.8885051		-8.510843
53	127	I	Iodine	5/2	100	2.81327	-71	5.38957
	129	I	Iodine (1.57E7 y)	7/2		2.6210	-48	3.5866
54	129	Xe	Xenon	1/2	26.4006	-0.777976		-7.45210
	131	Xe	Xenon	3/2	21.2324	0.691862	-11.4	2.209077
55	133	Cs	C(a)esium	7/2	100	2.582025	-0.343	3.533256
56	135	Ba	Barium	3/2	6.592	0.838627	16.0	2.677690
	137	Ba	Barium	3/2	11.232	0.93734	24.5	2.99287
57	137	La	Lanthanum (6E4 y)	7/2		2.695	26	3.688
57	138	La	Lanthanum (1.05E11 y)	5	0.090	3.713646	45	3.557240
	139	La	Lanthanum	7/2	99.910	2.7830455	20	3.808333
58	139	Ce	Cerium (137.64 d)	3/2		*1.06*		3.38
	141	Ce	Cerium (32.508 d)	7/2		*1.09*		1.49
59	141	Pr	Praeseodymium	5/2	100	4.2754	-5.89	8.1907
60	143	Nd	Neodymium	7/2	12.2	-1.065	-63	-1.4574
	145	Nd	Neodymium	7/2	8.3	-0.656	-33	-0.898
61	145	Pm	Promethium (17.7 y)	5/2		3.8	21	7.3
62	147	Sm	Samarium (1.06E11 y)	7/2	14.99	-0.8148	-25.9	-1.115
	149	Sm	Samarium	7/2	13.82	-0.6717	7.5	-0.9192
63	151	Eu	Europium	5/2	47.81	3.4717	90.3	6.6510
	153	Eu	Europium	5/2	52.19	1.5324	241	2.9357
64	155	Gd	Gadolinium	3/2	14.80	-0.2572	127	-0.8212
	157	Gd	Gadolinium	3/2	15.65	-0.3373	135	-1.0770
65	159	Tb	Terbium	3/2	100	2.014	143.2	6.431
66	161	Dy	Dysprosium	5/2	18.889	-0.480	251	-0.920
	163	Dy	Dysprosium	5/2	24.896	0.673	265	1.289
67	163	Ho	Holmium (4570 y)	7/2		4.23	360	5.79
	165	Ho	Holmium	7/2	100	4.132	358	5.654
	166	Ho	Holmium (1200 y)	7		*3.60*	-340	2.46
68	167	Er	Erbium	7/2	22.869	-0.5639	357	-0.7716
	169	Er	Erbium (9.40 d)	1/2		0.4850		4.646
69	169	Tm	Thulium	1/2	100	-0.231		-2.21
	171	Tm	Thulium (1.92 y)	1/2		-0.228		-2.18
70	171	Yb	Ytterbium	1/2	14.28	0.49367		4.7288
	173	Yb	Ytterbium	5/2	16.13	-0.67989	280	-1.30251
71	175	Lu	Lutetium	7/2	97.41	2.232	349	3.0547

NMR Properties of Selected Isotopes

A	Sym	ν_o [MHz]	$R_M(H)$	$R_{NA}(C)$	Reference	Ξ [MHz]
79	Se	5.2072	2.97E–03			
79	Br	25.1404	7.94E–02	2.37E+02	0.01 M NaBr in D_2O	25.053980
81	Br	27.0997	9.95E–02	2.88E+02	0.01 M NaBr in D_2O	27.006518
83	Kr	3.8617	1.90E–03	1.28E+00	Kr gas	3.847600
85	Rb	9.6916	1.06E–02	4.50E+01	0.01 M RbCl in D_2O	9.654943
87	Rb	32.8436	1.77E–01	2.90E+02	0.01 M RbCl in D_2O	32.720454
87	Sr	4.3508	2.72E–03	1.12E+00	0.5 M $SrCl_2$ in D_2O	4.333822
89	Y	4.9203	1.19E–04	7.00E–01	$Y(NO_3)_3$ in H_2O/D_2O	4.900198
91	Zr	9.3354	9.49E–03	6.26E+00	$Zr(C_5H_5)_2Cl_2$ in CH_2Cl_2 (sat.) + 5% C_6D_6	9.296298
93	Nb	24.5488	4.88E–01	2.87E+03	$K[NbCl_6]$ in CH_3CN / CD_3CN (sat.)	24.476170
95	Mo	6.5467	3.27E–03	3.06E+00	2 M Na_2MoO_4 in D_2O	6.516926
97	Mo	6.6849	3.49E–03	1.96E+00	2 M Na_2MoO_4 in D_2O	6.653695
99	Mo	13.4272	2.42E–03			
99	Tc	22.6161	3.82E–01		NH_4TcO_4 in H_2O / D_2O	22.508326
99	Ru	4.5903	1.13E–03	8.46E–01	0.3 M $K_4[Ru(CN)_6]$ in D_2O	4.605151
101	Ru	5.1274	1.57E–03	1.58E+00	0.3 M $K_4[Ru(CN)_6]$ in D_2O	5.161369
103	Rh	3.1652	3.17E–05	1.86E–01	$Rh(acac)_3$ in $CDCl_3$ (sat.)	3.186447
105	Pd	4.5975	1.13E–03	1.49E+00	K_2PdCl_6 in D_2O (sat.)	4.576100
107	Ag	4.0704	6.74E–05	2.05E–01	$AgNO_3$ in D_2O (sat.)	4.047819
109	Ag	4.6795	1.02E–04	2.90E–01	$AgNO_3$ in D_2O (sat.)	4.653533
111	Cd	21.3003	9.66E–03	7.27E+00	Me_2Cd neat liq.	21.215480
113	Cd	22.2820	1.11E–02	7.94E+00	Me_2Cd neat liq.	22.193175
113	In	21.9963	3.51E–01	8.85E+01	0.1 M $In(NO_3)_3$ in D_2O + 0.5 M DNO_3	21.865755
115	In	22.0436	3.53E–01	1.99E+03	0.1 M $In(NO_3)_3$ in D_2O + 0.5 M DNO_3	21.912629
115	Sn	32.8994	3.56E–02	7.11E–01	Me_4Sn + 5% C_6D_6	32.718749
117	Sn	35.8430	4.60E–02	2.08E+01	Me_4Sn + 5% C_6D_6	35.632259
119	Sn	37.4986	5.27E–02	2.66E+01	Me_4Sn + 5% C_6D_6	37.290632
121	Sb	24.0858	1.63E–01	5.48E+02	$KSbCl_6$ in CH_3CN / CD_3CN (sat.)	23.930577
123	Sb	13.0425	4.66E–02	1.17E+02	$KSbCl_6$ in CH_3CN / CD_3CN (sat.)	12.959217
125	Sb	13.4527	5.11E–02			
123	Te	26.3870	1.84E–02	9.61E–01	Me_2Te + 5% C_6D_6	26.169742
125	Te	31.8136	3.22E–02	1.34E+01	Me_2Te + 5% C_6D_6	31.549769
127	I	20.1462	9.54E–02	5.60E+02	0.01 M KI in D_2O	20.007486
129	I	13.4067	5.06E–02			
129	Xe	27.8560	2.16E–02	3.35E+01	$XeOF_4$ neat liq.	27.810186
131	Xe	8.2575	2.82E–03	3.51E+00	$XeOF_4$ neat liq.	8.243921
133	Cs	13.2073	4.84E–02	2.84E+02	0.1 M $CsNO_3$ in D_2O	13.116142
135	Ba	10.0092	5.01E–03	1.94E+00	0.5 M $BaCl_2$ in D_2O	9.934457
137	Ba	11.1874	7.00E–03	4.62E+00	0.5 M $BaCl_2$ in D_2O	11.112928
137	La	13.7852	5.50E–02			
138	La	13.2970	9.40E–02	4.97E–01	$LaCl_3$ in D_2O / H_2O	13.194300
139	La	14.2356	6.06E–02	3.56E+02	0.01 M $LaCl_3$ in D_2O	14.125641
139	Ce	12.6514	1.01E–02			
141	Ce	5.5755	3.64E–03			
141	Pr	30.6168	3.35E–01	1.97E+03		
143	Nd	5.4476	3.39E–03	2.43E+00		
145	Nd	3.3555	7.93E–04	3.87E–01		
145	Pm	27.2124	2.35E–01			
147	Sm	4.1678	1.52E–03	1.34E+00		
149	Sm	3.4358	8.52E–04	6.92E–01		
151	Eu	24.8614	1.79E–01	5.04E+02		
153	Eu	10.9737	1.54E–02	4.73E+01		
155	Gd	3.0697	1.45E–04	1.26E–01		
157	Gd	4.0258	3.26E–04	3.00E–01		
159	Tb	24.0376	6.94E–02	4.08E+02		
161	Dy	3.4374	4.74E–04	5.26E–01		
163	Dy	4.8195	1.31E–03	1.91E+00		
163	Ho	21.6369	2.13E–01			
165	Ho	21.1356	1.98E–01	1.16E+03		
166	Ho	9.2072	5.83E–02		(+6 keV excited state)	
167	Er	2.8842	5.04E–04	6.77E–01		
169	Er	17.3658	5.24E–03			
169	Tm	8.2711	5.66E–04	3.32E+00		
171	Tm	8.1637	5.44E–04			
171	Yb	17.6762	5.52E–03	4.63E+00	0.171 M $Yb(\eta\text{-}C_5Me_5)_2(THF)_2$ in THF	17.499306
173	Yb	4.8688	1.35E–03	1.28E+00		
175	Lu	11.4185	3.13E–02	1.79E+02		

NMR Properties of Selected Isotopes

Z	A	Sym	Name	*I*	NA (%)	μ_z / μ_N	*Q* [fm^2]	γ [10^7 rad s^{-1} T^{-1}]
	176	Lu	Lutetium (3.78E10 y)	7	2.59	3.169	497	2.168
72	177	Hf	Hafnium	7/2	18.60	0.7935	337	1.0858
	179	Hf	Hafnium	9/2	13.62	-0.641	379	-0.682
73	179	Ta	Tantalum (1.82 y)	7/2		2.289	337	3.132
	180	Ta	Tantalum (1.2E15 y)	9	0.012	4.825	495	2.568
	181	Ta	Tantalum	7/2	99.988	2.3705	317	3.2438
74	183	W	Tungsten (Wolfram)	1/2	14.31	0.11778476		1.1282407
75	185	Re	Rhenium	5/2	37.40	3.1871	218	6.1057
	187	Re	Rhenium (4.35E10 y)	5/2	62.60	3.2197	207	6.1682
76	187	Os	Osmium	1/2	1.96	0.06465189		0.6192897
	189	Os	Osmium	3/2	16.15	0.659933	85.6	2.107130
77	191	Ir	Iridium	3/2	37.3	0.1507	81.6	0.4812
	193	Ir	Iridium	3/2	62.7	0.1637	75.1	0.5227
78	195	Pt	Platinum	1/2	33.832	0.60952		5.8385
79	197	Au	Gold, Aurum	3/2	100	0.148158	54.7	0.473060
80	199	Hg	Mercury, Hydrargyrum	1/2	16.87	0.5058855		4.845793
	201	Hg	Mercury	3/2	13.18	-0.560226	38.6	-1.788770
81	203	Tl	Thallium	1/2	29.52	1.6222579		15.539339
	205	Tl	Thallium	1/2	70.48	1.6382146		15.692186
82	205	Pb	Lead (1.73E7 y)	5/2		0.7117	23	1.3635
	207	Pb	Lead (Plumbum)	1/2	22.1	0.58219		5.5767
83	209	Bi	Bismuth	9/2	100	4.1103	-51.6	4.3747
84	209	Po	Polonium (102 y)	1/2		0.68		6.51
86	211	Rn	Radon (14.6 h)	1/2		0.601		5.76
87	212	Fr	Francium (19.3 m)	5		4.62	-10	4.43
88	225	Ra	Radium (14.9 d)	1/2		-0.734		-7.03
89	227	Ac	Actinium (21.77 y)	3/2		1.1	170	3.5
90	229	Th	Thorium (7.34E3 y)	5/2		0.46	430	0.88
91	231	Pa	Protactinium (3.25E4 y)	3/2	100	*2.01*	-172	6.42
92	233	U	Uranium (1.592E5 y)	5/2		*0.59*	366.3	1.13
	235	U	Uranium (7.04E8 y)	7/2	0.7204	-0.38	493.6	-0.52
	238	U	Uranium (4.468E9 y)	0	99.274		1390	
93	237	Np	Neptunium (2.14E6 y)	5/2		3.14	386.6	6.02
94	239	Pu	Plutonium (2.410E4 y)	1/2		0.203		1.94
	241	Pu	Plutonium (14.4 y)	5/2		-0.68	560	-1.30
95	241	Am	Americium (432.7 y)	5/2		1.58	314	3.03
	243	Am	Americium (7.37E3 y)	5/2		1.50	286	2.87
96	243	Cm	Curium (29.1 y)	5/2		*0.41*		0.79
	245	Cm	Curium (8.48E3 y)	7/2		*0.5*		0.68
	247	Cm	Curium (1.56E7 y)	9/2		*0.37*		0.39
97	247	Bk	Berkelium (1.4E2 y)	(3/2)		*no data*		
	249	Bk	Berkelium (320 d)	7/2		*2.0*		2.7
98	251	Cf	Californium (9.0E2 y)	1/2		*no data*		
99	252	Es	Einsteinium (472 d)	(5)		*no data*		
	253	Es	Einsteinium (20.47 d)	7/2		4.10	670	5.61
100	253	Fm	Fermium (3.0 d)	(1/2)		*no data*		
	257	Fm	Fermium (100.5 d)	(9/2)		*no data*		

This Table (updated Oct. 2009) was assembled and calculated by W.E. Hull using information from the following sources:

De Laeter et al. *Pure Appl Chem* 75 (2003) 683-800. (isotope abundances)
Harris RK, et al. *Pure Appl Chem* 73 (2001) 1795-1818 and 80 (2008) 59-84. (shift references)
Mills I, et al. *Quantities, Units and Symbols in Physical Chemistry* (IUPAC recommendations 1993, corrections 1995). Blackwell Scientific (1993, 1995).
Pyykkö P. Spectroscopic nuclear quadrupole moments. Mol. Phys. 99 (2001) 1617-1629.

NMR Properties of Selected Isotopes

A	Sym	ν_o [MHz]	$R_M(H)$	$R_{NA}(C)$	Reference	Ξ [MHz]
176	Lu	8.1049	3.98E–02	6.05E+00		
177	Hf	4.0588	1.40E–03	1.53E+00		
179	Hf	2.5502	5.47E–04	4.38E–01		
179	Ta	11.7085	3.37E–02			
180	Ta	9.5979	1.06E–01	7.48E–02	(+77 keV excited state)	
181	Ta	12.1254	3.74E–02	2.20E+02	$KTaCl_6$ in CH_3CN (sat.)	11.989600
183	W	4.2174	7.50E–05	6.31E–02	1 M Na_2WO_4 in D_2O	4.166387
185	Re	22.8233	1.39E–01	3.05E+02	0.1 M $KReO_4$ in D_2O	22.524600
187	Re	23.0568	1.43E–01	5.26E+02	0.1 M $KReO_4$ in D_2O	22.751600
187	Os	2.3149	1.24E–05	1.43E–03	0.98 M OsO_4 in CCl_4	2.282331
189	Os	7.8765	2.44E–03	2.32E+00	0.98 M OsO_4 in CCl_4	7.765400
191	Ir	1.7986	2.91E–05	6.38E–02		
193	Ir	1.9538	3.73E–05	1.37E–01		
195	Pt	21.8243	1.04E–02	2.07E+01	1.2 M Na_2PtCl_6 in D_2O	21.496784
197	Au	1.7683	2.76E–05	1.62E–01		
199	Hg	18.1136	5.94E–03	5.89E+00	Me_2Hg neat liq. (toxic!)	17.910822
201	Hg	6.6864	1.49E–03	1.16E+00	Me_2Hg neat liq. (toxic!)	6.611583
203	Tl	58.0862	1.96E–01	3.40E+02	$Tl(NO_3)_3$	57.123200
205	Tl	58.6575	2.02E–01	8.36E+02	$Tl(NO_3)_3$	57.683838
205	Pb	5.0966	1.54E–03			
207	Pb	20.8458	9.06E–03	1.18E+01	Me_4Pb + 5% C_6D_6	20.920599
209	Bi	16.3525	1.44E–01	8.48E+02	$Bi(NO_3)_2$ sat. in conc. HNO_3 + 50% D_2O	16.069288
209	Po	24.3479	1.44E–02			
211	Rn	21.5193	9.97E–03			
212	Fr	16.5423	1.81E–01			
225	Ra	26.2814	1.82E–02			
227	Ac	13.1288	1.13E–02			
229	Th	3.2941	4.17E–04			
231	Pa	23.9899	6.90E–02	4.06E+02		
233	U	4.2251	8.80E–04			
235	U	1.9437	1.54E–04	6.53E–03	UF_6 + 10% C_6D_6	1.841400
238	U					
237	Np	22.4860	1.33E–01			
239	Pu	7.2686	3.84E–04			
241	Pu	4.8696	1.35E–03			
241	Am	11.3146	1.69E–02			
243	Am	10.7417	1.45E–02			
243	Cm	2.9361	2.95E–04			
245	Cm	2.5576	3.51E–04			
247	Cm	1.4720	1.05E–04			
249	Bk	10.2302	2.25E–02			
253	Es	20.9719	1.94E–01			

Stone NJ. *Table of Nuclear Magnetic Dipole and Electric Quadrupole Moments (2001)* [http://www.nndc.bnl.gov/nndc/stone_moments/nuclear-moments.pdf].
LBNL Isotopes Project Nuclear Data Dissemination Home Page. *Table of Nuclear Moments* [http://ie.lbl.gov/toipdf/mometbl.pdf].
NUDAT 2 half-life data: http://www.nndc.bnl.gov/

NMR Tables

Properties of Selected Deuterated Solvents for NMR

Solvent	Formula	MW_{ave}	Density $[d_4^{20}]$	MP [°C]	BP [°C]	RI $[n_D^{20}]$	Dielec. [ε]	^{1}H shift (Mult.) [ppm]	J(HD) [Hz]	^{13}C Shift (Mult.) [ppm]	J(CD) [Hz]	H_2O/HDO Shift [ppm]
Acetic Acid-d4	$C_2D_4O_2$	64.08	1.119	15.9	115.5	1.368	6.1	11.65 2.04 (5)	2.2	178.99 20 (7)	20	11.5
Acetone-d6	C_3D_6O	64.12	0.872	–93.8	55.5	1.3554	20.7	2.05 (5)	2.2	29.92 (7) 206.68 (13)	19.4 0.9	2.84/ 2.81
Acetonitrile-d3	C_2D_3N	44.07	0.844	–46	80.7	1.3406	37.5	1.94 (5)	2.5	1.39 (7) 118.69	21	2.12
Benzene-d6	C_6D_6	84.15	0.950	6.8	79.1	1.4986	2.3	7.16		128.39 (3)	24.3	0.4
Chloroform-d1	$CDCl_3$	120.38	1.500	–64.1	60.9	1.4445	4.8	7.24		77.23 (3)	32	1.55
Cyclohexane-d12	$C_6D_{12}O$	96.24	0.890	7	78		2	1.38		26.43 (5)	19	0.80
Deuterium oxide	D_2O	20.03	1.107	3.8	101.4	1.328	78.5	4.81				
1,2-Dichloroethane-d4	$C_2D_4Cl_2$	102.99	1.307	–35	83	1.443		3.72 (5)		43.6 (5)	23.5	
Dichloromethane-d2	CD_2Cl_2	86.95	1.362	–97	39.5	1.362		5.32 (3)	1.1	54 (5)	27.2	1.52
Diethylether-d10	$C_4D_{10}O$	84.19	0.78	–116.3	34.6			3.34 (m) 1.07 (m)		65.3 (5) 14.5 (7)	21 19	
Diethylene glycol dimethyl ether-d14 (diglyme-d14)	$C_6D_{14}O_3$	148.26	0.95	–68	162			3.49 (br) 3.40 (br) 3.22 (5)	1.5	70.7 (5) 70 (5) 57.7 (7)	21 21 21	
1,2-Dimethoxyethane-d10 (glyme-d10)	$C_4D_{10}O_2$	100.18	0.86	–58	83			3.40 (m) 3.22 (5)	1.6	71.7 (5) 57.8 (7)	21 21	
N,N-Dimethyl-formamide-d7	C_3D_7NO	80.14	1.04	–60	153	1.428	36.7	8.03 2.92 (5) 2.75 (5)	1.9 1.9	163.15 (3) 34.89 (7) 29.76 (7)	29.4 21.0 21.1	3.45
Dimethyl sulfoxide-d6	C_2D_6OS	84.17	1.190	20.2	190	1.4758	46.7	2.50 (5)	1.9	39.51 (7)	21.0	3.3
1,4-Dioxane-d6	$C_4D_8O_2$	96.16	1.129	12	99	1.4198	2.2	3.53 (m)		66.66 (5)	21.9	2.4
Ethanol-d6	C_2D_6O	52.11	0.888	–114.5	78	1.358	24.5	5.29 3.56 1.11 (m)		56.96 (5) 17.31 (7)	22 19	5.2
Methanol-d4	CD_4O	36.07	0.89	–99	65	1.3256	32.7	4.87 3.31 (5)	1.7	49.15 (7)	21.4	4.86
Methyl cyclohexane-d14	C_7D_{14}	112.27	0.77	–126	101	1.4189						
Nitrobenzene-d5	$C_6D_5NO_2$	128.14	1.253	6	211	1.5498		8.11 (br) 7.67 (br) 7.50 (br)		148.6 134.8 (3) 129.5 (3) 123.5 (3)	24.5 25 26	2.42
Nitromethane-d3	CD_3NO_2	64.06	1.19	–26	100	1.3795		4.33 (5)		62.8 (7)	22	2.2
2-Propanol-d8	C_3D_8O	68.15	0.786	–89.5	82.4	1.3728		5.12 3.89 (br) 1.10 (br)		62.9 (3) 24.2 (7)	21.5 19	
Pyridine-d5	C_5D_5N	84.13	1.02	–41	114	1.5079	12.4	8.74 7.58 7.22		150.35 (3) 135.91 (3) 123.87 (3)	27.5 24.5 25	4.97
Tetrachloroethane-d2	$C_2D_2Cl_4$	169.86	1.7	–43	146	1.493		5.91 (5)		74.2 (5)		1.5
Tetrahydrofuran-d8	C_4D_8O	80.16	0.99	–108	64	1.4035	7.6	3.58 1.73		67.57 (5) 25.37 (5)	22.2 20.2	2.42

Solvent	Formula	MW_{ave}	Density [d_4^{20}]	MP [°C]	BP [°C]	RI [n_D^{20}]	Dielec. [ε]	^{1}H shift (Mult.) [ppm]	J(HD) [Hz]	^{13}C Shift (Mult.) [ppm]	J(CD) [Hz]	H_2O/HDO Shift [ppm]
Toluene-d8	C_7D_8	100.19	0.94	–85	109	1.4932	2.4	7.09 (m) 7.00 6.98 (m) 2.09 (5)	 2.3	137.86 129.24 (3) 128.33 (3) 125.49 (3) 20.4 (7)	 23 24 24 19	0.45
2,2,2-Trifluoroacetic Acid-d1	$C_2DF_3O_2$	115.03	1.50	–15	71	1.30		11.50		164.2 (4) 116.6 (4)		11.5
2,2,2-Trifluoroethanol-d3	$C_2D_3F_3$	87.06	1.42	–44	77	1.30		5.02 3.88 (4x3)	 2 (9)	126.3 (4) 61.5 (4x5)	 22	5

This Table summarizes the physical properties of deuterated solvents and the chem. shifts (rel. to TMS) and deuterium couplings for the solvent signals and the approximate shifts for residual water (last column).

MRI Tables

Abbreviations and Acronyms Used in Magnetic Resonance Imaging

Method	Description	Equivalent acronyms
SINGLEPULSE	Basic pulse-and-acquire spectroscopy	FID
NSPECT	Non-localized spectroscopy with NOE and decoupling options	FID
CSI	Chemical shift imaging with optional PRESS localization	
PRESS	Localized MRS with double spin echo	
STEAM	Localized MRS with stimulated echo (for short TE)	
ISIS	Localized MRS with inversion-based voxel definition	OSIRIS
DtiEpi	Diffusion tensor imaging with EPI (SE and STE)	PGSE-EPI
DtiStandard	Diffusion tensor imaging with 2DFT (SE and STE)	PGSE
EPI	Echo-Planar Imaging (GE and SE), single-shot or interleaved, with navigator-based phase stabilization and automatic ghost correction	
FAIR_EPI	Pulsed arterial spin labelling-based perfusion imaging with EPI	
FC2D_ANGIO	Time-of-flight angiography flow-compensated	TOF-angio
FL2D_ANGIO	Time-of-flight angiography w/o flow-comp. (short TE)	
FISP	Fast gradient echo with steady state signal selection (FID, echo or fully balanced), and optional inversion recovery for T1 mapping.	FLASH, FAST, FISP, PSIF, CE-FAST, SSFP, GRASS, TrueFISP
FLASH	Gradient echo	FISP, GRASS, FAST
GEFC	Gradient echo with flow compensation	
MDEFT	T1-weghted hi-res imaging with inversion-recovery preparation	MPRAGE
MGE	Multiple gradient echo	
MSME	Multiple spin echo including T2 mapping	
RARE	Fast spin echo based on CPMG sequence	FSE, TSE
RAREVTR	RARE with variable TR for simultaneous T1&T2 mapping	
RAREst	Fast spin echo for short TE using slew-rate-optimized gradients	HASTE
FLOW_MAP	Quantitative flow mapping and PC-angio	
UTE	Ultra-short TE radial scan	
FieldMap	Quantitative B0 mapping, part of the MAPSHIM tool for localized high-order shimming	
SPIRAL	Fast MRI with spiral k-space scan	
IntraGate-FLASH	Cardiac and respiration-cine with retrospective (trigger-free) gating	

Chemical Shifts of Residual Protons in Common Deuterated Solvents

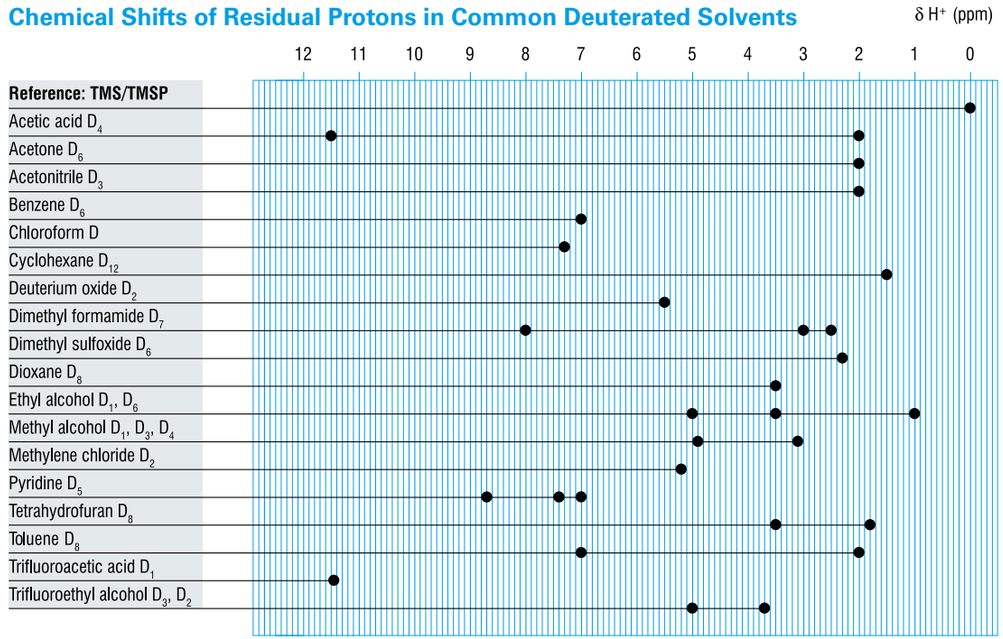

^{1}H Chemical Shifts in Organic Compounds

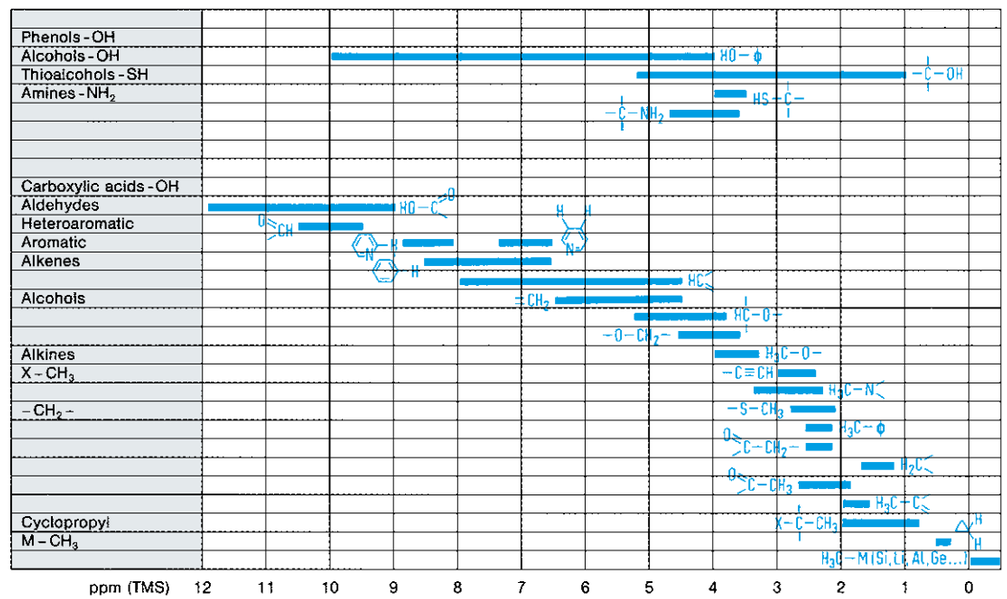

^{13}C Chemical Shifts in Organic Compounds*

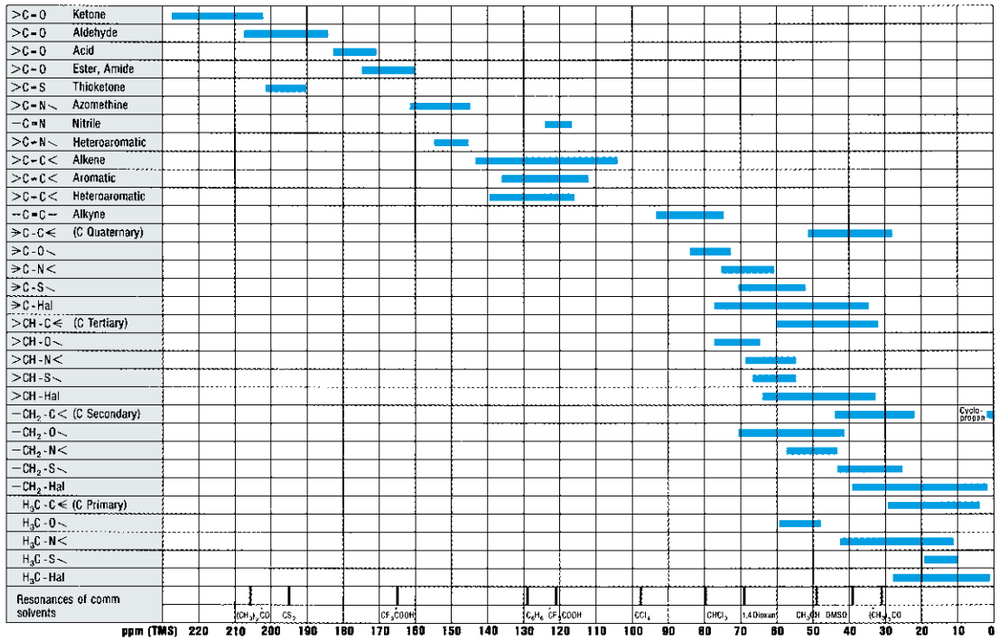

* Relative to internal tetramethylsilane.

^{11}B Chemical Shifts*

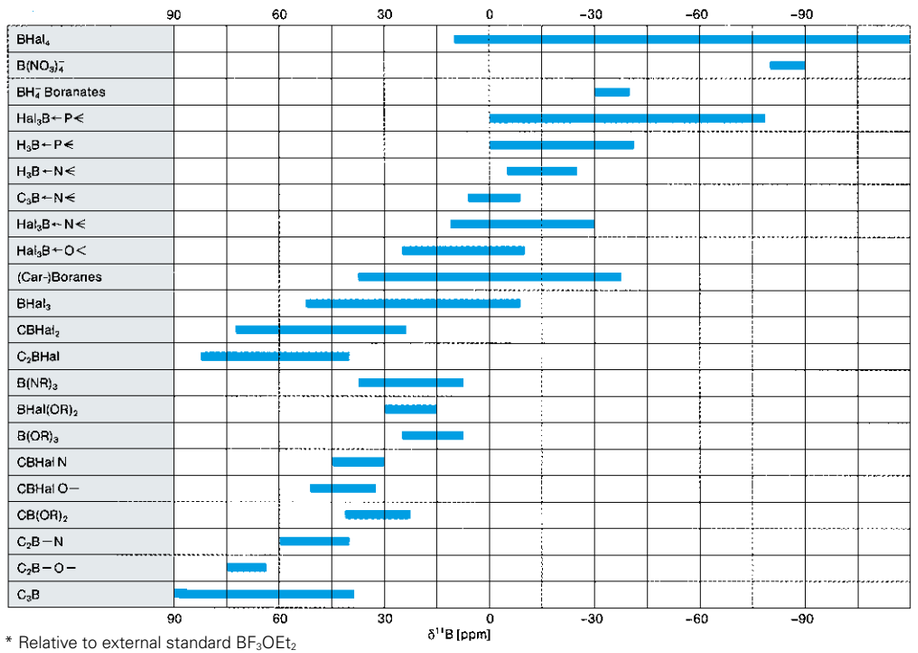

* Relative to external standard BF_3OEt_2

^{17}O Chemical Shifts*

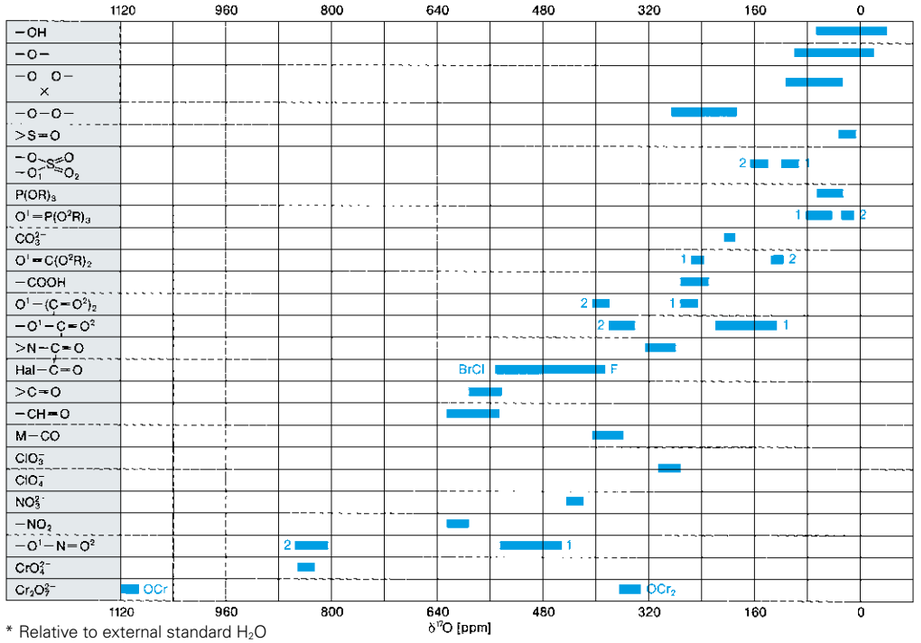

* Relative to external standard H_2O

^{15}N Chemical Shifts in Organic Compounds*

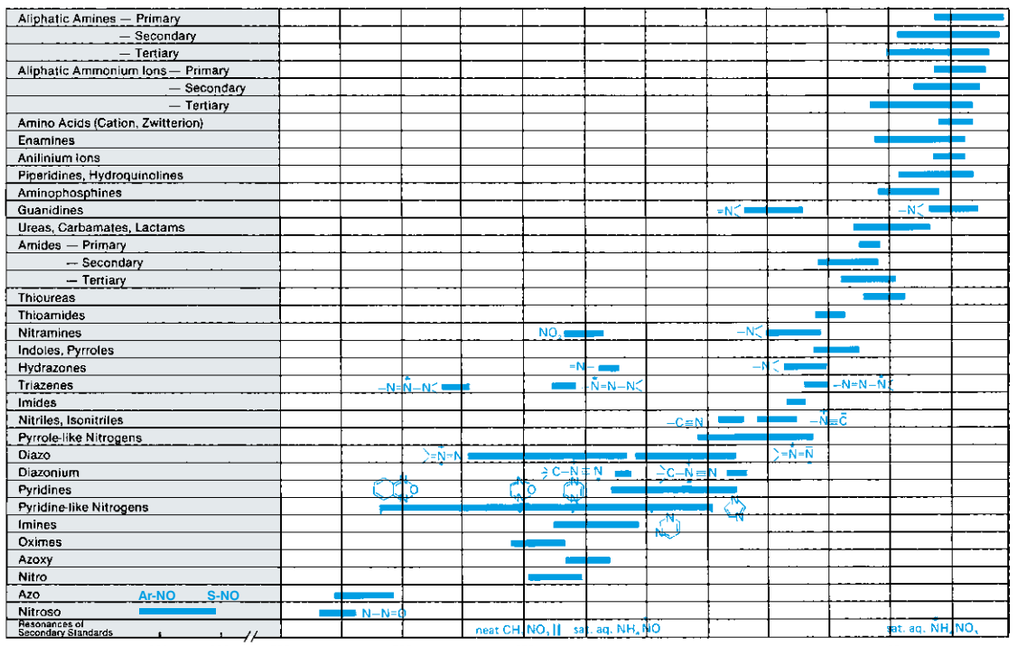

* Relative to external liquid ammonia at 25°C. Data taken from: G. C. Levy and R. L. Lichter: "Nitrogen-15 Nuclear Magnetic Resonance Spectroscopy", J. Wiley, 1979.

^{27}Al Chemical Shifts*

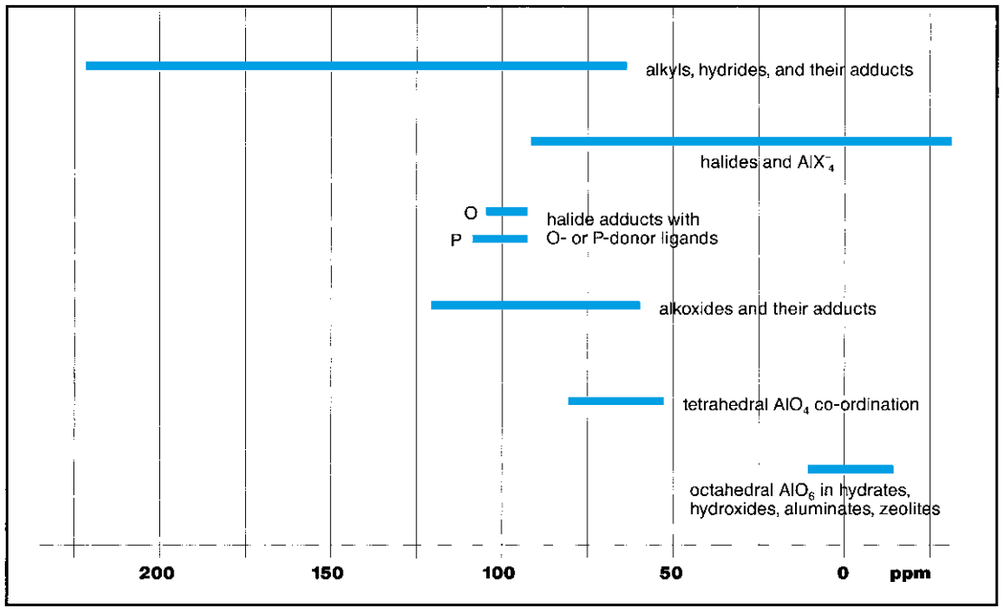

* Relative to $Al(H_2O)^{3+}_6$.

^{29}Si Chemical Shifts*

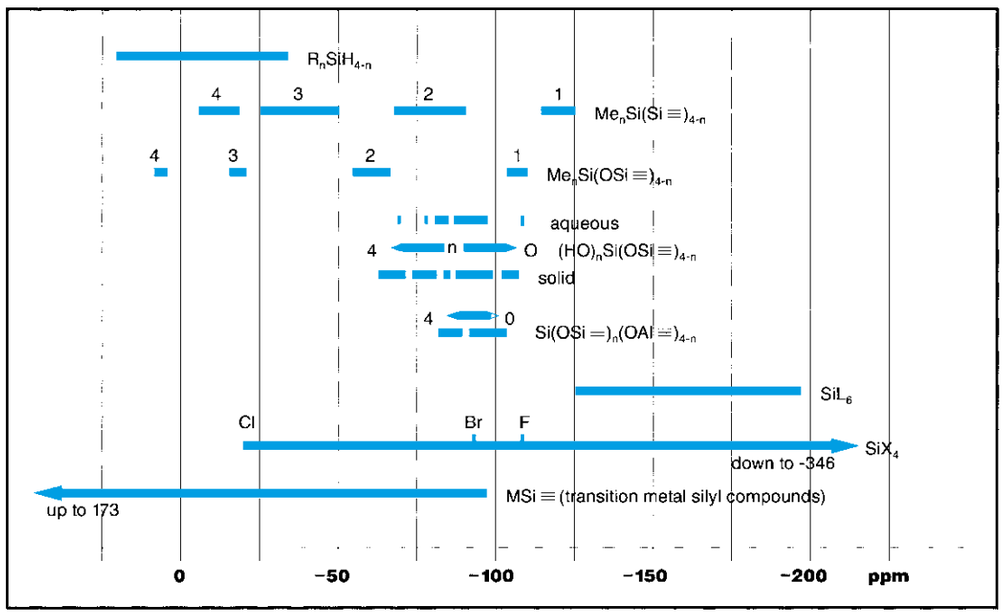

* Relative to $Si(CH_3)_4$.

Some Representative ^{19}F Chemical Shifts Referenced to $CFCl_3$

	δ / ppm		δ / ppm		δ / ppm
MeF	-271.9	$CFBr_3$	7.4	$FCH=CH_2$	-114
EtF	-213	CF_2Br_2	7	$F_2C=CH_2$	-81.3
CF_2H_2	-1436	CFH_2Ph	-207	$F_2C=CF_2$	-135
CF_3R	-60 to -70	CF_2Cl_2	-8	C_6F_6	-163
AsF_5	-66	$[AsF_6]^-$	-69.5	$[BeF_4]^-$	-163
BF_3	-131	ClF_3	116; -4	ClF_5	247; 412
IF_7	170	MoF_6	-278	ReF_7	345
SeF_6	55	$[SbF_6]^-$	-109	SbF_5	-108
$[SiF_6]^{2-}$	-127	TeF_6	-57	WF_6	166
XeF_2	258	XeF_4	438	XeF_6	550

Some Representative ^{31}P Chemical Shifts Referenced to 85 % H_3PO_4

(a) Phosphorus (III) compounds			
	δ / ppm		δ / ppm
PMe_3	-62	$PMeF_2$	245
PEt_3	-20	$PMeH_2$	-163.5
$P(n\text{-}Pr)_3$	-33	$PMeCl_2$	192
$P(i\text{-}Pr)_3$	-19.4	$PMeBr_2$	184
$P(n\text{-}Bu)_3$	-32.5	PMe_2F	186
$P(i\text{-}Bu)_3$	-45.3	PMe_2H	-99
$P(s\text{-}Bu)_3$	7.9	PMe_2Cl	96.5
$P(t\text{-}Bu)_3$	63	PMe_2Br	90.5

(b) Phosphorus (V) compounds			
	δ / ppm		δ / ppm
Me_3PO	36.2	Me_3PS	59.1
Et_3PO	48.3	Et_3PS	54.5
$[ME_4P]^+$	24.4	$[Et_4P]^+$	40.1
$[PO_4]^{3-}$	6.0	$[PS_4]^{3-}$	87
PF_5	-80.3	$[PF_6]^-$	-145
PCl_5	-80	$[PCl_4]^+$	86
$MePF_4$	-29.9	$[PCl_6]^-$	-295
Me_3PF_2	-158	Me_2PF_3	8.0

Chemical Shift Ranges and Standards for Selected Nuclei

Nucleus	Spin	Chemical Shift Range δ [ppm]	Standard	Nucleus	Spin	Chemical Shift Range δ [ppm]	Standard
^{1}H	1/2	12 to -1	$SiMe_4$	^{43}Ca	7/2	40 to -40	$CaCl_2$
^{6}Li	1	5 to -10	1M LiCl in H_2O	^{51}V	7/2	0 to -2000	$VOCl_3$
^{7}Li	3/2	5 to -10	1M LiCl in H_2O	^{67}Zn	5/2	100 to -2700	$ZnClO_4$
^{11}B	3/2	100 to -120	$BF_3 \cdot OEt_2$	^{77}Se	1/2	1600 to -1000	$SeMe_2$
^{13}C	1/2	240 to -10	$SiMe_4$	^{93}NB	9/2	0 to -2000	$K[NbCl_6]$
^{15}N	1/2	1200 to -500	$MeNO_2$	^{99}Ru	3/2	3000 to -3000	RuO_3/CCl_4
^{17}O	5/2	1400 to -100	H_2O	^{119}Sn	1/2	5000 to -3000	$SnMe_4$
^{19}F	1/2	100 to -300	$CFCl_3$	^{121}Sb	5/2	1000 to -2700	Et_4NSbCl_6
^{23}Na	3/2	10 to -60	1M NaCl in H_2O	^{129}Xe	1/2	2000 to -6000	$XeOF_4$
^{27}Al	5/2	200 to -200	$[Al(H_2O)_6]^{3+}$	^{133}Cs	7/2	300 to -300	CsBr
^{29}Si	1/2	100 to -400	$SiMe_4$	^{195}Pt	1/2	9000 to -6000	Na_2PtCl_6
^{31}P	1/2	230 to -200	H_3PO_4	^{199}Hg	1/2	500 to -3000	$HgMe_2$

Some Important Silylated Compounds Used as ^{1}H Shift References

Name	Chemical formula	Abbreviation	Molecular weigth	Boiling or melting point (°C)	δ ^{1}H ppm rel. TMS
Tetramethylsilane	$(CH_3)_4Si$	TMS	88.2	BP = 26.3	0
Hexamethyldisilane	$(CH_3)_3Si–Si(CH_3)_3$	HMDS	146.4	BP = 112.3	0.037
Hexamethyldisiloxane	$(CH_3)_3Si–O–Si(CH_3)_3$	HMDSO	162.4	BP = 100	0.055
Hexamethyldisilazane	$(CH_3)_3Si–NH–Si(CH_3)_3$	HMDSA	161.4	BP = 125	0.042
3-(trimethylsilyl)propane sulfonic acid soduim salt 4,4-dimethyl-4-silapentane sodium sulfonate	$(CH_3)_3Si(CH_2)_3SO_3Na$	TSPSA DSS	218.3	MP = 200	0.015
3-(trimethylsilyl)propionic acid sodium salt 4,4-dimethyl-4-silapentane sodium carboxylate	$(CH_3)_3Si(CH_2)_2COONa$	TSP DSC	168.2	MP > 300	0.000
3-(trimethylsilyl) 2,2,3,3-tetra-deuteropropionic acid sodium salt	$(CH_3)_3Si(CD_2)_2COONa$	TSP-d_4	172.2	MP > 300	0.000
Octamethylcyclotetrasiloxane	$(CH_3)_2Si[O–Si(CH_3)_2]_3–O$	OCTS	296.8	BP = 175 MP = 16.8	0.085
1,1,3,3,5,5-hexakis-(trideutero-methyl)-1,3,5-trisilacyclohexane	$(CD_3)_2Si–CH_2–Si(CD_3)_2$ $CH_2–Si(CD_3)_2–CH_2$	CS-d_{18}	216.6	BP = 208	-0.327
Tetrakis-(trimethylsilyl)-methane	$[(CH_3)_3Si]_4C$	TTSM	304.8	MP = 307	0.236

Enhancement Factors η_{NOE} and η_{INEPT} for X {^{1}H} Nuclear Overhauser and INEPT Experiments

X	^{19}F	^{31}P	^{11}B	^{13}C	^{15}N	^{29}Si	^{57}Fe	^{103}Rh	^{109}Ag	^{119}Sn	^{183}W
η_{NOE}[a]	0.53	1.24	1.56	1.99	–4.93	–2.52	15.41	–15.80	–10.68	–1.33	11.86
η_{INEPT}[b]	1.06	2.47	3.12	3.98	–9.86	–5.03	30.82	–31.59	–21.37	–2.67	23.71

[a] The maximum possible intensity enhancement is equal to 1 + η_{NOE} in the extreme narrowing limit.
[b] For ^{19}F or ^{31}P as polarization source (irradiated nucleus) the factors η_{NOE} and η_{INEPT} are reduced by the factor 0.941 [$\gamma(^{19}F)/\gamma(^{1}H)$] and 0.405 [$\gamma(^{31}P)/\gamma(^{1}H)$]

^{1}H, ^{1}H Coupling Constants in Selected Organic Molecules

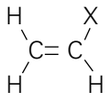

X	$^{3}J_{cis}$	$^{3}J_{trans}$	^{2}J
H	11.6	19.1	2.5
Li	19.3	23.9	7.1
COOH	10.2	17.2	1.7
CN	11.75	17.92	0.91
C_6H_5	11.48	18.59	1.08
CH_3	10.02	16.81	2.08
OCH_3	7.0	14.1	-2.0
Cl	1.3	14.6	-1.4
Br	7.1	15.2	-1.8
F	4.65	12.75	-3.2

$H_3C\text{-}CH_2\text{-}X$

X	^{3}J
Li	8.90
$Si(C_2H_5)_3$	8.0
H	7.5
C_6H_5	7.62
CN	7.60
I	7.45
Br	7.33
CH_3	7.26
Cl	7.23
$N(C_2H_5)_2$	7.13
OC_2H_5	6.97
$^{+}O(C_2H_5)_2$	4.7

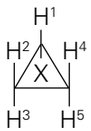

X	$^{3}J(1,2)$	$^{3}J(1,3)$	$^{3}J(2,4)$	$^{3}J(3,5)$	$^{3}J(2,5)$	$^{2}J(2,3)$
H	8.97	5.58	8.97	8.97	5.58	-4.34
Cl	7.01	3.58	10.26	10.58	7.14	-6.01
Br	7.13	3.80	10.16	10.45	7.01	-6.12
I	7.51	4.37	9.89	9.97	6.63	-5.94
NH_2	6.63	3.55	9.65	9.89	6.18	-4.29
CN	8.43	5.12	9.18	9.49	7.08	-4.72
COOH	8.04	4.57	9.26	9.66	7.14	-4.00
COCl	7.88	4.43	9.19	9.99	7.59	-4.46
$COCH_3$	7.96	4.55	8.76	9.60	6.94	-3.41

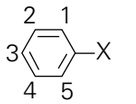

X	$^{3}J(1,2)$	$^{4}J(1,3)$	$^{5}J(1,4)$	$^{4}J(1,5)$	$^{3}J(2,3)$	$^{4}J(2,4)$
H	7.54	1.37	0.66	1.37	7.54	1.37
Li	6.73	1.54	0.77	0.74	1.42	1.29
CH_3	7.64	1.25	0.60	1.87	7.52	1.51[a]
$COOCH_3$	7.86	1.35	0.63	1.79	7.49	1.31
I	7.93	1.14	0.47	1.88	7.47	1.75
Br	8.05	1.12	0.46	2.1	7.44	1.78
Cl	8.05	1.13	0.48	2.27	7.51	1.72
NH_2	8.02	1.11	0.47	2.53	7.39	1.60
$N(CH_3)_2$	8.40	1.01	0.43	2.76	7.29	1.76
$N(CH_3)_3$	8.55	0.92	0.48	3.05	7.46	1.69
NO_2	8.36	1.18	0.55	2.40	7.47	1.48
OH	8.17	1.09	0.49	2.71	7.40	1.74
OCH_3	8.30	1.03	0.44	2.94	7.36	1.76
F	8.36	1.07	0.43	2.74	7.47	1.82[b]

[a] $^{4}J(1, CH_3)$ -0.75
$^{5}J(2, CH_3)$ 0.36
$^{6}J(3, CH_3)$ -0.62

[b] $^{3}J(1, F)$ 8.91
$^{4}J(2, F)$ 5.69
$^{5}J(3, F)$ 0.22

Substituent Effect S(*i,j*) for J_{HH} in Monosubstituted Benzenes

pos. *i,j*	F	Cl	Br	I	NO_2	OCH_3
1,2	+0.81	+0.61	+0.53	+0.39	+0.77	+0.79
1,3	–0.34	–0.23	–0.27	–0.25	–0.20	–0.32
1,4	–0.24	–0.16	–0.20	–0.19	–0.16	–0.22
1,5	+1.21	+0.87	–0.71	+0.51	+1.02	+1.33
2,3	–0.04	+0.03	–0.05	–0.04	–0.07	–0.16
2,4	+0.39	+0.34	+0.36	+0.37	+0.08	+0.38

Additivity Parameters for ^{13}C Chemical Shifts in Substituted Benzenes

$\delta_i = 128.5 + S_i(\delta_i)$, $S_i(\delta_i)$ refers to the carbon atom bearing the substituent

Substituent	$S_i(\delta_i)$	$S_i(\delta_o)$	$S_i(\delta_m)$	$S_i(\delta_p)$	Substituent	$S_i(\delta_i)$	$S_i(\delta_o)$	$S_i(\delta_m)$	$S_i(\delta_p)$
–H	0.0	0.0	0.0	0.0	**–I**	–32.3	9.9	2.6	–0.4
–CH_3	9.3	0.6	0.0	–3.1	**–OH**	26.9	–12.7	1.4	–7.3
–CH_2CH_3	15.7	–0.6	–0.1	–2.8	**–OCH_3**	30.2	–14.7	0.9	–8.1
–$CH(CH_3)_2$	20.1	–2.0	0.0	–2.5	**–NH_2**	19.2	–12.4	1.3	–9.5
–$C(CH_3)_3$	22.1	–3.4	–0.4	–3.1	**–$N(CH_3)_2$**	22.4	–15.7	0.8	–11.8
–Cyclopropyl	15.1	–3.3	–0.6	–3.6	**–$N(C_6H_5)_2$**	19.3	–4.4	0.6	–5.9
–CH_2Cl	9.1	0.0	0.2	–0.2	**–NO_2**	19.6	–5.3	0.8	6.0
–CH_2Br	9.2	0.1	0.4	–0.3	**–CN**	–16.0	3.5	0.7	4.3
–CF_3	2.6	–2.2	0.3	3.2	**–NCO**	5.7	–3.6	1.2	–2.8
–CH_2OH	13.0	–1.4	0.0	–1.2	**–$SC(CH_3)_3$**	4.5	9.0	–0.3	0.0
–$CH=CH_2$	7.6	–1.8	–1.8	–3.5	**–COH**	9.0	1.2	1.2	6.0
–C≡CH	–6.1	3.8	0.4	–0.2	**–$COCH_3$**	9.3	0.2	0.2	4.2
–C_6H_5	13.0	–1.1	0.5	–1.0	**–COOH**	2.4	1.6	–0.1	4.8
–F	35.1	–14.3	0.9	–4.4	**–COO^-**	7.6	0.8	0.0	2.8
–Cl	6.4	0.2	1.0	–2.0	**–$COOCH_3$**	2.1	1.2	0.0	4.4
–Br	–5.4	3.3	2.2	–1.0	**–COCl**	4.6	2.9	0.6	7.0

Nuclear Magnetic Relaxation Rates $(1/T_1)°$ in s^{-1} at Infinite Dilution of Quadrupolar Relaxing Ionic Nuclei in Various Solvents

Ionic nucleus	H_2O	$HCONH_2$	NMF	DMF	DMA	MeOH	EtOH	HCOOH	CH_3CN	$(CH_3)_2CO$	DMSO	HMPT
$^{7}Li^+$	0.027*	0.2	0.18	0.15	0.15	0.035	0.18	0.14	0.05	0.07	0.17	0.36
$^{23}Na^+$	16.2	95	130	90	83	41	95	50	20	30	140	60
$^{39}K^+$	17.8	–	–	–	–	33	–	–	–	–	–	–
$^{87}Rb^+$	386	2400	4000	2900	–	1380	5500	1400	≈342	–	4400	–
$^{133}Cs^+$	0.086	0.45	0.75	0.5	0.67	0.20	1.1	0.27	–	–	0.95	–
$^{35}Cl^-$	26.5	250	340	800	–	400	1300	950	40	–	100	–
$^{81}Br^-$	1050	420	11700	5400	–	11800	43000	28000	700	≈3000	1100	–
$^{127}I^-$	4600	13200	33000	4700	–	46000	$>10^5$	70000	1200	–	4000	–
$^{25}Mg^{2+}$	3.85	–	–	–	–	–	–	–	–	–	–	–
$^{43}Ca^{2+}$	0.80	–	–	–	–	–	–	–	–	–	–	–
$^{87}Sr^{2+}$	170	–	–	–	–	–	–	–	–	–	–	–
$^{137}Ba^{2+}$	4000	–	–	–	–	–	–	–	–	–	–	–
$^{67}Zn^{2+}$	51.8	–	–	–	–	–	–	–	–	–	–	–
$^{27}Al^{3+}$	≈5.7	–	–	–	–	–	–	–	–	–	–	–
$^{45}Sc^{3+}$	≈69	–	–	–	–	–	–	–	–	–	–	–
$^{69}Ga^3$	≦350	–	–	–	–	–	–	–	–	–	–	–
$^{139}La^{3+}$	368	–	–	–	–	–	–	–	–	–	–	–

* in D_2O

Table by courtesy of Dr. M. Holz (Dept. Phys. Chem. University of Karlsruhe, FRG)

NMR Tables

Typical Stray Field Data for NMR Magnet Systems

Magnet System ^1H MHz/mm Bore	Axial Distance (m) from Magnet Center to 5 Gauss (0.5 mT) Line	Radial Distance (m) from Magnet Center to 5 Gauss (0.5 mT) Line
300/54 UltraShield	0.90	0.60
300/89 UltraShield WB	1.60	1.10
400/54 UltraShield	1.50	1.00
400/54 UltraShield Plus	1.00	0.50
400/89 UltraShield WB	2.00	1.40
500/54 UltraShield	1.90	1.30
500/54 UltraShield	1.90	1.30
500/54 UltraShield Plus	1.20	0.60
500/89 UltraShield WB	2.50	1.80
600/54 UltraShield	2.50	1.80
600/54 UltraShield Plus	1.40	0.70
600/89 UltraShield WB	3.50	2.70
700/54 UltraShield	3.10	1.90
750/89 UltraStabilized WB	7.80	6.20
800/54 UltraStabilized	7.60	6.10
800/54 US²	3.40	2.20
800/54 USPlus	2.50	1.50
850/54 US²	3.40	2.20
850/89 US² WB	4.60	3.30
900/54 UltraStabilized	9.80	7.80
900/54 US²	4.60	3.30
950/54 US²	4.60	3.30

Relevant Properties of Cryogenic Fluids

(Liquid helium and nitrogen are used in supercon magnets)

Cryogen	Normal Boiling Point (K)	Latent Heat (J/g)	Amount of Liquid Evaporated by 1 Watt (l/hour)	Liquid Density (g/ml)	Gas Density at NTP (g/ml)	Liquid to NTP Gas Volume Ratio	Enthalpy Change (gas) B.P. to 77 K (J/mole)	Enthalpy Change (gas) 77 to 300 K (J/mole)
Liquid Helium	4.2	20.9	1.038	0.125	1.79×10^{-4}	1 : 700	384	1157
Liquid Hydrogen	20.39	443	0.115	0.071	8.99×10^{-5}	1 : 790	590	2900
Liquid Nitrogen	77.55	198	0.023	0.808	1.25×10^{-3}	1 : 650	–	234
Liquid Oxygen	90.19	212.5	0.015	1.014	1.43×10^{-3}	1 : 797	–	From BP: 193

NTP = normal room temperature and atmospheric pressure

Abbreviations and Acronyms Used in Magnetic Resonance

2D	Two-Dimensional
3D	Three-Dimensional
ACCORDION	2D technique, simultaneous incrementing of evolution and mixing times
ADA	**A**lternated **D**elay **A**cquisition
ADC	**A**nalog-to-**D**igital **C**onverter, **A**pparent **D**iffusion **C**onstant
ADEQUATE	**A**stonishingly Sensitive **D**oubl**E** **QUA**ntum **T**ransfer **E**xperiment
ADLF	**A**diabatic **D**emagnetization in the **L**aboratory **F**rame
ADRF	**A**diabatic **D**emagnetization in the **R**otating **F**rame
A.E.COSY	**A**lternative **E**xclusive **COSY**
AFP	**A**diabtic **F**ast **P**assage
AHT	**A**verage **H**amiltonian **T**heory
AJCP	**A**diabatic **J** **C**ross **P**olarization
AMCP	**A**mplitude-**M**odulated **C**ross **P**olarization
ANGIO	MR **ANGIO**graphy
APHH-CP	**A**diabatic-**P**assage **H**artmann-**H**ahn **C**ross **P**olarization
APT	**A**ttached **P**roton **T**est
AQ	**A**c**Q**uisition
ARP	**A**diabatic **R**apid **P**assage
ASIS	**A**romatic **S**olvent-**I**nduced **S**hift
ASL	**A**rterial **S**pin **L**abeling
ASTM	**A**merican **S**ociety for **T**esting and **M**aterials
BASE	**BA**sis imaging with **SE**lective-inversion preparation
BB	**B**road**B**and, as in decoupling
BDR	**B**roadband **D**ipolar **R**ecoupling
bEPI	**b**lipped **EPI**
bFFE	**b**alanced **F**ast-**F**ield **E**cho
BIRD	**BI**linear **R**otation **D**ecoupling
BIRD/2	half **BIRD**, bilinear π**/2** pulse
BLEW	A windowless multiple-pulse decoupling sequence
BLEW-*n*	**B**urum-**L**inder-**E**rnst **W**indowless homonuc. dipolar dec. sequence of ***n*** pulses
BMS	**B**ulk **M**agnetic **S**usceptibility
BOLD	**B**lood **O**xygenation **L**evel-**D**ependent contrast (MRI)
BOSS	**B**im**O**dal **S**lice-**S**elective
BP	**B**i**P**hasic
BPP	**B**loembergen/**P**urcell/**P**ound (theory)
BR-*n*	**B**urum-**R**him homonuclear dipolar decoupling sequence of ***n*** pulses
BSP	**B**loch-**S**iegert **P**hase
BURP	**B**and-selective **U**niform **R**esponse **P**ure-phase pulse
bTFE	**b**alanced **T**urbo **F**ield **E**cho
BW	**B**and**W**idth
BWR	**B**loch-**W**angsness-**R**edfield theory
CA	**C**ontrast **A**gent
CAMELSPIN	**C**ross-relaxation **A**ppropriate for **M**inimolecules **E**mulated by **L**ocked **SPIN**s
CBCA(CO)NH	**C*b***(i-1) and **C*a***(i-1), **N**(i), H_N(i) 3D correl.
CBCANH	**C*b***(i,i-1) and **C*a***(i,i-1), **N**(i), H_N(i) 3D correl.
CCPPA	**C**oupled **C**luster **P**olarization **P**ropagator **A**pproximation
CE	**C**ontrast-**E**nhanced
CEST	**C**hemical **E**xchange **S**aturation **T**ransfer
CH-COSY	**C**arbon-**H**ydrogen **CO**rrelation **S**pectroscop**Y**
CHESS	**CHE**mical **S**hift **S**elective Imaging Sequence
CHIRP	rf pulse with linear freq. modulation
CIDEP	**C**hemically **I**nduced **D**ynamic **E**lectron **P**olarization
CIDNP	**C**hemically **I**nduced **D**ynamic **N**uclear **P**olarization
CINE	"movie-like" MRI
CISS	**C**onstructive **I**nterference **S**teady **S**tate
CNR	**C**ontrast-to-**N**oise **R**atio
COLOC	**CO**rrelated Spectroscopy via **LO**ng-Range **C**oupling
COLOC-S	**COLOC** with **S**uppression of one-bond correlations
CONOESY	Combined **COSY/NOESY**
CORMA	**CO**mplete **R**elaxation **M**atrix **A**nalysis
CORY-*n*	**CORY** modification of **BR-*n***
COSS	**CO**rrelation with **S**hift **S**caling
COSY	**CO**rrelated **S**pectroscop**Y**
COSY-45	**COSY** with **45°** mixing pulse
COSYDEC	**COSY** with F_1 **DEC**oupling
COSYLR	**COSY** for **L**ong-**R**ange couplings
CP	**C**ross **P**olarization**, C**ircular **P**olarization
CPD	**C**omposite-**P**ulse **D**ecoupling
CPMAS	**C**ross **P**olarization **M**agic-**A**ngle **S**pinning
CPMG	**C**arr-**P**urcell-**M**eiboom-**G**ill Sequence
CRAMPS	**C**ombined **R**otation **A**nd **M**ultiple **P**ulse **S**pectroscopy
CRAZED	**C**orrelated Spectroscopy **R**evamped by **A**symmetric **Z**-gradient **E**cho **D**etection
CRINEPT	**C**ross-correlated **R**elaxation-enhanced **INEPT**
CS	**C**ontiguous **S**lice
CSA	**C**hemical **S**hift **A**nisotropy
CSCM	**C**hemical **S**hift **C**orrelation **M**ap
CSI	**C**hemical **S**hift **I**maging
CT	**C**onstant **T**ime
CW	**C**ontinuous **W**ave
CYCLCROP	**CYCL**ic **CRO**ss **P**olarization
CYCLOPS	**CYCL**ically **O**rdered **P**hase **S**equence
CYCLPOT	**CYCL**ic **PO**larization **T**ransfer
DAC	**D**igital-to-**A**nalog **C**onverter
DAISY	**D**irect **A**ssignment **I**nterconnection **S**pectroscop**Y**
DANTE	**D**elay **A**lternating with **N**utation for **T**ailored **E**xcitation
DAS	**D**ynamic **A**ngle **S**pinning
DCNMR	NMR in Presence of an Electric **D**irect **C**urrent
DD	**D**ipole-**D**ipole
DE	**D**ual **E**cho**,** **D**riven **E**quilibrium

NMR Tables

Abbreviations and Acronyms Used in Magnetic Resonance

DECSY	**D**ouble-quantum **E**cho **C**orrelated **S**pectroscop**Y**
DEFT	**D**riven **E**quilibrium **F**ourier **T**ransform
DEPT	**D**istortionless **E**nhancement by **P**olarization **T**ransfer
DEPTH	spin-echo sequence for spatial localization
DEPTQ	**DEPT** including quaternary carbons
DFT	**D**iscrete **F**ourier **T**ransformation
DICE	**DI**rect **C**onnectivity **E**xperiment
DICOM	**D**igital **I**maging and **CO**mmunications in **M**edicine
DIGGER	**D**iscreet **I**solation from **G**radient-**G**overned **E**limination of **R**esonances
DIPSI	Composite-pulse **D**ecoupling **I**n the **P**resence of **S**calar **I**nteractions
DISCO	**DI**fferences and **S**ums within **COSY**
DLB	**D**ifferential **L**ine **B**roadening
DNMR	**D**ynamic **NMR**
D.NOESY	**D**irect cross-relaxation **NOESY**
DNP	**D**ynamic **N**uclear **P**olarization
DOC	**D**ouble **CO**nstant-Time sequence
DOPT	**D**ipolar **O**rder **P**olarization **T**ransfer
DOR	**D**ouble-**O**rientation **R**otation
DOSY	**D**iffusion-**O**rdered **S**pectroscop**Y**
DOUBTFUL	**DOUB**le Quantum **T**ransition for **F**inding **U**nresolved **L**ines
DPFGSE	**D**ouble **P**ulsed **F**ield **G**radient **S**pin **E**cho
DQ	**D**ouble **Q**uantum
DQC	**D**ouble **Q**uantum **C**oherence
DQF	**D**ouble **Q**uantum **F**ilter
DQF-COSY	**D**ouble **Q**uantum **F**iltered **COSY**
DQSY	**D**ouble-**Q**uantum CO**SY**
DQ/ZQ	**D**ouble **Q**uantum/**Z**ero **Q**uantum Spectroscopy
DRAMA	**D**ipolar **R**ecovery **A**t the **M**agic **A**ngle
DREAM	**D**ouble-quantum **R**elay **E**nhancement by **A**diabatic **M**ixing
DRESS	**D**epth **RES**olved **S**pectrosocpy
DRIVE	**DRIV**en **E**quilibrium
DRYCLEAN	**D**iffusion-**R**educed water signals in spectroscop**Y** of mole**C**ules moving s**L**ow**E**r th**AN** water
DSA	**D**ata-**S**hift **A**cquisition
DSC	**D**ynamic **S**usceptibility **C**ontrast
DSE	**D**ual **S**pin **E**cho
DTI	**D**iffusion **T**ensor **I**maging
DTRCF	**D**ouble **T**ilted **R**otating **C**oordinate **F**rame
DTSE	**D**ouble **T**urbo **S**pin **E**cho
DUMBO	**D**ecoupling **U**sing **M**ind-**B**oggling **O**ptimization – a numerically optimized phase-modulated homonuc. dipolar dec. sequence
DWI	**D**iffusion-**W**eighted **I**maging
E-BURP	**E**xcitation **BURP** pulse
EC	**E**ddy **C**urrents
E.COSY	**E**xclusive **CO**rrelation **S**pectroscop**Y**
ECO-WURST	**WURST** decoupling with **E**limination of **C**ycling **O**scillations
EFG	**E**lectric **F**ield **G**radient
EM	**E**xponential **M**ultiplication
EMF	**E**lectro**M**agnetic **F**ield **E**lectro**M**otive **F**orce
ENDOR	**E**lectron-**N**uclear **DO**uble **R**esonance
ENMR	**E**lectrophoretic **NMR**
EPI	**E**cho-**P**lanar **I**maging
EPR	**E**lectron **P**aramagnetic **R**esonance
EPS	**E**cho-**P**lanar **S**pectroscopy
ES, ESP	**E**cho **S**pacing
E-SHORT	**E**nhanced **SHORT** repetition MRI
ESR	**E**lectron **S**pin **R**esonace
E.TACSY	**E**xclusive **TACSY**
EXORCYCLE	4-step phase cycle for spin echoes
EXSY	**EX**change **S**pectroscop**Y**
FA	**F**lip **A**ngle
FADE	**FA**SE Acq. with **D**ouble **E**cho
FAIR	**F**low-sensitive **A**lternating **I**nversion **R**ecovery
FASE	**F**ast **A**dvanced **S**pin **E**cho
FAST	**F**ourier-**A**cquired **ST**eady State
FASTMAP	**FAST** B_0 Field **MAP**ping for shimming
FATE	**FA**st **T**urbo **E**cho
FC	**F**low **C**ompensation
FC2D_ANGIO	**F**low-**C**ompensated time-of-flight **2D ANGIO**graphy
FE	**F**ield **E**cho**,** **F**requency **E**ncoding
FFE	**F**ast **F**ield **E**cho
FFLG	**F**lip-**F**lop **L**ee-**G**oldburg decoupling
FFT	**F**ast **F**ourier **T**ransform
FGRE	**F**ast **G**radient-**R**ecalled **E**cho
FID	**F**ree **I**nduction **D**ecay
FIDS	**FI**tting of **D**oublets and **S**inglets
FieldMap	B_0 **Field Map**ping for localized shimming
FIRFT	**F**ast **I**nversion-**R**ecovery **F**ourier **T**ransform
FISP	**F**ast **I**maging with **S**teady-state **P**recession
FL2D_ANGIO	**FL**ow-sensitive **2D ANGIO**graphy
FLAIR	**FL**uid **A**ttenuation **I**nversion-**R**ecovery
FLASH	**F**ast **L**ow-**A**ngle **SH**ot imaging
FLOCK	Long-range HETCOR using 3 BIRD pulses
FLOPSY	**F**lip-**FLOP** **S**pectroscop**Y**
FLOW_MAP	Quantitative **FLOW MAP**ping and PC-angiography
FMP	**F**ast **M**ulti**P**lanar
fMRI	**f**unctional **MRI**
FOCSY	**FO**ldover-**C**orrected **S**pectrospcop**Y**
FONAR	Field-focusing MRI
FOV	**F**ield **O**f **V**iew
FPT	**F**inite **P**erturbation **T**heory
FR	**F**requency **E**ncoding
FS	**F**at **S**aturation**,** **F**ast **S**can

Abbreviations and Acronyms Used in Magnetic Resonance

FSE	**F**ast **S**pin **E**cho
FSLG	**F**requency-**S**witched **L**ee-**G**oldburg – a homonuc. dipolar dec. scheme
FSPGR	**F**ast **SP**oiled **GR**adient Echo
FT	**F**ourier **T**ransform
FUCOUP	**FU**lly **COUP**led Spectroscopy
FWHM	**F**ull (line) **W**idth at **H**alf **M**aximum
GARP	**G**lobaly Optimized **A**lternating Phase **R**ectangular **P**ulses
GE	**G**radient **E**cho
GEFC	**G**radient **E**cho with **F**low **C**ompensation
gem-COSY	**gem**inal-filtered **COSY**
GES	**G**radient-**E**cho **S**pectroscopy
GFE	**G**radient **F**ield **E**cho
GRASE	**GRA**dient and **S**pin **E**cho
GRASP	**GR**adient-**A**ccelerated **SP**ectroscopy
GRASS	**G**radient-**R**ecalled **A**cquisition in the **S**teady **S**tate
GRE	**G**radient-**R**ecalled **E**cho
GRECCO	**GR**adient-**E**nhanced **C**arbon **CO**upling
GROESY	**G**radient-Enhanced Selective 1D **ROESY**
GROPE	**G**eneralized compensation for **R**esonance **O**ffset and **P**ulse length **E**rrors
GS	**G**radient **S**pectroscopy
gs- ...	**g**radient-**s**elected ... (e.g. gs-COSY)
H,X-COSY	**H,X** shift correlation (X-detected)
HASTE	**H**alf-Fourier **A**cquisition **S**ingle-shot **T**urbo spin **E**cho
HBHA (CBCA CO) NH	**H***b*(*i*-1) and **H***a*(*i*-1), **N**(*i*), $\mathbf{H_N}$(*i*) 3D correl.
HCACO	**H***a*(*i*), **C***a*(*i*), **C'O**(*i*) 3D correl.
HCACON	**H***a*(*i*), **C***a*(*i*), **C'O**(*i*), **N**(*i*+1) 4D correl.
HCA(CO)N	**H***a*(*i*), **C***a*(*i*), **N**(*i*+1) 3D correl.
HCA(CO) NNH	**H***a*(*i*), **C***a*(*i*), **N**(*i*+1), $\mathbf{H_N}$(*i*+1) 4D correl.
HCANNH	**H***a*(*i*), **C***a*(*i*), **N**(*i*), $\mathbf{H_N}$(*i*) 3D correl.
(H)CC(CO) NH	**C***a,b,...*(*i*), **N**(*i*+1), $\mathbf{H_N}$(*i*+1) 3D correl.
HCCH-COSY	**H***a*(*i*), **C***a*(*i*), **H***b*(*i*) 3D correl.
HCCH-TOCSY	total correlation of side-chain H and C
HDQC	**H**eteronuclear **D**ouble-**Q**uantum **C**orrelation
HEED	**H**ahn spin-**E**cho **E**xtende**D** sequence
HET2DJ	**HET**eronuclear **2D J**-correlated
HETCOR	**HET**eronuclear **COR**relation Spectroscopy
HETLOC	**HET**eronuclear **LO**ng-range **C**ouplings
HEHAHA	**HE**teronuclear **HA**rtmann **HA**hn
HMBC	**H**eteronuclear **M**ultiple-**B**ond **C**orrelation
HMQ	**H**eteronuclear **M**ultiple-**Q**uantum
HMQC	**H**eteronuclear **M**ultiple-**Q**uantum **C**oherence
HMSC	**H**eteronuclear **M**ultiple- and **S**ingle-bond **C**orrelation
HNCA	$\mathbf{H_N}$(*i*), **N**(*i*), **Ca**(*i*) and **Ca**(*i*-1) 3D shift correlation
HNCA-J	3D **HNCA** to measure $^3J(H_N,H\alpha)$
HN(CA)NNH	$\mathbf{H_N}$(*i*), **N**(*i*), **N**(*i*+1) and **N**(*i*-1) 3D correl.
HN(CA)CO	$\mathbf{H_N}$(*i*), **N**(*i*), **C'O**(*i*), and **C'O**(*i*-1) 3D shift correlation
H(N)CACO	$\mathbf{H_N}$(*i*), **Ca**(*i*), **C'O**(*i*) 3D shift correlation
HNCAHA	$\mathbf{H_N}$(*i*), **N**(*i*), **Ca**(*i*), **Ha**(*i*) 4D shift correlation
HNCO	$\mathbf{H_N}$(*i*), **N**(*i*), **C'O**(*i*-1) 3D shift correlation
HN(CO)CA	$\mathbf{H_N}$(*i*), **N**(*i*), **Ca**(*i*-1) 3D shift correlation
H(N)COCA	$\mathbf{H_N}$(*i*+1), **C'O**(*i*), **Ca**(*i*) 3D shift correlation
HN(CO) CAHA	$\mathbf{H_N}$(*i*+1), **N**(*i*+1), **Ca**(*i*), **Ha**(*i*) 4D shift correlation
HOESY	**H**eteronuclear **O**verhauser **E**ffect **S**pectroscop**Y**
HOHAHA	**HO**monuclear **HA**rtmann-**HA**hn Spectroscopy
HORROR	double-quantum **HO**mo-nuclea**R RO**tary **R**esonance
HQQC	**H**eteronuclear **Q**uadruple-**Q**uantum **C**orrelation
HR	**H**igh **R**esolution
HRPA	**H**igher **R**andom **P**hase **A**pproximation
HS	**H**omo**S**poil
HSL	**H**eteronuclear **S**pin **L**ock
HSQC	**H**eteronuclear **S**ingle-**Q**uantum **C**oherence
HTQC	**H**eteronuclear **T**riple-**Q**uantum **C**orrelation
I-BURP	**I**nversion **BURP** pulse
ICE	**I**ndirect **C**onnectivity **E**xperiment
IDESS	**I**mproved **DE**pth **S**elective single surface coil **S**pectroscopy
IDR	**I**nverted **D**irect **R**esponse
IEPI	**I**nterleaved **EPI**
IFT	**I**nverse **FT**
IGLO	**I**ndividual **G**auge for different **L**ocalized **O**rbitals
INADE-QUATE	**I**ncredible **N**atural **A**bu-dance **DoubI E QUA**natum **T**ransfer **E**xperiment
INAPT	**INEPT** with selective 1H excitation
INDOR	**IN**ternuclear **DO**uble **R**esonance
INEPT	**I**nsensitive **N**uclei **E**nhanced by **P**olarization **T**ransfer
INEPT+	**INEPT** with refocusing period for in-phase multiplets
INEPT-R	**INEPT R**efocused for 1H-dec. spectra
INSIPID	**IN**adequate **S**ensitivity **I**mprovement by **P**roton **I**ndirect **D**etection
IntraGate-FLASH	Cardiac and respiration cine MRI with retrospective (trigger-free) gating
INVERSE	H, X correlation via ^{1}H detection
IPAP	**I**n-**P**hase **A**nti-**P**hase (in 2D)
IR	**I**nversion-**R**ecovery
IRMA	**I**terative **R**elaxation **M**atrix **A**nalysis
ISECR	**I**n-pha**SE CR**oss peaks (method)

Abbreviations and Acronyms Used in Magnetic Resonance

ISIS	**I**mage-**S**elected **I**n-vivo **S**pectroscopy (single-voxel)
IST	**I**rreducible **S**pherical **T**ensor
IVIM	**I**ntra**V**oxel **I**ncoherent **M**otion
JCP	**J C**ross-**P**olarization
J-mod	**J mod**ulation
JR	**J**ump-and-**R**eturn sequence (90_y-τ-90_{-y})
J-res	**J-res**olved 2D
LAS	**L**aboratory **A**xis **S**ystem
LASE	**L**ow-**A**ngle **SE**
LB	**L**ine **B**roadening (via EM)
LG	**L**orentz-**G**auss window function
LIS	**L**anthanide **I**nduced **S**hift
LORG	**L**ocal **ORiG**in
LOSY	**LO**calized **S**pectroscop**Y**
LP	**L**inear **P**olarization, **L**inear **P**rediction
LPSVD	**L**inear **P**rediction using **S**ingular **V**alue **D**ecomposition
LSR	**L**anthanide **S**hift **R**eagent
LUT	**L**ook**U**p **T**able
MAGROFI	**MA**gnetization **G**rid **RO**tating-**F**rame **I**maging
MARCO POLO	**M**ultiple **A**nalysis by **R**eduction of **C**ross peaks and **O**rdering of **P**atterns in an **O**verdetermined **L**ibrary **O**rganization
MARDI-GRAS	**M**atrix **A**nalysis of **R**elaxati-on for **DI**stance **G**eomet**R**y of an **A**queous **S**tructure
MARF	**M**agic **A**ngle in the **R**otating **F**rame
MAS	**M**agic-**A**ngle **S**pinning
MASS	**M**agic-**A**ngle **S**ample **S**pinning
MAST	**M**otion **A**rtifact **S**uppression **T**echnique
MDEFT	**M**odified **D**riven **E**quilibrium **FT** method
ME	**M**ulti**E**cho
MEDUSA	Technique for the Determination of Dynamic Structures
MEM	**M**aximum **E**ntropy **M**ethod
MEMP	**M**ulti**E**cho **M**ulti**P**lanar
MESS	**M**ulti**E**cho **S**ingle **S**hot
MFISP	**M**irrored **FISP** (PSIF)
MGE	**M**ultiple **G**radient **E**cho
MINIP	**MIN**inmum **I**ntensity **P**rojection
MIP	**M**aximum **I**ntensity **P**rojection
MLEV	M. Levitt's CPD sequence
MLM	**M**aximum **L**ikelihood **M**ethod
MOTSA	**M**ultiple **O**verlapping **T**hin **S**lab(Slice) **A**cquisition
MP	**M**ultiple **P**ulse, **M**ulti**P**lanar, **M**agnetization-**P**repared
MPF*n*	**M**ultiple-**P**ulse Decoupling with **P**hase and **F**requency Switching with ***n*** offsets
MP-GR	**M**ulti**P**lanar **G**radient-**R**e-called Acq. in Steady State
MPR	**M**ulti**P**lanar **R**econstruction
MP-RAGE	**M**agnetization-**P**repared **RA**pid **G**radient **E**cho (MP-GRE)
MQ	**M**ultiple-**Q**uantum
MQC	**M**ultiple-**Q**uantum **C**oherence
MQF	**M**ultiple-**Q**uantum **F**ilter
MQHPT	**M**ultiple-**Q**uantum **H**eteronuclear **P**olarization **T**ransfer
MQS	**M**ultiple-**Q**uantum **S**pectroscopy
MR	**M**agnetic **R**esonance
MRA	**MR A**ngiography
MREV-*n*	**M**ansfield-**R**him-**E**lleman-**V**aughan homonuc. dipolar dec. cycle of ***n*** pulses
MRV	**MR V**enography
MRI	**M**agnetic **R**esonance **I**maging
MRS	**M**agnetic **R**esonance **S**pectroscopy
MRSI	**M**agnetic **R**esonance **S**pectroscopic **I**maging
MRT	**M**agnetic **R**esonance **T**omography
MS	**M**ulti**S**lice
mSENSE	**m**odified **SENSE**
MS-EPI	**M**ulti**S**hot **EPI**
MSHOT-*n*	**M**agic **S**andwich **H**igh-**O**rder **T**runcation homo-nuc. dipolar decoupling sequence with ***n*** TREV-4 sandwiches
MSME	**M**ulti**S**lice **M**ulti**E**cho (T2 mapping)
MSOFT	**M**ulti**S**lice **O**ff-resonance **FaT** Suppression
MSP	**M**ultiple **S**ensitive **P**oint
MSPGSE	**M**ultiple-**S**tepped **PGSE**
MT	**M**agnetization **T**ransfer
MTC	**M**agnetization **T**ransfer **C**ontrast
MTSA	**M**ultiple **T**hin-**S**lab **A**cquisition
MUSIC	**MU**ltiplicity-**S**elective **I**n-phase **C**oherence transfer
MVS	**M**ultiple **V**olume **S**pectroscopy
NEDOR	**N**uclear **E**lectronic **DO**uble **R**esonance
NERO	**N**onlinear **E**xcitation with **R**ejection on **R**esonance
NEWS	**N**arrow-gap non-**E**xcitation for **W**ater **S**uppression
NEX	**N**umber of **EX**citations
NMR	**N**uclear **M**agnetic **R**esonance
NOE	**N**uclear **O**verhauser **E**ffect
NOE-DIFF	**NOE-DIFF**erence spectroscopy
NOESY	**NOE**-based 2D shift correlation
NOVEL	**N**uclear **O**rientation **V**ia **E**lectron spin **L**ocking
NPW	**N**o **P**hase **W**rap
NQCC	**N**uclear **Q**uadrupole **C**oupling **C**onstant
NQR	**N**uclear **Q**uadrupole **R**esonance
NQS	**N**on-**Q**uaternary **S**uppression
NSPECT	**N**on-localized **SPECT**roscopy
OBTUSE	**O**ffset **B**inomial **T**ailored for **U**niform **S**pectral **E**xcitation
OCS	**O**ptimized **C**osine-**S**ine pulse
ODMR	**O**ptically **D**etected **M**agnetic **R**esonance
OS	**O**vercontiguous **S**lices
OSIRIS	**O**uter-Volume-**S**uppressed **I**mage-**R**elated **I**n vivo **S**pectroscopy – a modification of ISIS
PACE	**P**rospective **A**cquisition **CorrE**ction
PAR	**P**hase-**A**lternated **R**otation of magnetization

Abbreviations and Acronyms Used in Magnetic Resonance

PARACEST	**PARA**magnetic **C**hemical **E**xchange **S**aturation **T**ransfer
PAS	**P**rincipal **A**xis **S**ystem
PC	**P**hase **C**ontrast
PCA	**P**hase **C**ontrast **A**ngio-graphy
P.COSY	**P**urged **COSY**
PD	**P**roton **D**ensity
PDLF	**P**roton-**D**etected **L**ocal **F**ield
PE	**P**hase **E**ncoding
P.E.COSY	**P**rimitive **E.COSY**, **P**urged **E**xclusive **COSY**
PEDRI	**P**roton-**E**lectron **D**ouble **R**esonance **I**maging
PELF	**P**roton-**E**ncoded **L**ocal **F**ield
PENDANT	**P**olarization **EN**hancement **D**uring **A**ttached **N**ucleus **T**esting
PEP	**P**reservation of **E**quivalent **P**athways
PFG	**P**ulsed **F**ield **G**radient
PFGSE	**P**ulsed **F**ield **G**radient **S**pin **E**cho
PGSE	**P**ulsed **G**radient **S**pin **E**cho
PISEMA	**P**olarization **I**nversion with **S**pin **E**xchange at the **M**agic **A**ngle
PITANSEMA	**P**olarization **I**nversion **T**ime **A**veraged **N**utation **S**pin **E**xchange at the **M**agic **A**ngle
PJR	**P**ower-adapted **J**ump and **R**eturn
PMFG	**P**ulsed **M**agnetic **F**ield **G**radient
PMLG	**P**hase-**M**odulated **L**ee-**G**oldburg dipolar decoupling
PMRFI	**P**hase-**M**odulated **R**otating-**F**rame **I**maging
POF	**P**roduct **O**perator **F**ormalism
POMMIE	**P**hase **O**scillations to **M**axi**MI**ze **E**diting
POST	**P**ermutationally **O**ffset-**ST**abilized
PRE	**P**roton **R**elaxation **E**nhancement
Presat	**Presat**uration (usually of solvent)
PRESS	**P**oint-**RES**olved **S**pectroscopy
PRFT	**P**artially **R**elaxed **F**ourier **T**ransform
PROPELLER	**P**eriodically **R**otated **O**ver-lapping **P**arall**EL** **L**ines with **E**nhanced **R**econstruction
PS	**P**artial **S**aturation
PS-COSY	**P**hase-**S**ensitive **COSY**
PSD	**P**hase-**S**ensitive **D**etection
PSIF	mirrored **FISP** (SE acquisition)
PT	**P**olarization **T**ransfer
PW	**P**ulse **W**idth
PWI	**P**erfusion-**W**eighted **I**maging
Q	**Q**uality **F**actor (of RF coil/circuit) **Q**uantitative ... (e.g. **QMRI**, **QCSI**)
Q.F	**Q**uadrupole moment/**F**ield gradient (interaction or relaxation mechanism)
Q. Flow	**Flow Q**uantification
QPD	**Q**uadrature **P**hase **D**etection
QUEST	**QU**ick **E**cho **S**plit Imaging **T**echnique
QUIPSS	**QU**antitative **I**maging of **P**erfusion using a **S**ingle **S**ubtraction
RAM	**R**apid **A**cquisition **M**atrix
RARE	**R**apid **A**cquisition **R**elaxation **E**nhanced
RAREst	**RARE** with **s**hort **t**E using slew-rate-optimized gradients
RAREVTR	**RARE** with **V**ariable **TR** (simultaneous T_1 & T_2 mapping)
RASE	**R**apid **A**cquisition **S**pin **E**cho
RBW	**R**eceiver **B**and**W**idth
RCF	**R**otating **C**oordinate **F**rame
RCT	**R**elayed **C**oherence **T**ransfer
RE	**R**apid **E**xcitation (MRI)
REAPDOR	**R**otational **E**cho **A**diabatic **P**assage **DO**uble **R**esonance
RE-BURP	**R**efocused **B**and-selective **U**niform **R**esponse **P**ure phase
RECSY	Multistep **RE**layed **C**oherence **S**pectroscop**Y**
REDOR	**R**otational **E**cho **DO**uble **R**esonance
RELAY	**RELAY**ed Correlation Spectroscopy
REPAY	**R**everse **E**diting of **P**rotons **A**ccording to multiplicit**Y**
REREDOR	**R**otor-**E**ncoded **REDOR**
REST	**RE**gional **S**aturation **T**echnique
RF	**R**adio **F**requency
RFDR	**RF**-**D**riven **R**ecoupling
RF-FAST	**RF**-spoiled **FAST**
RFOV	**R**ectangular **FOV**
RICE	**R**apid **I**maging using **C**om-posite **E**cho
RIDE	**RI**ng **D**own **E**limination
RINEPT	**R**everse **INEPT**
RISE	**R**apid **I**maging using **S**pin **E**cho
RMSD	**R**oot-**M**ean-**S**quare **D**eviation
ROAST	**R**esonant **O**ffset **A**veraging in the **ST**eady State
RODI	**RO**tatin-grame relaxation **D**ispersion **I**maging
ROE	**R**otating-frame **O**verhauser **E**ffect
ROESY	**ROE**-based 2D shift correlation
ROI	**R**egion **O**f **I**nterest
ROPE	**R**espiratory **O**rdered **PE**
ROTO	**RO**ESY-**TO**CSY Relay
RPA	**R**andom **P**hase **A**pproximation
RR	**R**otational **R**esonance
RSSARGE	**RF**-**S**poiled **SARGE**
RT	**R**espiratory **T**rigger
RUFIS	**R**otating **U**ltra**F**ast **I**maging **S**equence
SA	**S**hielding **A**nisotropy
SAR	**S**pecific **A**bsorption **R**ate (RF)
SARGE	**S**poiled steady-state **A**cquisition with **R**ewinded **G**radient **E**cho
SAT	**SAT**uration
SB	**S**ine-**B**ell window function
SC	**S**calar **C**oupling
S.COSY	**COSY** with shift **S**caling in F1
SCT	**SC**an **T**ime
SCUBA	**S**timulate **C**ross peaks **U**nder **B**leached **A**lphas
SD	**S**pin **D**ipolar

NMR Tables

Abbreviations and Acronyms Used in Magnetic Resonance

SDDS	**S**pin **D**ecoupling **D**ifference **S**pectroscopy
SDEPT	**S**elective **DEPT**
SE	**S**pin **E**cho
SECSY	**S**pin-**E**cho **C**orrelated **S**pectroscop**Y**
SEDOR	**S**pin-**E**cho **DO**uble **R**esonance
SEDRA	**S**imple **E**xcitation for **D**ephasing of **R**otational echo **A**mplitudes
SEDUCE	**SE**lective **D**ecoupling **U**sing **C**rafted **E**xcitation
SEFT	**S**pin-**E**cho **F**ourier **T**ransform Spectroscopy (with J modulation)
SELCOSY	**SEL**ective **COSY**
SELTICS	**S**ideband **EL**imination by **T**emporary **I**nterruption of the **C**hemical **S**hift
SELINCOR	**SEL**ective **IN**verse **COR**relation
SELINQUATE	**SEL**ective **INADEQUATE**
SELRESOLV	**SEL**ective **RES**olution of C,H Coupling
SEMS	**S**pin-**E**cho **M**ulti**S**lice
SEMUT	**S**ubspectral **E**diting Using a **MU**ltiple-Quantum **T**rap
SENSE	**SENS**itivity **E**ncoding
sEPI	**s**piral **EPI**
SEPT	**S**elective IN**EPT**
SERF	**SE**lective **R**e**F**ocussing
SESAM	**SE**mi-**S**elective **A**cquisition **M**odulated (Decoupling)
SFAM	**S**imultaneous **F**req. and **A**mpl. **M**odulation
SFORD	**S**ingle **F**requency **O**ff-**R**esonance **D**ecoupling
SGSE	**S**teady-**G**radient **S**pin-**E**cho
SHECOR	**S**elective **HE**teronuclear **COR**relation
SHORT	**SHORT** repetition techniques
SI	**S**pectroscopic **I**maging
SIAM	**S**imultaneous acq. of **I**n-phase and **A**ntiphase **M**ultiplets
SIP	**S**aturation **I**nversion **P**rojection
SIMBA	**S**elective **I**nverse **M**ultiple-**B**ond **A**nalysis
SINEPT	**SINE**-dependent **PT**
SINGLE PULSE	**SINGLE PULSE**-acquire spectroscopy
SIS	**S**ubstituent-**I**nduced **S**hift
SJR	**S**econd-order **J**ump and **R**eturn
SKEWSY	**SKEW**ed Exchange **S**pectroscop**Y**
SL	**S**pin-**L**ock pulse
SLF	**S**eparated **L**ocal **F**ield
SLITDRESS	**SLI**ce in**T**erleaved **D**epth **RE**solved **S**urface coil **S**pectroscopy
SLOPT	**S**pin-**LO**cking **P**olarization **T**ransfer
SMART	**S**himadzu **M**otion **A**rtifact **R**eduction **T**echnique
SMASH	**S**hort **M**inimum **A**ngle **SH**ot, **S**i**M**ultaneous **A**cquisition of **S**patial **H**armonics
SNR or S/N	**S**ignal-to-**N**oise **R**atio
SOPPA	**S**econd-**O**rder **P**olarization **P**ropagator **A**pproach
SORS/STC	**S**lice-selective **O**ff-**R**eso-nance **S**inc Pulse / **S**atura-tion **T**ransfer **C**ontrast
SPACE	**SPA**tial and **C**hemical-Shift **E**ncoded **E**xcitation
SPAIR	**SP**ectral **S**election **A**ttenu-ated **I**nversion **R**ecovery
SPECIFIC-CP	**SPEC**trally **I**nduced **F**iltering **I**n **C**ombination with **C**ross **P**olarization
SPEED	**S**wap **P**has**E**-**E**ncoded **D**ata
SPGR	**SP**oiled **G**radient-**R**ecalled
SPI	**S**elective **P**opulation **I**nversion
SPIDER	**S**teady-state **P**rojection **I**maging with **D**ynamic **E**cho **T**rain **R**eadout
SPIO	**S**uper**P**aramagnetic **I**ron **O**xide
SPIR	**S**pectral **P**resaturation **I**nversion-**R**ecovery
SPIRAL	MRI with **SPIRAL** *k*-space scan
SPRITE	**S**ingle-**P**oint **R**amped **I**ma-ging with **T**1 **E**nhancement
SPT	**S**elective **P**opulation **T**ransfer
SQ	**S**ingle-**Q**uantum
SQC	**S**ingle-**Q**uantum **C**oherence
SQF	**S**ingle-**Q**uantum **F**ilter
SR	**S**aturation-**R**ecovery
SRP	**S**elf-**R**efocusing **P**ulse
SS	**S**lice **S**election (gradient), **S**ingle **S**lice
SSB	**S**hifted **S**ine-**B**ell window function
SSFP	**S**teady-**S**tate **F**ree **P**recession
SSFSE	**S**ingle-**S**hot **FSE**
SSI	**S**olid **S**tate **I**maging
SSMP	**S**ingle-**S**lice **M**ultiple-**P**hase
ssNMR	**s**olid-**s**tate **NMR**
SSTSE/T2	**S**ingle-**S**hot **TSE** with **T2** weighting
ST	**S**aturation **T**ransfer, **S**lice **T**hickness
STAGE	**S**mall **T**ip **A**ngle **GE**
STE	**ST**imulated **E**cho
STEAM	**ST**imulated **E**cho **A**cquisiti-on **M**ode for imaging
STEP	**STE P**rogressive Imaging
STERF	**S**teady-State **TE**chnique with **R**efocused **F**ID
STIR	**S**hort **T1** **I**nversion-**R**ecovery
STREAM	**S**uppressed **T**issue with **RE**freshment **A**ngiography **M**ethod
STUD	**S**ech/**T**anh **U**niversal **D**ecoupling – an adiabatic decoupling scheme
SUBMERGE	**SU**ppression **B**y **M**istuned **E**cho and **R**epetitive **G**radient **E**pisodes
SUSAN	**S**pin decoupling employing **U**ltra-broadband inversion sequences generated via **S**imulated **AN**nealing
SWATTR	**S**elective **W**ater **A**ttenuati-on by **T2** and **T1** **R**elaxation
SVS	**S**ingle-**V**olume **S**pectroscopy
T1 ...	**T1**-weighted ... (method)
T1W	**T1-W**eighted
T2 ...	**T2**-weighted ... (method)
T2W	**T2-W**eighted
T2*W	**T2*-W**eighted
TACSY	**TA**ylored **C**orrelation **S**pectroscop**Y**
TANGO	**T**esting for **A**djacent **N**uclei with a **G**yration **O**perator

Abbreviations and Acronyms Used in Magnetic Resonance

TART	**T**ip **A**ngle **R**educed T_1 Imaging
TD	**T**rigger **D**elay, **T**ime **D**ifference
TCF	**T**ime **C**orrelation **F**unction
TE	**T**ime delay between excitation and **E**cho maximum
TEDOR	**T**ransferred-**E**cho **DO**uble **R**esonance
TEI	**TE** **I**nterleaved
TF	**T**urbo **F**actor
TFE	**T**urbo **F**ield **E**cho
TGSE	**T**urbo **G**radient **S**pin **E**cho
THRIVE	**T**1W **H**igh-**R**esolution **I**sotropic **V**olume **E**xamination
TI	**T**ime following **I**nversion
TIR	**T**urbo **IR**
TMR	**T**opical **M**agnetic **R**esonance
TOBSY	**TO**tal through-**B**ond correlation **S**pectroscop**Y**
TOCSY	**TO**tal **C**orrelation **S**pectroscop**Y**
TOF	**T**ime-**O**f-**F**light
TOE	**T**runcated N**OE**
TONE	**T**ilt-**O**ptimized **N**onsaturated **E**xcitation
TORO	**TO**CSY-**RO**ESY Relay
TOSS	**TO**tal **S**uppression of **S**idebands
TPPI	**T**ime-**P**roportional **P**hase **I**ncrementation
TPPM	**T**wo-**P**ulse **P**hase **M**odulation
TPR	**T**ime and **P**hase **R**eversal
TQ	**T**riple-**Q**uantum
TQF	**T**riple-**Q**uantum **F**ilter
TR	**T**ime for **R**epetition of excitation
T/R	**T**ransmit/**R**eceive
TRAPDOR	**TRA**nsfer of **P**opulations in **DO**uble **R**esonance
TRCF	**T**ilted **R**otating **C**oordinate **F**rame
TREV-*n*	**T**ime-**REV**ersal echo sequence of ***n*** pulses for homonuc. dipolar dec.
TRNOE	**TR**ansferred **NOE**
TROSY	**T**ransverse **R**elaxation **O**ptimized **S**pectroscop**Y**
T-ROESY	**T**ransverse **ROESY**

TrueFISP	**FISP** with balanced gradient waveform
TS	**T**ime of **S**aturation
TSE	**T**urbo **S**pin **E**cho
TSETSE	double-resonance **T**wo-**S**pin **E**ffect for correlation spectroscopy
TSR	**T**otal **SR**
Turbo-FLASH	**FLASH** sequence during one IR period
U-BURP	**U**niversal **BURP** pulse
UE	**U**npaired **E**lectron (relaxation mechanism)
UFSE	**U**ltra**F**ast **SE**
UNCOSY	**UN**iform excitation **COSY**
USPIO	**U**ltra**S**mall **P**aramagnetic **I**ron **O**xide
UTE	**U**ltra-short **TE** radial scan
UTSE	**U**ltra-short **TSE**
VAPRO	**VA**riable **PRO**jection method
VAS	**V**ariable **A**ngle **S**pinning
VE	**V**elocity-**E**ncoded
VEC	**V**elocity-**E**ncoded **C**ine (MRI)
VEMP	**V**ariable-**E**cho **M**ulti**P**lanar
VENC	**V**elocity **ENC**oding value
VEST	**V**olume **E**xcitation **ST**imulated echoes
VIGRE	**V**olumetric **I**nterpolated **GR**adient **E**cho
VOI	**V**olume **O**f **I**nterest
VOSING	**VO**lume-selective **S**pectral edit**ING**
VOSY	**VO**lume-Selective **S**pectroscop**Y**
VPS	**V**olumes **P**er **S**egment
VSOP	**V**ery **S**mall superparamagnetic iron **O**xide **P**articles
WAHUHA	**WA**ugh-**HU**ber-**HA**eberlen Sequence
WALTZ	CPD Sequence Containing the Elements 1-2-3
WATER-GATE	**WATER** suppression through **GR**adient **T**ailored **E**xcitation
WATR	**W**ater **A**ttenuation by **T**ransverse **R**elaxation
WEFT	**W**ater **E**liminated **F**ourier **T**ransform
WET	**W**ater suppression **E**nhanced through **T**1 effects

WFOP	**W**ater **F**at **O**pposed **P**hase
WFS	**W**ater **F**at **S**eparation (Shift Difference)
WHH-*n*	**WAHUHA** dec. cycle of ***n*** pulses
WIM-*n*	**W**indowless **I**sotropic **M**ixing dec. cycle of ***n*** pulses
WURST	**W**ideband, **U**niform **R**ate, and **S**mooth **T**runcation – an adiabatic decoupling sequence
XCORFE	H, **X** **COR**relation using a **F**ixed **E**volution time
XD-NOESY	e**X**change-**D**ecoupled **NOESY**
X-FILTER	Selection of ^{1}H-^{1}H correlation when both H are coupled to X
X-HALF-FILTER	Selection of ^{1}H-^{1}H correlation when one H is coupled to X
Z-COSY	**Z**-filtered **COSY**
Z-FILTER	pulse sandwich for elimination of signal components with dispersive phase
ZECSY	**Z**ero-Quantum-**E**cho **C**orrelation **S**pectroscop**Y**
ZIP	**Z**ero-fill **I**nterpolation **P**rocessing
ZQ	**Z**ero **Q**uantum
ZQC	**Z**ero-**Q**uantum **C**oherence
ZQF	**Z**ero-**Q**uantum **F**ilter
ZZ-Spectroscopy	Selection of coherences involving ZZ or longitudinal two-spin order
ZZZ-Spectroscopy	Selection of coherences involving longitudinal 3-spin order
β-COSY	COSY with low-angle mixing pulse
Ψ-COSY	pseudo-COSY using incremented freq.-selective excitation

Symbols for NMR and Related Quantities*

Roman alphabet	
a or *A*	Hyperfine (electron-nucleus) coupling constant
$A_q^{(l,m)}$	The *m*th component of an irreducible tensor of order *l* representing the nuclear spin operator for an interaction of type *q*
$\boldsymbol{B}$	Magnetic field (strictly the magnetic flux density or magnetic induction)
$\boldsymbol{B}_0$	Static magnetic field of an NMR spectrometer
$\boldsymbol{B}_1$, $\boldsymbol{B}_2$	Radiofrequency magnetic fields associated with frequencies ν_1, ν_2
$\boldsymbol{B}_L$	Local magnetic field of random field or dipolar origin
$\boldsymbol{C}$	Spin-rotation interaction tensor
C_X	Spin-rotation coupling constant of nuclide X
$\boldsymbol{D}$	Dipolar interaction tensor
$D_{i,j}$	Dipolar coupling constant between nuclei (*i* and *j*), in Hz
D^C	Nuclear receptivity relative to that of ^{13}C
D^P	Nuclear receptivity relative to that of ^{1}H
$\boldsymbol{E}$	Electric field strength
F	Spectral width
F_1, F_2 or f_1, f_2	The two frequency dimensions of a two-dimensional spectrum
$\hat{\boldsymbol{F}}_G$	Nuclear spin operator for a group, G, of nuclei
F_G	Magnetic quantum number associated with $\hat{\boldsymbol{F}}_G$
g	Nuclear or electronic *g* factor (Landé splitting factor)
G	Magnetic field gradient amplitude
$\hat{\boldsymbol{H}}$	Hamiltonian operator
$H_{i,j}$	Matrix element of Hamiltonian operator
$\hat{\boldsymbol{I}}_j$	Nuclear spin operator for nucleus *j*
$\hat{I}_{j+}$, $\hat{I}_{j-}$	'Raising' and 'lowering' spin operators for nucleus *j*
I_j	Magnetidc quantum number associated with $\hat{\boldsymbol{I}}_j$
$\boldsymbol{J}$	Indirect coupling tensor
$^nJ_{AB}$	Spin-spin coupling constant for nuclei A and B through *n* bonds in Hz
$J(\omega)$	Spectral density of fluctuations at angular frequency ω
$^nK_{AB}$	Reduced nuclear spin-spin coupling constant $K_{AB} = 4\pi^2 J_{AB}/h\gamma_A\gamma_B$) in T^2J^{-1}

$\boldsymbol{L}$	Angular momentum
m_j	Eigenvalue of $\hat{\boldsymbol{I}}_{j\,z}$ (magnetic component quantum number)
m_{tot}	Total magnetic component quantum number for a spin system (eigenvalue of $\sum_j \hat{\boldsymbol{I}}_{j\,z}$)
$m_{tot}(X)$	Total magnetic component quantum number for X-type nuclei
$\boldsymbol{M}_0$	Equilibrium macroscopic magnetization per unit volume in the presence of $\boldsymbol{B}_0$
M_x, M_y, M_z	Components of macroscopic magnetization per volume
M_n	*n*th moment of spectrum (M_2 = second moment, etc.)
n_α, n_β	Populations of the α and β spin states
N	Total number of nuclei of a given type per unit volume in the sample
$\boldsymbol{q}$	Electric field gradient tensor in units of the elementary charge
eQ	Nuclear quadrupole moment, Q is in m^2 and e is the elementary charge in C
R_1^X	Spin-lattice (longitudinal) relaxation rate constant for nucleus X
R_2^X	Spin-spin (transverse) relaxation rate constant for nucleus X
$R_{1\rho}^X$	Longitudinal relaxation rate constant for nucleus X in the reference frame rotating with $\boldsymbol{B}_1$
S	Signal intensity
$\hat{\boldsymbol{S}}$	Electron (or, occasionally, nuclear) spin operator; cf. $\hat{\boldsymbol{I}}$
t_1, t_2	Time dimensions for two-dimensional NMR
T_c	Coalescence temperature under chem. exchange for signals in an NMR spectrum
T_1^X	Spin-lattice (longitudinal) relaxation time of the X nucleus
T_2^X	Spin-spin (transverse) relaxation time of the X nucleus
T_2'	Net dephasing time for M_x or M_y
$T_{1\rho}^X$	Longitudinal relaxation time for the X nucleus in the reference frame rotating with $\boldsymbol{B}_1$
T_d	Pulse (recycle) delay
$T_{a\,c}$	Acquisition time
$T_q^{(l,m)}$	The *m*th component of an irreducible tensor of order *l* representing the strength of an interaction of type *q*

** IUPAC Recommendations: Magnetic Resonance in Chemistry, Vol. 36, 145-149 (1998)*

Symbols for NMR and Related Quantities*

$\boldsymbol{V}$	Electric field gradient tensor. $\boldsymbol{V} = e\boldsymbol{q}$, where e is the elementary charge
$V_{\alpha\beta}$	Elements of Cartesian electric field gradient tensor
W_0, W_1, W_2	Relaxation rate constants (transition probabilities per time) between energy levels differing by 0, 1 and 2 in m_{tot}
W_{rs}	Transition probability between spin states r and s
Greek alphabet	
α	Nuclear spin wavefunction (eigenfunction of $\hat{I}_z$) for the $m_I = + ½$ state of a spin-½ nucleus
α_E	The Ernst angle (for optimum sensitivity)
β	Nuclear spin wavefunction (eigenfunction of $\hat{I}_z$) for the $m_I = - ½$ state of a spin-½ nucleus
γ_X	Magnetogyric ratio of nucleus X
δ_X	Chemical shift (for the resonance) of nucleus of element X, usually in ppm
Δn	Population difference between nuclear states (Δn_0 at Boltzmann equilibrium)
$\Delta\delta$	Change or difference in δ
$\Delta\nu_{1/2}$	Full width in frequency units of a resonance line at half-height
$\Delta\sigma$	Anisotropy in σ [$\Delta\sigma = \sigma_{zz} - ½(\sigma_{xx} + \sigma_{yy})$]
$\Delta\chi$	(i) Susceptibility anisotropy ($\Delta\chi = \chi_{\parallel} - \chi_{\perp}$); (ii) difference in electronegativities
ε_0	Permittivity of the vacuum
ζ	Anisotropy in shielding, expressed as $\sigma_{zz} - \sigma_{iso}$
η	(i) Nuclear Overhauser enhancement; (ii) tensor asymmetry factor; (iii) viscosity
κ	Skew of a tensor
θ	Angle, especially for that between a given vector and $\boldsymbol{B}_0$
$\boldsymbol{\mu}$	(i) Magnetic dipole moment (component μ_z along $\boldsymbol{B}_0$); (ii) electric dipole moment
μ_0	Permeability of the vacuum
μ_B	Bohr magneton (earlier β_e)
μ_N	Nuclear magneton (earlier β_N)
ν_j	Larmor or resonance frequency of nucleus j (in Hz)
ν_0	(i) Spectrometer operating frequency; (ii) Basic Larmor or resonance frequency for a given isotope

ν_1	Frequency of primary RF magnetic field B_1 (excitation, detection)
ν_2	Frequency of secondary RF magnetic field B_2 (decoupling)
Ξ_X	Normalized resonance frequency for nucleus X relative to ν_H for tetramethylsilane (TMS) at the same $\boldsymbol{B}_0$ field; $\Xi_X = 100\ \nu_X/\nu_H$ (TMS)
ρ	Density matrix
$\hat{\rho}$	Density operator
ρ_{ij}	Element of matrix representation of $\hat{\rho}$
$\boldsymbol{\sigma}$	Shielding tensor
σ_j	(Isotropic) shielding constant of nucleus j
$\sigma_{\parallel}$, $\sigma_{\perp}$	Components of shielding tensor σ parallel and perpendicular to the symmetry axis
$\hat{\sigma}$	Reduced density operator
τ	(i) Time between RF pulses or recovery time following inversion (ii) lifetime in dynamic NMR studies
τ_c	Correlation time for molecular motion, especially for isotropic molecular tumbling
τ_d	Dwell time for data sampling
τ_{null}	Recovery time leading to null M_z after a 180° pulse
τ_p	Pulse duration
τ_{sc}	Correlation time for relaxation by the scalar mechanism
τ_{sr}	Correlation time for spin-rotation relaxation
$\tau_{\parallel}$, $\tau_{\perp}$	Correlation times for molecular tumbling parallel and perpendicular to the symmetry axis
χ	(i) Magnetic susceptibility; (ii) nuclear quadrupole coupling constant ($\chi = e^2 q_{ZZ} Q/h$)
$\omega_j, \omega_0, \omega_1, \omega_2$	As for ν_j, ν_0, ν_1, ν_2 but in angular frequency units (rad/s)
Ω	Span of a tensor
Ω_1, Ω_2	Angular frequency of RF fields $\boldsymbol{B}_1$, $\boldsymbol{B}_2$

* *IUPAC Recommendations: Magnetic Resonance in Chemistry, Vol. 36, 145-149 (1998)*

^{1}H Chemical Shifts for Common Contaminants in Deuterated Solvents

	Proton	mult., J	$CDCl_3$	$(CD_3)_2CO$	$(CD_3)_2SO$	C_6D_6	CD_3CN	CD_3OD	D_2O
residual solvent H			7.26	2.05	2.50	7.16	1.94	3.31	4.79
H_2O		s	1.56	2.84 [a]	3.33 [a]	0.40	2.13	4.87	
acetic acid	CH_3	s	2.10	1.96	1.91	1.55	1.96	1.99	2.08
acetone	CH_3	s	2.17	2.09	2.09	1.55	2.08	2.15	2.22
acetonitrile	CH_3	s	2.10	2.05	2.07	1.55	1.96	2.03	2.06
benzene	CH	s	7.36	7.36	7.37	7.15	7.37	7.33	
t-butanol	CH_3	s	1.28	1.18	1.11	1.05	1.16	1.40	1.24
	OH [c]	s			4.19	1.55	2.18		
t-butyl methyl ether	CCH_3	s	1.19	1.13	1.11	1.07	1.14	1.15	1.21
	OCH_3	s	3.22	3.13	3.08	3.04	3.13	3.20	3.22
BHT [b]	ArH	s	6.98	6.96	6.87	7.05	6.97	6.92	
	OH [c]	s	5.01		6.65	4.79	5.20		
	$ArCH_3$	s	2.27	2.22	2.18	2.24	2.22	2.21	
	$ArC(CH_3)_3$	s	1.43	1.41	1.36	1.38	1.39	1.40	
chloroform	CH	s	7.26	8.02	8.32	6.15	7.58	7.90	
cyclohexane	CH_2	s	1.43	1.43	1.40	1.40	1.44	1.45	
1,2-dichloroethane	CH_2	s	3.73	3.87	3.90	2.90	3.81	3.78	
dichloromethane	CH_2	s	5.30	5.63	5.76	4.27	5.44	5.49	
diethyl ether	CH_3	t, 7	1.21	1.11	1.09	1.11	1.12	1.18	1.17
	CH_2	q, 7	3.48	3.41	3.38	3.26	3.42	3.49	3.56
diglyme	CH_2	m	3.65	3.56	3.51	3.46	3.53	3.61	3.67
	CH_2	m	3.57	3.47	3.38	3.34	3.45	3.58	3.61
	OCH_3	s	3.39	3.28	3.24	3.11	3.29	3.35	3.37
1,2-dimethoxyethane	CH_3	s	3.40	3.28	3.24	3.12	3.28	3.35	3.37
	CH_2	s	3.55	3.46	3.43	3.33	3.45	3.52	3.60
dimethylacetamide	CH_3CO	s	2.09	1.97	1.96	1.60	1.97	2.07	2.08
	NCH_3	s	3.02	3.00	2.94	2.57	2.96	3.31	3.06
	NCH_3	s	2.94	2.83	2.78	2.05	2.83	2.92	2.90
dimethylformamide	CH	s	8.02	7.96	7.95	7.63	7.92	7.97	7.92
	CH_3	s	2.96	2.94	2.89	2.36	2.89	2.99	3.01
	CH_3	s	2.88	2.78	2.73	1.86	2.77	2.86	2.85
dimethylsulfoxide	CH_3	s	2.62	2.52	2.54	1.68	2.50	2.65	2.71
dioxane	CH_2	s	3.71	3.59	3.57	3.35	3.60	3.66	3.75
ethanol	CH_3	t, 7	1.25	1.12	1.06	0.96	1.12	1.19	1.17
	CH_2	q, 7 [d]	3.72	3.57	3.44	3.34	3.54	3.60	3.65
	OH	s [c,d]	1.32	3.39	4.63		2.47		
ethyl acetate	CH_3CO	s	2.05	1.97	1.99	1.65	1.97	2.01	2.07
	CH_2CH_3	q, 7	4.12	4.05	4.03	3.89	4.06	4.09	4.14
	CH_2CH_3	t, 7	1.26	1.20	1.17	0.92	1.20	1.24	1.24
ethyl methyl ketone	CH_3CO	s	2.14	2.07	2.07	1.58	2.06	2.12	2.19
	CH_2CH_3	q, 7	2.46	2.45	2.43	1.81	2.43	2.50	3.18
	CH_2CH_3	t, 7	1.06	0.96	0.91	0.85	0.96	1.01	1.26
ethylene glycol	CH	s [e]	3.76	3.28	3.34	3.41	3.51	3.59	3.65
"grease" [f]	CH_3	m	0.86	0.87		0.92	0.86	0.88	
	CH_2	br s	1.26	1.29		1.36	1.27	1.29	
n-hexane	CH_3	t	0.88	0.88	0.86	0.89	0.89	0.90	
	CH_2	m	1.26	1.28	1.25	1.24	1.28	1.29	
HMPA [g]	CH_3	d, 9.5	2.65	2.59	2.53	2.40	2.57	2.64	2.61
methanol	CH_3	s [h]	3.49	3.31	3.16	3.07	3.28	3.34	3.34
	OH	s [c,h]	1.09	3.12	4.01		2.16		
nitromethane	CH_3	s	4.33	4.43	4.42	2.94	4.31	4.34	4.40
n-pentane	CH_3	t, 7	0.88	0.88	0.86	0.87	0.89	0.90	
	CH_2	m	1.27	1.27	1.27	1.23	1.29	1.29	

*Reprinted with permission from: J. Org. Chem. 1997, **62**, 7512-7515*

^{1}H Chemical Shifts for Common Contaminants in Deuterated Solvents (continued)

	Proton	mult.	$CDCl_3$	$(CD_3)_2CO$	$(CD_3)_2SO$	C_6D_6	CD_3CN	CD_3OD	D_2O
i-propanol	CH_3	d, 6	1.22	1.10	1.04	0.95	1.09	1.50	1.17
	CH	sep, 6	4.04	3.90	3.78	3.67	3.87	3.92	4.02
pyridine	CH(2)	m	8.62	8.58	8.58	8.53	8.57	8.53	8.52
	CH(3)	m	7.29	7.35	7.39	6.66	7.33	7.44	7.45
	CH(4)	m	7.68	7.76	7.79	6.98	7.73	7.85	7.87
silicone grease[i]	CH_3	s	0.07	0.13		0.29	0.08	0.10	
tetrahydrofuran	CH_2	m	1.85	1.79	1.76	1.40	1.80	1.87	1.88
	CH_2O	m	3.76	3.63	3.60	3.57	3.64	3.71	3.74
toluene	CH_3	s	2.36	2.32	2.30	2.11	2.33	2.32	
	CH(*o*/*p*)	m	7.17	7.1-7.2	7.18	7.02	7.1-7.3	7.16	
	CH(*m*)	m	7.25	7.1-7.2	7.25	7.13	7.1-7.3	7.16	
triethylamine	CH_3	t, 7	1.03	0.96	0.93	0.96	0.96	1.05	0.99
	CH_2	q, 7	2.53	2.45	2.43	2.40	2.45	2.58	2.57

[a] In these solvents the intermolecular rate of exchange is slow enough that a peak due to HDO is usually also observed; it appears at 2.81 and 3.30 ppm in acetone and DMSO, respectively. In the former solvent, it is often seen as a 1:1:1 triplet, with $^2J_{H,D}$ = 1 Hz. [b] 2,6-di-*tert*-butyl-4-methylphenol. [c] The signals from exchangeable protons were not always identified. [d] In some cases (see note *a*), the coupling interaction between the CH_2 and the OH protons may be observed (J = 5 Hz). [e] In CD_3CN, the OH proton was seen as a multiplet at δ = 2.69, and extra coupling was also apparent on the methylene peak. [f] Long-chain, linear aliphatic hydrocarbons. Their solubility in DMSO was too low to give visible peaks. [g] Hexamethylphosphoramide. [h] In some cases (see notes *a, d*), the coupling interaction between the CH_3 and the OH protons may be observed (J = 5.5 Hz). [i] Poly(dimethylsiloxane). Its solubility in DMSO was too low to give visible peaks.

^{13}C Chemical Shifts for Common Contaminants in Deuterated Solvents

		$CDCl_3$	$(CD_3)_2CO$	$(CD_3)_2SO$	C_6D_6	CD_3CN	CD_3OD	D_2O
solvent signals		77.16	29.84	39.52	128.06	1.32	49.00	
			206.26			118.26		
acetic acid	CO	175.99	172.31	171.93	175.82	173.21	175.11	177.21
	CH_3	20.81	20.51	20.95	20.37	20.73	20.56	21.03
acetone	CO	207.07	205.87	206.31	204.43	207.43	209.67	215.94
	CH_3	30.92	30.60	30.56	30.14	30.91	30.67	30.89
acetonitrile	CN	116.43	117.60	117.91	116.02	118.26	118.06	119.68
	CH_3	1.89	1.12	1.03	0.20	1.79	0.85	1.47
benzene	CH	128.37	129.15	128.30	128.62	129.32	129.34	
t-butanol	C	69.15	68.13	66.88	68.19	68.74	69.40	70.36
	CH_3	31.25	30.72	30.38	30.47	30.68	30.91	30.29
t-butyl methyl ether	OCH_3	49.45	49.35	48.70	49.19	49.52	49.66	49.37
	C	72.87	72.81	72.04	72.40	73.17	74.32	75.62
	CCH_3	26.99	27.24	26.79	27.09	27.28	27.22	26.60
BHT	C(1)	151.55	152.51	151.47	152.05	152.42	152.85	
	C(2)	135.87	138.19	139.12	136.08	138.13	139.09	
	CH(3)	125.55	129.05	127.97	128.52	129.61	129.49	
	C(4)	128.27	126.03	124.85	125.83	126.38	126.11	
	CH_3Ar	21.20	21.31	20.97	21.40	21.23	21.38	
	CH_3C	30.33	31.61	31.25	31.34	31.50	31.15	
	C	34.25	35.00	34.33	34.35	35.05	35.36	
chloroform	CH	77.36	79.19	79.16	77.79	79.17	79.44	
cyclohexane	CH_2	26.94	27.51	26.33	27.23	27.63	27.96	
1,2-dichloroethane	CH_2	43.50	45.25	45.02	43.59	45.54	45.11	
dichloromethane	CH_2	53.52	54.95	54.84	53.46	55.32	54.78	
diethyl ether	CH_3	15.20	15.78	15.12	15.46	15.63	15.46	14.77
	CH_2	65.91	66.12	62.05	65.94	66.32	66.88	66.42

NMR Tables

^{13}C Chemical Shifts for Common Contaminants in Deuterated Solvents (continued)

		$CDCl_3$	$(CD_3)_2CO$	$(CD_3)_2SO$	C_6D_6	CD_3CN	CD_3OD	D_2O
diglyme	CH_3	59.01	58.77	57.98	58.66	58.90	59.06	58.67
	CH_2	70.51	71.03	69.54	70.87	70.99	71.33	70.05
	CH_2	71.90	72.63	71.25	72.35	72.63	72.92	71.63
1,2-dimethoxyethane	CH_3	59.08	58.45	58.01	58.68	58.89	59.06	58.67
	CH_2	71.84	72.47	17.07	72.21	72.47	72.72	71.49
dimethylacetamide	CH_3	21.53	21.51	21.29	21.16	21.76	21.32	21.09
	CO	171.07	170.61	169.54	169.95	171.31	173.32	174.57
	NCH_3	35.28	34.89	37.38	34.67	35.17	35.50	35.03
	NCH_3	38.13	37.92	34.42	37.03	38.26	38.43	38.76
dimethylformamide	CH	162.62	162.79	162.29	162.13	163.31	164.73	165.53
	CH_3	36.50	36.15	35.73	35.25	36.57	36.89	37.54
	CH_3	31.45	31.03	30.73	30.72	31.32	31.61	32.03
dimethyl sulfoxide	CH_3	40.76	41.23	40.45	40.03	41.31	40.45	39.39
dioxane	CH_2	67.14	67.60	66.36	67.16	67.72	68.11	67.19
ethanol	CH_3	18.41	18.89	18.51	18.72	18.80	18.40	17.47
	CH_2	58.28	57.72	56.07	57.86	57.96	58.26	58.05
ethyl acetate	CH_3CO	21.04	20.83	20.68	20.56	21.16	20.88	21.15
	CO	171.36	170.96	170.31	170.44	171.68	172.89	175.26
	CH_2	60.49	60.56	59.74	60.21	60.98	61.50	62.32
	CH_3	14.19	14.50	14.40	14.19	14.54	14.49	13.92
ethyl methyl ketone	CH_3CO	29.49	29.30	29.26	28.56	29.60	29.39	29.49
	CO	209.56	208.30	208.72	206.55	209.88	212.16	218.43
	CH_2CH_3	36.89	36.75	35.83	36.36	37.09	37.34	37.27
	CH_2CH_3	7.86	8.03	7.61	7.91	8.14	8.09	7.87
ethylene glycol	CH_2	63.79	64.26	62.76	64.34	64.22	64.30	63.17
"grease"	CH_2	29.76	30.73	29.20	30.21	30.86	31.29	
n-hexane	CH_3	14.14	14.34	13.88	14.32	14.43	14.45	
	CH_2(2)	22.70	23.28	22.05	23.04	23.40	23.68	
	CH_2(3)	31.64	32.30	30.95	31.96	32.36	32.73	
HMPA[b]	CH_3	36.87	37.04	36.42	36.88	37.10	37.00	36.46
methanol	CH_3	50.41	49.77	48.59	49.97	49.90	49.86	49.50[c]
nitromethane	CH_3	62.50	63.21	63.28	61.16	63.66	63.08	63.22
n-pentane	CH_3	14.08	14.29	13.28	14.25	14.37	14.39	
	CH_2(2)	22.38	22.98	21.70	22.72	23.08	23.38	
	CH_2(3)	34.16	34.83	33.48	34.45	34.89	35.30	
i-propanol	CH_3	25.14	25.67	25.43	25.18	25.55	25.27	24.38
	CH	64.50	63.85	64.92	64.23	64.30	64.71	64.88
pyridine	CH(2)	149.90	150.67	149.58	150.27	150.76	150.07	149.18
	CH(3)	123.75	124.57	123.84	123.58	127.76	125.53	125.12
	CH(4)	135.96	136.56	136.05	135.28	136.89	138.35	138.27
silicone grease	CH_3	1.04	1.40		1.38		2.10	
tetrahydrofuran	CH_2	25.62	26.15	25.14	25.72	26.27	26.48	25.67
	CH_2O	67.97	68.07	67.03	67.80	68.33	68.83	68.68
toluene	CH_3	21.46	21.46	20.99	21.10	21.50	21.50	
	C(*i*)	137.89	138.48	137.35	137.91	138.90	138.85	
	CH(*o*)	129.07	129.76	128.88	129.33	129.94	129.91	
	CH(*m*)	128.26	129.03	128.18	128.56	129.23	129.20	
	CH(*p*)	125.33	126.12	125.29	125.68	126.28	126.29	
triethylamine	CH_3	11.61	12.49	11.74	12.35	12.38	11.09	9.07
	CH_2	46.25	47.07	45.74	46.77	47.10	46.96	47.19

[a] See footnotes for Table 1. [b] $^2J_{PC}$ = 3 Hz. [c] Reference material; see text.

*Reprinted with permission from J. Org. Chem. 1997, **62**, 7512-7515*

NMR Formulae

Quantity	Formula (bold face = vectors)	Definitions (SI units) (see SI section for constants and units)
Magnetic Field Magnetic Force	$\boldsymbol{B} = \mu_o\ \boldsymbol{H}$ $\boldsymbol{F} = Q\ \boldsymbol{v}\times\boldsymbol{B}$	$\boldsymbol{B}$ = magn. flux density, magn. induction (T) $\boldsymbol{H}$ = magn. field strength (A m^{-1}) μ_o = permeability of vacuum ($4\pi\times10^{-7}$ H m^{-1}) Q = elec. charge (C); v = velocity (m/s)
Nuclear Spin Spin Angular Mom. Magn. Moment	$\boldsymbol{I}$ $\hbar\ m_I$ $\boldsymbol{\mu}_I = \gamma_I \hbar_I\ \boldsymbol{I} = g_I\beta_N\ \boldsymbol{I}$	γ = magnetogyric ratio (rad s^{-1} T^{-1}); $\hbar = h/2\pi$ $\beta_N = \mu_B$ (nuclear magneton); g_I = nuclear g factor m_I = quantum no. ($-I, -I+1, \ldots +I$)
Zeeman Interaction Larmor Freq. Nutation Vector	$\mathrm{H} = -\boldsymbol{\mu}_I \cdot \boldsymbol{B}_0$, $E = -m_I\ \gamma_I\ \hbar\ B_0$ $\omega_0 = \gamma_I B_0$, $\nu_0 = \nu_I\ B_0$ $\boldsymbol{\omega} = -\gamma_I\ \boldsymbol{B}$	ω in rad s^{-1}, ν in Hz ($\Delta m_I = \pm1$), $\nu = \gamma/2\pi$ (clockwise precession in lab frame for $\gamma > 0$)
Boltzmann Pop. Diff. Equil. Magn.	$\Delta N/N \sim \gamma_I\ \hbar/2kT\ (\Delta m_I = \pm1)$ $M_0 = B_0\ [N\gamma_I^2\hbar^2\ I(I+1)\ /\ 3kT]$	N = number of nuclei with spin I T = temperature (K)
Rotating Frame (r.f.) and residual field	$\gamma\ \Delta\boldsymbol{B}_0 = \gamma\ \boldsymbol{B}_0 + \boldsymbol{\omega}_{\mathbf{r.f.}}$ $\boldsymbol{\Omega} = -\gamma\ \Delta\boldsymbol{B}_0 = \boldsymbol{\omega}_0 - \boldsymbol{\omega}_{\mathbf{r.f.}}$	$\boldsymbol{\omega}_{\mathbf{r.f.}}$ = rot. frame vector (detector freq.) in direction $\boldsymbol{\omega}_0$ (-z axis for $\gamma > 0$) $\Delta\boldsymbol{B}_0$ = residual field in r.f. $\boldsymbol{\Omega}$ = precession freq. in r.f. (clockwise in r.f. for $\omega_0 > \omega_{r.f.}$)
Effective RF Field Amplitude and Tilt Nutation	$\boldsymbol{\omega}_1 = -\gamma\ \boldsymbol{B}_1$, $\boldsymbol{B}_{\mathbf{eff}} = \boldsymbol{B}_1 + \Delta\boldsymbol{B}_0$ $B_{eff} = [B_1^2 + \Delta B_0^2]^{1/2}$, $\tan\theta = \Delta B_0/B_1$ $\boldsymbol{\beta}_{\mathbf{eff}}$ (in rad) $= -\gamma\ \boldsymbol{B}_{\mathbf{eff}}\ \tau_p$ $\nu_{B_{eff}}$ (in Hz) $= 1/(4\tau_{90})$	$\boldsymbol{B}_1$ = RF field vector in xy plane; nutation is ccw around $\boldsymbol{\omega}_{\mathbf{eff}} = -\gamma\ \boldsymbol{B}_{\mathbf{eff}}$; θ = tilt angle between $\boldsymbol{B}_{\mathbf{eff}}$ and xy-plane; for $\Delta B_0/B_1 < 0.1$: $\theta < 6°$, $B_{eff} \approx B_1$ τ_p = RF pulse width (s); τ_{90} = 90° pulse
Optimum flip angle	$\cos\beta_{opt} = \exp(-TR/T_1)$	TR = pulse repetition time
Relaxation rates	spin-lattice: $R_1 = 1/T_1$ spin-spin: $R_2 = 1/T_2 = \pi\Delta\nu_o$	$\Delta\nu_o$ = natural Lorentzian linewidth at half-height
Bulk Susceptibility Correction	for cylindrical samples with external ref. in coaxial capillary $\delta_{corr} = \delta_{obs} + C\ (\chi_{ref} - \chi_{sample})$	$C = +2\pi/3$ (tube perpendicular to B_0) $C = -4\pi/3$ (tube parallel to B_0)
Spin-echo amplitude in constant B_0 gradient	$M(2\ \tau) =$ $M_0\ \exp[-2\ \tau/T_2 - (2/3)(\gamma\ G)^2 D\tau^3]$	90-τ-180-τ Hahn echo with gradient G D = diffusion coeff. in gradient direction
Spin-echo attenuation in PFG-SE experiment	$\ln\ (S_{echo}\ /\ S_0) = -bD$ $b = (\gamma\delta\ G)^2(\Delta - \delta/3)$	$G = B_0$ gradient pulse amplitude (T/m) δ = pulse width; Δ = pulse spacing
Rotational Correlation Time	Stokes-Einstein Relation $\tau_c = (4\pi\eta\ r^3)\ /\ (3kT)$	τ_c = rot. correlation time for isotropic tumbling η = viscosity; r = molecular radius (sphere)
Nuclear Oberhauser Enhancement	$M_S\{I\}/M_S(0) = 1 + 0.5(\gamma_I/\gamma_S)(R_1^{IS}/R_1^S)$ (extreme narrowing; $\omega_S\tau_C << 1$)	enhancement of spin S due to continuous irradiation of spin I; R_1^{IS} = dipolar relaxation of S via I; R_1^S = relaxation of S via all mechanisms
Polarization Transfer	$M_S\{PT\}/M_S(0) = \gamma_I/\gamma_S$	PT from I to S via J_{IS}
Lorentzian Lineshape	$a(\omega) = R_2\ /\ [R_2^2 + \Delta\omega^2]$ $d(\omega) = \Delta\omega\ /\ [R_2^2 + \Delta\omega^2]$	$a(\omega)$, $d(\omega)$ = absorption, dispersion signals $\Delta\omega = \omega - \Omega$

NMR Formulae

NMR Relaxation

Mechanisms (isotropic tumbling, SI units)	Remarks
Intramolecular Heteronuclear Dipole-Dipole Spin I relaxed by Spin S $R_1^I = E_{IS}\ r_{IS}^{-6}\ [(1/12)J_0(\omega_I - \omega_S) + (3/2)J_1(\omega_I) + (3/4)J_2(\omega_I + \omega_S)]$ $R_2^I = E_{IS}\ r_{IS}^{-6}\ [(1/6)J_0(0) + (1/24)J_0(\omega_I - \omega_S) + (3/4)J_1(\omega_I) +$ $(3/2)J_1(\omega_S) + (3/8)J_2(\omega_I + \omega_S)]$ where $E_{IS} = (\mu_0/4\pi)^2\ (\gamma_I\ \gamma_S\ \hbar)^2\ S(S+1)$ Extreme narrowing: $R_1^I = (4/3)\ E_{IS}\ r_{IS}^{-6}\ \tau_c\ (\omega\tau_c << 1)$ For several spins S: use $\sum r_{IS}^{-6}$ NB: $T_1^I = 1/R_1^I$ only when S is saturated	Factor $(\mu_0/4\pi) = 10^{-7}$ is required for conversion from cgs-Gauss units to MKSA (SI) units. Spectral Densities for random isotropic rotation $J_q(\omega) = C_q\ [\tau_c/(1 + \omega^2\tau_c^2)]$ $(q = 0,1,2)$ $C_0 = 24/15$; $C_1 = 4/15$; $C_2 = 16/15$ extreme narrowing: $J_q(\omega) = C_q\ \tau_c$
Intramolecular Homonuclear Dipole-Dipole Spin I_k relaxed by Spin I_l $R_1^I = E_I\ r_{kl}^{-6}\ (3/2)\ [J_1(\omega_I) + J_2(2\omega_I)]$ $R_{1\rho}^I = E_I\ r_{kl}^{-6}\ [(3/8)J_0(\omega_1) + (15/4)J_1(\omega_I) + (3/8)J_2(2\omega_I)]$ $R_2^I = E_I\ r_{kl}^{-6}\ [(3/8)J_0(0) + (15/4)J_1(\omega_I) + (3/8)J_2(2\omega_I)]$ where $E_I = (\mu_0/4\pi)^2\ \gamma_I^4\ \hbar^2\ I(I+1)$ Extreme narrowing: $R_1^I = R_2^I = 2\ E_I\ r_{kl}^{-6}\ \tau_c\ (\omega\tau_c << 1)$ For several spins I: use $\sum r_{kl}^{-6}$	
Intermolecular Heteronuclear Dipole-Dipole Spin I on mol. A relaxed by Spin S on mol. B ($\omega\tau_C << 1$) $R_1^I = 16\pi\ c_S\ E_{IS}\ /\ (27\ r_{IS}\ D_{trans})$ (pair distribution function = step function)	$E_{IS} = (\mu_0/4\pi)^2\ (\gamma_I\ \gamma_S\ \hbar)^2\ S(S+1)$ c_S = conc. of spins S r_{IS} = distance of closest approach $D_{trans} = (D_A + D_B)\ /\ 2$
Intermolecular Homonuclear Dipole-Dipole Spin I on mol. A relaxed by Spin I on mol. B ($\omega\tau_C << 1$) $R_1^I = 8\pi c_I\ E_I\ /\ (9\ r_{II}\ D_{trans})$ also found in the literature is: $R_1^I = (4\pi/3)\ c_I\ E_I\ (\tau/r_{II}^3)\ [1 + (2r_{II}^2/5\ D_{trans}\ \tau)]$	$E_I = (\mu_0/4\pi)^2\ \gamma_I^4\ \hbar^2\ I(I+1)$ c_I = conc. of spins I r_{II} = distance of closest approach τ = mol. jump time

Spherical Harmonics

Spherical harmonics up to rank 2 expressed in polar and orthogonal Cartesian coordinates

$Y_{0,0}$	=	$\sqrt{\frac{1}{4\pi}}$		
$Y_{1,0}$	=	$\sqrt{\frac{3}{4\pi}}\ \cos\theta$	=	$\sqrt{\frac{3}{4\pi}}\ \frac{z}{r}$
$Y_{1,\pm1}$	=	$\mp\sqrt{\frac{3}{8\pi}}\ \sin\theta\ e^{\pm i\varphi}$	=	$\mp\sqrt{\frac{3}{8\pi}}\ \frac{x \pm iy}{r}$
$Y_{2,0}$	=	$\sqrt{\frac{5}{16\pi}}\ (3\cos^2\theta - 1)$	=	$\sqrt{\frac{5}{16\pi}}\ \frac{2z^2 - x^2 - y^2}{r^2}$
$Y_{2,\pm1}$	=	$\mp\sqrt{\frac{15}{8\pi}}\ \cos\theta\ \sin\theta\ e^{\pm i\varphi}$	=	$\mp\sqrt{\frac{15}{8\pi}}\ \frac{(x \pm iy)z}{r^2}$
$Y_{2,\pm2}$	=	$\sqrt{\frac{15}{32\pi}}\ \sin^2\theta\ e^{\pm 2i\varphi}$	=	$\sqrt{\frac{15}{32\pi}}\ \frac{(x \pm iy)^2}{r^2}$

NMR Formulae

Mechanisms (isotropic tumbling, SI units)	**Remarks**
Chemical Shift Anisotropy (CSA) molecular tumbling modulates the interaction of the chem. shift tensor with the B_0 field. $R_1 = (2/5)\ E_{CSA}\ [\tau_c / (1 + \omega^2\tau_c^2)]$ $R_2 = (1/90)\ E_{CSA}\ \{8\tau_c + [6\tau_c + (1 + \omega^2\tau_c^2)]\}$	predominant relaxation mech. for non-protonated X nuclei $E_{CSA} = \gamma^2\ B_0^2\ \Delta\sigma^2$ $\Delta\sigma = \sigma_\perp - \sigma_\parallel$ (in ppm) (assuming axial symmetry of tensor)
Quadrupole Relaxation ($I > 1/2$) $R_1 = R_2 = (3/40)\ C_i\ [1 + \eta^2/3]\ C_{QF}^2\ \tau_c \quad (\omega\tau_c << 1)$	$C_i = (2I + 3) / [I^2(2I - 1)]$ $C_{QF} = e^2\ Q\ q_{zz} / \hbar$ = quadrupolar coupling in Hz; η = asymmetry param.
Spin-Rotation Interaction (SR) Relaxation arises from the interaction of the nuclear spin with magnetic fields generated by the rotation of a molecular magnetic moment modulated by molecular collisions: $\left(\frac{1}{T_1}\right)_{SR} = \frac{2\ I_i\ kT}{3\ \hbar^2}\ C_{eff}^2\ \tau_J$ I_i = moment of inertia of the molecule C_{eff} = effective spin-rotational coupling constant τ_J = angular momentum correlation time With $\tau_c \cdot \tau_J = \frac{I_i}{6kT}$, we can introduce the reorientational correlation time and we obtain: $\left(\frac{1}{T_1}\right)_{SR} = \frac{I_i^2}{9\ \hbar^2}\ C_{eff}^2 \cdot \frac{1}{\tau_c}$	
Scalar Coupling (SC) This relaxation mechanism can occur if the nucleus I in question is scalar coupled (with coupling constant J) to a second spin ($S \geq ½$) and the coupling is modulated by either chemical exchange (**SC relaxation of the first kind**) or the relaxation of spin S, e.g. if $S > ½$, (**SC relaxation of the second kind**). In this case spin splittings disappear and single lines are observed. $\left(\frac{1}{T_1}\right)_{SC} = \frac{8\pi^2\ J^2\ S\ (S+1)}{3}\ \left[\frac{\tau_{SC}}{1 + (\omega_I - \omega_S)^2\ \tau_{SC}^2}\right]$ $\left(\frac{1}{T_2}\right)_{SC} = \frac{4\pi^2\ J^2\ S\ (S+1)}{3}\ \left[\tau_{SC} + \frac{\tau_{SC}}{1 + (\omega_I - \omega_S)^2\ \tau_{SC}^2}\right]$ τ_{SC} = τ_e, if exchange time $\tau_e \ll T_1$ of either spin (first kind) τ_{SC} = T_1^S (the relaxation time of spin S) if $T_1^S \ll \tau_e$, $1/2\pi J$ (second kind) ω_I and ω_S are the resonance of I and S at the magnetic field in which $\left(\frac{1}{T_{1,2}}\right)_{SC}$ is measured.	

X-ray Diffractometry Tables

Space Groups

Point groups and space groups without centers of inversion or mirror planes are printed in italics. Those space groups which are uniquely determinable from the systematic absences and the symmetry of the diffraction pattern are printed in bold type.

Crystal System	Point Group	SG #	Condensed Symbol	Full Symbol
triclinic	*1*	*1*	*P1*	
	-1	2	P-1	
monoclinic	*2*	*3*	*P2*	*P 1 2 1*
		4	*P2(1)*	*P 1 2(1) 1*
		5	*C2*	*C 1 2 1*
	m	6	Pm	P 1 m 1
		7	Pc	P 1 c 1
		8	Cm	C 1 m 1
		9	Cc	C 1 c 1
	2/m	10	P2/m	P 1 2/m 1
		11	P2(1)/m	P 1 2(1)/m 1
		12	C2/m	C 1 2/m 1
		13	P2/c	P 1 2/c 1
		14	**P2(1)/c**	**P 1 2(1)/c 1**
		15	C2/c	C 1 2/c 1
orthorhombic	*222*	*16*	*P222*	*P 2 2 2*
		17	***P222(1)***	***P 2 2 2(1)***
		18	***P2(1)2(1)2***	***P 2(1)2(1) 2***
		19	***P2(1)2(1)2(1)***	***P 2(1) 2(1) 2(1)***
		20	***C222(1)***	***C 2 2 2(1)***
		21	*C222*	*C 2 2 2*
		22	*F222*	*F 2 2 2*
		23	*I222*	*I 2 2 2*
		24	*I2(1)2(1)2(1)*	*I 2(1) 2(1) 2(1)*
	mm2	25	Pmm2	P m m 2
		26	Pmc2(1)	P m c 2(1)
		27	Pcc2	P c c 2
		28	Pma2	P m a 2
		29	Pca2(1)	P c a 2(1)
		30	Pnc2	P n c 2
		31	Pmn2(1)	P m n 2(1)
		32	Pba2	P b a 2
		33	Pna2(1)	P n a 2(1)
		34	Pnn2	P n n 2
		35	Cmm2	C m m 2
		36	Cmc2(1)	C m c 2(1)
		37	Ccc2	C c c 2
		38	Amm2	A m m 2
		39	Abm2	A b m 2
		40	Ama2	A m a 2
		41	Aba2	A b a 2
		42	Fmm2	F m m 2
		43	**Fdd2**	**F d d 2**
		44	Imm2	I m m 2
		45	Iba2	I b a 2
		46	Ima2	I m a 2
	mmm	47	Pmmm	P 2/m 2/m 2/m
		48	**Pnnn**	**P 2/n 2/n 2/n**
		49	Pccm	P 2/c 2/c 2/m
		50	**Pban**	**P 2/b 2/a 2/n**
		51	Pmma	P 2(1)/m 2/m 2/a
		52	**Pnna**	**P 2/n 2(1)/n 2/a**
		53	Pmna	P 2/m 2/n 2(1)/a
		54	**Pcca**	**P 2(1)/c 2/c 2/a**
		55	Pbam	P 2(1)/b 2(1)/a 2/m
		56	**Pccn**	**P 2(1)/c 2(1)/c 2/n**
		57	Pbcm	P 2/b 2(1)/c 2(1)/m
		58	Pnnm	P 2(1)/n 2(1)/n 2/m
		59	Pmmn	P 2(1)/m 2(1)/m 2/n
		60	**Pbcn**	**P 2(1)/b 2/c 2(1)/n**
		61	**Pbca**	**P 2(1)/b 2(1)/c 2(1)/a**
		62	Pnma	P 2(1)/n 2(1)/m 2(1)/a
		63	Cmcm	C 2/m 2/c 2(1)/m
		64	Cmca	C 2/m 2/c 2(1)/a
		65	Cmmm	C 2/m 2/m 2/m
		66	Cccm	C 2/c 2/c 2/m
		67	Cmma	C 2/m 2/m 2/a
		68	**Ccca**	**C 2/c 2/c 2/a**
		69	Fmmm	F 2/m 2/m 2/m
		70	**Fddd**	**F 2/d 2/d 2/d**
		71	Immm	I 2/m 2/m 2/m
		72	Ibam	I 2/b 2/a 2/m
		73	Ibca	I 2(1)/b 2(1)/c 2(1)/a
		74	Imma	I 2(1)/m 2(1)/m 2(1)/a
tetragonal	*4*	*75*	*P4*	*P 4*
		76	***P4(1)***	***P 4(1)***
		77	*P4(2)*	*P 4(2)*
		78	***P4(3)***	***P 4(3)***
		79	*I4*	*I 4*
		80	***I4(1)***	***I 4(1)***
	-4	81	P-4	P -4
		82	I-4	I -4
	4/m	83	P4/m	P 4/m
		84	P4(2)/m	P 4 (2)/m
		85	**P4/n**	**P 4/n**
		86	**P4(2)/n**	**P 4(2)/n**
		87	I4/m	I 4/m
		88	**I4(1)/a**	**I 4(1)/a**
	422	*89*	*P422*	*P 4 2 2*
		90	***P42(1)2***	***P 4 2(1) 2***
		91	*P4(1)22*	*P 4(1) 2 2*
		92	***P4(1)2(1)2***	***P 4(1) 2(1) 2***
		93	***P4(2)22***	***P 4(2)2 2***
		94	***P4(2)2(1)2***	***P 4(2) 2(1) 2***
		95	***P4(3)22***	***P 4(3) 2 2***
		96	***P4(3)2(1)2***	***P 4(3) 2(1) 2***
		97	*I422*	*I 4 2 2*
		98	***I4(1)22***	***I 4(1) 2 2***
	4mm	99	P4mm	P 4 m m
		100	P4bm	P 4 b m
		101	P4(2)cm	P 4(2) c m
		102	P4(2)nm	P 4(2) n m
		103	P4cc	P 4 c c
		104	P4nc	P 4 n c
		105	P4(2)mc	P 4(2) m c
		106	P4(2)bc	P 4(2) b c
		107	I4mm	I 4 m m
		108	I4cm	I 4 c m
		109	I4(1)md	I 4(1) m d
		110	**I4(1)cd**	**I 4(1) c d**
	-42m	111	P-42m	P -4 2 m
		112	P-42c	P -4 2 c
		113	P-42(1)m	P -4 2(1) m
		114	**P-42(1)c**	**P -4 2(1) c**
		115	P-4m2	P -4 m 2
		116	P-4c2	P -4 c 2
		117	P-4b2	P -4 b 2
		118	P-4n2	P -4 n 2
		119	I-4m2	I -4 m 2
		120	I-4c2	I -4 c 2
		121	I-42m	I -4 2 m
		122	I-42d	I -4 2 d
	4/mmm	123	P4/mmm	P 4/m 2/m 2/m
		124	P4/mcc	P 4/m 2/c 2/c
		125	**P4/nbm**	**P 4/n 2/b 2/m**

Crystal System	Point Group	SG #	Condensed Symbol	Full Symbol
		126	**P4/nnc**	**P 4/n 2/n 2/c**
		127	P4/mbm	P 4/m 2(1)/b 2/m
		128	P4/mnc	P 4/m 2(1)/n 2/c
		129	**P4/nmm**	**P 4/n 2(1)/m 2/m**
		130	**P4/ncc**	**P 4/n 2(1)/c 2/c**
		131	P4(2)/mmc	P 4(2)/m 2/m 2/c
		132	P4(2)/mcm	P 4(2)/m 2/c 2/m
		133	**P4(2)/nbc**	**P 4(2)/n 2/b 2/c**
		134	**P4(2)/nnm**	**P 4(2)/n 2/n 2/m**
		135	P4(2)/mbc	P 4(2)/m 2(1)/b 2/c
		136	P4(2)/mnm	P 4(2)/m 2(1)/n 2/m
		137	**P4(2)/nmc**	**P 4(2)/n 2(1)/m 2/c**
		138	**P4(2)/ncm**	**P 4(2)/n 2(1)/c 2/m**
		139	I4/mmm	I 4/m 2/m 2/m
		140	I4/mcm	I 4/m 2/c 2/m
		141	**I4(1)/amd**	**I 4(1)/a 2/m 2/d**
		142	**I4(1)/acd**	**I 4(1)/a 2/c 2/d**
trigonal	*3*	*143*	*P3*	*P 3*
		144	*P3(1)*	*P 3(1)*
		145	*P3(2)*	*P 3(2)*
		146	*R3*	*R 3*
	-3	147	P-3	P -3
		148	R-3	R -3
	32	*149*	*P312*	*P 3 1 2*
		150	*P321*	*P 3 2 1*
		151	***P3(1)12***	***P 3(1) 1 2***
		152	***P3(1)21***	***P 3(1) 2 1***
		153	***P3(2)12***	***P 3(2) 1 2***
		154	***P3(2)21***	***P 3(2) 2 1***
		155	*R32*	*R 3 2*
	3m	156	P3m1	P 3 m 1
		157	P31m	P 3 1 m
		158	P3c1	P 3 c 1
		159	P31c	P 3 1 c
		160	R3m	R 3 m
		161	R3c	R 3 c
	-3m	162	P-31m	P -3 1 2/m
		163	P-31c	P -3 1 2/c
		164	P-3m1	P -3 2/m 1
		165	P-3c1	P -3 2/c 1
		166	R-3m	R -3 2/m
		167	R-3c	R -3 2/c
hexagonal	*6*	*168*	*P6*	*P 6*
		169	***P6(1)***	***P 6(1)***
		170	***P6(5)***	***P 6(5)***
		171	***P6(2)***	***P 6(2)***
		172	***P6(4)***	***P 6(4)***
		173	*P6(3)*	*P 6(3)*
	-6	174	P-6	P -6
	6/m	175	P6/m	P 6/m
		176	P6(3)/m	P 6(3)/m
	622	*177*	*P622*	*P 6 2 2*
		178	***P6(1)22***	***P 6(1)2 2***
		179	***P6(5)22***	***P 6(5) 2 2***
		180	***P6(2)22***	***P 6(2) 2 2***
		181	***P6(4)22***	***P 6(4) 2 2***
		182	***P6(3)22***	***P 6(3) 2 2***
	6mm	183	P6mm	P 6 m m
		184	P6cc	P 6 c c
		185	P6(3)cm	P 6(3) c m
		186	P6(3)mc	P 6(3) m c
	-6m	187	P-6m2	P -6 m 2
		188	P-6c2	P -6 c 2
		189	P-62m	P -6 2 m
		190	P-62c	P -6 2 c
	6/mmm	191	P6/mmm	P 6/m 2/m 2/m
		192	P6/mcc	P 6/m 2/c 2/c
		193	P6(3)/mcm	P 6(3)/m 2/c 2/m
		194	P6(3)/mmc	P 6(3)/m 2/m 2/c

Crystal System	Point Group	SG #	Condensed Symbol	Full Symbol
cubic	*23*	*195*	*P23*	*P 2 3*
		196	*F23*	*F 2 3*
		197	*I23*	*I 2 3*
		198	***P2(1)3***	***P 2(1) 3***
		199	*I2(1)3*	*I 2(1) 3*
	m-3	200	Pm-3	P 2/m -3
		201	**Pn-3**	**P 2/n -3**
		202	Fm-3	F 2/m -3
		203	**Fd-3**	**F 2/d -3**
		204	Im-3	I 2/m -3
		205	**Pa-3**	**P 2(1)/a -3**
		206	**Ia-3**	**I 2(1)/a -3**
	432	*207*	*P432*	*P 4 3 2*
		208	***P4(2)32***	***P 4(2) 3 2***
		209	*F432*	*F 4 3 2*
		210	***F4(1)32***	***F 4(1) 3 2***
		211	*I432*	*I 4 3 2*
		212	***P4(3)32***	***P 4(3) 3 2***
		213	***P4(1)32***	***P 4(1) 3 2***
		214	*I4(1)32*	*I 4(1) 3 2*
	-43m	215	P-43m	P -4 3 m
		216	F-43m	F -4 3 m
		217	I-43m	I -4 3 m
		218	P-43n	P -4 3 n
		219	F-43c	F -4 3 c
		220	**I-43d**	**I -4 3 d**
	m-3m	221	Pm-3m	P 4/m -3 2/m
		222	**Pn-3n**	**P 4/n -3 2/n**
		223	Pm-3n	P 4(2)/m -3 2/n
		224	**Pn-3m**	**P 4(2)/n -3 2/m**
		225	Fm-3m	F 4/m -3 2/m
		226	Fm-3c	F 4/m -3 2/c
		227	**Fd-3m**	**F 4(1)/d -3 2/m**
		228	**Fd-3c**	**F 4(1)/d -3 2/c**
		229	Im-3m	I 4/m -3 2/m
		230	**Ia-3d**	**I 4(1)/a -3 2/d**

X-ray Diffractometry Tables

Bond Lengths of Main Group Elements

	H	B	C	N	O	F		Al	Si	P	S	Cl		Ga	Ge	As	Se	Br		In	Sn	Sb	Te	I
H	**68**	115	111	99	92	86		152	147	143	135	130		152	154	154	148	144		176	172	174	169	167
B	115	**162**	157	145	138	131		199	195	190	181	176		199	201	200	194	191		224	219	221	216	213
C	111	157	**158**	148	143	137		192	188	185	182	178		193	196	197	195	193		216	213	215	211	210
N	99	145	148	**146**	142	138		179	175	173	172	173		180	184	186	185	186		203	200	202	199	199
O	92	138	143	142	**144**	142		171	168	167	166	168		173	177	180	179	181		195	193	195	192	193
F	86	131	137	138	142	**148**		163	161	160	160	163		166	170	173	173	176		187	185	188	185	186
Al	152	199	192	179	171	163		**244**	236	227	217	210		239	238	237	229	225		268	261	261	253	249
Si	147	195	188	175	168	161		236	**230**	222	213	206		234	234	232	225	222		260	255	256	249	245
P	143	190	185	173	167	160		227	222	**218**	210	204		227	229	228	222	219		251	247	249	244	241
Si	135	181	182	172	166	160		217	213	210	**206**	202		218	220	222	219	216		241	238	240	235	235
Cl	130	176	178	173	168	163		210	206	204	202	**202**		211	215	217	215	216		234	231	233	230	230
Ga	152	199	193	180	173	166		239	234	227	218	211		**238**	238	237	230	226		263	259	260	253	250
Ge	154	201	196	184	177	170		238	234	229	220	215		238	**240**	239	233	230		263	258	260	255	252
As	154	200	197	186	180	173		237	232	228	222	217		237	239	**240**	235	231		261	257	259	254	253
Se	148	194	195	185	179	173		229	225	222	219	215		230	233	235	**232**	230		254	250	252	248	248
Br	144	191	193	186	181	176		225	222	219	216	216		226	230	231	230	**230**		249	246	248	245	245
In	175	223	216	202	195	187		268	260	251	241	234		263	262	260	253	249		**292**	285	285	277	273
Sn	172	219	213	200	193	185		261	255	247	238	231		259	258	257	250	246		285	**280**	281	273	270
Sb	174	221	215	202	195	188		261	256	249	240	233		260	260	259	252	248		285	281	**282**	275	272
Te	169	216	211	199	192	185		253	249	244	235	230		253	255	254	248	245		278	273	275	**270**	267
I	167	213	210	199	193	186		249	245	241	235	230		250	252	253	248	245		274	270	272	267	**266**

Bond valences s may be calculated from experimental bond lengths (d) after Pauling's correlation equation (Pauling, The Nature of Chemical Bond) using this single bond length (d_0). The constant b is commonly taken to be 37 pm.

$$s = \exp\left[(d_0 - d)/b\right] \qquad d = d_0 - (b \ln s)$$

The single bond lengths are listed in pm. They are calculated from the modified Schomaker-Stevenson equation (Blom, Haaland, *J. Mol. Struc.* 128 (1985) 21-27).

Laue Classes and Point Groups

Crystal System	Laue Class	Point Group
Triclinic	-1	*1* -1
Monoclinic	2/m	*2* m 2/m
Orthorhombic	mmm	*222* mm2 mmm
Tetragonal	4/m 4/mmm	*4* -4 4/m *422* -42m 4mm 4/mmm

Crystal System	Laue Class	Point Group
Trigonal/Hexagonal	-3	*3* -3
	-3m1 (-31m)	*321 (312)* 3m1 (31m) -3m1 (-31m)
	6/m	*6* -6 6/m
	6/mmm	*622* -62m 6mm 6/mmm
Cubic	m-3	*23* m-3
	m-3m	*432* -43m m-3m

Periodic Table of Elements

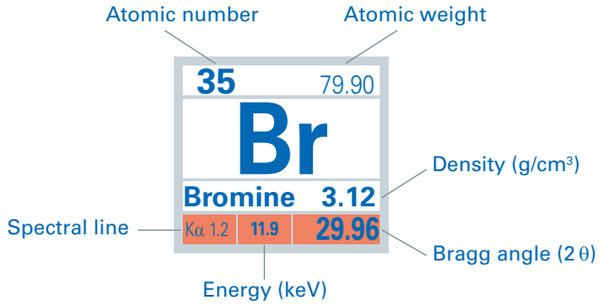

$$\lambda\ (\text{nm}) = \frac{1.24}{E\ (\text{keV})}$$

$$n\lambda = 2d \sin\theta$$

1 H 1.01 Hydrogen 0.0007																	2 He 4.00 Helium 0.0002
3 Li 6.94 Lithium 0.534	4 Be 9.01 Beryllium 1.85 Kα 1.2 0.108 74.34											5 B 10.81 Boron 2.34 Kα 1.2 0.18 42.51	6 C 12.01 Carbon 2.27 Kα 1.2 0.28 107.24 Kα 1.2 0.28 43.31	7 N 14.01 Nitrogen 0.001 Kα 1.2 0.39 70.14 Kα 1.2 0.39 33.60	8 O 16.00 Oxygen 0.001 Kα 1.2 0.53 50.90 Kα 1.2 0.53 25.10	9 F 19.00 Fluorine 0.001 Kα 1.2 0.68 38.91 Kα 1.2 0.68 90.60	10 Ne 20.18 Neon 0.0009 Kα 1.2 0.85 30.8 Kα 1.2 0.85 69.1
11 Na 22.99 Sodium 0.97 Kα 1.2 1.0 25.00 Kα 1.2 1.0 55.08 Kβ 1 1.1 24.40	12 Mg 24.31 Magnesium 1.74 Kα 1.2 1.3 20.70 Kα 1.2 1.3 136.72 Kβ 1 1.3 20.00											13 Al 26.98 Aluminium 2.70 Kα 1.2 1.5 145.12 Kα 1.2 1.5 17.45 Kβ 1 1.5 131.86 Kα 1 1.5 35.31	14 Si 28.09 Silicon 2.33 Kα 1.2 1.7 109.21 Kα 1.2 1.7 144.58 Kβ 1 1.8 101.67 Kα 1 1.7 30.04	15 P 30.97 Phosphorus 1.82 Kα 1.2 2.0 89.56 Kα 1.2 2.0 141.03 Kβ 1 2.1 83.20 Kα 1 2.0 25.88	16 S 32.07 Sulphur 2.07 Kα 1.2 2.3 75.85 Kα 1.2 2.3 110.69 Kβ 1 2.5 70.28 Kα 1 2.3 22.53	17 Cl 35.45 Chlorine 0.003 Kα 1.2 2.6 65.49 Kα 1.2 2.6 92.76 Kβ 1 2.8 60.49	18 Ar 39.95 Argon 0.002 Kα 1.2 3.0 57.32 Kα 1.2 3.0 79.86 Kβ 1 3.2 52.79
19 K 39.10 Potassium 0.86 Kα 1.2 3.3 136.67 Kα 1.2 3.3 50.69 Kβ 1 3.6 118.10	20 Ca 40.08 Calcium 1.54 Kα 1.2 3.7 113.07 Kβ 1 3.7 45.20 Kα 1 4.0 100.21 Lα 1 0.3 82.68 Lβ 1 0.3 81.61	21 Sc 44.96 Scandium 2.99 Kα 1.2 4.1 97.68 Kβ 1 4.5 87.28 Kα 1 4.5 40.59 Lα 1 0.4 69.50 Lβ 1 0.4 68.67	22 Ti 47.87 Titanium 4.54 Kα 1.2 4.5 86.12 Kβ 1 4.9 77.25 Kα 1 4.5 36.67 Lα 1 0.5 59.83 Lβ 1 0.5 58.97	23 V 50.94 Vanadium 6.11 Kα 1.2 5.0 76.92 Kα 1.2 5.0 123.17 Kβ 1 5.4 69.12 Kα 1 5.0 52.35 Lα 1 0.5 51.49	24 Cr 52.00 Chromium 7.15 Kα 1.2 5.4 69.34 Kα 1.2 5.4 107.11 Kβ 1 6.0 62.35 Kα 1 5.4 46.33 Lα 1 0.6 45.49	25 Mn 54.94 Manganese 7.44 Kα 1.2 5.9 62.96 Kα 1.2 5.9 95.20 Kβ 1 6.5 56.63 Kα 1 5.9 41.45 Lα 1 0.6 40.65	26 Fe 55.85 Iron 7.87 Kα 1.2 6.4 57.51 Kα 1.2 6.4 85.73 Kβ 1 7.1 51.72 Kα 1 6.4 37.30 Lα 1 0.7 36.60	27 Co 58.93 Cobalt 8.56 Kα 1.2 6.9 52.79 Kα 1.2 6.9 77.89 Kβ 1 7.7 47.46 Kα 1 6.9 33.77 Lα 1 0.8 33.12	28 Ni 58.69 Nickel 8.91 Kα 1.2 7.5 48.67 Kα 1.2 7.5 71.26 Kβ 1 8.3 43.72 Lα 1 0.9 30.70 Lβ 1 0.9 30.08 Kα 1 7.5 134.33 Kβ 1 8.3 112.81	29 Cu 63.55 Copper 8.93 Kα 1.2 8.0 45.02 Kα 1.2 8.0 65.55 Kβ 1 8.9 40.45 Lα 1 0.9 28.06 Lβ 1 1.0 27.45 Kα 1 8.0 117.85 Kβ 1 8.9 101.26	30 Zn 65.41 Zinc 7.13 Kα 1.2 8.6 41.80 Kα 1.2 8.6 60.58 Kβ 1 9.6 37.52 Lα 1 1.0 25.74 Lβ 1 1.0 25.18 Kα 1 8.6 105.87 Kβ 1 9.6 91.98	31 Ga 69.72 Gallium 5.91 Kα 1.2 9.2 38.91 Kα 1.2 9.2 56.20 Kβ 1 10.3 34.90 Lα 1 1.1 23.69 Lβ 1 1.2 23.12 Kα 1 9.2 96.35 Kβ 1 10.3 84.24	32 Ge 72.64 Germanium 5.32 Kα 1.2 9.9 36.32 Kα 1.2 9.9 52.31 Kβ 1 11.0 32.56 Lα 1 1.2 21.88 Lβ 1 1.2 21.33 Kα 1 9.9 88.44 Kβ 1 11.0 77.64	33 As 74.92 Arsenic 5.78 Kα 1.2 10.5 33.99 Kα 1.2 10.5 48.83 Kβ 1 11.7 30.44 Lα 1 1.3 20.25 Lβ 1 1.3 19.71 Kα 1 10.5 81.69 Kβ 1 11.7 71.90	34 Se 78.96 Selenium 4.81 Kα 1.2 11.2 31.89 Kα 1.2 11.2 45.71 Kβ 1 12.5 28.52 Lα 1 1.4 18.82 Lβ 1 1.4 18.28 Kα 1 11.2 75.84 Kβ 1 12.5 66.86	35 Br 79.90 Bromine 3.12 Kα 1.2 11.9 29.96 Kα 1.2 11.9 42.88 Kβ 1 13.3 26.79 Lα 1 1.5 17.52 Lβ 1 1.5 16.99 Kα 1 11.9 70.69 Kβ 1 13.3 62.39	36 Kr 83.80 Krypton 0.003 Kα 1.2 12.6 28.21 Kα 1.2 12.6 40.32 Kβ 1 14.1 25.20 Lα 1 1.6 126.81 Lβ 1 1.6 120.14
37 Rb 85.47 Rubidium 1.53 Kα 1.2 13.4 26.61 Kα 1.2 13.4 37.99 Kβ 1 15.0 23.75 Lα 1 1.7 113.68 Lβ 1 1.8 108.08 Kα 1 13.4 62.00 Kβ 1 15.0 54.79	38 Sr 87.62 Strontium 2.64 Kα 1.2 14.1 25.15 Kα 1.2 14.1 35.85 Kβ 1 15.8 22.42 Lα 1 1.8 103.45 Lβ 1 1.9 98.53 Kα 1 14.1 58.31 Kβ 1 15.8 51.54	39 Y 88.91 Yttrium 4.47 Kα 1.2 14.9 23.79 Kα 1.2 14.9 33.90 Kβ 1 16.7 21.19 Lα 1 1.9 95.07 Lβ 1 2.0 90.57 Kα 1 14.9 54.95 Kβ 1 16.7 48.57	40 Zr 91.22 Zirconium 6.51 Kα 1.2 15.8 22.50 Kα 1.2 15.8 32.04 Kβ 1 17.7 20.07 Lα 1 2.0 87.96 Lβ 1 2.1 83.76 Kα 1 15.8 51.75 Kβ 1 17.7 45.28	41 Nb 92.91 Niobium 8.57 Kα 1.2 16.6 21.35 Kα 1.2 16.6 30.38 Kβ 1 18.6 19.03 Lα 1 2.2 81.81 Lβ 1 2.3 77.84 Kα 1 16.6 48.95 Kβ 1 18.6 43.39	42 Mo 95.94 Molybdenum 10.22 Kα 1.2 17.5 20.28 Kα 1.2 17.5 28.84 Kβ 1 19.6 18.06 Lα 1 2.3 76.41 Lβ 1 2.4 72.63 Kα 1 17.5 46.39 Kβ 1 19.6 41.11	43 Tc (98) Technetium 11.5 Kα 1.2 18.4 19.29 Kα 1.2 18.4 27.42 Kβ 1 20.6 17.17 Lα 1 2.4 71.62 Lβ 1 2.5 67.98 Kα 1 18.4 44.03 Kβ 1 20.6 39.01	44 Ru 101.07 Ruthenium 12.37 Kα 1.2 19.3 18.37 Kα 1.2 19.3 26.10 Kβ 1 21.7 16.34 Lα 1 2.6 67.33 Lβ 1 2.7 63.82 Kα 1 19.3 41.64 Kβ 1 21.7 37.07	45 Rh 102.91 Rhodium 12.41 Kα 1.2 20.2 17.51 Kα 1.2 20.2 24.87 Kβ 1 22.7 15.57 Lα 1 2.7 63.46 Lβ 1 2.8 60.05 Kα 1 20.2 39.82 Kβ 1 22.7 35.51	46 Pd 106.42 Palladium 12.02 Kα 1.2 21.2 16.71 Kα 1.2 21.2 23.73 Kβ 1 23.8 14.85 Lα 1 2.8 59.95 Lβ 1 3.0 56.63 Kα 1 21.2 37.34 Kβ 1 23.8 33.60	47 Ag 107.87 Silver 10.55 Kα 1.2 22.2 15.96 Kα 1.2 22.2 22.66 Kβ 1 24.9 14.18 Lα 1 3.0 56.75 Lβ 1 3.2 53.50 Kα 1 22.2 36.19 Kβ 1 24.9 32.04	48 Cd 112.41 Cadmium 8.69 Kα 1.2 23.1 15.27 Kα 1.2 23.1 21.66 Kβ 1 26.1 13.55 Lα 1 3.1 53.82 Lβ 1 3.3 50.63 Kα 1 23.1 34.65 Kβ 1 26.1 30.59	49 In 114.82 Indium 7.31 Kα 1.2 24.2 14.61 Kα 1.2 24.2 20.72 Kβ 1 27.3 12.96 Lα 1 3.3 51.12 Lβ 1 3.5 47.99 Kα 1 24.2 33.04 Kβ 1 27.3 29.24	50 Sn 118.71 Tin 7.29 Kα 1.2 25.2 13.99 Kα 1.2 25.2 19.84 Kβ 1 28.5 12.41 Lα 1 3.4 48.64 Lβ 1 3.7 45.56 Kα 1 25.2 31.62 Kβ 1 28.5 27.97	51 Sb 121.76 Antimony 6.64 Kα 1.2 26.4 13.41 Kα 1.2 26.4 19.01 Kβ 1 29.7 11.89 Lα 1 3.6 46.34 Lβ 1 3.8 43.31 Kα 1 26.4 30.28 Kβ 1 29.7 26.78	52 Te 127.60 Tellurium 6.23 Kα 1.2 27.4 12.87 Kα 1.2 27.4 18.23 Kβ 1 31.0 11.40 Lα 1 3.8 44.20 Lβ 1 4.0 41.21 Kα 1 27.5 29.02 Kβ 1 31.0 25.67	53 I 126.90 Iodine 4.93 Kα 1.2 28.6 12.35 Kα 1.2 28.6 17.50 Kβ 1 32.3 10.94 Lα 1 3.9 42.22 Lβ 1 4.2 39.27 Kα 1 28.6 27.84 Kβ 1 32.3 24.62	54 Xe 131.29 Xenon 0.005 Kα 1.2 29.7 11.85 Kα 1.2 29.7 16.81 Kβ 1 33.6 10.50 Lα 1 4.1 40.37 Lβ 1 4.4 37.42
55 Cs 132.91 Caesium 1.87 Kα 1 30.9 16.16 Lα 1 4.3 91.80 Lβ 1 4.6 83.58	56 Ba 137.33 Barium 3.59 Kα 1 32.1 15.54 Lα 1 4.5 87.16 Lβ 1 4.8 79.24	57 La 138.91 Lanthanium 6.15 Kα 1 33.4 14.96 Lα 1 4.7 82.90 Lβ 1 5.0 75.27	72 Hf 178.49 Hafnium 13.31 Kα 1 55.8 8.95 Lα 1 7.9 45.87 Lβ 1 9.0 39.90 Mα 1 1.6 119.17 Lα 1 7.8 121.27 Lβ 1 9.0 99.46	73 Ta 180.95 Tantalum 16.65 Kα 1 57.6 8.68 Lα 1 8.2 44.41 Lβ 1 9.3 38.47 Mα 1 1.7 112.11 Lα 1 8.1 115.36 Lβ 1 9.3 94.92	74 W 183.84 Tungsten 19.25 Lα 1 8.4 43.01 Lβ 1 9.7 37.12 Mα 1 1.8 106.03 Lα 1 8.4 110.13 Lβ 1 9.7 90.75	75 Re 186.21 Rhenium 21.02 Lα 1 8.7 41.68 Lβ 1 10.0 35.82 Mα 1 1.8 100.66 Lα 1 8.7 105.43 Lβ 1 10.0 86.90	76 Os 190.23 Osmium 22.61 Lα 1 8.9 40.42 Lβ 1 10.4 34.59 Mα 1 1.9 95.64 Lα 1 8.9 101.16 Lβ 1 10.4 83.33	77 Ir 192.22 Iridium 22.65 Lα 1 9.2 39.21 Lβ 1 10.7 33.42 Mα 1 2.0 91.50 Lα 1 9.2 97.24 Lβ 1 10.7 80.01	78 Pt 195.08 Platinum 21.46 Lα 1 9.4 38.06 Lβ 1 11.1 32.29 Mα 1 2.0 87.53 Lα 1 9.4 93.62 Lβ 1 11.1 76.91	79 Au 196.97 Gold 19.28 Lα 1 9.7 36.96 Lβ 1 11.4 31.22 Mα 1 2.1 83.83 Lα 1 9.7 90.27 Lβ 1 11.4 73.56	80 Hg 200.59 Mercury 13.53 Lα 1 10.0 35.90 Lβ 1 11.8 30.19 Mα 1 2.1 80.49 Lα 1 10.0 87.13 Lβ 1 11.8 71.22	81 Tl 204.37 Thallium 11.86 Lα 1 10.3 34.92 Lβ 1 12.2 29.20 Mα 1 2.3 77.30 Lα 1 10.3 84.20 Lβ 1 12.2 68.62	82 Pb 207.20 Lead 11.34 Lα 1 10.6 33.93 Lβ 1 12.6 28.25 Mα 1 2.3 74.41 Lα 1 10.6 81.45 Lβ 1 12.6 66.16	83 Bi 208.98 Bismuth 9.81 Lα 1 10.8 33.00 Lβ 1 13.0 27.34 Mα 1 2.4 71.67 Lα 1 10.8 78.86 Lβ 1 13.0 63.82	84 Po (209) Polonium 9.32 Lα 1 11.1 32.11 Lβ 1 13.4 26.47 Lα 1 11.1 76.41 Lβ 1 13.4 61.59	85 At (210) Astatine 7.00 Lα 1 11.4 31.26 Lβ 1 13.9 25.64	86 Rn (222) Radon 0.01 Lα 1 11.7 30.44 Lβ 1 14.3 24.84
87 Fr (223) Francium 1.87 Lα 1 12.0 29.65 Lβ 1 14.8 24.06	88 Ra (226) Radium 5.5 Lα 1 12.3 28.89 Lβ 1 15.2 23.31	89 Ac (227) Actinium 10.07 Lα 1 12.7 28.17 Lβ 1 15.7 22.59															

Lanthanides, Actinides:

58 Ce 140.12 Cerium 6.77 Lα 1 4.8 128.13 Lα 1 4.8 79.00 Lβ 1 5.3 71.61	59 Pr 140.91 Praseodymium 6.77 Lα 1 5.0 119.69 Lα 1 5.0 75.41 Lβ 1 5.5 68.23	60 Nd 144.24 Neodymium 7.01 Lα 1 5.2 112.66 Lα 1 5.2 72.12 Lβ 1 5.7 65.10	61 Pm (145) Promethium 7.26 Lα 1 5.4 106.48 Lα 1 5.4 69.03 Lβ 1 6.0 62.19	62 Sm 150.36 Samarium 7.52 Lα 1 5.6 101.12 Lα 1 5.6 66.22 Lβ 1 6.2 59.49	63 Eu 151.96 Europium 5.24 Lα 1 5.9 96.23 Lα 1 5.9 63.55 Lβ 1 6.5 56.96	64 Gd 157.25 Gadolinium 7.90 Lα 1 6.1 91.87 Lα 1 6.1 61.09 Lβ 1 6.7 54.59	65 Tb 158.93 Terbium 8.23 Lα 1 6.3 87.87 Lα 1 6.3 58.78 Lβ 1 7.0 52.36	66 Dy 162.50 Dysprosium 8.55 Lα 1 6.5 84.15 Lα 1 6.5 56.59 Lβ 1 7.2 50.27	67 Ho 164.93 Holmium 8.80 Lα 1 6.7 80.73 Lα 1 6.7 54.53 Lβ 1 7.5 48.30	68 Er 167.26 Erbium 9.07 Lα 1 7.0 77.58 Lα 1 7.0 52.60 Lβ 1 7.8 46.43	69 Tm 168.93 Thulium 9.32 Lα 1 7.2 74.63 Lα 1 7.2 50.78 Lβ 1 8.1 44.67	70 Yb 173.04 Ytterbium 6.97 Lα 1 7.4 71.89 Lα 1 7.4 49.06 Lβ 1 8.4 42.99 Lα 1 7.4 136.36 Lβ 1 8.4 110.04	71 Lu 174.47 Lutetium 9.84 Lα 1 7.7 69.31 Lα 1 7.7 47.42 Lβ 1 8.7 41.40 Lα 1 7.7 128.12 Lβ 1 8.7 104.46
90 Th 232.04 Thorium 11.72 Lα 1 13.0 39.22 Lα 1 13.0 27.46 Lβ 1 16.2 21.90 Lα 1 13.0 64.12 Lβ 1 16.2 50.29	91 Pa 231.04 Protactinium 15.37 Lα 1 13.3 38.23 Lα 1 13.3 26.79 Lβ 1 16.7 21.24 Lα 1 13.3 62.39 Lβ 1 16.7 48.68	92 U 238.03 Uranium 18.45 Lα 1 13.6 37.29 Lα 1 13.6 26.14 Lβ 1 17.2 20.59 Lα 1 13.6 60.75 Lβ 1 17.2 47.13	93 Np (237) Neptunium 20.25 Lα 1 14.0 36.38 Lα 1 14.0 25.51 Lβ 1 17.8 19.96	94 Pu (244) Plutonium 19.84 Lα 1 14.3 35.50 α 14.3 24.90 Lβ 1 18.3 19.39	95 Am (243) Americium 13.69 Lα 1 14.6 34.65 Lα 1 14.6 24.32 Lβ 1 18.8 18.81	96 Cm (247) Curium 13.51 Lα 1 15.0 33.84 Lα 1 15.0 23.76 Lβ 1 19.4 18.26	97 Bk (247) Berkelium 14.79 Lα 1 15.3 33.04 Lα 1 15.3 23.20 Lβ 1 20.0 17.74	98 Cf (251) Californium 15.1 Lα 1 15.7 32.38 Lα 1 15.7 22.68 Lβ 1 20.6 17.22	99 Es (252) Einsteinium 13.5	100 Fm (257) Fermium	101 Md (258) Mendelevium	102 No (259) Nobelium	103 Lr (262) Lawrencium

Analyser crystal	Name, material	2d-value (nm)
XS-B	La/B_4C multilayer	19.0
XS-C	Ti/$_3C$ multilayer	12.0
XS-N	Ni/BN multilayer	11.0
XS-55	W/Si multilayer	5.5
XS-CEM	Specific structure	2.75
TIAP	Thallium biphthalate	2.576
ADP	Ammonium dihydrogen phosphate	1.064
PET	Pentaerythrite	0.874
InSb	Indium antimonide	0.748
Ge	Germanium	0.653
LiF (200)	Lithium fluoride	0.403
LiF (220)	Lithium fluoride	0.285
LiF (420)	Lithium fluoride	0.180

X-ray Diffractometry Tables

Conversion from the 2Θ Bragg angle using Ag, Mo and Cu radiation to resolution and vice versa.

Calculations based on Bragg's Law: $2\,d \sin\Theta = n\,\lambda$

For λ, the mean of α_1 and α_2 $(2/3\ \alpha_1 + 1/3\ \alpha_2)$ was taken, resulting in following wavelengths:

Ag	0.56083 Å
Mo	0.71073 Å
Cu	1.54178 Å

$2\Theta_{Ag}$ (°)	$2\Theta_{Mo}$ (°)	$2\Theta_{Cu}$ (°)	d (Å)	sin Θ/λ	$2\Theta_{Ag}$ (°)	$2\Theta_{Mo}$ (°)		d (Å)	sin Θ/λ
3.21	4.07	8.84	**10.000**	0.050	**50.00**	64.77		0.664	0.754
3.63	4.61	**10.00**	8.845	0.057	53.32	69.30		0.625	**0.800**
6.43	8.15	17.74	**5.000**	**0.100**	53.82	**70.00**		0.620	0.807
7.24	9.18	**20.00**	4.439	0.113	**60.00**	78.64		0.561	0.892
7.89	**10.00**	21.80	4.077	0.123	60.96	**80.00**		0.553	0.904
10.00	12.68	27.73	3.217	0.155	67.83	**90.00**		0.503	0.995
10.73	13.61	29.78	**3.000**	0.167	68.23	90.59		**0.500**	**1.000**
10.80	13.70	**30.00**	2.979	0.168	**70.00**	93.25		0.489	1.023
12.88	16.34	35.92	2.500	**0.200**	74.38	**100.00**		0.464	1.078
14.29	18.14	**40.00**	2.254	0.222	**80.00**	109.09		0.436	1.146
15.75	**20.00**	44.26	2.046	0.244	80.54	**110.00**		0.434	1.153
16.12	20.47	45.34	**2.000**	0.250	84.60	117.05		0.417	**1.200**
17.69	22.47	**50.00**	1.824	0.274	86.22	**120.00**		0.410	1.219
19.37	24.62	55.10	1.667	**0.300**	89.02	125.35		**0.400**	1.250
20.00	25.43	57.03	1.615	0.310	**90.00**	127.30		0.397	1.261
20.96	26.65	**60.00**	1.542	0.324	91.31	**130.00**		0.392	1.275
21.55	27.41	61.85	**1.500**	0.333	95.72	**140.00**		0.378	1.322
23.57	**30.00**	68.31	1.373	0.364	99.32	**150.00**		0.368	1.359
24.09	30.66	**70.00**	1.344	0.372	**100.00**	152.24		0.366	1.366
25.93	33.03	76.15	1.250	**0.400**	101.99	**160.00**		0.361	1.386
27.04	34.47	**80.00**	1.199	0.417	103.47	168.56		0.357	**1.400**
29.81	38.05	**90.00**	1.090	0.459	103.64	**170.00**		0.357	1.402
30.00	38.29	90.72	1.083	0.461	104.20	**180.00**		0.355	1.407
31.31	**40.00**	95.80	1.039	0.481	**110.00**			0.342	1.461
32.36	41.36	**100.00**	1.006	0.497	**120.00**			0.324	1.544
32.57	41.63	100.87	**1.000**	**0.500**	127.62			0.313	**1.600**
34.67	44.37	**110.00**	0.941	0.531	**130.00**			0.309	1.616
36.72	47.06	**120.00**	0.890	0.562	138.36			**0.300**	1.667
38.50	49.39	**130.00**	0.851	0.588	**140.00**			0.298	1.676
38.96	**50.00**	132.92	0.841	0.595	**150.00**			0.290	1.722
39.33	50.48	135.36	0.833	**0.600**	**160.00**			0.285	1.756
39.97	51.34	**140.00**	0.820	0.609	**170.00**			0.281	1.776
40.00	51.37	140.19	0.820	0.610	**180.00**			0.280	1.783
41.04	52.75	149.00	**0.800**	0.625					
41.14	52.88	**150.00**	0.798	0.626					
41.98	54.00	**160.00**	0.783	0.639					
42.49	54.67	**170.00**	0.774	0.646					
42.66	54.90	**180.00**	0.771	0.649					
46.23	59.67		0.714	**0.700**					
46.48	**60.00**		0.711	0.704					
47.23	61.02		**0.700**	0.714					

EPR/ENDOR Frequency Table

Z	A	E	Spin I	Nat. Abund. [%] (Half-life)	calc. X-Band ENDOR Freq. [MHz at 0.350 T] (free nucleus)	$g = \mu / (I\ \mu_N)$	$g\ \mu_N / g_e\ \mu_B$	Quadrupole Moment Q [fm² = 0.01 barn]
0	1	n	1/2		10.2076432	−3.8260854	1.040669 E−03	
1	1 2 3	H H H	1/2 1 1/2	99.9885 0.0115 (12.32 y)	14.9021186 2.28756617 15.8951945	5.58569468 0.857438228 5.95792488	−1.519270 E−03 −2.332173 E−04 −1.620514 E−03	0.286
2	3	He	1/2	0.000134	11.3519357	−4.25499544	1.157329 E−03	
3	6 7	Li Li	1 3/2	7.59 92.41	2.193146 5.791961	0.8220473 2.1709750	−2.235912 E−04 −5.904902 E−04	−0.0808 −4.01
4	9	Be	3/2	100.0	2.09429	−0.784993	2.13513 E−04	5.288
5	10 11	B B	3 3/2	19.9 80.1	1.601318 4.782045	0.600214927 1.792433	−1.632543 E−04 −4.875293 E−04	8.459 4.059
6	13	C	1/2	1.07	3.747940	1.404824	−3.821023 E−04	
7	14 15	N N	1 1/2	99.636 0.364	1.077197 1.511043	0.40376100 −0.56637768	−1.098202 E−04 1.540508 E−04	2.044
8	17	O	5/2	0.038	2.02098	−0.757516	2.06039 E−04	−2.558
9	19	F	1/2	100.0	14.01648	5.253736	−1.428980 E−03	
10	21	Ne	3/2	0.27	1.177076	−0.441198	1.20003 E−04	10.155
11	22 23	Na Na	3 3/2	(2.6019 y) 100.0	1.5527 3.944334	0.5820 1.4784371	−1.583 E−04 −4.021247 E−04	 10.4
12	25	Mg	5/2	10.00	0.91290	−0.34218	9.3071 E−05	19.94
13	27	Al	5/2	100.0	3.886082	1.4566028	−3.961859 E−04	14.66
14	29	Si	1/2	4.685	2.96293	−1.11058	3.02070 E−04	
15	31	P	1/2	100.0	6.03801	2.26320	−6.15575 E−04	
16	33	S	3/2	0.75	1.145104	0.429214	−1.16743 E−04	−6.78
17	35 36 37	Cl Cl Cl	3/2 2 3/2	75.76 (3.01 E5 y) 24.24	1.461790 1.71476 1.216786	0.5479162 0.642735 0.4560824	−1.490294 E−04 −1.748195 E−04 −1.240513 E−04	−8.165 −1.80 −6.435
18	39	Ar	7/2	(269 y)	1.21	−0.454	1.234 E−04	
19	39 40 41	K K K	3/2 4 3/2	93.258 0.0117 6.730	0.696337 0.865803 0.382209	0.2610049 −0.324525 0.143261827	−7.099152 E−05 8.82686 E−05 −3.896623 E−05	5.85 −7.3 7.11
20	41 43	Ca Ca	7/2 7/2	(1.02 E5 y) 0.135	1.215637 1.004386	−0.4556517 −0.3764694	1.239341 E−04 1.023971 E−04	−6.7 −4.08
21	45	Sc	7/2	100.0	3.625677	1.358996	−3.696376 E−04	−22.0
22	47 49	Ti Ti	5/2 7/2	7.44 5.41	0.84144 0.84166	−0.31539 −0.315477	8.5784 E−05 8.58076 E−05	30.2 24.7
23	50 51	V V	6 7/2	0.250 99.750	1.487665 3.924649	0.5576148 1.4710588	−1.516674 E−04 −4.001178 E−04	21 −5.2
24	53	Cr	3/2	9.501	0.844019	−0.31636	8.6048 E−05	−15 or −2.8
25	53 55	Mn Mn	7/2 5/2	(3.74 E6 y) 100.0	3.8296 3.701688	1.4354 1.38748716	−3.9043 E−04 −3.773869 E−04	 33

EPR/ENDOR Frequency Table

Z	A	E	Spin	NA [%]	ENDOR Freq.	$g = \mu / (I\ \mu_N)$	$g\ \mu_N / g_e\ \mu_B$	Q [fm²]
26	57	Fe	1/2	2.119	0.483548	0.18124600	–4.92977 E–05	
27	59 60	Co Co	7/2 5	100.0 (1925 d)	3.527 2.027	1.322 0.7598	–3.596 E–04 –2.067 E–04	42 44
28	61	Ni	3/2	1.1399	1.33399	–0.50001	1.3600 E–04	16.2
29	63 65	Cu Cu	3/2 3/2	69.15 30.85	3.961568 4.2359	1.484897 1.5877	–4.038817 E–04 –4.318525 E–04	–22.0 –20.4
30	67	Zn	5/2	4.102	0.933986	0.35008196	–9.521988 E–05	15
31	69 71	Ga Ga	3/2 3/2	60.108 39.892	3.58672 4.55726	1.34439 1.70818	–3.6567 E–04 –4.6461 E–04	17.1 10.7
32	73	Ge	9/2	7.76	0.521409	–0.1954373	5.315759 E–05	–19.6
33	75	As	3/2	100.0	2.56025	0.959647	–2.61017 E–04	31.4
34	77 79	Se Se	1/2 7/2	7.63 (2.95 E5 y)	2.855058 0.7760	1.0701486 –0.2909	–2.910730 E–04 7.911 E–05	 80
35	79 81	Br Br	3/2 3/2	50.69 49.31	3.746454 4.038433	1.404267 1.513708	–3.819508 E–04 –4.117181 E–04	30.5 25.4
36	83 85	Kr Kr	9/2 9/2	11.500 (10.756 y)	0.575479 0.596	–0.215704 –0.2233	5.86701 E–05 6.075 E–05	25.9 43.3
37	85 87	Rb Rb	5/2 3/2	72.17 27.83	1.444247 4.894398	0.5413406 1.834545	–1.472409 E–04 –4.989836 E–04	27.6 13.35
38	87	Sr	9/2	7.00	0.648363	–0.243023	6.61005 E–05	33.5
39	89	Y	1/2	100.0	0.733223	–0.2748308	7.475208 E–05	
40	91	Zr	5/2	11.22	1.39118	–0.521448	1.41830 E–04	–17.6
41	93	Nb	9/2	100.0	3.6583	1.37122	–3.72963 E–04	–32
42	95 97	Mo Mo	5/2 5/2	15.90 9.56	0.9756 0.9962	–0.3657 –0.3734	9.9462 E–05 1.016 E–04	–2.2 25.5
43	99	Tc	9/2	(2.1 E5 y)	3.3703	1.2633	–3.4360 E–04	–12.9
44	99 101	Ru Ru	5/2 5/2	12.76 17.06	0.684 0.764	–0.256 –0.286	6.97 E–05 7.79 E–05	7.9 45.7
45	103 105	Rh Rh	1/2 7/2	100.0 (35.36 h)	0.47169 3.39	–0.17680 1.27	4.8088 E–05 –3.46 E–04	
46	105	Pd	5/2	22.33	0.685	–0.257	6.98 E–05	66
47	107 109	Ag Ag	1/2 1/2	51.839 48.161	0.606574 0.69734	–0.2273593 –0.26138	6.184016 E–05 7.1094 E–05	
48	111 113	Cd Cd	1/2 1/2	12.80 12.22	3.174203 3.320483	–1.1897722 –1.2446018	3.236098 E–04 3.385231 E–04	
49	113 115	In In	9/2 9/2	4.29 95.71	3.2779 3.2850	1.2286 1.2313	–3.3418 E–04 –3.3490 E–04	79.9 81
50	115 117 119	Sn Sn Sn	1/2 1/2 1/2	0.34 7.68 8.59	4.9027 5.34136 5.5881	–1.8377 –2.00208 –2.09456	4.9983 E–04 5.44552 E–04 5.69706 E–04	
51	121 123 125	Sb Sb Sb	5/2 7/2 7/2	57.21 42.79 (2.75856 y)	3.5893 1.9436 2.00	1.34536 0.72851 0.75	–3.65929 E–04 –1.9815 E–04 –2.04 E–04	–36 or –45 –49

EPR/ENDOR Frequency Table

Z	A	E	Spin	NA [%]	ENDOR Freq.	$g = \mu / (I\ \mu_N)$	$g\ \mu_N / g_e\ \mu_B$	Q [fm²]
52	123 125	Te Te	1/2 1/2	0.89 7.07	3.932218 4.740899	–1.4738956 –1.7770102	4.008894 E–04 4.833345 E–04	
53	127 129	I I	5/2 7/2	100.0 (1.57 E7 y)	3.00222 1.9979	1.125308 0.7489	–3.060760 E–04 –2.0368 E–04	–71 –48
54	129 131	Xe Xe	1/2 3/2	26.4006 21.2324	4.15114 1.230549	–1.555952 0.461241	4.232082 E–04 –1.254545 E–04	 –11.4
55	133 134 135 137	Cs Cs Cs Cs	7/2 4 7/2 7/2	100.0 (2.0652 y) (2.3 E6 y) (30.07 y)	1.968173 1.9967 2.0828 2.163	0.7377214 0.74843 0.78069 0.8109	–2.006551 E–04 –2.0357 E–04 –2.12341 E–04 –2.205 E–04	–0.343 38.9 5.0 5.1
56	133 135 137	Ba Ba Ba	1/2 3/2 3/2	(10.51 y) 6.592 11.232	4.11749 1.491586 1.66716	–1.54334 0.559085 0.62489	4.19778 E–04 –1.520672 E–04 –1.69967 E–04	 16.0 24.5
57	137 138 139	La La La	7/2 5 7/2	(6 E4 y) 0.090 99.910	2.054 1.981533 2.121403	0.7700 0.7427292 0.7951559	–2.094 E–04 –2.020172 E–04 –2.1627690 E–04	26 45 20
59	141	Pr	5/2	100.0	4.5625	1.71016	–4.65152 E–04	–5.89
60	143 145	Nd Nd	7/2 7/2	12.2 8.3	0.8118 0.5000	–0.3043 –0.1874	8.2764 E–05 5.0979 E–05	–63 –33
61	147	Pm	7/2	(2.623 y)	1.97	0.737	–2.00 E–04	74
62	147 149 151	Sm Sm Sm	7/2 7/2 5/2	14.99 13.82 (90 y)	0.6211 0.5120 0.3874	–0.2328 –0.1919 –0.1452	6.332 E–05 5.220 E–05 3.949 E–05	–25.9 7.5 71
63	151 152 153 154 155	Eu Eu Eu Eu Eu	5/2 3 5/2 3 5/2	47.81 (13.537 y) 52.19 (8.593 y) (4.753 y)	3.70487 1.7253 1.6353 1.783 1.62	1.38868 0.6467 0.6130 –0.6683 0.608	–3.77711 E–04 –1.759 E–04 –1.667 E–04 1.818 E–04 –1.65 E–04	90.3 271 241 280 240
64	155 157	Gd Gd	3/2 3/2	14.80 15.65	0.4575 0.5999	–0.1715 –0.2249	4.664 E–05 6.116 E–05	127 135
65	157 158 159	Tb Tb Tb	3/2 3 3/2	(71 y) (180 y) 100.0	3.57 1.563 3.5821	1.34 0.5860 1.3427	–3.64 E–04 –1.594 E–04 –3.6520 E–04	141 270 143.2
66	161 163	Dy Dy	5/2 5/2	18.889 24.896	0.512 0.718	–0.192 0.269	5.22 E–05 –7.32 E–05	251 265
67	165	Ho	7/2	100.0	3.150	1.181	–3.211 E–04	358
68	167	Er	7/2	22.869	0.4298	–0.1611	4.382 E–05	357
69	169 171	Tm Tm	1/2 1/2	100.0 (1.92 y)	1.23 1.22	–0.462 –0.456	1.257 E–04 1.240 E–04	
70	171 173	Yb Yb	1/2 5/2	14.28 16.13	2.6341 0.72555	0.98734 –0.27196	–2.6855 E–04 7.3970 E–05	 280
71	173 174 175 176	Lu Lu Lu Lu	7/2 1 7/2 7	(1.37 y) (3.31 y) 97.41 2.59	1.74 5.1 1.7016 1.208	0.651 1.9 0.6378 0.4527	–1.772 E–04 –5.2 E–04 –1.735 E–04 –1.231 E–04	 349 497

EPR/ENDOR Frequency Table

Z	A	E	Spin	NA [%]	ENDOR Freq.	$g = \mu / (I\ \mu_N)$	$g\ \mu_N / g_e\ \mu_B$	Q [fm^2]
72	177 179	Hf Hf	7/2 9/2	18.60 13.62	0.6049 0.380	0.2267 –0.142	–6.166 E–05 3.87 E–05	337 379
73	181	Ta	7/2	99.988	1.8069	0.67729	–1.8422 E–04	317
74	183	W	1/2	14.31	0.628478	0.2355695	–6.407328 E–05	
75	185 187	Re Re	5/2 5/2	37.40 62.60	3.4012 3.4359	1.2748 1.2879	–3.4675 E–04 –3.5029 E–04	218 207
76	187 189	Os Os	1/2 3/2	1.96 16.15	0.344971 1.173760	0.12930378 0.439955	–3.516974 E–05 –1.196648 E–04	 85.6
77	191 193	Ir Ir	3/2 3/2	37.3 62.7	0.26804 0.2912	0.10047 0.1091	–2.7326 E–05 –2.9684 E–05	81.6 75.1
78	195	Pt	1/2	33.832	3.25229	1.21904	–3.31570 E–04	
79	197	Au	3/2	100.0	0.26351	0.098772	–2.6865 E–05	54.7
80	199 201	Hg Hg	1/2 3/2	16.87 13.18	2.699312 0.996420	1.011771 –0.3734838	–2.751947 E–04 1.015850 E–04	 38.6
81	203 204 205	Tl Tl Tl	1/2 2 1/2	29.52 (3.78 y) 70.48	8.656069 0.12 8.741211	3.24451580 0.045 3.2764292	–8.824859 E–04 –1.22 E–05 –8.911661 E–04	
82	207	Pb	1/2	22.1	3.1065	1.1644	–3.1670 E–04	
83	207 209	Bi Bi	9/2 9/2	(32.9 y) 100.0	2.419 2.437	0.9069 0.9134	–2.4667 E–04 –2.4844 E–04	–58 –51.6
84	209	Po	1/2	(102 y)	3.63	1.36	–3.70 E–04	
86	211	Rn	1/2	(14.6 h)	3.207	1.202	–3.269 E–04	
87	212	Fr	5	(20 min)	2.47	0.924	–2.51 E–04	–10
88	225	Ra	1/2	(14.9 d)	3.916	–1.468	3.993 E–04	
89	227	Ac	3/2	(21.77 y)	2.0	0.73	–1.99 E–04	170
90	229	Th	5/2	(7.34 E3 y)	0.491	0.184	–5.00 E–05	430
91	231	Pa	3/2	100.0 (3.25 E4 y)	3.57	1.34	–3.64 E–04	–172
92	233 235	U U	5/2 7/2	(1.592 E5 y) 0.7204 (7.04 E8 y)	0.630 0.290	0.236 –0.109	–6.42 E–05 2.95 E–05	366.3 493.6
93	237	Np	5/2	(2.14 E6 y)	3.351	1.256	–3.416 E–04	386.6
94	239 241	Pu Pu	1/2 5/2	(2.410 E4 y) (14.4 y)	1.08 0.726	0.406 –0.272	–1.104 E–04 7.40 E–05	 560
95	241 243	Am Am	5/2 5/2	(432.7 y) (7.37 E3 y)	1.69 1.60	0.632 0.60	–1.72 E–04 –1.63 E–04	314 286
96	243 245 247	Cm Cm Cm	5/2 7/2 9/2	(29.1 y) (8.48 E3 y) (1.56 E7 y)	0.438 0.38 0.22	0.164 0.14 0.082	–4.46 E–05 –3.89 E–05 –2.24 E–05	
97	249	Bk	3.5	(320 d)	1.5	0.6	–1.6 E–04	
99	253	Es	3.5	(20.47 d)	3.13	1.17	–3.19 E–04	670

revision 2009 based on NMR Properties Table, W. E. Hull; no. of decimal places reflects precision.

EPR Tables

Useful Relationships for EPR

Magn. Moment of the electron $\mu_e = g_e\ \mu_B\ S = g_e\ \mu_B / 2$ (g_e defined as negative) alternatively: $\mu_e = -g_e\ \mu_B / 2$ (with g_e positive) $\mu_B = \beta_e$ = Bohr magneton	**Magn. Moment for nucleus n** with spin I_n $\mu_n = g_n\ \mu_N\ I_{n=}\ \gamma_n\ \eta\ I_n$ $\mu_N = \beta_N$ = nuclear magneton
Resonance Condition - EPR $\nu_e = \lvert g\rvert\ \mu_B\ B_0 / h$ ν_e [GHz] = 13.996246 $\lvert g\rvert\ B_0$ [T] B_0 [T] = 0.071447730 ν_e [GHz] / $\lvert g\rvert$ $\lvert g\rvert$ = 0.071447730 ν_e [GHz] / B_0 [T] $\lvert g\rvert$ = 3.04198626 ν_e [GHz] / ν_{H2O} [MHz]	**Resonance Condition - NMR** $\nu_n = \lvert g_n\rvert\ \mu_N\ B_0 / h\ =\ \lvert\gamma_n\rvert B_0 / 2\pi$ for ^{1}H: ν_{H2O} [MHz] = 42.5763875 B_0 [T] B_0 [T] = 0.0234871970 ν_{H2O} [MHz]
Hyperfine Coupling A [MHz] = 2.99792458 $\times 10^4$ A [cm^{-1}] = 13.996246 $\lvert g\rvert$ A [mT] = 1.3996246 $\lvert g\rvert$ A [G]	A [cm^{-1}] = 0.333564095 $\times$ 10^{-4} A [MHz] = 4.6686451 $\times$ 10^{-4} $\lvert g\rvert$ A [mT] = 0.46686451 $\times$ 10^{-4} $\lvert g\rvert$ A [G]
Magnetic Field (flux density) = B_0 [in Tesla]	1 T = 10^4 G = 10 kG; 1 mT = 10 G; 1 G = 0.1 mT

see Physical Tables for Fundamental Constants

Skin Depth Table

Material	Specific Resistivity x 10^{-6} ohm-cm	Depth at 9.6 GHz		Depth at 100 kHz	
		μm	μin	mm	in
Silver	1.629	0.656	25.8	0.203	0.008
Copper. annealed	1.724	0.674	26.6	0.209	0.008
Gold	2.440	0.802	31.6	0.249	0.010
Aluminum	2.824	0.863	34.0	0.267	0.011
Rhodium	5.040	1.153	45.4	0.357	0.014
Tungsten	5.600	1.216	47.9	0.377	0.015
Molybdenum	5.700	1.226	48.3	0.380	0.015
Zinc	5.800	1.237	48.7	0.383	0.015
Brass	ca. 7.	1.359	53.5	0.421	0.017
Cadmium	7.600	1.416	55.8	0.439	0.017
Nickel	7.800	1.435	56.5	0.444	0.017
Platinum	10.000	1.624	64.0	0.503	0.020
Palladium	11.0	1.704	67.1	0.528	0.021
Tin	11.5	1.742	68.6	0.540	0.021
Lead	22.0	2.409	94.9	0.747	0.029

EPR Tables

Table for Various Free Radicals Generated in Aqueous Solution

Radical	Sample solution	T (°C) *p*H	T_1 (µs)
$^{\bullet}CH_3$	0.1-0.5 M DMSO 1.0 M NaOH	19 *p*H = 14	0.2
$^{\bullet}CH_2COO^-$	0.5 M NaOAc 1.0 M NaOH	17-19 *p*H = 14	2.0
$^{\bullet}CH(COO^-)_2$	0.5 M malonic acid 2.0 M NaOH	18 *p*H = 14	2.9
$^-OC^{\bullet}(COO^-)_2$	0.1 M tartronic acid 1.2 M NaOH	17 *p*H = 14	3.6 $3.5 \le T_1 < 4.0$
$^-OCH^{\bullet}COO^-$	0.1 M tartronic acid 1.2 M NaOH	17 *p*H = 14	1.4
$^{\bullet}CH_2O^-$	0.5 M CH_3OH 0.1 M NaOH	10 *p*H = 13	~0.1 $0.08 \le T_1 < 0.15$
$CH_3C^{\bullet}OH$	0.5 M CH_3CH_2OH 1.0 M NaOH	18 *p*H = 14	0.7
$(CH_3)_2CO^{\bullet-}$	0.5 M *i*-propanol 1.0 M NaOH	16 *p*H = 14	1.6

Radical	Sample solution	T (°C) *p*H	T_1 (µs)
$^{\bullet}CH_2OH$	0.5-1.0 M CH_3OH 1.0 M phosphate buffer	17 *p*H = 6.6-6.8	0.6
$CH_3C^{\bullet}HOH$	0.5 M CH_3CH_2OH 1.0 M phosphate buffer	18 *p*H = 6.6-6.8	1.3
$(CH_3)_2C^{\bullet}OH$	0.25 M *i*-propanol 0.5 M phosphate buffer	17 *p*H = 6.8	2.7
CH_2OD	0.5 M CH_3OH in D_2O acidif with H_2SO_4	9 *p*D = 3.6 19 *p*D = 3.2	0.72 0.53
$(CH_3)_2C^{\bullet}OD$	0.5 M *i*-propanol in D_2O acidif with H_2SO_4 0.5 M isopropanol in D_2O; 0.5 M phosphate buffer	19 *p*D = 3.5 19 *p*D = 7.0	2.2 2.5

Relaxation Times of Some Organic Free Radicals (Saturation-Recovery Method)

Radical	T_1 (µs)	T_2 (µs)
1,2-dicarboxylvinyl	9.0±1	7.0±2
chelidonic acid trianion	5.0±0.5	4.5±1
ascorbate radical	2.3±0.5	1.0±0.3
p-benzosemiquinone anion	2.0±0.3	1.8±0.5
2,5-di-*t*-butyl-benzosemiquinone anion	11.5±0.5	. . .

Values of T_2 for Various Organic Radicals at 77 K (ESE Method)

Radical	Matrix	T_2 (µs)
naphthalene anion	MTHF	3.4
naphtalene-d_8 anion	MTHF	3.2
1.3,5-triphenylbenzene anion	MTHF	3.2
triphenylene anion	MTHF	3.2
DPPH	MTHF	3.2
DPPH	fluorolube (FS-5)	10.0
perylene cation	sulfuric acid	10.4
anthracene cation	sulfuric acid	10.4
naphthacene cation	sulfuric acid	10.4
thianthrene cation	sulfuric acid	10.0
anthracene-d_{10} cation	sulfuric acid-d_2	200.0
anthracene cation	boric acid	14.6
biphenyl cation	boric acid	14.6
p-terphenyl cation	boric acid	14.2
naphthalene cation	boric acid	13.2
1,3,5-triphenylbenzene cation	boric acid	13.8
coronene cation	boric acid	10.0
triphenylene cation	boric acid	9.8
thianthrene cation	boric acid	10.0

IR Spectroscopy Tables

Conversion Table for Transmittance and Absorbance Units

Transmittance [%]	Absorbance	Transmittance [%]	Absorbance	Transmittance [%]	Absorbance	Transmittance [%]	Absorbance
1.0	2.000	26.0	.585	51.0	.292	76.0	.119
2.0	1.699	27.0	.569	52.0	.284	77.0	.114
3.0	1.523	28.0	.553	53.0	.276	78.0	.108
4.0	1.398	29.0	.538	54.0	.268	79.0	.102
5.0	1.301	30.0	.523	55.0	.260	80.0	.097
6.0	1.222	31.0	.509	56.0	.265	81.0	.092
7.0	1.155	32.0	.495	57.0	.244	82.0	.086
8.0	1.097	33.0	.481	58.0	.237	83.0	.081
9.0	1.046	34.0	.469	59.0	.229	84.0	.076
10.0	1.000	35.0	.456	60.0	.222	85.0	.071
11.0	.959	36.0	.444	61.0	.215	86.0	.066
12.0	.921	37.0	.432	62.0	.208	87.0	.060
13.0	.886	38.0	.420	63.0	.201	88.0	.056
14.0	.854	39.0	.409	64.0	.194	89.0	.051
15.0	.824	40.0	.398	65.0	.187	90.0	.046
16.0	.796	41.0	.387	66.0	.180	91.0	.041
17.0	.770	42.0	.377	67.0	.174	92.0	.036
18.0	.745	43.0	.367	68.0	.167	93.0	.032
19.0	.721	44.0	.357	69.0	.161	94.0	.027
20.0	.699	45.0	.347	70.0	.155	95.0	.022
21.0	.678	46.0	.337	71.0	.149	96.0	.018
22.0	.658	47.0	.328	72.0	.143	97.0	.013
23.0	.638	48.0	.319	73.0	.137	98.0	.009
24.0	.620	49.0	.310	74.0	.131	99.0	.004
25.0	.602	50.0	.301	75.0	.125	100.0	.000

Near-Infrared Table

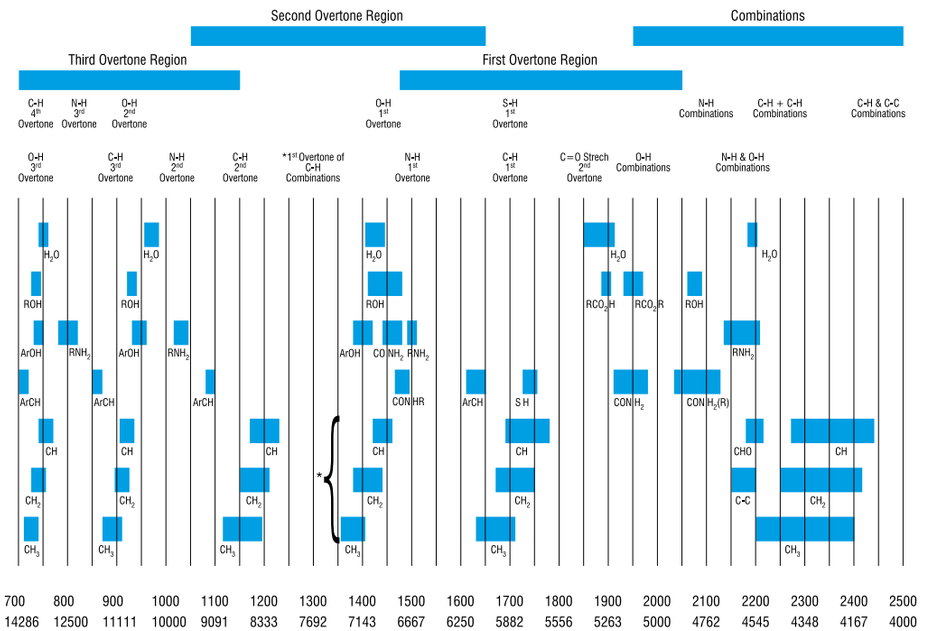

Conversion Table for Energy and Wavelength Units

Wavenumber [cm^{-1}]	Wavelength [µm]	Wavelength [nm]	Frequency [GHz]	Electron Volt [eV]
2.0	5 000.00	5 000 000	60	.00 025
4.0	2 500.00	2 500 000	120	.00 050
6.0	1 666.67	1 666 667	180	.00 074
8.0	1 250.00	1 250 000	240	.00 099
10.0	1 000.00	1 000 000	300	.00 124
12.0	833.33	833 333	360	.00 149
14.0	714.29	714 286	420	.00 174
16.0	625.00	625 000	480	.00 198
18.0	555.56	555 556	540	.00 223
20.0	500.00	500 000	600	.00 248
22.0	454.55	454 545	660	.00 273
24.0	416.57	416 667	719	.00 298
26.0	384.62	384 615	779	.00 322
28.0	357.14	357 143	839	.00 347
30.0	333.33	333 333	898	.00 372
32.0	312.50	312 500	959	.00 397
34.0	294.12	294 118	1 019	.00 422
36.0	277.78	277 778	1 079	.00 446
38.0	263.16	263 158	1 139	.00 471
40.0	250.00	250 000	1 199	.00 496
50.0	200.00	200 000	1 499	.00 620
60.0	166.67	166 667	1 799	.00 744
70.0	142.86	142 857	2 099	.00 868
80.0	125.00	125 000	2 398	.00 992
90.0	111.11	111 111	2 698	.01 116
100.0	100.00	100 000	2 988	.01 240
110.0	90.91	90 909	3 298	.01 364
120.0	83.33	83 333	3 597	.01 488
130.0	76.92	76 923	3 897	.01 612
140.0	71.43	71 429	4 197	.01 736
150.0	66.67	66 667	4 497	.01 860
160.0	62.50	62 500	4 797	.01 984
170.0	58.82	58 824	5 096	.02 108
180.0	55.56	55 556	5 396	.02 232
190.0	52.63	52 632	5 696	.02 356
200.0	50.00	50 000	5 996	.02 480
220.0	45.45	45 455	6 595	.02 728
240.0	41.67	41 667	7 195	.02 976
260.0	38.46	38 462	7 795	.03 224
280.0	35.71	35 714	8 394	.03 472
300.0	33.33	33 333	8 994	.03 720
320.0	31.25	31 250	9 593	.03 967
340.0	29.41	29 412	10 193	.04 215
360.0	27.78	27 778	10 792	.04 463
380.0	26.32	26 316	11 329	.04 711
400.0	25.00	25 000	11 992	.04 959
500.0	20.00	20 000	14 990	.06 199
600.0	16.67	16 667	17 987	.07 439
700.0	14.29	14 286	20 985	.08 679
800.0	12.50	12 500	23 983	.09 919
900.0	11.11	11 111	26 981	.11 159

Wavenumber [cm^{-1}]	Wavelength [µm]	Wavelength [nm]	Frequency [GHz]	Electron Volt [eV]
1 000.0	10.00	10 000	29 979	.12 398
1 100.0	9.09	9 091	32 977	.13 638
1 200.0	8.33	8 333	35 975	.14 878
1 300.0	7.69	7 692	38 973	.16 118
1 400.0	7.14	7 143	41 971	.17 358
1 500.0	6.67	6 667	44 968	.18 598
1 600.0	6.25	6 250	47 966	.19 837
1 700.0	5.88	5 882	50 964	.21 077
1 800.0	5.56	5 556	53 962	.22 317
1 900.0	5.26	5 263	56 960	.23 557
2 000.0	5.00	5 000	59 958	.24 797
2 200.0	4.55	4 545	65 954	.27 276
2 400.0	4.17	4 167	71 950	.29 756
2 600.0	3.58	3 846	77 945	.32 236
2 800.0	3.57	3 571	83 941	.34 716
3 000.0	3.33	3 333	89 937	.37 195
3 200.0	3.13	3 125	95 933	.39 675
3 400.0	2.94	2 941	101 929	.42 155
3 600.0	2.78	2 778	107 924	.44 634
3 800.0	2.63	2 632	113 920	.47 141
4 000.0	2.50	2 500	119 916	.49 594
5 000.0	2.00	2 000	149 895	.61 992
6 000.0	1.67	1 667	179 874	.74 390
7 000.0	1.43	1 429	209 853	.86 789
8 000.0	1.25	1 250	239 832	.99 187
9 000.0	1.11	1 111	269 811	1.11 586
10 000.0	1.00	1 000	299 790	1.23 984
11 000.0	.91	909	329 769	1.36 382
12 000.0	.83	833	359 748	1.48 781
13 000.0	.77	769	389 727	1.61 179
14 000.0	.71	714	419 706	1.73 578
15 000.0	.67	667	449 685	1.85 976
16 000.0	.62	625	479 664	1.98 374
17 000.0	.59	588	509 643	2.10 773
18 000.0	.56	556	539 622	2.23 171
19 000.0	.53	526	569 601	2.35 570
20 000.0	.50	500	599 580	2.47 968
22 000.0	.45	455	659 538	2.72 765
24 000.0	.42	417	719 496	2.97 562
26 000.0	.38	385	779 454	3.22 358
28 000.0	.36	357	839 412	3.47 155
30 000.0	.33	333	899 370	3.71 952
32 000.0	.31	312	959 328	3.96 749
34 000.0	.29	294	1 019 286	4.21 546
36 000.0	.28	278	1 079 244	4.46 342
38 000.0	.26	263	1 139 202	4.71 139
40 000.0	.25	250	1 199 160	4.95 936
50 000.0	.20	200	1 498 950	6.19 921

Sources

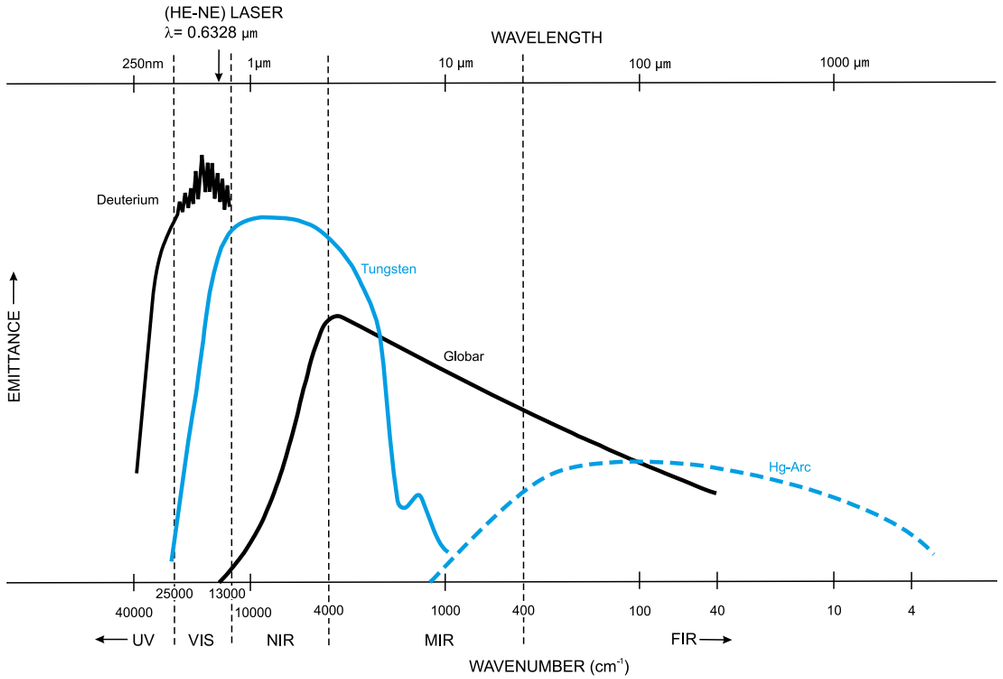

Detectors

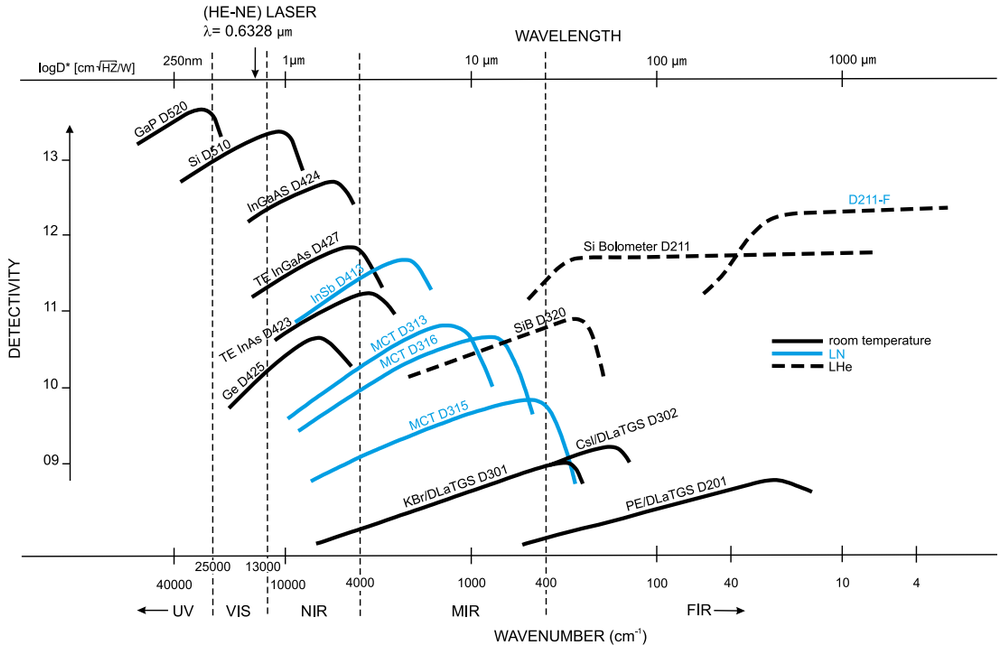

IR Spectroscopy Tables

Beamsplitters

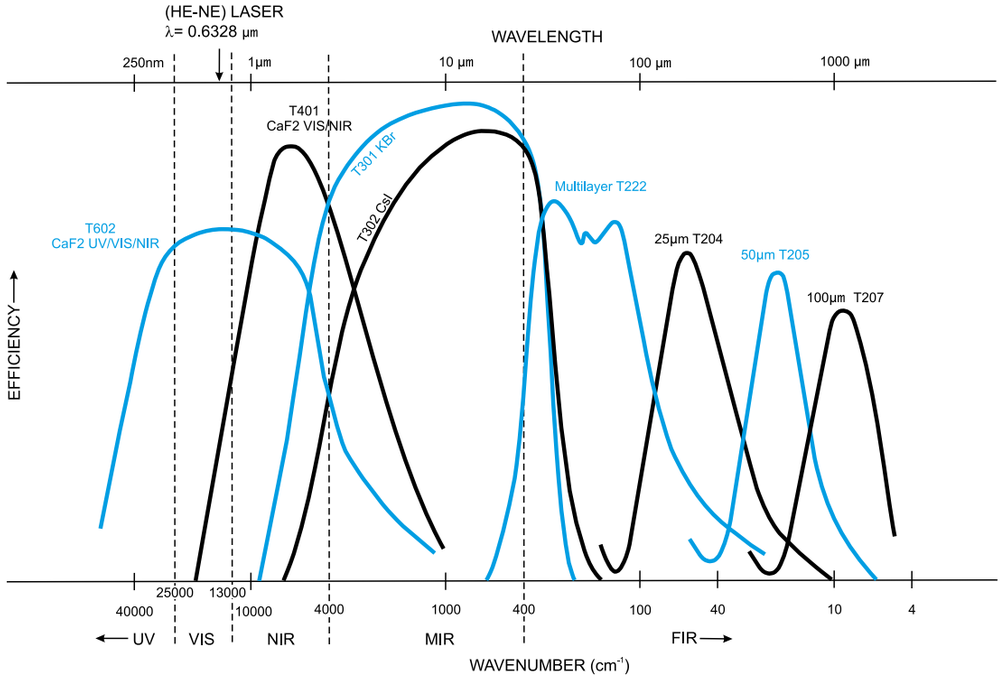

Optical Components Used in FT-IR Spectroscopy

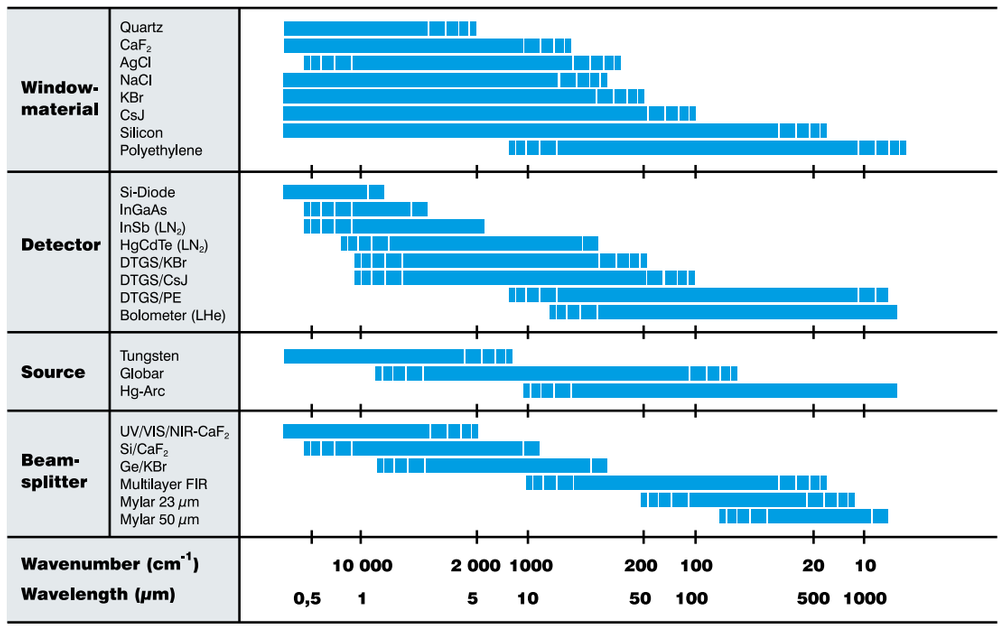

IR Window Materials

Material	Transmission Range [cm $^{-1}$] ([micrometers])	Refractive Index n at 2000 cm^{-1}	Reflectance loss per surface	Hardness (Knoop)	Chemical Properties
Infrasil SiO_2	57,000-2,800 (0.175-3.6)	1.46	~ 3.3%	461	Insoluble in water; soluble in HF.
UV Sapphire AL_2O_3	66,000-2,000 (0.15-5.0)	1.75	~ 7.3%	1370	Very slightly soluble in acids and bases.
Silicon Si	10,000-100 (1.0-100)	3.42	~ 30%	1150	Insoluble in most acids and bases; soluble in HF and HNO_3.
Calcium Fluoride CaF_2	66,000-1,200 (0.15-8.0)	1.40	~ 2.8%	158	Insoluble in water; resists most acids and bases; soluble in NH_4 salts.
Barium Fluoride BaF_2	50,000-900 (0.2-11)	1.45	~ 3.3%	82	Low water solubility; soluble in acid and NH_4Cl.
Zinc Sulfide, Cleartran ZnS	22,000-750 (0.45-13.0)	2.25	~ 15%	355	Soluble in acid; insoluble in water.
Germanium Ge	5,000-600 (2.0-17)	4.01	~ 36%	550	Insoluble in water; soluble in hot H_2SO_4 and aqua regia.
Sodium Chloride NaCl	28,000-700 (0.35-15)	1.52	~ 4.5%	15	Hygroscopic; slightly soluble in alcohol and NH_3.
AMTIR GeAsSe Glass	11,000-900 (0.9-11)	2.50	~ 18%	170	Insoluble in water. Soluble in bases.
Zinc Selenide ZnSe	20,000-500 (0.5-20)	2.43	~ 17%	150	Soluble in strong acids; dissolves in HNO_3.
Silver Chloride AgCl	23,000-400 (0.42-25)	2.00	~ 11%	10	Insoluble in water; soluble in NH_4OH.
Potassium Bromide KBr	33,000-400 (0.3-25)	1.54	~ 4.5%	7	Soluble in water, alcohol, and glycerine; hygroscopic.
Cesium Iodide CsI	33,000-150 (0.3-70)	1.74	~ 7.3%	20	Soluble in water and alcohol; hygroscopic.
KRS-5 TlBr/I	16,000-200 (0.6-60)	2.38	~ 17%	40	Soluble in warm water; soluble in bases; insoluble in acids.
Polyethylene PE (high density)	600-10 (16-1,000)	1.52	~ 4.5%	5	Resistant to most solvents.
Diamond C	45,000-10 (0.22-1,000)	2.40	~ 17%	7000	Insoluble in water, acids, and bases.
TPX(TM) Methylpentene Resin	350-10 (28-1,000)	1.43	~ 3.3%		Similar to PE but transparent and more rigid

Absorption of Commonly Used IR Solvents*

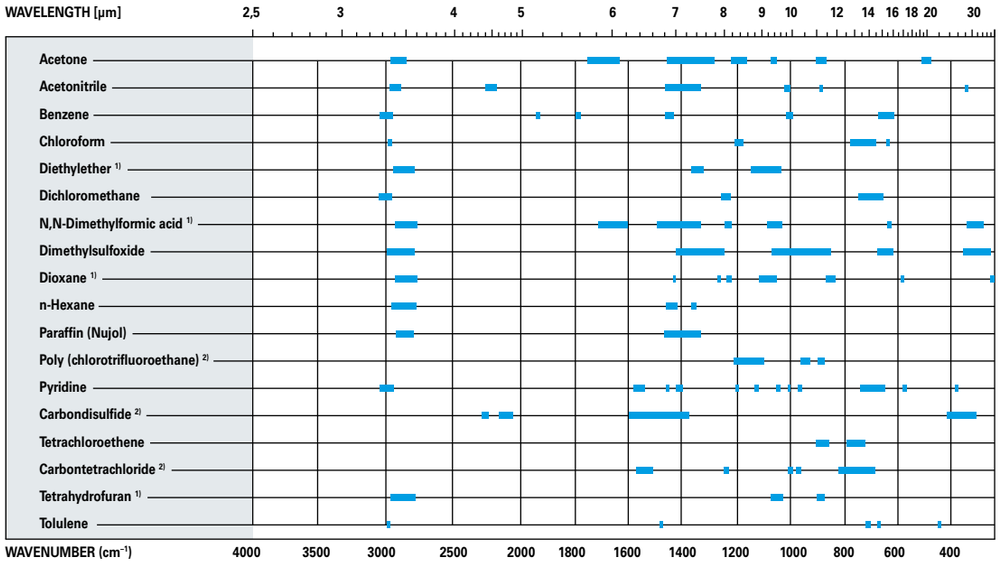

* This chart shows ranges with transmission less than 20 %; standard thickness: 100 μm; except for: (1) 20 μm; (2) 200 μm.

Infrared and Raman Tables

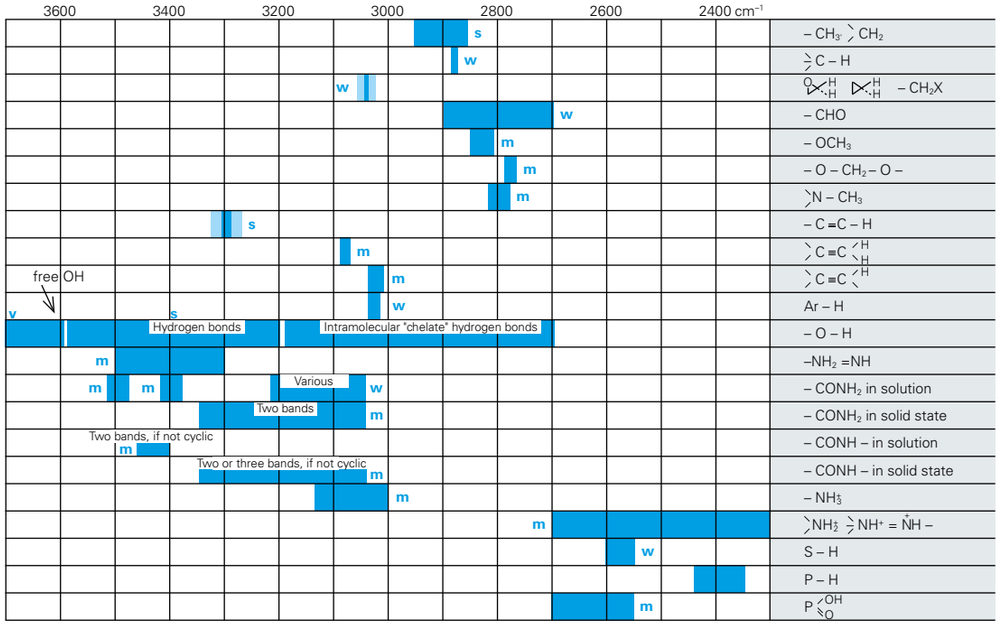

Positions of Stretching Vibrations of Hydrogen (in the hatched ranges the boundaries are not well defined;
Band intensity: **s** = strong, **m** = medium, **w** = weak, **v** = varying.

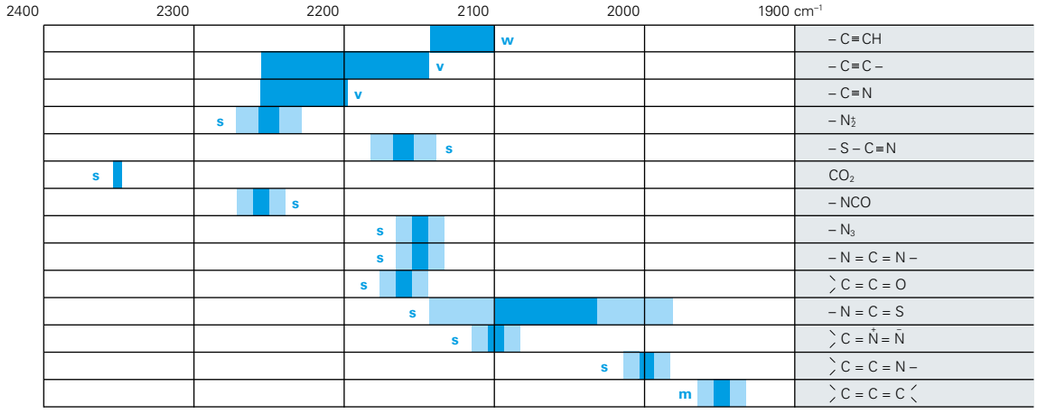

Positions of Stretching Vibrations of Triple Bonds and Cumulated Double Bonds
(**s** = strong, **m** = medium, **w** = weak, **v** = varying)

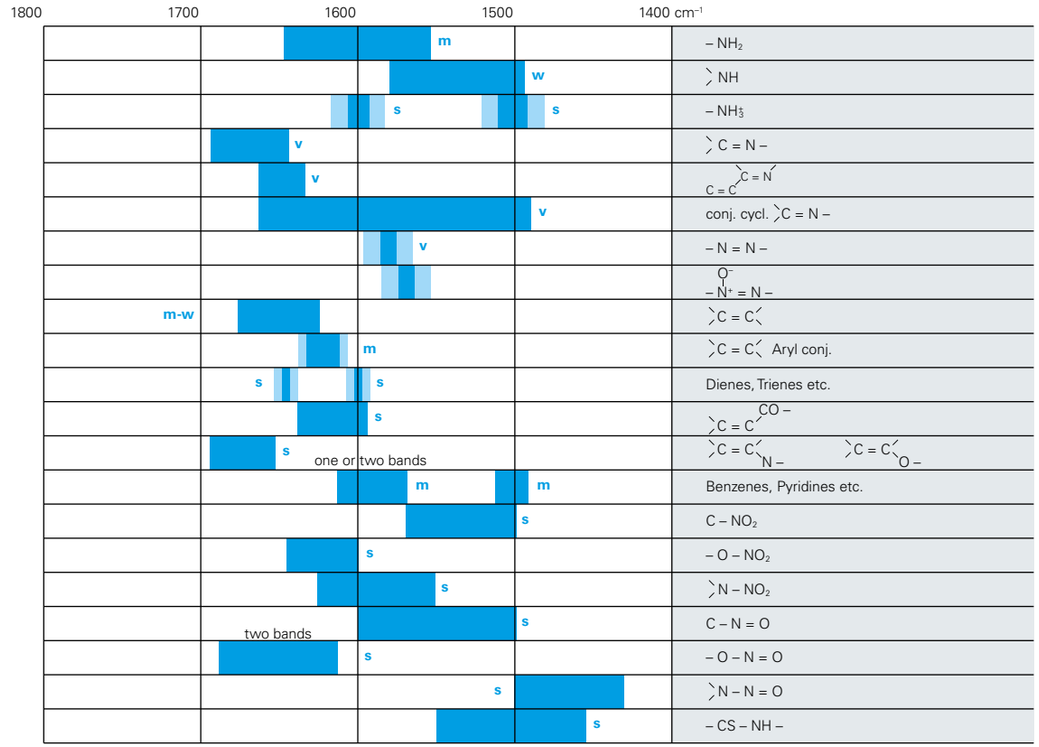

Positions of the Double Bond Stretching Vibrations and N-H Bending Vibrations
(**s** = strong, **m** = medium, **w** = weak, **v** = varying)

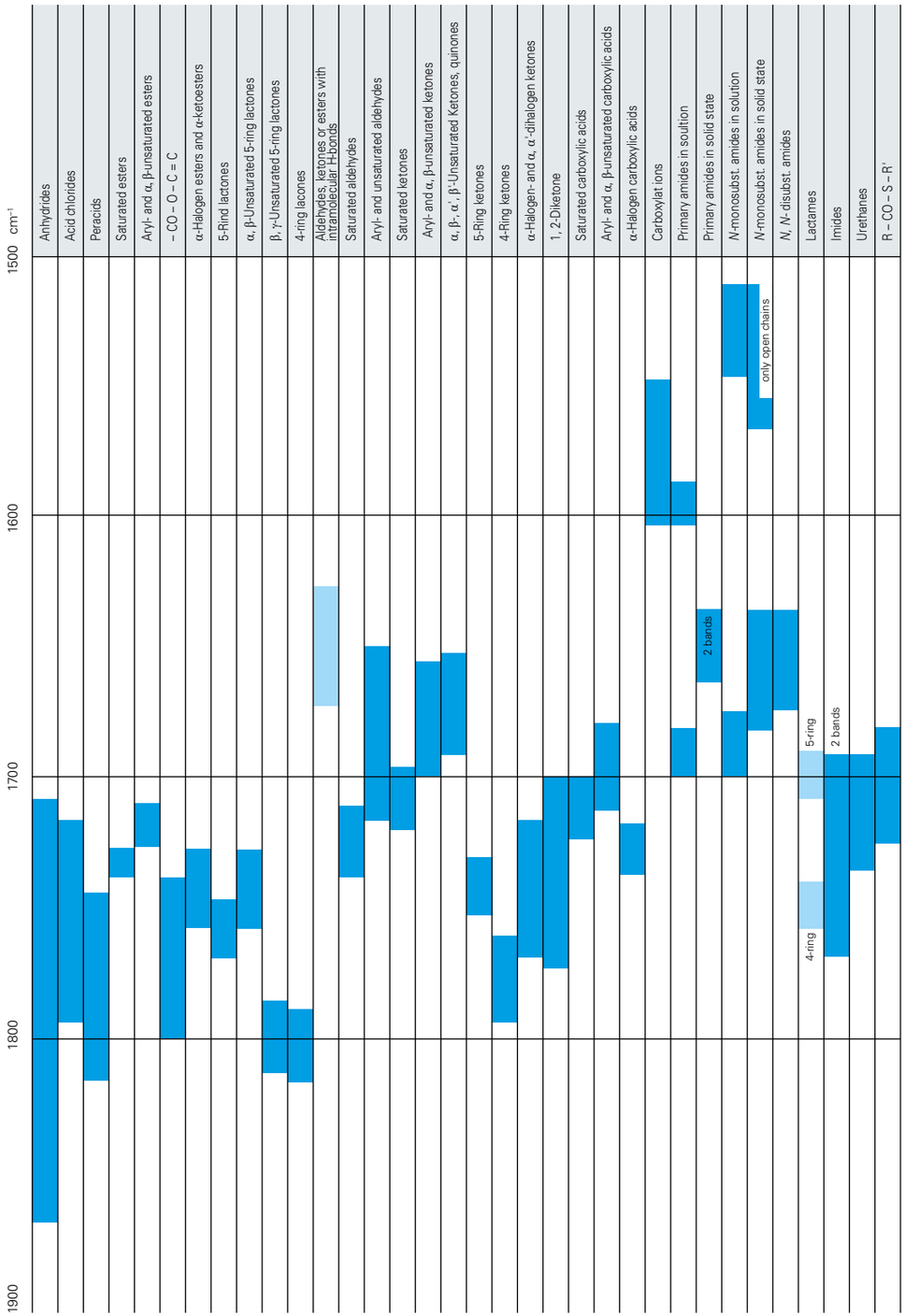

Positions of Carbonyl Stretching Vibrations (all bands are strong)

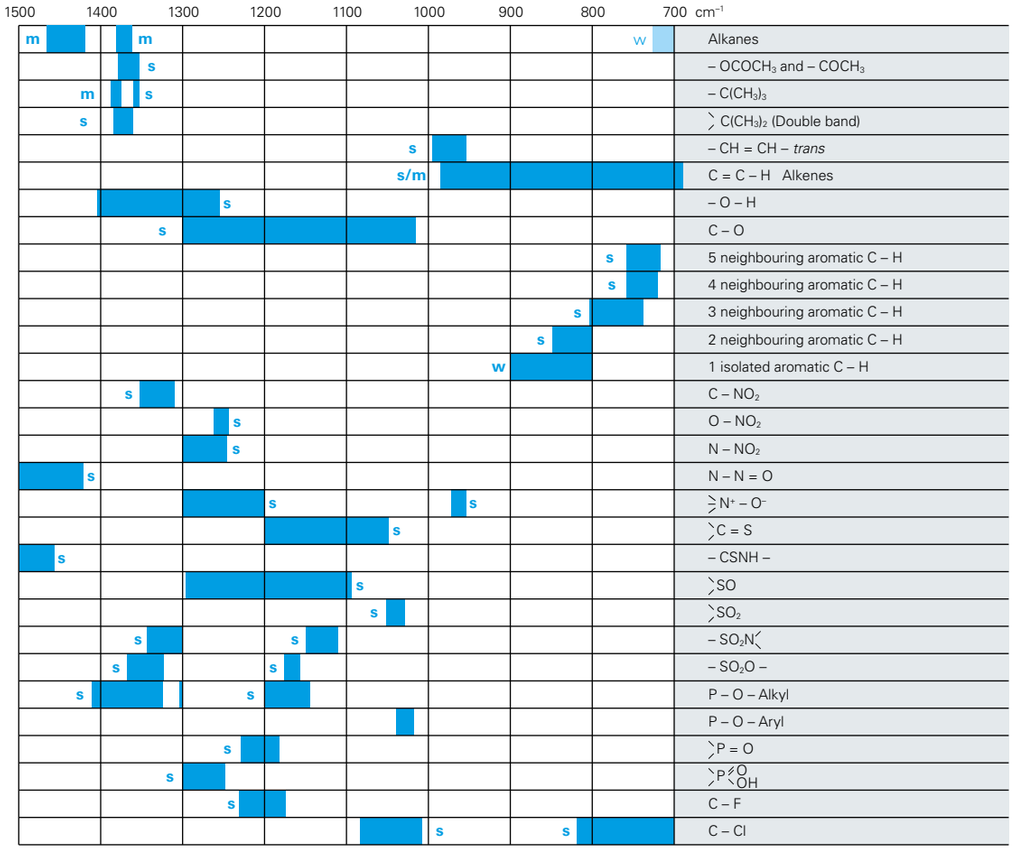

Characteristic Absorptions in the Fingerprint Region (**s** = strong, **m** = medium, **w** = weak)

Stokes Shifts (0-3500 cm^{-1}) of Various Laser Sources

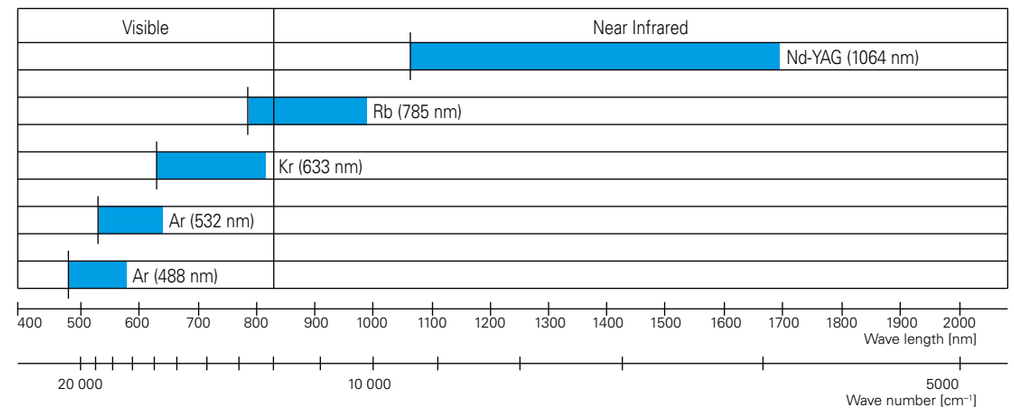

Nd-YAG: Neodynium YAG Laser **Rb:** Ruby Laser **Kr:** Krypton Ion Laser **Ar:** Argon Ion Laser

Vibrational Spectroscopy

Selected Force Constants and Bond Orders (according to Siebert) of Organic and Inorganic Compounds

Bond A-B	Force Const. f (N cm^{-1})	Bond Order	Compound	Bond A-B	Force Const. f (N cm^{-1})	Bond Order	Compound
H-H	5.14	0.77	H_2	**C-S**	3.3	1.0	$S(CH_3)_2$
Li-Li	1.24	1.2	Li_2	**C-Cl**	3.12	0.93	CCl_4
B-B	3.58	1.2	B_2	**C-Ni**	2.91	1.2	Ni_4CO
C-C	16.5	3.8	HCCH	**C-Ni**	1.43	0.68	NiCO
N-N	22.42	3.2	N_2	**C-Se**	5.94	1.8	CSe_2
O-O	11.41	1.4	O_2	**C-Br**	2.42	0.86	CBr_4
F-F	4.45	0.58	F_2	**C-Rh**	2.4	1.2	$(Rh(CN)_6)^{3-}$
Na-Na	0.17	0.24	Na_2	**C-Ag**	2.0	0.99	$(Ag(CN)_2)^-$
Si-Si	4.65	2.0	Si_2	**C-I**	1.69	0.79	CI_4
Si-Si	~1.7	~0.9	Si_2H_6	**N-H**	7.05	1.1	NH_3
P-P	5.56	2.1	P_2	**N-B**	7.2	1.6	BN_2^{3-}
P-P	2.07	0.95	P_4	**N-C**	18.07	3.0	HCN
S-S	4.96	1.7	S_2	**N-N**	22.42	3.2	N_2
S-S	2.5	0.99	S_8	**N-N**	16.01	2.4	N-NNH
Cl-Cl	3.24	1.1	Cl_2	**N-N**	13.15	2.0	$N\text{-}N\text{-}N^-$
Ni-Ni	0.11	0.2	Ni solid	**N-O**	25.07	3.1	$N\text{-}O^+$
As-As	3.91	1.8	As_2	**N-O**	17.17	2.3	NO^+_2
Se-Se	3.61	1.6	$^{80}Se_2$	**N-O**	15.49	2.1	NO
Br-Br	2.36	1.1	Br_2	**N-O**	15.18	2.0	ONCl
Rb-Rb	0.08	0.2	Rb_2	**N-O**	11.78	1.7	NNO
Cd-Cd	1.11	1.0	Cd_2^{2+}	**N-F**	4.16	0.66	NF_3
Sb-Sb	2.61	1.9	Sb_2	**N-Si**	3.8	1.1	$((CH_3)_3Si)_2NH$
Te-Te	2.37	1.7	Te_2	**N-S**	12.54	2.5	NSF_3
I-I	1.70	1.2	I_2	**N-S**	8.3	1.9	HNSO
Hg-Hg	1.69	1.5	Hg_2^{2+}	**N-S**	3.1	0.87	$H_3N\text{-}SO_3$
Pb-Pb	4.02	3	Pb_2	**O-Li**	1.58	0.66	LiO
Bi-Bi	1.84	1.6	Bi_2	**O-Be**	7.51	1.8	BeO
H-B	2.75	0.68	BH_3	**O-B**	13.66	2.5	BO
H-C	5.50	1.0	CH_4	**O-B**	6.35	1.3	BO_3^{3-}
H-N	7.05	1.1	NH_3	**O-O**	16.59	2.0	O^+_2
H-O	8.45	1.1	H_2O	**O-O**	11.41	1.4	O_2
H-O	7.40	1.0	HO^-	**O-O**	6.18	0.89	O^-_2
H-F	8.85	1.1	HF	**O-O**	5.70	0.83	O_3
H-Al	1.76	0.60	AlH^-_4	**O-Na**	~3.2	~1.1	Na-OH
H-Si	2.98	0.84	SiH_4	**O-Mg**	3.5	1.1	MgO
H-P	3.11	0.82	PH_3	**O-Al**	5.66	1.5	AlO
H-S	4.29	1.0	H_2S	**O-Al**	3.8	1.1	$Al(OH)^-_4$
H-Cl	4.81	1.0	HCl	**O-Si**	9.25	2.1	SiO
H-Ge	2.81	0.82	GeH_4	**O-Si**	4.75	1.2	SiO^{-4}_4
H-As	2.85	0.81	AsH_3	**O-P**	9.41	2.0	PO
H-Se	3.51	0.93	H_2Se	**O-P**	6.16	1.4	PO^{3-}_4
H-Br	3.84	0.98	HBr	**O-S**	10.01	2.0	SO_2
H-Sn	2.03	0.76	SnH_4	**O-Cl**	4.26	1.0	ClO^-_2
H-Sb	2.09	0.77	SbH_3	**O-Cl**	3.30	0.82	ClO^-
H-I	2.92	0.97	HI	**O-Ca**	2.85	1.2	CaO
C-H	5.50	1.0	CH_4	**O-Ti**	7.19	2.4	TiO
C-B	3.82	1.1	$B(CH_3)_3$	**O-V**	7.36	2.3	VO
C-C	16.5	3.2	HCCH	**O-Cr**	5.82	1.9	CrO
C-C	9.15	1.9	H_2CCH_2	**O-Mn**	5.16	1.6	MnO
C-C	7.6	1.7	C_6H_6	**O-Fe**	5.67	1.7	FeO
C-C	4.4	1.1	H_3CCH_3	**O-Cu**	2.97	0.93	CuO
C-N	18.07	3.0	HCN	**O-Ge**	7.53	1.8	^{74}GeO
C-N	11.84	2.1	CN_2^{2-}	**O-Se**	6.45	1.5	SeO
C-N	6.54	1.3	$NNCH_2$	**O-Mo**	3.05	1.2	Ba_2CaMoO_6 (solid)
C-O	18.56	2.8	CO	**O-Ru**	6.70	2.2	RuO_4
C-O	15.61	2.4	CO_2	**O-Ag**	2.00	0.79	AgO
C-O	12.76	2.0	OCH_2	**O-Sn**	5.53	1.7	SnO
C-O	7.86	1.3	CO_3^{2-}	**O-Te**	5.31	1.6	TeO
C-O	5.1	0.96	$O(CH_3)_2$	**O-Ba**	3.79	1.8	BaO
C-F	6.98	1.1	CF_4	**O-Ce**	6.33	2.6	CeO
C-P	8.95	2.4	HCP	**O-Pr**	5.68	2.4	PrO
C-S	7.67	2.0	CS_2	**O-Nd**	3.5	1.6	$NdAc_3{\cdot}H_2O$ (polymer)

MS: Exact Masses of the Isotopes

Atomic Masses and Representative Abundances of the Isotopes (NIST)

The masses and abundances of the isotopes we use for generating molecular formulas, simulating patterns and SNAP peak finding basically are taken from the National Institute of Standards and Technology (NIST).

Z = Atomic number, M = mass number; Abund. = isotope abundance.

Z	E	M	Exact Mass	Abund.	Valency
1	**H**	**1**	1.007825032	0.999885	1
	H (D)	**2**	2.014101778	0.000115	
	H (T)	**3**	3.016049267 5		
2	**He**	**3**	3.016029309 7	1.37e-06	0
		4	4.002603249 7	0.99999863	
3	**Li**	**6**	6.015122 3	0.0759	1
		7	7.016004	0.9241	
4	**Be**	**9**	9.012182 1	1	2
5	**B**	**10**	10.012937	0.199	3
		11	11.009305 5	0.801	
6	**C**	**12**	12	0.9893	4
		13	13.003354 837 8	0.0107	
		14	14.003241 988		
7	**N**	**14**	14.003074 005 2	0.99632	3
		15	15.000108 898 4	0.00368	
8	**O**	**16**	15.994914 622 1	0.99757	2
		17	16.999131 5	0.00038	
		18	17.999160 4	0.00205	
9	**F**	**19**	18.998403 2	1	1
10	**Ne**	**20**	19.992440 175 9	0.9048	0
		21	20.993846 74	0.0027	
		22	21.991385 51	0.0925	
11	**Na**	**23**	22.989769 67	1	1
12	**Mg**	**24**	23.985041 9	0.7899	2
		25	24.985837 02	0.1	
		26	25.982593 04	0.1101	
13	**Al**	**27**	26.981538 44	1	3
14	**Si**	**28**	27.976926 532 7	0.92229607770392	4
		29	28.976494 72	0.04683195316804 7	
		30	29.973770 22	0.03087196912803 1	
15	**P**	**31**	30.973761 51	1	3
		32	31.973907 16		
16	**S**	**32**	31.972070 69	0.9493	2
		33	32.971458 5	0.0076	
		34	33.967866 83	0.0429	
		36	35.967080 88	0.0002	
17	**Cl**	**35**	34.968852 71	0.7578	1
		37	36.965902 6	0.2422	
18	**Ar**	**36**	35.967546 28	0.003365	0
		38	37.962732 2	0.000632	
		40	39.962383 123	0.996003	
19	**K**	**39**	38.963706 9	0.932581	1
		40	39.963998 67	0.000117	
		41	40.961825 97	0.067302	
20	**Ca**	**40**	39.962591 2	0.96941	2
		42	41.958618 3	0.00647	
		43	42.958766 8	0.00135	
		44	43.955481 1	0.02086	
		46	45.953692 8	4E-05	
		48	47.952534	0.00187	
21	**Sc**	**45**	44.955910 2	1	3
22	**Ti**	**46**	45.952629 5	0.0825	4
		47	46.951763 8	0.0744	
		48	47.947947 1	0.7372	
		49	48.947870 8	0.0541	
		50	49.944792 1	0.0518	
23	**V**	**50**	49.947162 8	0.0025	5
		51	50.943963 7	0.9975	
24	**Cr**	**50**	49.946049 6	0.04345	3
		52	51.940511 9	0.83789	
		53	52.940653 8	0.09501	
		54	53.938884 9	0.02365	
25	**Mn**	**55**	54.938049 6	1	2
26	**Fe**	**54**	53.939614 8	0.05845	2
		56	55.934942 1	0.91754	
		57	56.935398 7	0.02119	
		58	57.933280 5	0.00282	
27	**Co**	**59**	58.933200 2	1	2
28	**Ni**	**58**	57.935347 9	0.680769	2
		60	59.930790 6	0.262231	
		61	60.931060 4	0.011399	
		62	61.928348 8	0.036345	
		64	63.927969 6	0.009256	

MS: Exact Masses of the Isotopes

Atomic Masses and Representative Abundances of the Isotopes (NIST)

The masses and abundances of the isotopes we use for generating molecular formulas, simulating patterns and SNAP peak finding basically are taken from the National Institute of Standards and Technology (NIST).
Z = Atomic number, M = mass number; Abund. = isotope abundance.

Z	E	M	Exact Mass	Abund.	Valency
29	Cu	63	62.9296011	0.6917	1
		65	64.9277937	0.3083	
30	Zn	64	63.9291466	0.4863	2
		66	65.9260368	0.279	
		67	66.9271309	0.041	
		68	67.9248476	0.1875	
		70	69.925325	0.0062	
31	Ga	69	68.925581	0.60108	3
		71	70.924705	0.39892	
32	Ge	70	69.9242504	0.2084	4
		72	71.9220762	0.2754	
		73	72.9234594	0.0773	
		74	73.9211782	0.3628	
		76	75.9214027	0.0761	
33	As	75	74.9215964	1	3
34	Se	74	73.9224766	0.0089	2
		76	75.9192141	0.0937	
		77	76.9199146	0.0763	
		78	77.9173095	0.2377	
		80	79.9165218	0.4961	
		82	81.9167	0.0873	
35	Br	79	78.9183376	0.5069	1
		81	80.916291	0.4931	
36	Kr	78	77.920386	0.0035	0
		80	79.916378	0.0228	
		82	81.9134846	0.1158	
		83	82.914136	0.1149	
		84	83.911507	0.57	
		86	85.9106103	0.173	
37	Rb	85	84.9117893	0.7217	1
		87	86.9091835	0.2783	
38	Sr	84	83.913425	0.0056	2
		86	85.9092624	0.0986	
		87	86.9088793	0.07	
		88	87.9056143	0.8258	
39	Y	89	88.9058479	1	3
40	Zr	90	89.9047037	0.5145	4
		91	90.905645	0.1122	
		92	91.9050401	0.1715	
		94	93.9063158	0.1738	
		96	95.908276	0.028	
41	Nb	93	92.9063775	1	5
42	Mo	92	91.90681	0.1484	6
		94	93.9050876	0.0925	
		95	94.9058415	0.1592	
		96	95.9046789	0.1668	
		97	96.906021	0.0955	
		98	97.9054078	0.2413	
		100	99.907477	0.0963	
43	Tc	97	96.906365		4
		98	97.907216		
		99	98.9062546		
44	Ru	96	95.907598	0.0554	3
		98	97.905287	0.0187	
		99	98.9059393	0.1276	
		100	99.9042197	0.126	
		101	100.9055822	0.1706	
		102	101.9043495	0.3155	
		104	103.90543	0.1862	
45	Rh	103	102.905504	1	3
46	Pd	102	101.905608	0.0102	2
		104	103.904035	0.1114	
		105	104.905084	0.2233	
		106	105.903483	0.2733	
		108	107.903894	0.2646	
		110	109.905152	0.1172	
47	Ag	107	106.905093	0.51839	1
		109	108.904756	0.48161	
48	Cd	106	105.906458	0.0125	2
		108	107.904183	0.0089	
		110	109.903006	0.1249	
		111	110.904182	0.128	
		112	111.9.027572	0.2413	
		113	112.9.044009	0.1222	
		114	113.9.033581	0.2873	
		116	115.904755	0.0749	

MS: Exact Masses of the Isotopes

Atomic Masses and Representative Abundances of the Isotopes (NIST)

The masses and abundances of the isotopes we use for generating molecular formulas, simulating patterns and SNAP peak finding basically are taken from the National Institute of Standards and Technology (NIST).
Z = Atomic number, M = mass number; Abund. = isotope abundance.

Z	E	M	Exact Mass	Abund.	Valency
49	In	113	112.904061	0.0429	3
		115	114.903878	0.9571	
50	Sn	112	111.904821	0.0097	4
		114	113.902782	0.0066	
		115	114.903346	0.0034	
		116	115.901744	0.1454	
		117	116.902954	0.0768	
		118	117.901606	0.2422	
		119	118.903309	0.0859	
		120	119.9021966	0.3258	
		122	121.9034401	0.0463	
		124	123.9052746	0.0579	
51	Sb	121	120.903818	0.5721	5
		123	122.9042157	0.4279	
52	Te	120	119.90402	0.0009	2
		122	121.9030471	0.0255	
		123	122.904273	0.0089	
		124	123.9028195	0.0474	
		125	124.9044247	0.0707	
		126	125.9033055	0.1884	
		128	127.9044614	0.3174	
		130	129.9062228	0.3408	
53	I	127	126.904468	1	1
54	Xe	124	123.9058958	0.0009	0
		126	125.904269	0.0009	
		128	127.9035304	0.0192	
		129	128.9047795	0.2644	
		130	129.9035079	0.0408	
		131	130.9050819	0.2118	
		132	131.9041545	0.2689	
		134	133.9053945	0.1044	
		136	135.90.722	0.0887	
55	Cs	133	132.905447	1	1
56	Ba	130	129.90631	0.00106	2
		132	131.905056	0.00101	
		134	133.904503	0.02417	
		135	134.905683	0.06592	
		136	135.90457	0.07854	
		137	136.905821	0.11232	
		138	137.905241	0.71698	
57	La	138	137.907107	0.0009	3
		139	138.906348	0.9991	
58	Ce	136	135.90714	0.00185	4
		138	137.905986	0.00251	
		140	139.905434	0.8845	
		142	141.90924	0.11114	
59	Pr	141	140.907648	1	3
60	Nd	142	141.907719	0.272	3
		143	142.90981	0.122	
		144	143.910083	0.238	
		145	144.912569	0.083	
		146	145.913112	0.172	
		148	147.916889	0.057	
		150	149.920887	0.056	
61	Pm	145	144.912749 (3)		
		147	146.9151385 (26)		
62	Sm	144	143.911995	0.0307	2
		147	146.914893	0.1499	
		148	147.914818	0.1124	
		149	148.91718	0.1382	
		150	149.917271	0.0738	
		152	151.919728	0.2675	
		154	153.922205	0.2275	
63	Eu	151	150.919846	0.4781	2
		153	152.921226	0.5219	
64	Gd	152	151.919788	0.002	3
		154	153.920862	0.0218	
		155	154.922619	0.148	
		156	155.92212	0.2047	
		157	156.923957	0.1565	
		158	157.924101	0.2484	
		160	159.927051	0.2186	
65	Tb	159	158.925343	1	3
66	Dy	156	155.924278	0.0006	3
		158	157.924405	0.001	
		160	159.925194	0.0234	
		161	160.92693	0.1891	
		162	161.926795	0.2551	
		163	162.928728	0.249	
		164	163.929171	0.2818	

MS: Exact Masses of the Isotopes

Atomic Masses and Representative Abundances of the Isotopes (NIST)

The masses and abundances of the isotopes we use for generating molecular formulas, simulating patterns and SNAP peak finding basically are taken from the National Institute of Standards and Technology (NIST).
Z = Atomic number, M = mass number; Abund. = isotope abundance.

Z	E	M	Exact Mass	Abund.	Valency
67	Ho	**165**	164.930.319	1	3
68	Er	**162**	161.928775	0.0014	3
		164	163.929197	0.0161	
		166	165.93029	0.3361	
		167	166.932045	0.2293	
		168	167.932368	0.2678	
		170	169.93546	0.1493	
69	Tm	**169**	168.934211	1	3
70	Yb	**168**	167.933894	0.0013	2
		170	169.934759	0.0304	
		171	170.936322	0.1428	
		172	171.9363777	0.2183	
		173	172.9382068	0.1613	
		174	173.9388581	0.3183	
		176	175.942568	0.1276	
71	Lu	**175**	174.9407679	0.9741	3
		176	175.9426824	0.0259	
72	Hf	**174**	173.94004	0.0016	4
		176	175.9414018 4	0.0526	
		177	176.94322	0.186	
		178	177.9436977	0.2728	
		179	178.9458151	0.1362	
		180	179.9465488	0.3508	
73	Ta	**180**	179.947466	0.00012	5
		181	180.947996	0.99988	
74	W	**180**	179.946706	0.0012	6
		182	181.948206	0.265	
		183	182.9502245	0.1431	
		184	183.9509326	0.3064	
		186	185.954362	0.2843	
75	Re	**185**	184.9529557	0.374	4
		187	186.9557508	0.626	
76	Os	**184**	183.952491	0.0002	3
		186	185.953838	0.0159	
		187	186.9557479	0.0196	
		188	187.955836	0.1324	
		189	188.9581449	0.1615	
		190	189.958445	0.2626	
		192	191.961479	0.4078	
77	Ir	**191**	190.960591	0.373	3
		193	192.962924	0.627	
78	Pt	**190**	189.95993	0.00014	2
		192	191.961035	0.00782	
		194	193.962664	0.32967	
		195	194.964774	0.33832	
		196	195.964935	0.25242	
		198	197.967876	0.07163	
79	Au	**197**	196.966552	1	1
80	Hg	**196**	195.965815	0.0015	2
		198	197.966752	0.0997	
		199	198.968262	0.1687	
		200	199.968309	0.231	
		201	200.970285	0.1318	
		202	201.970626	0.2986	
		204	203.973476	0.0687	
81	Tl	**203**	202.972329	0.29524	3
		205	204.974412	0.70476	
82	Pb	**204**	203.973029	0.014	4
		206	205.974449	0.241	
		207	206.975881	0.221	
		208	207.976636	0.524	
83	Bi	**209**	208.980383	1	5
90	Th	**232**	232.0380504	1	4
91	Pa	**231**	231.0358789	1	4
92	U	**234**	234.0409456	5.5e-05	3
		235	235.0439231	0.0072	
		238	238.0507826	0.992745	

References:
Coursey, J.S., Schwab, D.J., and Dragoset, R.A. (2003), Atomic Weights and Isotopic Compositions (version 2.3.1). [Online] Available: http://physics.nist.gov/Comp [2004, February 26]. National Institute of Standards and Technology, Gaithersburg, MD.
Originally published as T.B. Coplen, Atomic Weights of the Elements 1999, Pure Appl. Chem. 73(4), 667 (2001); K.J.R. Rosman and P.D.P. Taylor, Isotopic Compositions of the Elements 1997, J. Phys. Chem. Ref. Data 27(6), 1275 (1998); and G. Audi and A.H. Wapstra, The 1995 Update To The Atomic Mass Evaluation, Nuclear Physics A 595(4), 409 (1995).
The following modifications/additions were made to the NIST Atomic Weights and Isotopic Compositions (version 2.3.1) table:
- Uun was renamed to Ds (Darmstadtium) which is now the official name.
- Additional elements Ct, Nt and Qt were defined which have an abundance of 95% of 13C, 15N and 18O and 5% of 12C, 14N and 16O. These elements were added to calculate isotopically marked substances.
- The valencies of the atoms are listed additionally. For quickly inspecting the valencies used, please refer to the Table of Valencies.

Solid Phase Peptides Synthesis

Mass Shift of Modifications, Protection Groups and Artifacts

m/z shift [Da]	Modification	Abbreviation	Sum formula change	Valid residues	Origin
-186,07931	Trp->Null		$-C_{11}H_{10}N_2O$	W	Deletion
-163,06333	Tyr->Null		$-C_9H_9NO_2$	Y	Deletion
-156,10111	Arg->Null		$-C_6H_{12}N_4O$	R	Deletion
-147,06841	Phe->Null		$-C_9H_9NO$	F	Deletion
-137,05891	His->Null		$-C_6H_7N_3O$	H	Deletion
-131,04049	Met->Null		$-C_5H_9NOS$	M	Deletion
-129,04259	Glu->Null		$-C_5H_7NO_3$	E	Deletion
-128,09496	Lys->Null		$-C_6H_{12}N_2O$	K	Deletion
-128,05858	Gln->Null		$-C_5H_8N_2O_2$	Q	Deletion
-115,02694	Asp->Null		$-C_4H_5NO_3$	D	Deletion
-114,04293	Asn->Null		$-C_4H_6N_2O_2$	N	Deletion
-113,08406	Ile->Null		$-C_6H_{11}NO$	I	Deletion
-113,08406	Leu->Null		$-C_6H_{11}NO$	L	Deletion
-101,04768	Thr->Null		$-C_4H_7NO_2$	T	Deletion
-99,06841	Val->Null		$-C_5H_9NO$	V	Deletion
-97,05276	Pro->Null		$-C_5H_7NO$	P	Deletion
-87,03203	Ser->Null		$-C_3H_5NO_2$	S	Deletion
-71,03711	Ala->Null		$-C_3H_5NO$	A	Deletion
-57,02146	Gly->Null		$-C_2H_3NO$	G	Deletion
-16,01872	Pyro-glutamination (N-term)		$-NH_2$	Q	N-terminal
0,98402	Deamidation		$-NH_2+OH$	NQ	Artefact
14,01565	Methylation		$+CH_2$	DEKR	Chemical Modification
14,01565	Methylation	Me	$-H+CH_3$	Y	Fmoc
15,99492	Oxidation	Ox	$+O$	MW	Artefact
16,01872	Amidation (C-term)		$-O+NH_2O$	all Amino acids	C-terminal
27,99492	Formylation	For	$-H+CHO$	W	Boc
28,03130	Dimethylation		$+C_2H_4$	KR	Chemical Modification
28,03130	Ethylation	Et	$-H+C_2H_5$	Y	Boc
29,00274	Formyl (N-term)		$+CHO$	M	N-terminal
31,98983	Double Oxidation Tryptophane		$+O_2$	W	Artefact
42,01057	Acetylation	Ac	$-H+C_2H_3O$	K	Fmoc
42,04695	Trimethylation		$+C_3H_6$	KR	Chemical Modification
44,98508	Nitration	NO2	$-H+NO_2$	Y	Chemical Modification
44,98508	Nitration	NO2	$-H+NO_2$	R	Boc
47,94445	Selenocystein		-S+Se	C	Chemical Modification
56,06260	Diethylation		$+C_4H_8$	K	Chemical Modification
56,06260	tert.-Butyl	tBu	$-H+C_4H_9$	CSTY	Fmoc
56,06260	tert.-Butyl	tBu	$-H+C_4H_9$	STY	Boc
57,02146	Gly->GG		$+C_2H_3NO$	G	Double coupling
68,06260	Piperidine	Pip	$+C_5H_8$	DE	Artefact
71,03711	Propionamidation		$+C_3H_5NO$	C	Cys-State
71,03711	Ala->AA		$+C_3H_5NO$	A	Double coupling
71,03711	Acetamidomethyl	Acm	$-H+C_3H_6NO$	C	Fmoc/Boc
72,05752	tert.-Butoxy	OtBu	$-H+C_4H_9O$	DE	Fmoc/Boc
79,96633	Phosphorylation		$-H+PO_3H_2$	STY	Chemical Modification
86,07317	tert.-Butoxymethyl	Bum	$-H+C_5H_{11}O$	H	Fmoc
87,03203	Ser->SS		$+C_3H_5NO_2$	S	Double coupling
88,03467	tert.-Butylthio	tButhio	$-H+C_4H_9S$	C	Fmoc
90,04695	Benzyl	Bzl	$-H+C_7H_7$	CST	Fmoc
90,04695	Benzyl	Bzl	$-H+C_7H_7$	CSTY	Boc
95,98230	Trifluoroacetylation	Tfa	$-H+C_2F_3O$	K	Fmoc/Boc
97,05276	Pro->PP		$+C_5H_7NO$	P	Double coupling
99,06841	Val->VV		$+C_5H_9NO$	V	Double coupling
100,05243	tert.-Butoxycarbonyl	Boc	$-H+C_5H_9O_2$	all Amino acids	Boc

Solid Phase Peptides Synthesis

Mass Shift of Modifications, Protection Groups and Artifacts

m/z shift [Da]	Modification	Abbreviation	Sum formula change	Valid residues	Origin
101,04768	Thr->TT		$+C_4H_7NO_2$	T	Double coupling
103,00918	Cys->CC		$+C_3H_5NOS$	C	Double coupling
104,06260	4-Methylbenzyl	MeBzl	$-H+C_8H_9$	C	Boc
106,04187	Benzyloxy	BzlO	$-H+C_7H_7O$	DE	Fmoc/Boc
113,08406	Ile->Il		$+C_6H_{11}NO$	I	Double coupling
113,08406	Leu->LL		$+C_6H_{11}NO$	L	Double coupling
114,04293	Asn->NN		$+C_4H_6N_2O_2$	N	Double coupling
115,02694	Asp->DD		$+C_4H_5NO_3$	D	Double coupling
118,07825	2-Phenylisopropyl	O-2-PhiPr	$-H+C_9H_{11}$	DE	Fmoc
120,05752	4-Methoxybenzyl	MeOBzl	$-H+C_8H_9O$	C	Fmoc/Boc
120,05752	Benzyloxymethyl	Bom	$-H+C_8H_9O$	H	Boc
128,05858	Gln->QQ		$+C_5H_8N_2O_2$	Q	Double coupling
128,09496	Lys->KK		$+C_6H_{12}N_2O$	K	Double coupling
129,04259	Glu->EE		$+C_5H_7NO_3$	E	Double coupling
131,04049	Met->MM		$+C_5H_9NOS$	M	Double coupling
134,03678	Benzyloxycarbonyl	Z	$-H+C_8H_7O_2$	K	Fmoc/Boc
137,05891	His->HH		$+C_6H_7N_3O$	H	Double coupling
147,06841	Phe->FF		$+C_9H_9NO$	F	Double coupling
148,08882	Adamantyloxy	O-1-Ada	$-H+C_{10}H_{13}O$	D	Fmoc/Boc
148,08882	Adamantyloxy	O-2-Ada	$-H+C_{10}H_{13}O$	D	Boc
154,00885	Tosyl	Tos	$-H+C_7H_7O_2S$	HR	Fmoc/Boc
156,10111	Arg->RR		$+C_6H_{12}N_4O$	R	Double coupling
157,96901	2,6-Dichlorobenzyl	di-Cl-Bzl	$-H+C_7H_5Cl_2$	Y	Fmoc/Boc
163,06333	Tyr->YY		$+C_9H_9NO_2$	Y	Double coupling
164,08373	1-(4,4-Dimethyl-2,6-dioxo-cyclohexylidene)-ethyl	Dde	$-H+C_{10}H_{13}O_2$	K	Fmoc
166,00146	2,4-Dinitrophenyl	Dnp	$-H+C_6H_3N_2O_4$	H	Boc
167,99781	2-Chlorobenzyloxycarbonyl	2-Cl-Z	$-H+C_8H_6ClO_2$	K	Fmoc/Boc
180,05752	Xanthyl	Xan	$-H+C_{13}H_9O$	NQ	Boc
180,07864	2,4,6-Trimethoxybenzyl	Tmob	$-H+C_{10}H_{13}O_3$	N	Fmoc
182,04015	Mesitylene-2-sulfonyl	Mts	$-H+C_9H_{11}O_2S$	R	Fmoc
182,04015	Mesitylene-2-sulfonyl	Mts	$-H+C_9H_{11}O_2S$	RW	Boc
186,07931	Trp->WW		$+C_{11}H_{10}N_2O$	W	Double coupling
206,13068	1-(4,4-Dimethyl-2,6-dioxo-cyclohexylidene)-3-methylbutyl	ivDde	$-H+C_{13}H_{19}O_2$	K	Fmoc
211,94729	2-Bromobenzyloxycarbonyl	2-Br-Z	$-H+C_8H_6BrO_2$	Y	Boc
212,05072	4-Methoxy-2,3,6-trimethyl-benzenesulfonyl	Mtr	$-H+C_{10}H_{13}O_3S$	R	Fmoc/Boc
222,06808	Fluorenylmethoxycarbonyl	Fmoc	$-H+C_{15}H_{11}O_2$	all Amino acids	Fmoc
226,07760	Biotinylation		$+C_{10}H_{14}N_2S_1O_2$	K	Chemical Modification
226,09938	4,4'-Dimethoxybenzhydryl	Mbh	$-H+C_{15}H_{15}O_2$	NQ	Fmoc
242,10955	Trityl	Trt	$-H+C_{19}H_{15}$	CHNQST	Fmoc
242,10955	Trityl	Trt	$-H+C_{19}H_{15}$	CHNQ	Boc
252,08202	2,2,4,6,7-Pentamethyl-dihydrobenzofurane-5-sulfonyl	Pbf	$-H+C_{13}H_{17}O_3S$	R	Fmoc
256,12520	4-Methyltrityl	Mtt	$-H+C_{20}H_{17}$	HK	Fmoc
266,09767	2,2,5,7,8-Pentamethyl-chromane-6-sulfonyl	Pmc	$-H+C_{14}H_{19}O_2S$	R	Fmoc
272,12012	4-Methoxytrityl	Mmt	$-H+C_{20}H_{17}O$	C	Fmoc
276,07058	2-Chlorotrityl	2-Cl-Trt	$-H+C_{19}H_{14}Cl$	Y	Fmoc
327,18344	4(N-[1-(4,4-Dimethyl-2,6-dioxo-cyclohexylidene)-3-methylbutyl]-amino)benzyloxy	ODmab	$-H+C_{20}H_{26}NO_3$	DE	Fmoc
388,08211	Fluorescein		$+C_{22}H_{14}N_1O_6$	C	Chemical Modification
421,07324	Fluoresceinisothiocyanat	FITC	$+C_{21}S_1H_{15}N_3O_5$	CKRS	Chemical Modification
431,26920	Biotinylation		$-H+C_{20}H_{40}N_4O_4S$	K	Chemical Modification
672,29816	CyDye-Cy3		$+C_{37}H_{44}N_4S_1O_6$	C	Chemical Modification

Peptide Fragmentation

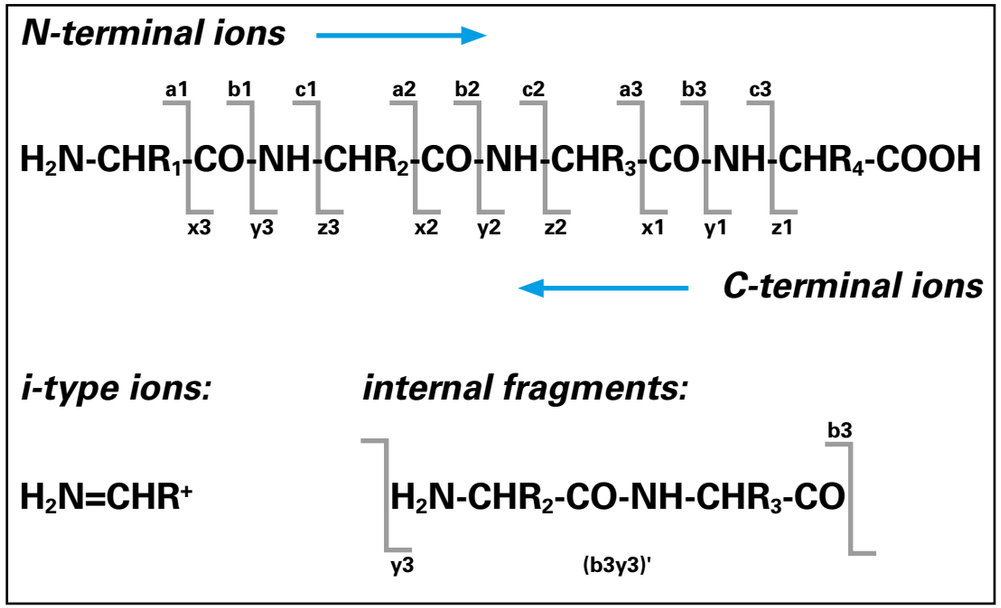

Typical fragment ions observed

- Low energy CID: b and y
- PSD: a, b, y and i, including neutral losses of NH_3 from a and b
- ISD: c and y
- ECD-FTICR: c and z

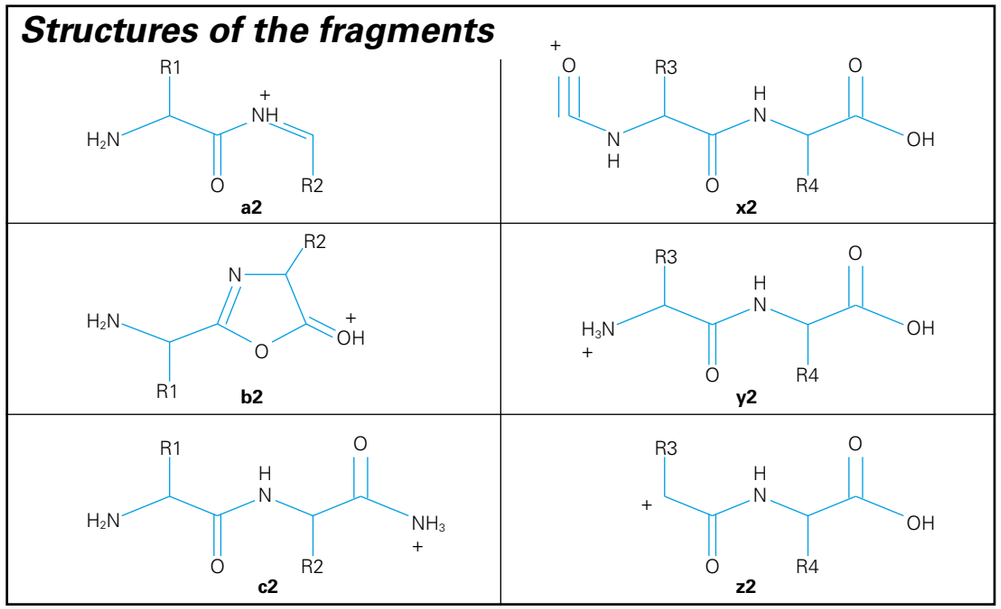

Molecular Weights of Amino Acid Residues

Amino Acid Structure	Name	Symbol	1 Letter Code	Elemental Composition (Residue)	Monoisotopic Mass (Residue)	Averaged Mass (Residue)
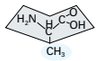	Alanine	Ala	A	C_3H_5NO	71.03712	71.08
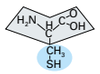	Cysteine	Cys	C	C_3H_5NOS	103.00919	103.15
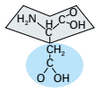	Aspartic acid	Asp	D	$C_4H_5NO_3$	115.02695	115.09
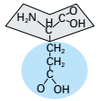	Glutamic acid	Glu	E	$C_5H_7NO_3$	129.0426	129.12
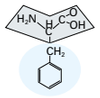	Phenylanaline	Phe	F	C_9H_9NO	147.06842	147.18
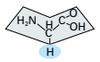	Glycine	Gly	G	C_2H_3NO	57.02146	57.05
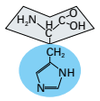	Histidine	His	H	$C_6H_7N_3O$	137.05891	137.14
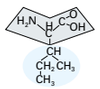	Isoleucine	Ile	I	$C_6H_{11}NO$	113.08407	113.16
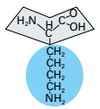	Lysine	Lys	K	$C_6H_{12}N_2O$	128.09497	128.17
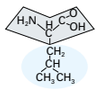	Leucine	Leu	L	$C_6H_{11}NO$	113.08407	113.16

Masses of Terminal Groups

C-Terminal Groups	Composition	Monoisotopic Mass	Averaged Mass
Free Acid	OH	17.00274	17.00735
Amide	NH_2	16.01872	16.02262

Amino Acid Structure	Name	Symbol	1 Letter Code	Elemental Composition (Residue)	Monoisotopic Mass (Residue)	Averaged Mass (Residue)
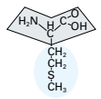	Methionine	Met	M	C_5H_9NOS	131.04049	131.20
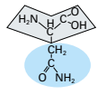	Asparagine	Asn	N	$C_4H_6N_2O_2$	114.04293	114.10
	Proline	Pro	P	C_5H_7NO	97.05277	97.12
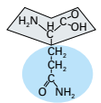	Glutamine	Gln	Q	$C_5H_8N_2O_2$	128.05858	128.13
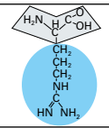	Arginine	Arg	R	$C_6H_{12}N_4O$	156.10112	156.19
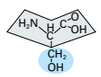	Serine	Ser	S	$C_3H_5NO_2$	87.03203	87.08
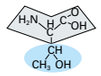	Threonine	Thr	T	$C_4H_7NO_2$	101.04768	101.11
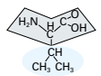	Valine	Val	V	C_5H_9NO	99.06842	99.13
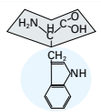	Tryptophan	Trp	W	$C_{11}H_{10}N_2O$	186.07932	186.21
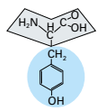	Tyrosine	Tyr	Y	$C_9H_9NO_2$	163.06333	163.18

N-Terminal Groups	Composition	Monoisotopic Mass	Averaged Mass
Hydrogen	H	1.00783	1.0079
N-Formyl	HCO	29.00274	29.01808
N-Acetyl	CH_3CO	43.01839	43.04447

Amino Acid Calculator Table

Residues Sorted by Molecular Weight

Sums and Differences of 2 Amino Acid Residues Residue Mass Differences

		G	A	S	P	V	T	C	I	L
		57.05203	**71.07902**	**87.07832**	**97.11704**	**99.13299**	**101.10531**	**103.14344**	**113.15998**	**113.15998**
G	**57.05203**	114.10406	14.02699	30.02629	40.06501	42.08097	44.05328	46.09141	56.10795	56.10795
A	**71.07902**	128.13105	**142.15804**	15.99931	26.03803	28.05398	30.02629	32.06442	42.08097	42.08097
S	**87.07832**	144.13035	158.15734	**174.15665**	10.03872	12.05467	14.02699	16.06512	26.08166	26.08166
P	**97.11704**	154.16907	168.19606	184.19537	**194.23409**	2.01595	3.98827	6.02640	16.04294	16.04294
V	**99.13299**	156.18502	170.21201	186.21132	196.25004	**198.26599**	1.97232	4.01045	14.02699	14.02699
T	**101.10531**	158.15734	172.18433	188.18363	198.22235	200.23831	**202.21062**	2.03813	12.05467	12.05467
C	**103.14344**	160.19547	174.22246	190.22176	200.26048	202.27644	204.24875	**206.28688**	10.01654	10.01654
I	**113.15998**	170.21201	184.23900	200.23831	210.27703	212.29298	214.26529	216.30342	**226.31997**	0.00000
L	**113.15998**	170.21201	184.23900	200.23831	210.27703	212.29298	214.26529	216.30342	226.31997	**226.31997**
N	114.10406	171.15609	185.18308	201.18238	211.22110	213.23705	215.20937	217.24750	227.26404	227.26404
D	**115.08866**	172.14069	186.16768	202.16699	212.20571	214.22166	216.19398	218.23211	228.24865	228.24865
Q	128.13105	185.18308	199.21006	215.20937	225.24809	227.26404	229.23636	231.27449	241.29103	241.29103
K	**128.17468**	185.22671	199.25370	215.25300	225.29172	227.30768	229.27999	231.31812	241.33466	241.33466
E	**129.11565**	186.16768	200.19467	216.19398	226.23270	228.24865	230.22096	232.25909	242.27564	242.27564
M	**131.19742**	188.24945	202.27644	218.27574	228.31446	230.33041	232.30273	234.34086	244.35740	244.35740
H	**137.14152**	194.19355	208.22054	224.21985	234.25857	236.27452	238.24684	240.28497	250.30151	250.30151
F	**147.17714**	204.22917	218.25616	234.25546	244.29418	246.31014	248.28245	250.32058	260.33712	260.33712
R	156.18813	213.24016	227.26714	243.26645	253.30517	255.32112	257.29344	259.33157	269.34811	269.34811
Y	**163.17645**	220.22848	234.25546	250.25477	260.29349	262.30944	264.28176	266.31989	276.33643	276.33643
W	186.21391	243.26594	257.29293	273.29224	283.33096	285.34691	287.31922	289.35735	299.37390	299.37390

Amino Acid Calculator Table

N	**D**	**Q**	**K**	**E**	**M**	**H**	**F**	**R**	**Y**	**W**
114.10406	**115.08866**	**128.13105**	**128.17468**	**129.11565**	**131.19742**	**137.14152**	**147.17714**	**156.18813**	**163.17645**	**186.21391**
57.05203	58.03664	71.07902	71.12265	72.06362	74.14539	80.08950	90.12511	99.13610	106.12442	129.16188
43.02504	44.00965	57.05203	57.09566	58.03664	60.11840	66.06251	76.09812	85.10911	92.09743	115.13490
27.02574	28.01034	41.05272	41.09636	42.03733	44.11910	50.06320	60.09882	69.10980	76.09812	99.13559
16.98702	17.97162	31.01400	31.05764	31.99861	34.08038	40.02448	50.06010	59.07108	66.05940	89.09687
14.97106	15.95567	28.99805	29.04169	29.98266	32.06442	38.00853	48.04415	57.05513	64.04345	87.08092
12.99875	13.98335	27.02574	27.06937	28.01034	30.09211	36.03621	46.07183	55.08282	62.07113	85.10860
10.96062	11.94522	24.98761	25.03124	25.97221	28.05398	33.99808	44.03370	53.04469	60.03301	83.07047
0.94407	1.92868	14.97106	15.01470	15.95567	18.03744	23.98154	34.01716	43.02814	50.01646	73.05393
0.94407	1.92868	14.97106	15.01470	15.95567	18.03744	23.98154	34.01716	43.02814	50.01646	73.05393
228.20812	0.98461	14.02699	14.07062	15.01160	17.09336	23.03747	33.07308	42.08407	49.07239	72.10985
229.19272	**230.17733**	13.04238	13.08602	14.02699	16.10875	22.05286	32.08848	41.09946	48.08778	71.12525
242.23510	243.21971	**256.26209**	0.04364	0.98461	3.06637	9.01048	19.04609	28.05708	35.04540	58.08287
242.27874	243.26335	256.30573	**256.34936**	0.94097	3.02274	8.96684	19.00246	28.01345	35.00176	58.03923
243.21971	244.20432	257.24670	257.29033	**258.23131**	2.08177	8.02587	18.06149	27.07247	34.06079	57.09826
245.30148	246.28608	259.32846	259.37210	260.31307	**262.39484**	5.94411	15.97972	24.99071	31.97903	55.01649
251.24558	252.23019	265.27257	265.31621	266.25718	268.33894	**274.28305**	10.03562	19.04660	26.03492	49.07239
261.28120	262.26581	275.30819	275.35182	276.29279	278.37456	284.31867	**294.35428**	9.01099	15.99931	39.03677
270.29219	271.27679	284.31917	284.36281	285.30378	287.38555	293.32965	303.36527	**312.37625**	6.98832	30.02579
277.28050	278.26511	291.30749	291.35113	292.29210	294.37386	300.31797	310.35359	319.36457	**326.35289**	23.03747
300.31797	301.30258	314.34496	314.38859	315.32957	317.41133	323.35544	333.39105	342.40204	349.39036	**372.42783**

Sum of 2 Residues

isobaric and close-to-isobaric mass differences are color coded
isobaric and close-to-isobaric substitutions by 2 residues are color coded

Matrices

Matrix name	Elemental Composition	Structure	MH_{mono}^{+} [Th]	Average Mass	Order No.
2,3,4-Trihydroxyacetophenone (2,3,4-THAP), 1 g	$C_8H_8O_4$	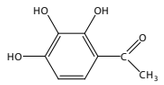	169,04953	168,15	**206148**
2,4,6-Trihydroxyacetophenone (2,4,6-THAP), 1 g	$C_8H_8O_4 \bullet H_2O$	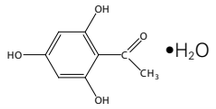	169,04953	186,16	**206154**
2,5-Dihydroxyacetophenon (2,5-DHAP), 1 g	$C_8H_8O_3$	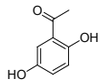	153,05462	152,20	**231829**
2,5-Dihydroxybenzoic acid (2,5-DHB), 1 g 2,5-Dihydroxybenzoic acid (2,5-DHB), 5 g	$C_7H_6O_4$	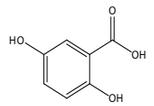	155,03388	154,12	**201346** **203074**
3-Hydroxypicolinic acid (3-HPA), 1 g 3-Hydroxypicolinic acid (3-HPA), 5 g	$C_6H_5NO_3$	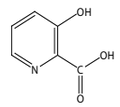	140,03422	139,11	**201224** **203070**
α-Cyano-4-hydroxycinnamic acid ester (CNME), 1 g	$C_{11}H_9NO_3$	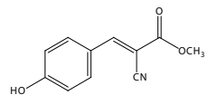	204,06552	203,19	**201225**
α-Cyano-4-hydroxycinnamic acid (HCCA), 1 g α-Cyano-4-hydroxycinnamic acid (HCCA), 5 g α-Cyano-4-hydroxycinnamic acid (HCCA), portioned, 10 tubes	$C_{10}H_7NO_3$	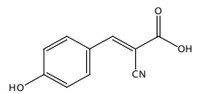	190,04987	189,17	**201344** **203072** **255344**
Dithranol (DIT), 1 g	$C_{14}H_{10}O_3$	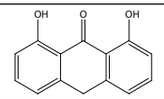	227,07027	226,23	**209783**
SDHB, 5 g	$C_7H_6O_4$ $C_8H_8O_4$	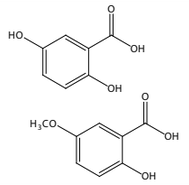		154,12 168,15	**209813**
Sinapinic acid (SA), 1 g Sinapinic acid (SA), 5 g	$C_{11}H_{12}O_5$	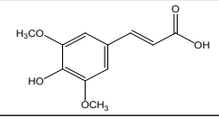	225,07575	224,22	**201345** **203073**
trans-Indole-3-acrylic acid (IAA), 1 g	$C_{11}H_9NO_2$	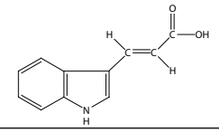	188,07060	187,20	**209803**
Peptide / Protein Matrix Kit	HCCA, 2,5-DHB and SA				**205931**

Bruker Matrix Selection Guide

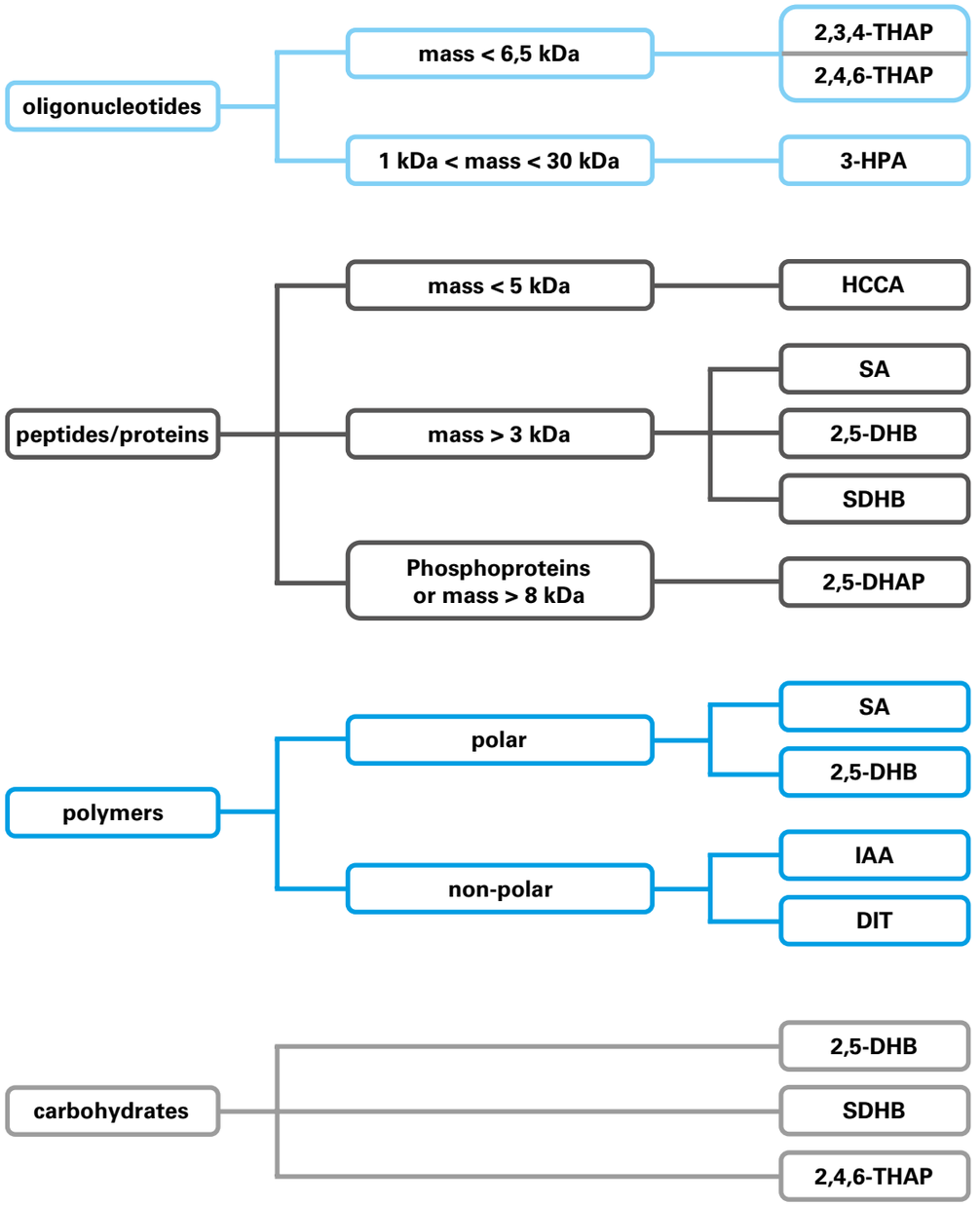

Please see page 74 for matrices details.

Molecular Weights

Molecular Weights of Selected Glycan Residues

Residue Name	Symbol	Elemental Composition	Monoisotopic Mass	Average Mass
Deoxyribose	dRib	$C_5H_8O_3$	116,04734	116,12
Arabinose	Ara	$C_5H_8O_4$	132,04226	132,11
Ribose	Rib	$C_5H_8O_4$	132,04226	132,11
Xylose	Xyl	$C_5H_8O_4$	132,04226	132,11
Fucose	Fuc	$C_6H_{10}O_4$	146,05791	146,14
Galactosamine	GalN	$C_6H_{11}NO_4$	161,06881	161,16
Glucosamin	GlcN	$C_6H_{11}NO_4$	161,06881	161,16
Galactose	Gal	$C_6H_{10}O_5$	162,05282	162,14
Glucose	Glc	$C_6H_{10}O_5$	162,05282	162,14
Mannose	Man	$C_6H_{10}O_5$	162,05282	162,14
Glucuronic acid	GlcA	$C_6H_8O_6$	176,03209	176,13
N-acetylgalactosamin	GalNAc	$C_8H_{13}NO_5$	203,07937	203,20
N-acetylglucosamin	GlcNAc	$C_8H_{13}NO_5$	203,07937	203,20
Muramic acid	Mur	$C_{11}H_{17}NO_7$	275,10050	275,26
N-acetylneuraminic acid	NANA	$C_{11}H_{17}NO_8$	291,09542	291,26

Molecular Weights of Nucleotide Residues (compatible to BioTools 3.2)

Nucleotide Residue	Elemental Composition	Monoisotopic Mass	Averaged Mass
AMP	$C_{10}H_{12}N_5O_6P$	329,05252	329,21
GMP	$C_{10}H_{12}N_5O_7P$	345,04744	345,21
UMP	$C_9H_{11}N_2O_8P$	306,02530	306,17
CMP	$C_9H_{12}N_3O_7P$	305,04129	305,18
dAMP	$C_{10}H_{12}N_5O_5P$	313,05761	313,21
dGMP	$C_{10}H_{12}N_5O_6P$	329,05252	329,21
dTMP	$C_{10}H_{13}N_2O_7P$	304,04604	304,20
dCMP	$C_9H_{12}N_3O_6P$	289,04637	289,18
Hypoxanthine	$C_{10}H_{11}N_4O_6P$	314,04162	314,19
7-deaza-dGMP	$C_{11}H_{13}N_4O_6P$	328,05727	328,22
7-deaza-dAMP	$C_{11}H_{13}N_4O_5P$	312,06236	312,22
2-amino-purine	$C_{10}H_{12}N_5O_5P$	313,05761	313,21
dAMP-thioCH3	$C_{11}H_{14}N_5O_4SP$	343,05041	343,30
dGMP-thioCH3	$C_{11}H_{14}N_5O_5SP$	359,04533	359,30
dTMP-thioCH3	$C_{11}H_{15}N_2O_6SP$	334,03885	334,29
dCMP-thioCH3	$C_{10}H_{14}N_3O_5SP$	319,03918	319,28
ddCMP	$C_9H_{12}N_3O_5P$	273,05146	273,19
ddAMP	$C_{10}H_{12}N_5O_4P$	297,06269	297,21
ddTMP	$C_{10}H_{13}N_2O_6P$	288,05112	288,20
ddGMP	$C_{10}H_{12}N_5O_5P$	313,05761	313,21

Conversion Factors for Important Physical Units

Energy Equivalents

	Joule	Hertz	cm^{-1}	Kelvin	eV
Joule	1	1.5091905 E+33	5.03411762 E+22	7.242964 E+22	6.24150974 E+18
Hertz	6.62606876 E–34	1	3.335640952 E–11	4.7992374 E–11	4.13566727 E–15
cm^{-1}	1.98644544 E–23	2.99792458 E+10	1	1.4387752	1.239841857 E–04
Kelvin	1.3806503 E–23	2.0836644 E+10	0.6950356	1	8.6173432 E–05
eV	1.602176462 E–19	2.417989491 E+14	8.06554477 E+03	1.1604506 E+04	1

based on the Fundamental constants with $E = mc^2 = hc/\lambda = h\nu = kT$ and 1 eV = (e/C) J

Force Units: SI unit = Newton (N), cgs unit = dyne, Weight = mass×g_n

	N	p (pond)	kp	dyne
N	1	101.9716	0.1019716	1.0 E+05
p	0.00980665	1	1.00 E–03	980.665
kp	9.80665	1000	1	980665
dyne	1.0 E–05	1.019716 E–03	1.019716 E–06	1

Energy and Work Units: SI unit = Joule (J), cgs unit: 1 erg = 10^{-7} Joule

	J = N m	kp m	kWh	kcal	BTU	eV
J	1	0.101972	2.777778 E–07	2.390057 E–04	9.478134 E–04	6.241512 E+18
kp m	9.80665	1	2.724069 E–06	2.343846 E–03	9.294874 E–03	6.120832 E+19
kWh	3.600 E+06	3.670978 E+05	1	860.4207	3412.128	2.246944 E+25
kcal	4184	426.6493	1.162222 E–03	1	3.965651	2.611448 E+22
BTU	1055.06	1.075862 E+02	2.930722 E–01	2.521654 E–01	1	6.585169 E+21
eV	1.602176 E–19	1.633765 E–20	4.450489 E–26	3.829293 E–23	1.518564 E–22	1

Power Units: SI unit = Watt (W)

	W = J s^{-1}	kW	kpm/s	PS	cal/s	kcal/h
W	1	1.0 E–03	0.1019716	1.341022 E–03	0.2390057	0.8604207
kW	1.0 E+03	1	101.9716	1.341022	239.0057	860.4207
kpm/s	9.80665	9.80665 E–03	1	1.315093 E–02	2.343846	8.437844
PS	745.7	0.7457	76.04024	1	178.2266	641.6157
cal/s	4.184	4.184 E–03	0.4266493	5.610835 E–03	1	3.6
kcal/h	1.162222	1.162222 E–03	0.1185137	1.558565 E–03	0.2777778	1

Pressure Units: SI unit = Pascal

	Pa = N/m^2	kp/m^2	atm	bar	Torr = mmHg	at = kp/cm^2
Pa = N/m^2	1	0.1019716	9.86923 E–06	1.0 E–05	7.500617 E–03	1.019716 E–05
kp/m^2	9.80665	1	9.67841 E–05	9.80665 E–05	7.355592 E–02	1.0 E–04
atm	1.01325 E+05	1.033227 E+04	1	1.01325	760	1.033227
bar	1.0 E+05	1.019716 E+04	0.9869233	1	750.0617	1.019716
Torr	133.3224	13.59510	1.315789 E–03	1.333224 E–03	1	1.359510 E–03
at = kp/cm^2	9.80665 E+04	1.0 E+04	0.9678411	9.800665 E–01	735.5592	1

Time Units: SI unit = second

	s	min	h	d	week	year
s	1	1.666667 E–02	2.777778 E–04	1.157407 E–05	1.653439 E–06	3.168874 E–08
min	60	1	1.666667 E–02	6.944444 E–04	9.920635 E–05	1.901324 E–06
h	3600	60	1	4.166667 E–02	5.952381 E–03	1.140795 E–04
d	86400	1440	24	1	1.428571 E–01	2.737907 E–03
week	604800	10080	168	7	1	1.916535 E–02
year	31556952	525949.2	8765.82	365.2425	52.1775	1

Temperature Conversion: SI unit = Kelvin

	Kelvin (K)	Centigrade (°C)	Fahrenheit (°F)	Rankine (°R)
K	1	$T_C = T_K - 273.15$	$T_F = (9/5)T_K - 459.67$	$T_R = (9/5)T_K$
°C	$T_K = T_C + 273.15$	1	$T_F = (9/5)T_C + 32$	$T_R = (9/5)(T_C + 273.15)$
°F	$T_K = (5/9)(T_F + 459.67)$	$T_C = (5/9)(T_F - 32)$	1	$T_R = T_F + 459.67$
°R	$T_K = (9/5)T_R$	$T_C = (5/9)T_R - 273.15$	$T_F = T_R - 459.67$	1

IUPAC Periodic Table of Elements

BRUKER

1 (IA)	2 (IIA)	3 (IIIB)	4 (IVB)	5 (VB)	6 (VIB)	7 (VIIB)	8 (VIII)	9 (VIII)	10 (VIII)	11 (IB)	12 (IIB)	13 (IIIA)	14 (IVA)	15 (VA)	16 (VIA)	17 (VIIA)	18 (VIIIA)
Hydrogen																	**Helium**
$^{1}H_{1}$ -259.34° -252.87° -240.18° +1-1 1.00794 91.0%																	$^{2}He_{2}$ -272.2° -268.93° -267.96° 0 4.002602 8.9%
Lithium	**Beryllium**											**Boron**	**Carbon**	**Nitrogen**	**Oxygen**	**Fluorine**	**Neon**
$^{2}_{1}Li_{3}$ 180.5° 1342° +1 6.941 $1.86\cdot10^{-7}$%	$^{2}_{2}Be_{4}$ 1287° 2471° +2 9.012182 $2.38\cdot10^{-9}$%											$^{2}_{3}B_{5}$ 2075° 4000° +3 10.811 $6.9\cdot10^{-8}$%	$^{2}_{4}C_{6}$ 4492† 3642s +2+4-4 12.0107 0.033%	$^{2}_{5}N_{7}$ -210.00° -195.79° -146.94° ±1±2±3+4+5 14.0067 0.0102%	$^{2}_{6}O_{8}$ -218.79° -182.95° -118.56° -2 15.9994 0.078%	$^{2}_{7}F_{9}$ -219.62° -188.12° -129.02° -1 18.9984032 $2.7\cdot10^{-6}$%	$^{2}_{8}Ne_{10}$ -248.59° -246.08° -228.7° 0 20.1797 0.0112%
Sodium	**Magnesium**											**Aluminum**	**Silicon**	**Phosphorus**	**Sulfur**	**Chlorine**	**Argon**
$^{2}_{8}_{1}Na_{11}$ 97.80° 883° +1 22.98976928 0.000187%	$^{2}_{8}_{2}Mg_{12}$ 650° 1090° +2 24.3050 0.00350%											$^{2}_{8}_{3}Al_{13}$ 660.32° 2519° +3 26.9815386 0.000277%	$^{2}_{8}_{4}Si_{14}$ 1414° 3265° +2+4-4 28.0855 0.00326%	$^{2}_{8}_{5}P_{15}$ 44.15° 280.5° 721° +3+5-3 30.973762 0.000034%	$^{2}_{8}_{6}S_{16}$ 115.21° 444.60° 1041° +4+6-2 32.065 0.00168%	$^{2}_{8}_{7}Cl_{17}$ -101.5° -34.04° 143.8° +1+5+7-1 35.453 0.000017%	$^{2}_{8}_{8}Ar_{18}$ -189.35° -185.85° -122.28° 0 39.948 0.000329%
Potassium	**Calcium**	**Scandium**	**Titanium**	**Vanadium**	**Chromium**	**Manganese**	**Iron**	**Cobalt**	**Nickel**	**Copper**	**Zinc**	**Gallium**	**Germanium**	**Arsenic**	**Selenium**	**Bromine**	**Krypton**
$^{2}_{8}_{8}_{1}K_{19}$ 63.38° 759° +1 39.0983 0.0000123%	$^{2}_{8}_{8}_{2}Ca_{20}$ 842° 1484° +2 40.078 0.000199%	$^{2}_{8}_{9}_{2}Sc_{21}$ 1541° 2836° +3 44.955912 $1.12\cdot10^{-7}$%	$^{2}_{8}_{10}_{2}Ti_{22}$ 1668° 3287° +2+3+4 47.867 $7.8\cdot10^{-6}$%	$^{2}_{8}_{11}_{2}V_{23}$ 1910° 3407° +2+3+4+5 50.9415 $9.6\cdot10^{-7}$%	$^{2}_{8}_{13}_{1}Cr_{24}$ 1907° 2671° +2+3+6 51.9961 0.000044%	$^{2}_{8}_{13}_{2}Mn_{25}$ 1246° 2061° +2+3+4+7 54.938045 0.000031%	$^{2}_{8}_{14}_{2}Fe_{26}$ 1538° 2861° +2+3 55.845 0.00294%	$^{2}_{8}_{15}_{2}Co_{27}$ 1495° 2927° +2+3 58.933195 $7.3\cdot10^{-6}$%	$^{2}_{8}_{16}_{2}Ni_{28}$ 1455° 2913° +2+3 58.6934 0.000161%	$^{2}_{8}_{18}_{1}Cu_{29}$ 1084.62° 2562° +1+2 63.546 $1.70\cdot10^{-6}$%	$^{2}_{8}_{18}_{2}Zn_{30}$ 419.53° 907° +2 65.38 $4.11\cdot10^{-6}$%	$^{2}_{8}_{18}_{3}Ga_{31}$ 29.76° 2204° +3 69.723 $1.23\cdot10^{-7}$%	$^{2}_{8}_{18}_{4}Ge_{32}$ 938.25° 2833° +2+4 72.64 $3.9\cdot10^{-7}$%	$^{2}_{8}_{18}_{5}As_{33}$ 817c 614s° 1400° +3+5-3 74.92160 $2.1\cdot10^{-8}$%	$^{2}_{8}_{18}_{6}Se_{34}$ 221° 685° 1493° +4+6-2 78.96 $2.03\cdot10^{-7}$%	$^{2}_{8}_{18}_{7}Br_{35}$ -7.2° 58.8° 315° +1+5-1 79.904 $3.8\cdot10^{-8}$%	$^{2}_{8}_{18}_{8}Kr_{36}$ -157.36° -153.22° -63.74° 0 83.798 $1.5\cdot10^{-7}$%
Rubidium	**Strontium**	**Yttrium**	**Zirconium**	**Niobium**	**Molybdenum**	**Technetium**	**Ruthenium**	**Rhodium**	**Palladium**	**Silver**	**Cadmium**	**Indium**	**Tin**	**Antimony**	**Tellurium**	**Iodine**	**Xenon**
$^{2}_{8}_{18}_{8}_{1}Rb_{37}$ 39.31° 688° +1 85.4678 $2.31\cdot10^{-8}$%	$^{2}_{8}_{18}_{8}_{2}Sr_{38}$ 777° 1382° +2 87.62 $7.7\cdot10^{-8}$%	$^{2}_{8}_{18}_{9}_{2}Y_{39}$ 1522° 3345° +3 88.90585 $1.51\cdot10^{-8}$%	$^{2}_{8}_{18}_{10}_{2}Zr_{40}$ 1855° 4409° +4 91.224 $3.72\cdot10^{-8}$%	$^{2}_{8}_{18}_{12}_{1}Nb_{41}$ 2477° 4744° +3+5 92.90638 $2.28\cdot10^{-9}$%	$^{2}_{8}_{18}_{13}_{1}Mo_{42}$ 2623° 4639° +6 95.96 $8.3\cdot10^{-9}$%	$^{2}_{8}_{18}_{13}_{2}Tc_{43}$ 2157° 4265° +4+6+7 [98]	$^{2}_{8}_{18}_{15}_{1}Ru_{44}$ 2334° 4150° +3 101.07 $6.1\cdot10^{-9}$%	$^{2}_{8}_{18}_{16}_{1}Rh_{45}$ 1964° 3695° +3 102.90550 $1.12\cdot10^{-9}$%	$^{2}_{8}_{18}_{18}_{0}Pd_{46}$ 1554.9° 2963° +2+4 106.42 $4.5\cdot10^{-9}$%	$^{2}_{8}_{18}_{18}_{1}Ag_{47}$ 961.78° 2162° +1 107.8682 $1.58\cdot10^{-9}$%	$^{2}_{8}_{18}_{18}_{2}Cd_{48}$ 321.07° 767° +2 112.411 $5.3\cdot10^{-9}$%	$^{2}_{8}_{18}_{18}_{3}In_{49}$ 156.60° 2072° +3 114.818 $6.0\cdot10^{-10}$%	$^{2}_{8}_{18}_{18}_{4}Sn_{50}$ 231.93° 2602° +2+4 118.710 $1.25\cdot10^{-8}$%	$^{2}_{8}_{18}_{18}_{5}Sb_{51}$ 630.63° 1587° +3+5-3 121.760 $1.01\cdot10^{-9}$%	$^{2}_{8}_{18}_{18}_{6}Te_{52}$ 449.51° 988° +4+6-2 127.60 $1.57\cdot10^{-8}$%	$^{2}_{8}_{18}_{18}_{7}I_{53}$ 113.7° 184.4° 546° +1+5+7-1 126.90447 $2.9\cdot10^{-9}$%	$^{2}_{8}_{18}_{18}_{8}Xe_{54}$ -111.75° -108.04° 16.58° 0 131.293 $1.5\cdot10^{-8}$%
Cesium	**Barium**	**Lanthanum**	**Hafnium**	**Tantalum**	**Tungsten**	**Rhenium**	**Osmium**	**Iridium**	**Platinum**	**Gold**	**Mercury**	**Thallium**	**Lead**	**Bismuth**	**Polonium**	**Astatine**	**Radon**
$^{2}_{8}_{18}_{18}_{8}_{1}Cs_{55}$ 28.44° 671° +1 132.9054519 $1.21\cdot10^{-9}$%	$^{2}_{8}_{18}_{18}_{8}_{2}Ba_{56}$ 727° 1897° +2 137.327 $1.46\cdot10^{-8}$%	$^{2}_{8}_{18}_{18}_{9}_{2}La_{57}$ † 918° 3464° +3 138.90547 $1.45\cdot10^{-9}$%	$^{2}_{8}_{18}_{32}_{10}_{2}Hf_{72}$ 2233° 4603° +4 178.49 $5.02\cdot10^{-10}$%	$^{2}_{8}_{18}_{32}_{11}_{2}Ta_{73}$ 3017° 5458° +5 180.94788 $6.75\cdot10^{-11}$%	$^{2}_{8}_{18}_{32}_{12}_{2}W_{74}$ 3422° 5555° +6 183.84 $4.34\cdot10^{-10}$%	$^{2}_{8}_{18}_{32}_{13}_{2}Re_{75}$ 3186° 5596° +4+6+7 186.207 $1.69\cdot10^{-10}$%	$^{2}_{8}_{18}_{32}_{14}_{2}Os_{76}$ 3033° 5012° +3+4 190.23 $2.20\cdot10^{-9}$%	$^{2}_{8}_{18}_{32}_{15}_{2}Ir_{77}$ 2446° 4428° +3+4 192.217 $2.16\cdot10^{-9}$%	$^{2}_{8}_{18}_{32}_{16}_{2}Pt_{78}$ 1768.4° 3825° +2+4 195.084 $4.4\cdot10^{-9}$%	$^{2}_{8}_{18}_{32}_{17}_{1}Au_{79}$ 1064.18° 2856° +1+3 196.966569 $6.1\cdot10^{-10}$%	$^{2}_{8}_{18}_{32}_{18}_{2}Hg_{80}$ -38.83° 356.73° 1477° +1+2 200.59 $1.11\cdot10^{-9}$%	$^{2}_{8}_{18}_{32}_{18}_{3}Tl_{81}$ 304° 1473° +1+3 204.3833 $6.0\cdot10^{-10}$%	$^{2}_{8}_{18}_{32}_{18}_{4}Pb_{82}$ 327.46° 1749° +2+4 207.2 $1.03\cdot10^{-8}$%	$^{2}_{8}_{18}_{32}_{18}_{5}Bi_{83}$ 271.40° 1564° +3+5 208.98040 $4.7\cdot10^{-10}$%	$^{2}_{8}_{18}_{32}_{18}_{6}Po_{84}$ 254° 962° +2+4 [209]	$^{2}_{8}_{18}_{32}_{18}_{7}At_{85}$ 302° [210]	$^{2}_{8}_{18}_{32}_{18}_{8}Rn_{86}$ -71° -61.7° 104° 0 [222]
Francium	**Radium**	**Actinium**	**Rutherfordium**	**Dubnium**	**Seaborgium**	**Bohrium**	**Hassium**	**Meitnerium**	**Darmstadtium**	Roentgenium	Copernicium						
$^{2}_{8}_{18}_{32}_{18}_{8}_{1}Fr_{87}$ 27° +1 [223]	$^{2}_{8}_{18}_{32}_{18}_{8}_{2}Ra_{88}$ 700° +2 [226]	$^{2}_{8}_{18}_{32}_{18}_{9}_{2}Ac_{89}$ ‡ 1051° 3198° +3 [227]	$^{2}_{8}_{18}_{32}_{32}_{10}_{2}Rf_{104}$ +4 [267]	$^{2}_{8}_{18}_{32}_{32}_{11}_{2}Db_{105}$ [268]	$^{2}_{8}_{18}_{32}_{32}_{12}_{2}Sg_{106}$ [271]	$^{2}_{8}_{18}_{32}_{32}_{13}_{2}Bh_{107}$ [272]	$^{2}_{8}_{18}_{32}_{32}_{14}_{2}Hs_{108}$ [277]	$^{2}_{8}_{18}_{32}_{32}_{15}_{2}Mt_{109}$ [276]	$^{2}_{8}_{18}_{32}_{32}_{16}_{2}Ds_{110}$ [281]	$^{2}_{8}_{18}_{32}_{32}_{17}_{2}Rg_{111}$ [280]	$^{2}_{8}_{18}_{32}_{32}_{18}_{2}Cn_{112}$ [285]						

† Lanthanides	Cerium	Praseodymium	Neodymium	Promethium	Samarium	Europium	Gadolinium	Terbium	Dysprosium	Holmium	Erbium	Thulium	Ytterbium	Lutetium
	$^{2}_{8}_{18}_{19}_{9}_{2}Ce_{58}$ 798° 3443° +3+4 140.116 $3.70\cdot10^{-9}$%	$^{2}_{8}_{18}_{21}_{8}_{2}Pr_{59}$ 931° 3520° +3 140.90765 $5.44\cdot10^{-10}$%	$^{2}_{8}_{18}_{22}_{8}_{2}Nd_{60}$ 1021° 3074° +3 144.242 $2.70\cdot10^{-9}$%	$^{2}_{8}_{18}_{23}_{8}_{2}Pm_{61}$ 1042° 3000° +3 [145]	$^{2}_{8}_{18}_{24}_{8}_{2}Sm_{62}$ 1074° 1794° +2+3 150.36 $8.42\cdot10^{-10}$%	$^{2}_{8}_{18}_{25}_{8}_{2}Eu_{63}$ 822° 1596° +2+3 151.964 $3.17\cdot10^{-10}$%	$^{2}_{8}_{18}_{25}_{9}_{2}Gd_{64}$ 1313° 3273° +3 157.25 $1.076\cdot10^{-9}$%	$^{2}_{8}_{18}_{27}_{8}_{2}Tb_{65}$ 1356° 3230° +3 158.92535 $1.97\cdot10^{-10}$%	$^{2}_{8}_{18}_{28}_{8}_{2}Dy_{66}$ 1412° 2567° +3 162.500 $1.286\cdot10^{-9}$%	$^{2}_{8}_{18}_{29}_{8}_{2}Ho_{67}$ 1474° 2700° +3 164.93032 $2.90\cdot10^{-10}$%	$^{2}_{8}_{18}_{30}_{8}_{2}Er_{68}$ 1529° 2868° +3 167.259 $8.18\cdot10^{-10}$%	$^{2}_{8}_{18}_{31}_{8}_{2}Tm_{69}$ 1545° 1950° +3 168.93421 $1.23\cdot10^{-10}$%	$^{2}_{8}_{18}_{32}_{8}_{2}Yb_{70}$ 819° 1196° +2+3 173.054 $8.08\cdot10^{-10}$%	$^{2}_{8}_{18}_{32}_{9}_{2}Lu_{71}$ 1663° 3402° +3 174.9668 $1.197\cdot10^{-10}$%
‡ Actinides	Thorium	Protactinium	Uranium	Neptunium	Plutonium	Americium	Curium	Berkelium	Californium	Einsteinium	Fermium	Mendelevium	Nobelium	Lawrencium
	$^{2}_{8}_{18}_{32}_{18}_{10}_{2}Th_{90}$ 1750° 4788° +4 232.03806 $1.09\cdot10^{-10}$%	$^{2}_{8}_{18}_{32}_{20}_{9}_{2}Pa_{91}$ 1572° +5+4 231.03588	$^{2}_{8}_{18}_{32}_{21}_{9}_{2}U_{92}$ 1135° 4131° +3+4+5+6 238.02891 $2.94\cdot10^{-11}$%	$^{2}_{8}_{18}_{32}_{22}_{9}_{2}Np_{93}$ 644° +3+4+5+6 [237]	$^{2}_{8}_{18}_{32}_{24}_{8}_{2}Pu_{94}$ 640° 3228° +3+4+5+6 [244]	$^{2}_{8}_{18}_{32}_{25}_{8}_{2}Am_{95}$ 1176° 2011° +3+4+5+6 [243]	$^{2}_{8}_{18}_{32}_{25}_{9}_{2}Cm_{96}$ 1345° +3 [247]	$^{2}_{8}_{18}_{32}_{27}_{8}_{2}Bk_{97}$ 1050° +3+4 [247]	$^{2}_{8}_{18}_{32}_{28}_{8}_{2}Cf_{98}$ 900° +3 [251]	$^{2}_{8}_{18}_{32}_{29}_{8}_{2}Es_{99}$ 860° +3 [252]	$^{2}_{8}_{18}_{32}_{30}_{8}_{2}Fm_{100}$ 1527° +3 [257]	$^{2}_{8}_{18}_{32}_{31}_{8}_{2}Md_{101}$ 827° +2+3 [258]	$^{2}_{8}_{18}_{32}_{32}_{8}_{2}No_{102}$ 827° +2+3 [259]	$^{2}_{8}_{18}_{32}_{32}_{9}_{2}Lr_{103}$ 1627° +3 [262]

Group

Element
K E_Z M.P.°
L B.P.°
M C.P.°
N Ox.States
O At.Weight
P Abundance%
Q

Key to Table

Key to Table: The IUPAC Group Numbers 1 to 18 are used (CAS group numbering in parentheses). Information presented: E_Z = element symbol and nuclear charge (protons); melting, boiling, critical point (MP, BP, CP) in °C (sublimation or critical temp. marked with s or t); population of electron levels K - Q; possible oxidation states; **IUPAC mean atomic weights updated 2005** based on terrestrial isotope abundances (^{12}C = 12.0000); for unnatural elements atom. wt. of most abundant isotope is given in brackets; total element abundance (%) in the solar system.

Adapted by W. E. Hull from the Table prepared by Richard B. Firestone (rbf@lbl.gov), Isotopes Project, Lawrence Berkeley National Laboratory; see R. B. Firestone, C. M. Baglin, and S.Y. F. Chu, 1999 Update to the 8th Edition of the *Table of Isotopes*, John Wiley & Sons, (1999); for Atomic Wt. updates see T. B. Coplen, Pure Appl Chem 73 (2001) 667-683 and R. D. Loss, Pure Appl Chem 75 (2003) 1107-1122.

Properties of Selected Nondeuterated Solvents

Solvent	Formula	MW_{ave}	Density d_4^{20} [g/mL]	Viscosity η^{25} [mPa•s, cP]	MP [°C]	BP [°C]	Refrac. Index n_D^{20}	Dielec. Const. ε	Dipole Mom. [D]	Chemical Shift δ_H (ppm)	Chemical Shift δ_C (ppm)
Acetic acid	$C_2H_4O_2$	60.05	1.049	1.13	16.5	118.1	1.3716	6.17	1.7	2.10 11.42	20.8 178.1
Acetone	C_3H_6O	58.08	0.788	0.306	–94.5	56.2	1.3587	20.7	2.8	2.05	30.50 205.4
Acetonitrile	C_2H_3N	41.05	0.784	0.35	–45.2	81.7	1.3441	37.5	3.44	1.93	1.6 117.8
Benzene	C_6H_6	78.11	0.8789	0.604	5.5	80.2	1.5011	2.29	0	7.16	128.5
1-Butanol	$C_4H_{10}O$	74.12	0.8097	2.55	–89.5	117.6	1.3993	17.7	1.70	1.0-1.5 3.5	14, 19 34, 63
2-Butanone (methyl ethyl ketone)	C_4H_8O	72.11	0.805	0.378	–86.7	79.6	1.3788	18.5	2.77	1.1, 2.2 2.5	7, 27.5 35, 207
Carbon disulfide	CS_2	76.14	1.270	0.363	–111.8	46.1	1.628	2.6	0		192.8
Carbon tetrachloride	CCl_4	153.82	1.590	0.908	–22.9	76.7	1.460	2.22	0		96.7
Chloroform	$CHCl_3$	119.38	1.480	0.537	–63.5	61.2	1.4458	4.81	1.08	7.26	77.2
Chloromethane	CH_3Cl	50.49	0.916	0.24	–97.5	–24.1	1.3389	12.6	1.87	3.06	25.6
Cyclohexane	C_6H_{12}	84.16	0.7786	0.894	6.5	80.8	1.4262	2.02	0	1.4	27.6
Cyclopentane	C_5H_{10}	70.13	0.745	0.44	–94.0	49.3	1.4065	1.94	0	1.5	26.5
Dibromomethane	CH_2Br_2	173.84	2.485		–52.7	96.9	1.5419	7.5	1.43	5.0	21.6
o-Dichlorobenzene	$C_6H_4Cl_2$	147.00	1.31	1.324	–17.2	180.3	1.5515	9.9	2.27	7.0-7.4	128-133
1,2-Dichloroethane	$C_2H_4Cl_2$	98.96	1.253	0.79	–35.7	83.4	1.4448	10.4	1.83	3.7	51.7
cis-1,2-Dichloroethylene	$C_2H_2Cl_2$	96.94	1.284		–80.0	60.6	1.4490	9.2	1.90	6.4	119.3
trans-1,2-Dichloroethylene	$C_2H_2Cl_2$	96.94	1.257		–49.8	47.7	1.4462	2.1	0	6.3	121.1
1,1-Dichloroethylene	$C_2H_2Cl_2$	96.94	1.213		–122.6	31.6	1.4254	4.6	1.34	5.5	115.5 128.9
Dichloromethane	CH_2Cl_2	84.93	1.326	0.41	–96.7	39.9	1.424	9.0	1.60	5.31	53.73
Diethylether	$C_4H_{10}O$	74.12	0.713	0.230	–116.3	34.6	1.3526	4.30	1.25	1.2 3.5	17.1 67.4
Diethylene glycol dimethyl ether (diglyme)	$C_6H_{14}O_3$	134.18	0.947	0.989	–64.1	162.0	1.407	7.1		3.3-3.6	59.0 70.5 72
1,2-Dimethoxyethane (glyme)	$C_4H_{10}O_2$	90.12	0.868	0.46	–69 –58	85	1.379	7.20	1.71	3.3 3.5	59 72
Dimethoxymethane	$C_3H_8O_2$	76.10	0.866		–105.2	42.3	1.3563	2.6		3.3 4.4	54.8 97.9
N,N-Dimethylacetamide	$C_4H_9N_O$	87.12	0.9415	2.14	–20	166	1.437	37.8	3.75	2.1 3	21.5 34, 38 169.6
Dimethylcarbonate	$C_3H_6O_3$	90.08	1.069		3	90.5	1.3688			3.65	54.8 156.9
Dimethylether	C_2H_6O	46.07			–139	–24.5				1.3	59.4
N,N-Dimethyl-formamide	C3H7NO	73.10	0.9487	0.92	–60.5	152.9	1.4305	36.7	3.86	2.8 2.9 8.0	30.10 35.2 162.5
Dimethylsulfoxide	C_2H_6OS	78.14	1.100	1.987	18.5	189.5	1.4783	46.7	4.0	2.49	39.50
1,4-Dioxane	$C_4H_8O_2$	88.11	1.034	1.18	11.9	101.2	1.4224	2.25	0.45	3.53	67.30
Ethanol	C_2H_6O	46.07	0.789	1.074	–114.4	78.4	1.3614	24.5	1.69	1.10	17.20 56.70
Ethyl acetate	$C_4H_8O_2$	88.11	0.896	0.426	–83.8	77.1	1.3724	6.0	1.8	1.2 2.0 4.1	14.3 20.7 60.1 170.4
Ethylene carbonate	$C_3H_4O_3$	88.06	1.321	1.93	36.4	244	1.416	89.6	4.91	4.2	65.0 155.8
Ethylene glycol	$C_2H_6O_2$	62.07	1.115	21 (20 °C)	–12.6	197.5	1.431	37.7		3.7	63.4
Formamide	CH_3NO	45.04	1.133	3.3	2.6	210.5	1.4475	110	3.38	7.2 8.1	165.1
Glycerol	$C_3H_8O_3$	92.10	1.26	940	17.9	290.1	1.474	42.5		3.4 3.7	64.5 73.7

Chemical Tables

Properties of Selected Nondeuterated Solvents

Solvent	Formula	MW_{ave}	Density d_4^{20} [g/mL]	Viscosity η^{25} [mPa•s, cP]	MP [°C]	BP [°C]	Refrac. Index n_D^{20}	Dielec. Const. ε	Dipole Mom. [D]	Chemical Shift δ_H (ppm)	Chemical Shift δ_C (ppm)
Hexamethyl-phosphoramide (HMPA)	$C_6H_{18}N_3OP$	179.20	1.027		7.2	233	1.4588	30.6	5.5	2.4 2.6	36.6
Hexane	C_6H_{14}	86.18	0.6594	0.294	–95.4	68.8	1.3749	1.89	0.08		
Methanesulfonic acid	CH_4O_3S	96.11	1.48	10.52	18	168	1.430			2.8	39.6
Methanol	CH_4O	32.04	0.791	0.544	–97.7	64.7	1.3284	32.6	1.70	3.31	49.0
Morpholine	C_4H_9NO	87.12	1.005	2.011	–3.1	128.9	1.4548	7.4	1.58	2.6 3.9	46.8 68.9
Nitromethane	CH_3NO_2	61.04	1.137	0.61	–28.7	100.9	1.3817	35.9	3.46	4.33	62.8
Pentane	C_5H_{12}	72.15	0.626	0.224	–129.7	36.1	1.3575	1.84	0.04		
2-Propanol	C_3H_8O	60.10	0.786	2.1	–87.9	82.4	1.3772	19	1.66	1.2 3.4	25.3 64.0
Pyridine	C_5H_5N	79.10	0.983	0.95	–41.8	115.4	1.510	12.4	2.3	7.21 7.57 8.72	123.5 135.5 149.5
Quinoline	C_9H_7N	129.16	1.098		–14.9	237.7	1.6293	9.0	2.2	7-8.8	121-151
1,1,2,2-Tetrachloroethane	$C_2H_2Cl_4$	167.85	1.60	1.58	–43.5	146.2	1.486	8.2	1.3	6.0	74.0
Tetrachloroethylene	C_2Cl_4	165.83	1.622	0.89	–22.2	121.1	1.504	2.3			120.4
Tetrahydrofuran	C_4H_8O	72.11	0.889	0.46	–108.6	66.0	1.407	7.5	1.68	1.72 3.57	25.26 67.2
Toluene	C_7H_8	92.14	0.867	0.56	–95.0	110.7	1.4969	2.38	0.36	2.09 7.01 7.09	21.3 138.5
Trichloroethylene	C_2HCl_3	131.39	1.465	0.545	–84.7	87.1	1.4767	3.4	0.81	6.4	116.7 124.0
Triethylamine	$C_6H_{15}N$	101.19	0.728	0.363	–114.7	89.2	1.401	2.42	0.87	1.0, 2.5	13, 51
Trifluoroacetic acid	$C_2HF_3O_2$	114.02	1.53	1.14	–15.4	72.5	1.285	42.1	2.26		115.7 163.8
2,2,2-Trifluoroethanol	$C_2H_3F_3O$	100.04	1.384	1.76	–44	74	1.291	8.55	2.52	3.9 5.0	62 126.3
Water	H_2O	18.02	0.9982	0.8909	0.0	100.0	1.3329	80.1	1.85	4.72	
o-Xylene	C_8H_{10}	106.17	0.88	0.76	–25.2	144.5	1.505	2.57	0.5	2.4 6.9	18 125-137

Data were revised 2006 from a variety of sources; density and refractive index are at 20°C, other parameters mainly at 25°C; exceptions occur when the solvent is not liquid at these temperatures; MP and BP are means or best values from the NIST Chem WebBook.

Electronegativities according to Pauling

Main group elements						
H 2.20						
Li 0.98	Be 1.57	B 2.04	C 2.55	N 3.04	O 3.44	F 3.98
Na 0.93	Mg 1.31	Al 1.61	Si 1.90	P 2.19	S 2.58	Cl 3.16
K 0.82	Ca 1.10	Ga 2.01	Ge 2.01	As 2.18	Se 2.55	Br 2.96
Rb 0.82	Sr 0.95	In 1.78	Sn 1.96	Sb 2.05	Tr 2.1	I 2.66
Cs 0.7	Ba 0.9	Tl 1.8	Pb 1.8	Bi 1.9	Po 2.0	At 2.2

d-block elements									
Sc 1.3	Ti 1.5	V 1.6	Cr 1.6	Mn 1.5	Fe 1.8	Co 1.8	Ni 1.8	Cu 1.9	Zn 1.6
Y 1.2	Zr 1.4	Nb 1.6	Mo 1.8	Tc 1.9	Ru 2.2	Rh 2.2	Pd 2.2	Ag 1.9	Cd 1.7
La 1.1	Hf 1.3	Ta 1.5	W 1.7	Re 1.9	Os 2.2	Ir 2.2	Pt 2.2	Au 2.4	Hg 1.9

f-block elements
All 1.1-1.3

Important Abbreviations and Acronyms

A	adenine
AA	anisylacetone
AAO	acetaldehyde oxime
AC	acetate
Ac	acetyl [$CH_3C(0)–$]
acac	acetylacetone
ACTH	adrenocorticotropic hormone (corticotropin)
ADMA	alkyldimethylamine
ADP	adenosine 5′-diphosphate
AIBN	azobis(isobutyronitrile)
Ala	alanine (A)
Am	amyl
AMP	adenosine 5′-monophosphate
AN	acetonitrile
APS	adenosine 5′-phosphosulfate
Ar	aryl
Arg	arginine (R)
Asn	asparagine (N)
Asp	aspartic acid (D)
ATA	anthranilamide
ATP	adenosine 5′-triphosphate
BA	benzyladenine
BaP (BAP)	benzo[*a*]pyrene
BBP	benzyl butyl phthalate
BHC	benzene hexachloride
BHT	2,6-di-*t*-butyl-4-methylphenol
bipy	2,2'-bipyridyl
Bn	benzyl (also Bz, BZL, or Bnz)
BN	benzonitrile
Boc	t-butyloxycarbonyl
BOM	benzyloxymethyl [$PhCH_2OCH_2–$]
BON	*β*-oxynaphthoic acid
BPBG	butyl phthalyl butyl glycolate
Bs	brosylate [$BrC_6H_4SO_2–$]
BSA	*O,N*-bistrimethylsilyl acetamide
BTA	benzoyltrifluoroacetone
Bu	butyl
Bz	benzoyl
C	cytosine
***p* CBA**	*p*-carboxybenzaldehyde
Cbz	carbobenzyloxy [$PhCH_2OC(O)–$]
CD	cyclodextrin
CDP	cytidine 5′-diphosphate
CE	cyanoethyl
CMP	cytidine 5′-monophosphate
CoA	coenzyme A
Cp (or cp)	cyclopentadiene
12-Crown-4	1,4,7,10-tetraoxacyclododecane
CTA	citraconic anhydride
Cys	cysteine (C)
DAA	diacetone acrylamide
DAP	dodecylammonium propionate
DCB	dicyanobenzene
DCEE	dichloroethyl ether
DDD	2,2′-dihydroxy-6,6′-dinaphthyl disulfide
DDH	1,3-dibromo-5,5-dimethylhydantoin
DDM	diphenyldiazomethane
DDT	1,1-bis(*p*-chlorophenyl)-2,2,2-trichloroethane
DEA	*N,N*-diethylaniline or diethyl amine
DEC	diethylaminoethyl chloride hydrochloride
DHA	dehydroacetic acid
DHP	dihydropyran
Diglyme	diethylene glycol dimethyl ether
Diox	dioxane
DMAc	*N,N*-dimethylacetamide
DMAA	*N,N*-dimethylacetoacetamide
DME	1,2-dimethoxyethane (glyme)
DMF	dimethylformamide
DML	dimyristoyl lecithin
DMS	dimethylsiloxane
DMSO	dimethyl sulfoxide
DMSO2	dimethyl sulfone
DMT	dimethyl terephthalate
DNA	deoxyribonucleic acid
DNF	2,4-dinitrofluorobenzene
DOCA	deoxycorticosterone acetate
DPG	2,3-diphosphoglycerate
DPL	dipalmitoyl lecithin
dpm	dipivaloylmethanato
DPPH	diphenylpicrylhydracyl
DST	disuccinimidyl tartrate
DTBN	di-t-butyl nitroxide
E	trans config. (entgegen)
EAA	ethyl acetoacetate
EAK	ethyl amyl ketone
EBA	*N*-ethyl-*N*-benzylaniline

Chemical Tables

Important Abbreviations and Acronyms

EBBA	*N*-(*p*-ethoxybenzylidene)-*p*-butylaniline
EDC	ethylene dichloride
EDTA	ethylenediaminetetraacetic acid
EGS	ethylene glycol bis(succinimidyl succinate)
en	ethylenediamine
Et	ethyl
EVA	ethylene vinyl acetate
FA	furfuryl alcohol
FAD	flavin adenine dinucleotide
FMA	fluoroscein mercuric acetate
Fmoc	9-fluorenylmethoxycarbonyl
Fuc	fucose
G	guanine
Gal	galactose
GDP	guanosine 5′-diphosphate
Glc	glucose
Gln	glutamine (Q)
Glu	glutamic acid (E)
Gly	glycine (G)
Glyme (glyme)	1,2-dimethoxyethane
HAB	4,4′-bis(heptyl)azoxybenzene
Hex	hexane (or hexyl) or hexose
HFA	hexafluoroacetone
His	histidine (H)
HMDS	hexamethyldisilazide
HMPA	hexamethylphosphoramide
HMPT	hexamethylphosphorous triamide
HOAB	*p-n*-heptyloxyazoxybenzene
HOAc	acetic acid
Hyp	hydroxyproline
IH	immobilized histamine
IHP	inositolhexaphosphate
Ile	isoleucine (I)
IMP	inosine 5′-monophosphate
IPN	isophthalonitrile
KDP	potassium dihydrogen phosphate
LAH	lithium aluminum hydride ($LiAlH_4$)
LAP	leucine aminopeptidase
LDH	lactic dehydrogenase
Leu	leucine (L)
Lys	lysine (K)
M	metal
MA	maleic anhydride
MAA	methoxyacetic acid
Man	mannose
MBBA	*N*-(*p*-methoxybenzylidene)-*p*-butylaniline
MCA	monochloroacetic acid
Me	methyl
MEM	*β*-methoxyethoxymethyl
Mes	mesityl = 2,4,6-trimethylphenyl
Met	methionine (M)
MMH	methylmercuric hydroxide
MOM	methoxymethyl
Ms	mesyl = methanesulfonyl = $CH_3SO_2–$
MSA	methanesulfonic acid
MTPA	*α*-methoxy-*α*-trifluoromethylphenylacetic acid
MVK	methyl vinyl ketone
NAC	*N*-acetyl
NAD(P)	nicotinamide adenine dinucleotide (phosphate)
NAD(P)H	nicotinamide adenine dinucleotide (phosphate)
NAI	*N*-acetylimidazole
NCA	*N*-chloroacetamide
Nf	nonaflate ($C_4F_9SO_2–$)
NM	nitromethane
NMA	*N*-methylacrylamide
NMF	*N*-methylformamide
Ns	*p*-nitrobenzenesulfonyl
NTA	nitrilotriacetic acid
OCBA	*o*-chlorobenzoic acid
OCT	*o*-chlorotoluene
ODCB	*o*-dichlorobenzene
P	polymer substituent
PAA	*p*-azoxyanisole
PAS	*p*-aminosalicylic acid
PBA	pyrene butyric acid
PBLG	poly(L-benzyl μ-glutamate)
PC	propylene carbonate
PCA	perchloric acid
PCB	polychlorinated biphenyl
PCP	pentachlorophenol
PDMS	poly(dimethylsiloxane)
PEG	polyethylene glycol
PET	
Ph	phenyl
Phe	phenylalanine (F)
phen	1,10-phenanthroline

Important Abbreviations and Acronyms

PMA	poly(methacrylic acid)
PMMA	poly(methyl methacrylate)
POC	cyclopentyloxycarbonyl
POM	poly(oxymethylene)
PPA	poly(phosphoric acid)
Pr	propyl
Pro	proline (P)
PS	polystyrene
PTFE	polytetrafluoroethylene
PVA	poly(vinyl alcohol)
PVC	poly(vinyl chloride)
PVF	poly(vinyl fluoride)
PVP	poly(vinyl pyrrolidone)
Pyr (or Py)	pyridine
RNA	ribonucleic acid
SDS	sodium dodecyl sulfate
Ser	serine (S)
SLS	sodium lauryl sulfate
T	thymine
TAB	trimethylammonium bromide (TMAB)
TBE	tetrabromoethane
TCA	trichloroacetic acid
TCNQ	tetracyanoquinodimethane
TEA	triethylamine
Tf	triflate [CF_3SO_2–]
TFA	trifluoroacetic acid

THF	tetrahydrofuran
THP	tetrahydropyran
Thr	threonine (T)
TIPS	triisopropylsilyl
TMB	*N,N,N′N′*-tetramethylbenzidine
TMM	trimethylenemethane
TMS	tetramethylsilyl
TMU	tetramethylurea
TNM	tetranitromethane
TNT	2,4,6-trinitrotoluene
Tol	p-tolyl
TP	thymolphthalein
TPC	thymolphthalein complexone
TPE	tetraphenylethylene
Tr	trityl = triphenylmethyl
Triglyme	triethylene glycol dimethyl ether
TRIS	tris(hydroxymethyl)aminomethane
Trp	tryptophan (W)
Ts	tosyl = *p*-toluenesulfonyl
Tyr	tyrosine (Y)
U	uracil
UTP	uridine 5′-triphosphate
Val	valine (V)
Xyl	xylose
Z	cis configuration (zusammen)

Concentration Units for Solutions

Name	Symbol	Definition
Weight percent	wt %	(Grams of solute per grams of solution) x 100
Mole fraction	X_A	Moles of A per total number of moles
Molar	*M*	Moles of solute per liter of solution
Normal	*N*	Equivalents of solute per liter of solution
Formal	*F*	Formula weights of solute per liter of solution
Molal	*m*	Moles of solute per kg of solvent
Weight formal	*f*	Formula weight of solute per kg of solvent

Acronyms and Abbreviations in Quantum Chemistry and Molecular Modeling

AEE	**A**verage **E**xcitation **E**nergy
AM1	**A**ustin **M**ethod **1**, a modified MNDO method (semi-empirical)
AMBER	**A**ssisted **M**odel **B**uilding and **E**nergy **R**efinement, P. Kollman's empirical force field for biopolymers
AMFI	**A**tomic **M**ean **FI**eld approximation for SO coupling
AO	**A**tomic **O**rbital
ARCS	**A**romatic **R**ing **C**urrent **S**hielding
BOMD	**B**orn-**O**ppenheimer **M**olecular **D**ynamics simulation
CC	**C**oupled **C**luster methods (ab initio)
CCSD(T)	**C**oupled **C**luster method at **S**ingles, **D**oubles, **T**riples level
CDFT	**C**urrent **D**ensity **F**unctional **T**heory (ab initio)
CFT	**C**rystal **F**ield **T**heory
CHARMM	**CH**emitry at **HAR**vard **M**acromolecular **M**echanics, empirical force field implementation of M. Karplus
CHF	**C**oupled **H**artree-**F**ock perturbation theory
CI	**C**onfiguration **I**nteraction
CNDO	**C**omplete **N**eglect of **D**ifferential **O**verlap (semi-empirical)
CNDO/*n*	**C**omplete **N**eglect of **D**ifferential **O**verlap (level ***n*** = 1 or 2)
CNDO/2H	CNDO/2 modified for hydrogen bonding
CPMD	**C**ar-**P**arrinello **M**olecular **D**ynamics simulation
CSGT	**C**ontinuous **S**et of **G**auge **T**ransformations (ab initio)
DFT	**D**ensity **F**unctional **T**heory (ab initio)
DFTB	**D**ensity **F**unctional **T**ight **B**inding method
DGEOM	**D**istance **GEOM**etry
DHF	relativistic four-component **D**irac-**H**artree-**F**ock method
DZ	**D**ouble **Z**eta, a basis set consisting of two STOs for each atomic orbital
EH	**E**xtended **H**ückel theory
EHT	**E**xtended **H**ückel MO **T**heory
EOM	**E**quation **O**f **M**otion
FEMO	**F**ree-**E**lectron **M**olecular **O**rbitals
FPT	**F**inite **P**erturbation **T**heory
GGA	**G**eneralized **G**radient **A**pproximation (DFT)
GIAO	**G**auge-**I**ncluding **A**tomic **O**rbitals, also used: **G**auge-**I**nvariant or **G**auge-**I**ndependent (ab initio)
GIPAW	**G**auge-**I**ncluding **P**rojector-**A**ugmented **W**aves (ab initio)
GTO	**G**aussian **T**ype atomic **O**rbital
HF	**H**artree-**F**ock method for self-consistent fields
HFC(C)	**H**yper**F**ine **C**oupling (**C**onstant)
HMO	**H**ückel **M**olecular **O**rbitals
HOMO	**H**ighest **O**ccupied **M**olecular **O**rbital
IGAIM	**I**ndividual **G**auge for **A**toms **I**n **M**olecules (ab initio)
IGLO	**I**ndividual **G**auge for **L**ocalized **O**rbitals (ab initio)
INDO	**I**ntermediate **N**eglect of **D**ifferential **O**verlap (semi-empirical)
INDO/S	**INDO** for **S**pectroscopy
JWKB	**J**effreys-**W**entzel-**K**ramers-**B**rillouin, a semiclassical approximation to quantum mechanics
K-LMG	split-valence basis set defined with K, L, M numbers of Gaussians

Chemical Tables

Acronyms and Abbreviations in Quantum Chemistry and Molecular Modeling

LCAO	**L**inear **C**ombination of **A**tomic **O**rbitals (ab initio)
LDA	**L**ocal **D**ensity **A**pproximation (DFT)
LUMO	**L**owest **U**noccupied **M**olecular **O**rbital (see HOMO)
MCSCF	**M**ulti**C**onfiguration **S**elf **C**onsistent **F**ield (ab initio)
MD	**M**olecular **D**ynamics (with any method)
MINDO	**M**odified **I**ntermediate **N**eglect to **D**ifferential **O**verlap (semi-empirical)
MINDO/*n*	**M**odified **I**ntermediate Neglect of **D**ifferential **O**verlap (***n*** = 1-3, semi-empirical)
MINDO/3H	MINDO/3 modified for hydrogen bonding
MM	**M**olecular **M**echanics (with empirical force field)
MMn	N. L. Allinger's empirical force field for small molecules (n = integer)
MNDO	**M**odified **N**eglect of **D**ifferential **O**verlap (semi-empirical)
MNDO/H	MNDO modified for hydrogen bonding
MO	**M**olecular **O**rbital
MP2	**M**øller-Plesset 2nd-order perturbation calc. (ab initio)
MR-CI	**M**ulti-**R**eference **C**onfiguration **I**nteraction
NDDO	**N**eglect of **D**iatomic **D**ifferential **O**verlap
NICS	**N**ucleus-**I**ndependent **C**hemical **S**hift (aromaticity)
OPLS	**O**ptimized **P**otentials for **L**iquid **S**imulations, W. Jorgensen's empirical force field for biopolymers
PM3	**P**arameterized **M**ethod **3** (a modification of AM1)
PPP	**P**ariser-**P**arr-**P**ople method (semi-empirical)
QSAR	**Q**uantitative **S**tructure-Activity **R**elationship
REX	**R**elativistic **EX**tended Hückel MOs
RHF	**R**estricted **H**artee-**F**ock method (for SCF calculations)
SCF	**S**elf-**C**onsistent **F**ield
SCPT	**S**elf-**C**onsistent **P**erturbation **T**heory
SCRF	**S**elf-**C**onsistent **R**eaction **F**ield for free radicals
SD	**S**pin-**D**ipolar term
SO	**S**pin-**O**rbit coupling
SOMO	**S**ingly **O**ccupied **M**olecular **O**rbital
SOS	**S**um **O**ver **S**tates perturbation theory
STO	**S**later **T**ype **O**rbital basis set (ab initio)
STO-*n*G	**S**later **T**ype **O**rbitals as a sum of *n* Gaussians
TFD	**T**homas-**F**ermi-**D**irac method, a statistical treatment of electron density
UCHF	**U**n**C**oupled **H**artree-**F**ock perturbation method
UHF	**U**nrestricted **H**artee-**F**ock method for SCF calculations
VB	**V**alence **B**ond theory
VSEPR	**V**alence-**S**hell **E**lectron **P**air **R**epulsion, a theory of molecular geometry
VWN	**V**osko, **W**ilk, **N**usair parameterization for LDA
WKB	**W**entzel-**K**ramers-**B**rillouin method, a semiclassical approximation to quantum mechanics
ZDO	**Z**ero **D**ifferential **O**verlap (semi-empirical)
ZFS	**Z**ero-**F**ield **S**plitting
ZINDO	**Z**erner's **INDO** method
ZORA	**Z**ero-**O**rder **R**egular **A**pproximatio

Physical Tables

Colour, Wave Length, Frequency, Wave Number and Energy of Light

Colour	λ [nm]	ν [Hz]	ν [cm^{-1}]	E [eV]	E [kJ mol^{-1}]
Infrared	1000	$3.00 \cdot 10^{14}$	$1.00 \cdot 10^{4}$	1.24	120
Red	700	$4.28 \cdot 10^{14}$	$1.43 \cdot 10^{4}$	1.77	171
Orange	620	$4.84 \cdot 10^{14}$	$1.61 \cdot 10^{4}$	2.00	193
Yellow	580	$5.17 \cdot 10^{14}$	$1.72 \cdot 10^{4}$	2.14	206
Green	530	$5.66 \cdot 10^{14}$	$1.89 \cdot 10^{4}$	2.34	226
Blue	470	$6.38 \cdot 10^{14}$	$2.13 \cdot 10^{4}$	2.64	254
Violet	420	$7.14 \cdot 10^{14}$	$2.38 \cdot 10^{4}$	2.95	285
Near Ultraviolet	300	$1.00 \cdot 10^{15}$	$3.33 \cdot 10^{4}$	4.15	400
Far Ultraviolet	200	$1.50 \cdot 10^{15}$	$5.00 \cdot 10^{4}$	6.20	598

Density of Water (H_2O)

t [°C]	ρ [kg/dm³]	t [°C]	ρ [kg/dm³]	t [°C]	ρ [kg/dm³]
0	0.999841	11	0.999606	22	0.997772
1	0.999900	12	0.999498	23	0.997540
2	0.999941	13	0.999377	24	0.997299
3	0.999965	14	0.999244	25	0.997047
4	0.999973	15	0.999099	26	0.996785
5	0.999965	16	0.998943	27	0.996515
6	0.999941	17	0.998775	28	0.996235
7	0.999902	18	0.998596	29	0.995946
8	0.999849	19	0.998406	30	0.995649
9	0.999782	20	0.998205		
10	0.999701	21	0.997994		

Viscosity of Water, η in mPa · s (cP)

t [°C]	η	t [°C]	η	t [°C]	η	t [°C]	η
0	1.7865	**20**	1.0019	**50**	0.5477	**90**	0.3155
5	1.5138	**25**	0.8909	**60**	0.4674	**100**	0.2829
10	1.3037	**30**	0.7982	**70**	0.4048	**125**	0.2200
15	1.1369	**40**	0.6540	**80**	0.3554	**150**	0.1830

Viscosities of Various Liquids, η in mPa · s (cP)

Liquid	0°C	10°C	20°C	30°C	40°C	50°C	60°C	70°C	100°C
Acetic acid	–	–	1.219	1.037	0.902	0.794	0.703	0.629	0.464
Acetone	0.397	0.358	0.324	0.295	0.272	0.251	–	–	–
Aniline	–	6.53	4.39	3.18	2.40	1.91	1.56	1.29	0.76
Benzene	–	0.757	0.647	0.560	0.491	0.435	0.389	0.350	–
Bromobenzene	1.556	1.325	1.148	1.007	0.889	0.792	0.718	0.654	0.514
Carbon disulfide	0.436	0.404	0.375	0.351	0.329	–	–	–	–
Carbon dioxide (liq.)	0.099	0.085	0.071	0.053	–	–	–	–	–
Carbon tetrachloride	1.348	1.135	0.972	0.845	0.744	0.660	0.591	0.533	0.400
Chloroform	0.704	0.631	0.569	0.518	0.473	0.434	0.399	–	–
Diethyl ether	0.294	0.267	0.242	0.219	0.199	0.183	0.168	0.154	0.119
Ethanol	1.767	1.447	1.197	1.000	0.830	0.700	0.594	0.502	–
Ethyl acetate	0.581	0.510	0.454	0.406	0.366	0.332	0.304	0.278	–
Ethyl formate	0.508	0.453	0.408	0.368	0.335	0.307	–	–	–
Formic acid	–	2.241	1.779	1.456	1.215	1.033	0.889	0.778	0.547
Mercury	1.681	1.661	1.552	1.499	1.450	1.407	1.367	1.327	1.232
Methanol	0.814	0.688	0.594	0.518	0.456	0.402	0.356	–	–
***n*-Octane**	0.710	0.618	0.545	0.485	0.436	0.494	0.358	0.326	0.255
Oil, castor	–	2420	986	451	231	125	74	43	16.9
Oil, olive	–	138	84	52	36	24.5	17	12.4	–
***n*-Pentane**	0.278	0.254	0.234	0.215	0.198	0.184	0.172	0.161	0.130
Sulfuric acid	56	49	27	20	14.5	11.0	8.2	6.2	–
Toluene	0.771	0.668	0.585	0.519	0.464	0.418	0.379	0.345	0.268

Self-Diffusion Coefficients *D* of Various Liquids at 25°C

Liquid	D [10^{-9} m^{2}s^{-1}]	Liquid	D [10^{-9} m^{2}s^{-1}]	Liquid	D [10^{-9} m^{2}s^{-1}]
Water (H_2O)	2.299	Acetonitrile	4.37	Cyclopentane	3.09
Water (D_2O)	1.872	Pyridine	1.54	Cyclooctane	0.55
Methanol (CH_3OH)	2.415	Nitromethane	2.39	*n*-Pentane	5.72
Methanol (CH_3OD)	2.30	Tetrahydrofuran	2.84	*n*-Hexane	4.26
Methanol (CD_3OH)	2.21	Benzene	2.21	*n*-Heptane	3.12
Methanol (CD_3OD)	2.11	Fluorobenzene	2.39	*n*-Octane	2.35_5
Ethanol	1.08	Hexafluorobenzene	1.46	*n*-Nonane	1.77
t-Butanol-d_1	0.28	Toluene	2.27	*N*-Decane	1.37
Formamide	0.55	Carbon disulfide	4.32	*n*-Undecane	1.07_6
N,*N*-Dimethylformamide	1.63	Carbon Tetrachloride	1.30	*n*-Dodecane	0.81
N,*N*-Dimethylacetamide	1.35	Chloroform	2.35	*n*-Tridecane	0.70
Dimethyl sulfoxide	0.73	Acetic acid	1.08	*n*-Tetradecane	0.52
Dioxane	1.09	Formic acid	1.08	Pentan-1-ol	0.29
Acetone	4.57	Cyclohexane	1.42	Octan-1-ol	0.14

Table by courtesy of Dr. M. Holz (Institute of Phys. Chem., University of Karlsruhe, FRG) and Prof. A Sacco (Dept. Chem., University of Bari, Italy).

Temperature Dependence of the Self-Diffusion Coefficient *D* of Water (H_2O)

t [°C]	D [10^{-9} m^{2}s^{-1}]	t [°C]	D [10^{-9} m^{2}s^{-1}]	t [°C]	D [10^{-9} m^{2}s^{-1}]	t [°C]	D [10^{-9} m^{2}s^{-1}]
-5	0.913	20	2.023	50	3.956	80	6.557
0	1.099	25	2.299	55	4.344	85	7.056
2.5	1.199	30	2.594	60	4.748	90	7.574
5	1.303	35	2.907	65	5.172	95	8.111
10	1.525	40	3.238	70	5.615	100	8.667
15	1.765	45	3.588	75	6.078		

Table by courtesy of Dr. M. Holz, Institute of Phys. Chem., University of Karlsruhe, FRG.

SI Unit System (Système International) adapted from NIST Publication 330 (2001)

Fundamental SI Base Units	Unit Name	Symbol
length (*l*, *λ*)	meter	m
mass (*m*)	kilogram	kg
time (*t*)	second	s
electric current (*I*)	ampere	A
thermodynamic temperature (*T*)	kelvin	K
amount of substance (*n*)	mole	mol
luminous intensity (I_v)	candela	cd
SI-derived Quantities	**Unit Name**	**Symbol**
area (*A*)	square meter	m^2
volume (*V*)	cubic meter	m^3
speed, velocity (***v***)	meter per second	m/s
acceleration (***a***)	meter per second squared	m/s^2
momentum (***p*** = *m****v***)	kilogram meter per second	kg m/s
moment or inertia (*I*, *J*)	kilogram square meter	kg m^2
mass density (*ρ*)	kilogram per cubic meter	kg/m^3
specific volume (*v*)	cubic meter per kilogram	m^3/kg
molar mass (*M*)	kg per mole	kg/mol
molar volume (V_m)	cubic meter per mole	m^3/mol
concentration (*c*)	mole per cubic meter	mol/m^3
molal concentration (*m*)	mole per kilogram	mol/kg
kinematic viscosity (*ν*) diffusion coefficient (*D*)	square meter per second	m^2/s
electric current density (*J*)	ampere per square meter	A/m^2
magnetic field strength (***H***) magnetization (***M*** = ***B***/μ_0 – ***H***)	ampere per meter	A/m
magnetic dipole moment (***m***, ***μ***)	ampere square meter	A m^2
wave number ($\tilde{\nu}$)	reciprocal meter	m^{-1}
luminance (L_v)	candela per square meter	cd/m^2
refractive index (*n*)	(dimensionless)	

SI Prefix	Symbol	Factor
yocto	y	10^{-24}
zepto	z	10^{-21}
atto	a	10^{-18}
femto	f	10^{-15}
pico	p	10^{-12}
nano	n	10^{-9}
micro	μ	10^{-6}
milli	m	10^{-3}
centi	c	10^{-2}
deci	d	10^{-1}
deka	da	10^{1}
hecto	h	10^{2}
kilo	k	10^{3}
mega	M	10^{6}
giga	G	10^{9}
tera	T	10^{12}
peta	P	10^{15}
exa	E	10^{18}
zetta	Z	10^{21}
yotta	Y	10^{24}

Special SI-derived Quantities	Unit Name	Symbol	SI-derived and Base Units
plane angle (*α* = *s*/*r*)	radian	rad	m m^{-1} = 1 [2π rad = 360°], 1 rad = 57.2957795°
solid angle (*Ω*= *A*/r^2)	steradian	sr	m^2 m^{-2} = 1 [4π sr = sphere]
frequency (*ν* , *f*)	hertz	Hz	s^{-1}
force (***F*** = *m****a***)	newton	N	m kg s^{-2}
pressure, stress (*p*, *P*, *σ* = ***F***/*A*)	pascal	Pa	N/m^2 = m^{-1} kg s^{-2}
energy, work, heat (*E*, *W*)	joule	J	N m = m^2 kg s^{-2}
power, radiant flux (*P*)	watt	W	J/s = m^2 kg s^{-3}
electric charge, quantity (*Q*), flux (*ψ*)	coulomb	C	s A
electric potential (*V*, *ϕ*), pot. difference (*U*), emf (*E*)	volt	V	W/A or J/C = m^2 kg s^{-3} A^{-1}
capacitance (*C*)	farad	F	C/V = m^{-2} kg^{-1} s^4 A^2
electric resistance (*R*), impedance (*Z*)	ohm	Ω	V/A = m^2 kg s^{-3} A^{-2}
electric conductance (*G* = 1/*R*)	siemens	S	A/V or Ω^{-1} = m^{-2} kg^{-1} s^3 A^2
magnetic flux (*Φ*)	weber	Wb	V s = m^2 kg s^{-2} A^{-1}
magnetic flux density, induction (***B***)	tesla	T	Wb/m^2 = V s m^{-2} = kg s^{-2} A^{-1}
inductance (*L*)	henry	H	Wb/A or V s A^{-1} = m^2 kg s^{-2} A^{-2}
Celsius temperature (*θ*, *t*)	degree Celsius	°C	°C = K – 273.15

Special SI-derived Quantities	Unit Name	Symbol	SI-derived and Base Units
luminous flux (F)	lumen	lm	cd sr = $m^2\ m^{-2}$ cd
illuminance (E_v)	lux	lx	lm/m^2 = $m^2\ m^{-4}$ cd = m^{-2} cd
activity, radioactive decay (A)	becquerel	Bq	s^{-1}
absorbed dose, specific energy	gray	Gy	J/kg = $m^2\ s^{-2}$
dose equivalent (personal, organ)	sievert	Sv	J/kg = $m^2\ s^{-2}$
catalytic activity	katal	kat	s^{-1} mol

Other SI-derived Quantities	Unit Name	SI Symbol	SI Base Units
angular velocity (ω)	radian per second	rad/s	s^{-1} [1 Hz = 2π rad s^{-1}]
angular acceleration	radian per second squared	rad/s^2	s^{-2}
moment of force ($\boldsymbol{M}$), torque ($\boldsymbol{T} = \boldsymbol{r} \times \boldsymbol{F}$)	newton meter	N m	m^2 kg s^{-2}
dynamic viscosity (η, μ)	pascal second	Pa s	N s/m^2 = m^{-1} kg s^{-1}
surface tension (γ, σ)	newton per meter	N/m	kg s^{-2}
specific energy	joule per kilogram	J/kg	$m^2\ s^{-2}$
molar energy	joule per mole	J/mol	m^2 kg s^{-2} mol^{-1}
energy density	joule per cubic meter	J/m^3	m^{-1} kg s^{-2}
heat flux density (I)	watt per square meter	W/m^2	kg s^{-3}
thermal conductivity (λ, k)	watt per meter kelvin	W/(m K)	m kg s^{-3} K^{-1}
heat capacity (C_v , C_p), entropy (S)	joule per kelvin	J/K	m^2 kg s^{-2} K^{-1}
specific heat capacity (c) or entropy	joule per kilogram kelvin	J/(kg K)	$m^2\ s^{-2}\ K^{-1}$
molar entropy, molar heat capacity (C_m)	joule per mole kelvin	J/(mol K)	m^2 kg s^{-2} K^{-1} mol^{-1}
electric field strength ($\boldsymbol{E}$)	volt per meter	V/m	m kg s^{-3} A^{-1}
electric field gradient (q_{ab})	volt per square meter	V/m^2	kg s^{-3} A^{-1}
electric charge density (ρ)	coulomb per cubic meter	C/m^3	m^{-3} s A
electric flux density ($\boldsymbol{D}$)	coulomb per square meter	C/m^2	m^{-2} s A
electric polarization ($\boldsymbol{P} = \boldsymbol{D} - \varepsilon_0\boldsymbol{E}$)	coulomb per square meter	C/m^2	m^{-2} s A
electric dipole moment (μ)	coulomb meter	C m	m s A
electric polarizability (α)		$C^2\ m^2\ J^{-1}$	F m^2 = kg^{-1} s^4 A^2
electric quadrupole moment (eQ)	coulomb square meter	C m^2	m^2 s A
electric resistivity ($\rho = E / j$)	ohm meter	Ω m	m^3 kg s^{-3} A^{-2}
electric conductivity ($\kappa = 1 / \rho$)	siemens per meter	S/m	m^{-3} kg^{-1} s^3 A^2
molar conductivity (Λ)	siemens square meter per mole	S m^2/mol	kg^{-1} s^3 A^2 mol^{-1}
permittivity (ε)	farad per meter	F/m	m^{-3} kg^{-1} s^4 A^2
permeability ($\mu = \boldsymbol{B}/\boldsymbol{H}$)	henry per meter	H/m	m kg s^{-2} A^{-2}
exposure (radiation), ion dose	coulomb per kilogram	C/kg	kg^{-1} s A
absorbed dose rate	gray per second	Gy/s	$m^2\ s^{-3}$
rf specific absorption rate (SAR)	watt per kg	W/kg	$m^2\ s^{-3}$
radiant intensity (I)	watt per steradian	W/sr	m^2 kg s^{-3}
radiance (L)	watt per square meter steradian	W/(m^2 sr)	kg s^{-3}
irradiance (E)	watt per square meter	W/m^2	kg s^{-3}
luminous energy (Q_v)	lumen second	lm s	s cd sr
catalytic activity concentration	katal per cubic meter	kat/m^3	m^{-3} s^{-1} mol

Accepted non-SI units	Unit Name	Symbol	Value in SI units
length	astronomical unit	ua, AU	1 ua = 1.495 978 70 (30) × 10^{11} m
	nautical mile	nmi, NM	1 nautical mile = 1852 m
	Ångström	Å	1 Å = 10^{-10} m = 0.1 nm
area	are	a	1 a = 1 dam^2 = 10^2 m^2
	hectare	ha	1 ha = 1hm^2 = 10^4 m^2
	barn	b	1 b = 100 fm^2 = 10^{-28} m^2
volume	liter	L (l)	1 L = 1 dm^3 = 10^{-3} m^3
concentration	moles per liter (molar, M)	mol/L	1 M = 1 mol/dm^3
time	minute	min	1 min = 60 s
	hour	h	1 h = 60 min = 3600 s
	day	d	1 d = 24 h = 86 400 s
angular measure	degree	°	1° = (π/180) rad = 60'
	minute	'	1' = (1/60)° = (π/10800) rad
	second	''	1'' = (1/60)' = (π/648000) rad
mass	atomic mass unit	u	1 u = 1.660 538 86 (28) × 10^{-27} kg
	metric ton	t	1 t = 1000 kg
velocity	knot = 1 naut. mile/h	kn	1 nmi/h = 0.514444444 m/s
energy	electronvolt	eV	1 eV = 1.602 176 53 (14) × 10^{-19} J
pressure	bar	bar	1 bar = 10^5 Pa = 1000 hPa
nat. log. intensity scale	neper	Np	1 Np = 1 (= 8.6858896 dB)
base-10 log. intensity scale	bel, decibel	B, dB	1 dB = (1n 10)/20 Np

CGS Units	Symbol	SI Value	CGS Units	Symbol	SI Value
erg	erg	1 g cm^2 s^{-2} = 10^{-7} J	dyne	dyn	1 g cm s^{-2} = 10^{-5} N
gal	Gal	1 cm/s^2 = 10^{-2} m/s^2	gauss	G	10^{-4} T = 0.1 mT
maxwell	Mx	10^{-8} Wb	oersted	Oe	(10^3/4π) A/m
phot	ph	10^4 lx	poise	P	1 dyn s /cm^2 = 10^{-1} Pa s
stilb	sb	1 cd/cm^2 = 10^4 cd/m^2	stokes	St	1 cm^2/s = 10^{-4} m^2 s^{-1}

non-SI Units	Symbol	SI Value	non-SI Units	Symbol	SI Value
acceleration	g_n	9.80665 m s^{-2}	atmosphere	atm	101325 Pa
bohr (au)	a_0, b	5.29177 × 10^{-11} m	calorie (therm.)	calth	4.184 J
calorie (intern.)	cal_{IT}	4.1868 J	carat (metric)	kt	200 mg
centipoise	cP	1 mPa s	curie	Ci	3.7 × 10^{10} Bq
dalton	Da, u	1.66053873 × 10^{-27} kg	debye	D	3.33564 × 10^{-30} C m
entropy unit	e.u.	4.184 J K^{-1} mol^{-1}	fermi	f, fm	1 fm = 10^{-15} m
footcandle		10.76391 lx	gamma	γ	1 nT = 10^{-9} T
horsepower	hp	745.6999 W	jansky	Jy	1 Jy = 10^{-26} W m^{-2} Hz^{-1}
lambert		$10^4/\pi$ = 3.183099 cd/m^2	light year	l.y.	9.46073047258 × 10^{15} m
mho		1 siemens	miles/gal. (US)	mpg	235.215/mpg = L/100 km
miles/h	mph	0.44704 m/s	parsec	pc	3.085677581 × 10^{16} m
point (1/72 in)	pt	0.3527778 mm	pound/in^2	psi	6.894757 kPa
quad (10^{15} Btu)		1.055056 × 10^{18} J	rad	rad	1 cGy = 10^{-2} Gy
rem	rem	1 cSv = 10^{-2} Sv	roentgen	R	1 R = 2.58 × 10^{-4} C/kg
svedberg	S, Sv	10^{-13} s	ton (TNT)		4.184 GJ
ton (register)		2.831685 m^3	torr (mm hg)	Torr	1/760 atm = 133.322 3684 Pa
X unit		ca. 1.002 × 10^{-4} nm	year (Gregorian)	a	365.2425 d 31 556 952 s

SI Values of US and Imperial Measures

Linear Measures (1 m = 10^2 cm = 10^3 mm)			
Name	**Symbol**	**Equivalents**	**Exact SI Value (m)**
mil; thou	mil	0.001 in	2.54 E-05
point (font sizes)	pt	1/72 in	3.527778 E-04
pica		12 pt	4.233333 E-03
inch (international)	**in**	**defined**	**0.0254**
inch (US survey)	in	defined: 39.3700 in = 1 m	0.0254000508001016
hand		4 in	0.1016
link (US survey)	li, lnk	33/50 ft	0.201168402336805
foot (int.)	**ft**	**12 in (int)**	**0.3048**
foot (US survey)	ft	defined: 1 ft = 12/39.37 m	0.304800609601219
yard (int.)	**yd**	**3 ft; 36 in (int)**	**0.9144**
yard (US survey)	yd	3 ft; 36 in	0.914401828803658
fathom (US survey)	fm	6 ft	1.82880365760732
rod (US survey)	rd	25 li; 5.5 yd; 16.5 ft	5.02921005842012
chain (US survey)	ch	4 rd; 100 li; 22 yd; 66 ft	20.1168402336805
furlong (US survey)	fur	10 ch; 40 rd; 220 yd; 660 ft	201.168402336805
cable (US survey)		120 fm; 720 ft	219.456438912878
mile (int.)	**mi**	**1760 yd; 5280 ft (int)**	**1609.344**
statute mile (US survey)	mi	25 rd; 80 ch; 5280 ft; 8000 li	1609.347219
nautical mile (int.)	**nmi**	**defined**	**1852**
sea mile (US survey)		6080.20 ft	1853.24866649733
league	lea	3 nautical miles	5556
Area Measures (1 m^2 = 10^4 cm^2 = 10^6 mm^2)			
Name	**Symbol**	**Equivalents**	**Exact SI Value (m^2)**
square inch (int.)	sq in, in^2		6.4516 E-04
square foot (int.)	sq ft, ft^2	144 in^2	0.09290304
square yard (int.)	sq yd, yd^2	9 ft^2; 1296 in^2	0.83612736
square rod (US survey)	sq rd, rd^2	30.25 yd^2; 272.25 ft^2	25.2929538117141
acre (international)		4840 yd^2; 43560 ft^2; 0.40468564 ha	4046.8564224
acre (US survey)		10 ch^2; 160 rd^2; 4840 yd^2; 43560 ft^2	4046.87260987425
square mile (int.)	sq mi, mi^2	3097600 yd^2	2.589988110336 E+06
square mile (US survey)	sq mi, mi^2	640 acre	2.58999847031952 E+06
Volume Measures (1 L = 1 dm^3 = 10^{-3} m^3; 1 mL = 1 cm^3 = 10^{-6} m^3; 1 μl = 1 mm^3 = 10^{-9} m^3)			
Name	**Symbol**	**Equivalents**	**Exact SI Value (L, dm^3)**
cubic inch (int.)	cu in, in^3	0.554 fl oz	0.016387064
cubic foot (int.)	cu ft, ft^3	1728 in^3	28.316846592
cubic yard (int.)	cu yd, yd^3	27 ft^3; 46656 in^3	764.554857984
displacement ton		defined as 35 ft^3	991.08963072
register ton		defined as 100 ft^3	2831.6846592
cubic mile (int.)	cu mi, mi^3	5.451776 E9 yd^3	4.168181825 E+12
Imperial dry and fluid measures (UK, Commonwealth)			
minim	min	1/480 fl oz	5.919388021 E-05
drop	gtt	1/288 fl oz; 5/3 min	9.865646701 E-05
dash		1/384 gi; 1/16 tsp	3.699617513 E-04
pinch		2 dash; 1/192 gi; 1/8 tsp	7.399235026 E-04
scruple	fl s	1/24 fl oz; 20 min	1.183877604 E-03
drachm	fl dr	1/8 fl oz; 60 min	3.551633000 E-03
teaspoon (Canada)	tsp	1/6 fl oz; 80 min	4.735510417 E-03
teaspoon	tsp	1/24 gi; 5/3 fl dr; 100 min	5.919388021 E-03
tablespoon (Canada)	tbsp	1/2 fl oz; 3 tsp; 240 min;	1.420653125 E-02
tablespoon	tbsp	1/8 gi; 5/8 fl oz; 3 tsp; 5 fl dr; 300 min	1.775816406 E-02
ounce (Imp)	**fl oz (Imp)**	**8 fl dr; 480 min**	**0.0284130625**
gill	gi (Imp)	5 fl oz	0.1420653125
cup (Canada)	c (CA)	8 fl oz	0.2273045

Imperial dry and fluid measures (UK, Commonwealth)			
Name	**Symbol**	**Equivalents**	**SI Value (L, dm^3)**
pint	pt (Imp)	4 gill; 20 fl oz	0.56826125
quart	qt (Imp)	2 pt; 40 fl oz	1.1365225
gallon (Imperial)	**gal (Imp)**	**defined as 160 oz av water at 62 °F; 4 qt; 8 pt; 32 gi; 160 fl oz**	**4.54609**
peck	pk	2 gal	9.09218
bucket	bkt	4 gal	18.18436
bushel	bu	8 gal	36.36872
barrel	bl	36 gal	163.65924
US fluid measures			
minim	min	1/480 fl oz	6.161151992 E-05
drop	gtt	1/360 fl oz; 4/3 min	8.214869323 E-05
dash		1/96 fl oz; 1/16 tsp	3.080575996 E-04
pinch		2 dash; 1/48 fl oz; 1/8 tsp	6.161151992 E-04
dram	fl dr	1/8 fl oz; 60 min	3.696691195 E-03
teaspoon	tsp	1/6 fl oz	4.928921594 E-03
tablespoon	tbsp	1/2 fl oz; 4 fl dr; 0.5 fl oz	1.478676478 E-02
ounce (US)	**fl oz (US)**	**1/128 gal; 8 fl dr; 480 min**	**0.0295735295625**
jigger		1.5 fl oz; 12 fl dr	0.044360294
gill	gi (US)	4 fl oz	0.118294118
cup	c (US)	8 fl oz	0.236588
pint	pt (US)	2 c; 16 fl oz	0.473176473
quart	qt (US)	2 pt; 32 fl oz	0.946353
gallon (US)	**gal (US)**	**defined as 231 in^3; 4 qt; 128 fl oz**	**3.785411784**
barrel	fl bl (US)	defined as 31.5 gal	119.240471196
barrel (oil)	bbl	defined as 42 gal (US)	158.987294928
US dry measures			
pint	pt	1/64 bu	0.5506104713575
quart	qt	1/32 bu; 2 pt	1.101220942715
board-foot	fbm	defined as 144 in^3	2.359737216
gal	gal	1/8 bu; 4 qt	4.40488377086
peck	pk	1/4 bu; 8 qt	8.80976754172
bushel (dry level)	bu (US lvl)	defined as 2150.42 in^3; 4 pk; 32 qt;	35.23907016688
barrel	bl	105 qt	115.628198985075
seam		8 bu	281.91256133504
cord	cd	128 ft^3	3624.556363776
Mass (1 kg = 10^3 g = 10^6 mg)			
Name	**Symbol**	**Equivalents**	**Exact SI Value (kg)**
avoirdupois	av		
grain	gr	1/7000 lb	6.479891 E-05
dram	dr av	1/256 lb; 7000/256 gr	1.7718451953125 E-03
ounce	oz av	1/16 lb; 16 dr	2.8349523125 E-02
pound	**lb av**	**defined**	**0.45359237**
stone (UK)		14 lb	6.35029318
quarter (UK)		2 stone; 28 lb	12.70058636
hundredweight (short, US)	net cwt	100 lb	45.359237
hundredweight (long, UK)	gross cwt	8 stone; 112 lb	50.80234544
short ton (US)	ton	20 cwt; 2000 lb	907.18474
long ton (UK)	ton	20 cwt (UK); 2240 lb	1016.0469088
troy or apothecary	t, ap		
grain	gr	same mass as in avoirdupois	6.479891 E-05
scruple	s ap	1/24 oz t; 20 gr	1.2959782 E-03
pennyweight	dwt, pwt	1/20 oz t; 24 gr	1.55517384 E-03
dram	dr t	1/8 oz t; 60 gr	3.8879346 E-03
ounce	oz t	1/12 lb t; 20 dwt; 8 dr t; 480 gr	3.11034768 E-02
pound	lb t	12 oz t; 96 dr t; 5760 gr	0.3732417216

Physical Tables

Fundamental Physical Constants (CODATA 2006) [a]

Quantity	Symbol	SI Value
Speed of Light (vacuum)	c, c_0	2.997 924 58 × 10^{8} m s^{-1} (defined)
Permeability of vacuum	μ_0	$4\pi \times 10^{-7}$ H m^{-1} or N A^{-2} (defined)
Permittivity of vacuum	$\varepsilon_0 = 1/(\mu_0 c_0^2)$	8.854 187 817 .... × 10^{-12} F m^{-1} (defined)
Planck Constant	h	6.626 068 96 (33) × 10^{-34} J s
	$\hbar = h / 2\pi$ (au)	1.054 571 628 (53) × 10^{-34} J s
Elementary Charge (au)	e	1.602 176 487 (40) × 10^{-19} C
Electron Rest Mass (au)	m_e	9.109 382 15 (45) × 10^{-31} kg
Proton Rest Mass	m_p	1.672 621 637 (83) × 10^{-27} kg
Proton/Electron Mass Ratio	m_p / m_e	1836.152 672 47 (80)
Neutron Rest Mass	m_n	1.674 927 211 (84) × 10^{-27} kg
Deuteron Rest Mass	m_d	3.343 583 20 (17) × 10^{-27} kg
Atomic Mass Unit (^{12}C/12)	m_u = 1 u = 1 Da	1.660 538 782 (83) × 10^{-27} kg
Avogadro's Number	N_A	6.022 141 79 (30) × 10^{23} mol^{-1}
Boltzmann Constant	k	1.380 6504 (24) × 10^{-23} J K^{-1}
Faraday Constant	F	9.648 533 99 (24) × 10^{4} C mol^{-1}
Gas Constant	R	8.314 472 (15) J mol^{-1} K^{-1}
Molar Volume of ideal gas [b]	$V_m = RT/p$	22.413 996 (39) × 10^{-3} m^3 mol^{-1}
Standard Atmosphere	atm	101.325 kPa (defined)
Fine Structure Constant	$\alpha = \mu_0 e^2 c_0 / 2h$	7.297 352 5376 (50) × 10^{-3}
Inverse Fine-Structure Constant	$1/\alpha$	137.035 999 679 (94)
Bohr Radius (au)	$a_0 = 4\pi\varepsilon_0\hbar^2 / m_e e^2$	0.529 177 208 59 (36) × 10^{-10} m
Hartree Energy (au)	$E_h = \hbar^2 / m_e a_0^2$	4.359 743 94 (22) × 10^{-18} J
Rydberg Constant	$R_\infty = E_h / 2hc_0$	1.097 373 156 8527 (73) × 10^{7} m^{-1}
Compton Wavelength (Electron)	$\lambda_C = h / m_e c_0$	2.426 310 2175 (33) × 10^{-12} m
Bohr Magneton (β, β_e)	$\mu_B = e\hbar / 2m_e$	9.274 009 15 (23) × 10^{-24} J T^{-1}
Electron Magnetic Moment	μ_e	–9.284 763 77 (23) × 10^{-24} J T^{-1}
Electron Magnetogyric Ratio	$\gamma_e = 2\,\mu_e / \hbar$	1.760 859 770 (44) × 10^{11} s^{-1} T^{-1}
	$\gamma_e / 2\pi$	28.024 953 64 (70) GHz T^{-1}
Free Electron Landé g factor	$g_e = 2\mu_e / \mu_B$	–2.002 319 304 3622 (15)
Nuclear Magneton (β_N)	$\mu_N = (m_e / m_p)\,\mu_B$	5.050 783 24 (13) × 10^{-27} J T^{-1}
Proton Magnetic Moment (free)	μ_p	1.410 606 662 (37) × 10^{-26} J T^{-1}
(shielded, H_2O sphere, 25°C)	μ_p'	1.410 570 419 (38) × 10^{-26} J T^{-1}
Proton Magnetogyric Ratio (free)	γ_p	2.675 222 099 (70) × 10^{8} s^{-1} T^{-1}
(shielded, H_2O sphere, 25°C)	γ_p'	2.675 153 362 (72) × 10^{8} s^{-1} T^{-1}
Proton MR freq. in H_2O	$\gamma_p' / 2\pi$	42.576 3881 (12) MHz T^{-1}
Electron/Proton Magn. Mom. Ratio	μ_e / μ_p	–658.210 6848 (54)
Deuteron Magnetic Moment	μ_d	0.433 073 465 (11) × 10^{-26} J T^{-1}
Gravitation Constant (Newtonian)	G	6.674 28 (67) × 10^{-11} m^3 kg^{-1} s^{-2}
Standard Acceleration (Earth gravity)	g_n	9.806 65 m s^{-2} (defined)
π = 3.141 592 653 59	e = 2.718 281 828 46	ln 10 = 2.302 585 092 99

[a] au = atomic units; uncertainty of last digits shown in ( ); source: http://physics.nist.gov/constants
[b] at STP of 273.15 K and 101.325 kPa = 1 atm.

International Dialing Codes / World Time Zones

Time Zones are listed as increment in hour:min relative to UTC / GMT for ST = standard time; DST = Daylight Savings (Summer) Time (where used).
Provences or Cities are listed for countries with more than one time zone.
NB: DST runs approximately from March to October in the northern hemisphere and October to March in the southern hemisphere; exact period depends on country and may change from year to year.
(data adapted by W.E. Hull from www.happyzebra.com and www.worldtimezone.com)

Country (Code) - Provinces / Cities	ST	DST
Afghanistan (+93)	+4:30	
Albania (+355)	+1	+2
Algeria (+213)	+1	
Angola (+244)	+1	
Argentina (+54) DST only in Buenos Aires and some provinces in the northeast	–3	–2
Armenia (+374)	+4	+5
Australia (+61) - W. Austr. (Perth)	+8	
Australia (+61) - N. Terr. (Darwin),	+9:30	
Australia (+61) - Queensland (Brisbane)	+10	
Australia (+61) - Cap. Terr. (Canberra), N.S.W. (Sydney), Victoria (Melbourne), S. Austr. (Adelaide), Tasmania (Hobart)	+10	+11
Austria (+43)	+1	+2
Azerbaijan (+994)	+4	+5
Bahamas (+1)	–5	–4
Bahrain (+973)	+3	
Bangladesh (+880)	+6	+7
Barbados (+1)	–4	
Belarus (+375)	+2	+3
Belgium (+32)	+1	+2
Belize (+501)	–6	
Benin (+229)	+1	
Bermuda (UK)	–4	–3
Bhutan (+975)	+6	
Bolivia (+591)	–4	
Bosnia-Herzegovina (+387)	+1	+2
Botswana (+267)	+2	
Brazil (+55) / Rio Branco	–5	
Brazil (+55) / Manaus	–4	
Brazil (+55) / Salvador, Recife	–3	
Brazil (+55) / Brasilia, Rio de Janeiro, Porto Alegre, Sao Paulo	–3	–2
Brazil (+55) / Fernando de Noronha	–2	
Brunei (+673)	+8	
Bulgaria (+359)	+2	+3
Burkina Faso (+226)	0	
Burundi (+257)	+2	
Cambodia (+855)	+7	
Cameroon (+237)	+1	
Canada (+1) - Newfoundland & Labrador	–3:30	–2:30
Canada (+1) - Pr. Edward Island, Nova Scotia, New Brunswick	–4	–3
Canada (+1) - Ontario (Toronto, Ottawa), Quebec (Montreal, Quebec)	–5	–4
Canada (+1) - Manitoba (Winnipeg)	–6	–5
Canada (+1) - Alberta (Edmonton, Calgary), NW Territories	–7	–6
Canada (+1) - Saskatchewan	–7	
Canada (+1) - British Columbia (Vancouver), Yukon Terr.	–8	–7
Canary Islands (Spain)	0	+1
Central African Republic (+236)	+1	
Chad (+235)	+1	
Chile (+56)	–4	–3
China (+86)	+8	
Colombia (+57)	–5	
Congo, Repub. (+242) / Kinshasa	+1	
Congo, Dem. Repub. (+243) / Lubumbashi	+2	
Costa Rica (+506)	–6	
Cote d'Ivoire (+225)	0	
Croatia (+385)	+1	+2
Cuba (+53)	–5	–4
Cyprus (+357)	+2	+3
Czech Republic (+420)	+1	+2
Denmark (+45)	+1	+2
Djibouti (+253)	+3	
Dominican Republic (+1)	–4	
Ecuador (+593)	–5	
Egypt (+20)	+2	+3
El Salvador (+503)	–6	
Eritrea (+291)	+3	
Estonia (+372)	+2	+3
Ethiopia (+251)	+3	
Fiji (+679)	+12	
Finland (+358)	+2	+3
France (+33)	+1	+2
French Guiana	–3	
Gabon (+241)	+1	
Galapagos Islands (Ecuador)	–6	
Gambia (+220)	0	
Gaza (+970)	+2	+3
Georgia (+995)	+4	
Germany (+49)	+1	+2
Ghana (+233)	0	
Gibraltar (UK)	+1	+2
Greece (+30)	+2	+3
Guatemala (+502)	–6	
Guadeloupe (France)	–4	
Guinea (+224)	0	
Guyana (+592)	–4	
Haiti (+509)	–5	
Honduras (+504)	–6	
Hungary (+36)	+1	+2
Iceland (+354)	0	
India (+91)	+5:30	
Indonesia (+62) - Papua	+9	
Indonesia (+62) - Bali, Kalimantan, Lombok, West Timor	+8	
Indonesia (+62) - Java, Sumatra	+7	
Iran (+98)	+3:30	+4:30
Iraq (+964)	+3	
Ireland (+353)	0	+1
Israel (+972)	+2	+3
Italy (+39)	+1	+2
Jamaica (+1)	–5	
Japan (+81)	+9	
Jordan (+962)	+2	+3
Kazakhstan (+7) / Almaty, Astana	+6	
Kazakhstan (+7) / Aqtau, Aqtobe	+5	
Kenya (+254)	+3	
Kosovo (+381)	+1	+2
Kuwait (+965)	+3	

International Dialing Codes / World Time Zones

Country (Code) - Provinces / Cities	ST	DST
Kyrgyzstan (+996)	+6	
Laos (+856)	+7	
Latvia (+371)	+2	+3
Lebanon (+961)	+2	+3
Lesotho (+266)	+2	
Liberia (+231)	0	
Libya (+218)	+2	
Liechtenstein (+423)	+1	+2
Lithuania (+370)	+2	+3
Luxembourg (+352)	+1	+2
Macedonia (+389)	+1	+2
Madagascar (+261)	+3	
Malawi (+265)	+2	
Malaysia (+60)	+8	
Maldives (+960)	+5	
Mali (+223)	0	
Malta (+356)	+1	+2
Martinique (France)	–4	
Mauritania (+222)	0	
Mauritius (+230)	+4	
Mexico (+52) - Aguascalientes, Fed. District (Mexico City), Guanajuato, Guerrero, Jalisco, Nuevo Leon, Quintana Roo, San Luis Potosi, Veracruz, Yucatan	–6	–5
Mexico (+52) - Chihuahua, Sinaloa	–7	–6
Mexico (+52) - Sonorro	–7	
Mexico (+52) - Baja California (Tijuana)	–8	–7
Moldova (+373)	+2	+3
Monaco (+377)	+1	+2
Mongolia (+976) / Choibalsan, Ulaanbaatar	+8	
Mongolia (+976) / Hovd	+7	
Montenegro (+382)	+1	+2
Morocco (+212)	0	+1
Mozambique (+258)	+2	
Myanmar (+95)	+6:30	
Namibia (+264)	+1	+2
Nepal (+977)	+5:45	
Netherlands (+31)	+1	+2
New Zealand (+64)	+12	+13
Nicaragua (+505)	–6	
Niger (+227)	+1	
Nigeria (+234)	+1	
North Korea (+850)	+9	
Norway (+47)	+1	+2
Oman (+968)	+4	
Pakistan (+92)	+5	+6
Panama (+507)	–5	
Papua New Guinea (+675)	+10	
Paraguay (+595)	–4	–3
Peru (+51)	–5	
Philippines (+63)	+8	
Poland (+48)	+1	+2
Portugal (+351)	0	+1
Puerto Rico (+1)	–4	
Qatar (+974)	+3	
Reunion (+262)	+4	
Romania (+40)	+2	+3
Russia (+7) / Kaliningrad	+2	+3
Russia (+7) / Kazan, Moscow, Murmansk, Novgorod, St. Petersburg	+3	+4
Russia (+7) / Samara	+4	+5
Russia (+7) / Chelyabinsk, Novosibirsk, Perm, Ufa, Yekaterinburg	+5	+6

Country (Code) - Provinces / Cities	ST	DST
Russia (+7) / Omsk	+6	+7
Russia (+7) / Krasnoyarsk	+7	+8
Russia (+7) / Irkutsk	+8	+9
Russia (+7) / Yakutsk	+9	+10
Russia (+7) / Vladivostok, Yuzhno-Sakhalinsk	+10	+11
Russia (+7) / Magadan	+11	+12
Russia (+7) / Anadyr, Kamchatka	+12	+13
Rwanda (+250)	+2	
Saudi Arabia (+966)	+3	
Senegal (+221)	0	
Serbia (+381)	+1	+2
Seychelles (+248)	+4	
Sierra Leone (+232)	0	
Singapore (+65)	+8	
Slovakia (+421)	+1	+2
Slovenia (+386)	+1	+2
Somalia (+252)	+3	
South Africa (+27)	+2	
South Korea (+82)	+9	
Spain (+34)	+1	+2
Sri Lanka (+94)	+5:30	
Sudan (+249)	+3	
Suriname (+597)	–3	
Swaziland (+268)	+2	
Sweden (+46)	+1	+2
Switzerland (+41)	+1	+2
Syria (+963)	+2	+3
Tahiti (France)	–10	
Taiwan (+886)	+8	
Tajikistan (+992)	+5	
Tanzania (+255)	+3	
Thailand (+66)	+7	
Timor-Leste (+670)	+9	
Togo (+228)	0	
Trinidad & Tobago (+1)	–4	
Tunisia (+216)	+1	
Turkey (+90)	+2	+3
Turkmenistan (+993)	+5	
UAE - Abu Dhabi, Dubai (+971)	+4	
Uganda (+256)	+3	
Ukraine (+380)	+2	+3
United Kingdom (+44) - England, Scotland, Wales, N. Ireland	0	+1
Uruguay (+598)	–3	–2
USA (+1) - Eastern Zone (New York, Boston, Miami, Philadelphia...)	–5	–4
USA (+1) - Central Zone (Chicago, Wichita, New Orleans, Pensicola)	–6	–5
USA (+1) - Mountain Zone (Helena, Denver, Santa Fe)	–7	–6
USA (+1) - Arizona	–7	
USA (+1) - Pacific Zone (Las Vegas, San Francisco, Los Angeles)	–8	–7
USA (+1) - Alaska (Anchorage)	–9	–8
USA (+1) - Hawaii (Honolulu)	–11	
Uzbekistan (+998)	+5	
Vatican City (+39)	+1	+2
Venezuela (+58)	–4:30	
Vietnam (+84)	+7	
Yemen (+967)	+3	
Zambia (+260)	+2	
Zimbabwe (+263)	+2	